THE UNIVERSITY OF CHICAGO

EVOLUTION OF FIN CONFIGURATION IN ACTINOPTERYGIAN FISH AND DEVELOPMENT OF THE PELVIC FINS IN ZEBRAFISH

A DISSERTATION SUBMITTED TO

THE FACULTY OF THE DIVISION OF THE BIOLOGICAL SCIENCES

AND THE PRITZKER SCHOOL OF MEDICINE

IN CANDIDACY FOR THE DEGREE OF

DOCTOR OF PHILOSOPHY

GRADUATE PROGRAM IN INTEGRATIVE BIOLOGY

BY

STEPHANIE SANG

CHICAGO, ILLINOIS

AUGUST 2022

To my parents, who have supported me in every step of my education.

Table of Contents

LIST OF FIGURES

LIST OF TABLES

ACKNOWLEDGEMENTS

I am grateful to everyone who has supported me during, and leading up to, the journey of earning my PhD. First, thank you to my co-advisors, Mike and Robert, who have made for a truly constructive co-advising experience. I appreciate that in our 4+ years of weekly meetings, I've been able to bring up segments of each project and receive input from you both. Having strong developmental and paleontological perspectives on my dissertation has most definitely deepened the quality of my discussions. Aside from the science, I have thoroughly enjoyed scrunching my face in confusion for 33% of each meeting when you both begin speaking about completely random topics (e.g. buried cockroaches, bird identification, the bug crisis). Thank you for being good sports and tolerating my constant shenanigans. In addition, thank you to my wonderful committee members – Graham, Urs, and Tim. Each of you individually has been integral to the completion of my project, ranging from sharing technical expertise, helping with the analysis, or diligently editing my writing. Thank you also to Vicky for providing input and making lunches in the conference room a much sought-after activity.

Secondly, my day-to-day life has been enriched by the presence of fantastic Ho, Coates, and Prince lab members. Thanks to Erin and Lindsey for being my academic "big sisters" and teaching me how to perform all the fundamental techniques. I am very excited to now be an "academic auntie"! Thanks Chris and Alana for being my nocturnal labmates and making timelapses at 1 AM to be much more bearable. The biggest thanks of course goes to Adam, without which all of the fish would have perished, and without whose company I probably would have descended into insanity during the initial pandemic years. I wish you many cruises and cryptocurrencies in the future. Thanks to Coates Lab members Ben, Vish, Abby, Elisabeth, Yunyan, Marco, Tetsuto, Kristen, and Aliss the Lungfish for making each week extremely wild

and special. The amount of chaos that this lab experiences on a near daily basis is unparalleled. I will miss the raccoon fights, lamprey brawls, and heated discussions about nemeses. Finally, thanks to Prince Lab members Ana, Manny, and Noor for being an excellent source of reagents and friendship when I wandered down to the second floor.

The friends I've acquired while here are undoubtedly the reasons why I could return to the lab after every failed experiment. Katie, you are my #1 and our bagel breaks gave me dear life. Tom and Melvin/Tony, you kept me caffeinated and strong – one day I'll top out on the climbing wall. Anatomy Crew – Kelsey, Sam, and JD – Human Anatomy is clearly the best part of this program, and it was made even better by having such wonderful friends by my side. For my friends from afar – you are too numerous to name – but I appreciate every one of you for rooting for me all this time. Your visits, phone calls, and encouraging messages made me feel incredibly supported.

I am also thankful to all the people and organizations that have helped me during my career thus far. Thank you to my undergraduate mentor, Warren, for getting me started - my undergraduate thesis propelled me to enter evolutionary and developmental biology. Thanks to my MSc advisor, Jill, for patiently teaching me the basics of developmental biology and how moss is boss.

Finally, thank you to my family – my extended relatives, my brother Brian, and my mom and dad, the original Dr. Sang and Dr. Hsieh. Your support has made it possible for me to become interested in science thanks to my participation in Science Olympiad, attend universities where I was able to study and perform research with the best in the field, and most importantly, to feel loved and supported no matter what happened. 感謝爸爸媽媽，你們一直都在照顧我。

ABSTRACT

Changes in development drive evolution to produce exceptionally diverse morphologies, but too often, there is insufficient knowledge about either a system's evolutionary history or developmental parameters to link the two together. The malleable fin configurations in the Actinopterygii (ray-finned fish), a clade of over 30,000 species, serve as a riveting case study for the chance to couple evolution and development to explain morphological diversity. Ray-finned fish possess two sets of paired fins, the pectoral and pelvic fins, and three unpaired median fins – the caudal, dorsal, and anal fins. While the positions of the fins, especially the paired fins (or the homologous forelimbs and hindlimbs), is constrained in the rest of jawed vertebrates, fin configuration is remarkably labile in actinopterygians. In this dissertation, I first attempt to characterize the evolutionary patterns of fin positioning in actinopterygians to gain an understanding of which groups were displaying the most pronounced changes, and to obtain a sense of how constrained these fin shifts might be (Chapter 2). Next, I investigate zebrafish (*Danio rerio*) pelvic fin development to determine where the pelvic fin precursor cells arise from (Chapter 3, 4). Finally, I present a synthesized view of how developmental changes in actinopterygian fish might have facilitated their diverse fin configurations (Chapter 5).

In Chapter 2, I quantify fin positions for almost 600 species of extant actinopterygian fish and 78 fossil species. I demonstrate that major lineages of actinopterygians occupy different areas of the pectoral-pelvic fin position morphospace; while the earliest lineages (e.g. non-teleosts, ostariophysans) of actinopterygians display posterior pelvic fins and ventral pectoral fins, the later lineages (e.g. percomorphs) move into the anterior pelvic fin and dorsally-shifted pectoral fin area of the morphospace. Fossil species are mostly located in the ventral-pelvic, dorsal-pectoral corner of the morphospace. I then find a major shift in adaptive optima in paired

fin positioning at the base of Neoteleostei, a teleostean group that encompasses the Acanthopterygii (spiny-rayed fish) and has received little attention for its synapomorphies. The nature of how the paired fins relate to one another appears to fundamentally shift in Neoteleostei. While there is no correlation in paired fin position in all actinopterygians (and Non-Neoteleost), I was able to recover a correlation ($p=0.03$) in Neoteleosts. I next investigated the positioning of the median fins and found an unexpected linkage between the positioning of the anterior limit of the dorsal fin and the position of the pelvic fins. These fins have stayed in register despite continuous shifts in position along the body axis, and this linkage appears to date to the Jurassic.

In Chapters 3, I generate a transgenic line *Tg(hsp:cre-ert2)* as part of a permanent lineage tracing system to show that cells from the posterior lateral plate mesoderm at the levels of somite 6-11 can contribute to the future pelvic fin bud, with greater support for cells likely arising from somite levels 7-11. These long-term lineage tracing results are coupled with embryonic fate-mapping and cell tracking of the lateral plate mesoderm. In Chapter 4, I find evidence that pelvic fin specification is likely late in the late larval stages, and not embryonic. Expression of candidate 'hindlimb' genes such as *tbx4* and *pitx1* was not detectable in embryos, and only appeared in the body wall 1-2 weeks (4-5 mm SL) prior to pelvic fin initiation (7 mm SL). These genes were also expressed in the ventral myosepta close to the prospective pelvic fin location. Furthermore, I find expression of caudal cluster Hox genes *hoxc10, hoxc9,* and *hoxc9* and EMT-associated gene *twist1b* in the same expression domains as the candidate 'hindlimb' genes. Taken together, in Chapter 5, I propose that the late specification of the pelvic fin field has allowed actinopterygian fish to shift their pelvic fin positions, and that this novelty has also been facilitated by changes to the migratory nature of the lateral plate mesoderm

Chapter 1 - INTRODUCTION

1.1 Overview

The ability to be highly mobile and navigate through an open environment is key to the story of vertebrate evolution. Though undulatory propulsion alone is sufficient to transport an organism, mobility is significantly enhanced by the addition of appendages – fins or limbs. In aquatic environments, fins both generate thrust and stabilize the body, allowing for fast and refined movement as well as station holding on the substrate or mid-water. Paired fins also allowed vertebrate life to join the Devonian 'nekton revolution' and rise from the benthos to occupy the water column (Klug et al., 2010). In terrestrial environments, limbs are the primary means of locomotion and interaction with the substrate for most vertebrates (excepting limbless vertebrates that have secondarily lost their limbs) and are often used for manipulating the environment. Finally, certain limb adaptations, such as the repeated evolution of wings, have allowed vertebrates to enter the aerial space.

This dissertation focuses on the evolution and development of fins in actinopterygian, or the ray-finned fish, and how the positioning of these fins along the body axes changes throughout actinopterygian evolution. Furthermore, this dissertation investigates the developmental underpinnings of pelvic fin development using zebrafish *Danio rerio* as a model system. Taken together, these chapters contribute to the study of how selective and developmental constraints might influence the positioning of fins in ray-finned fish.

Actinopterygians are characterized by three median fins, which are positioned on the dorsal and ventral midline of the body, and two sets of paired fins (Figure 1.1A). The median fins – dorsal, anal, and caudal fins – can vary in the size, length along the body, and in the case of the dorsal fin, in number. The dorsal and anal fins consist of pterygiophores/radials, which are endoskeletal internal bony or cartilaginous supports for muscle attachments, and dermal fin rays that extend outside the body. The pectoral fins are composed of an endoskeletal pectoral girdle, which is attached to endochondrally-derived fin radials, which are in turn attached to the dermal lepidotrichia (Figure 1.1B). Pectoral fins, if present, are commonly located on the lateral side of the body and can vary in dorsoventral position. However, as the pectoral girdle is articulated with the skull, these fins are constrained to the anterior region of the fish. The pelvic fins similarly are composed of a pelvic girdle, fewer radials in comparison to the pectoral fins, and lepidotrichia (Figure 1.1C). Actinopterygian pelvic fins lie ventrally on the body. Unlike tetrapods, the pelvic girdle is not articulated to the axial skeleton, and can stray from a pre-pectoral to a pre-anal position. As a rule, the pelvic fin is never located posterior to the anus. While the position of the anus relative to the entire body length can shift (e.g. flatfish, where the anus has been shifted anteriorly), the pelvic fins must remain anterior to this landmark. This is because the lateral plate mesoderm, the tissue layer that gives rise to the paired fins, only extends to the anus.

Actinopterygian fins have been repeatedly modified in shape, number, and function. In many lineages of actinopterygians, the lepidotrichia of the fins are spinous, which have been hypothesized to be a defensive trait (Price, Friedman, & Wainwright, 2015). Fins have been frequently lost, duplicated, or evolved *de novo* such as the adipose fin (Larouche, Zelditch, &

Cloutier, 2018; Stewart, Smith, & Coates, 2014). Given the importance and diversity of fin morphology, the study of actinopterygian fin evolution and development is a rich area for testing macroevolutionary questions.

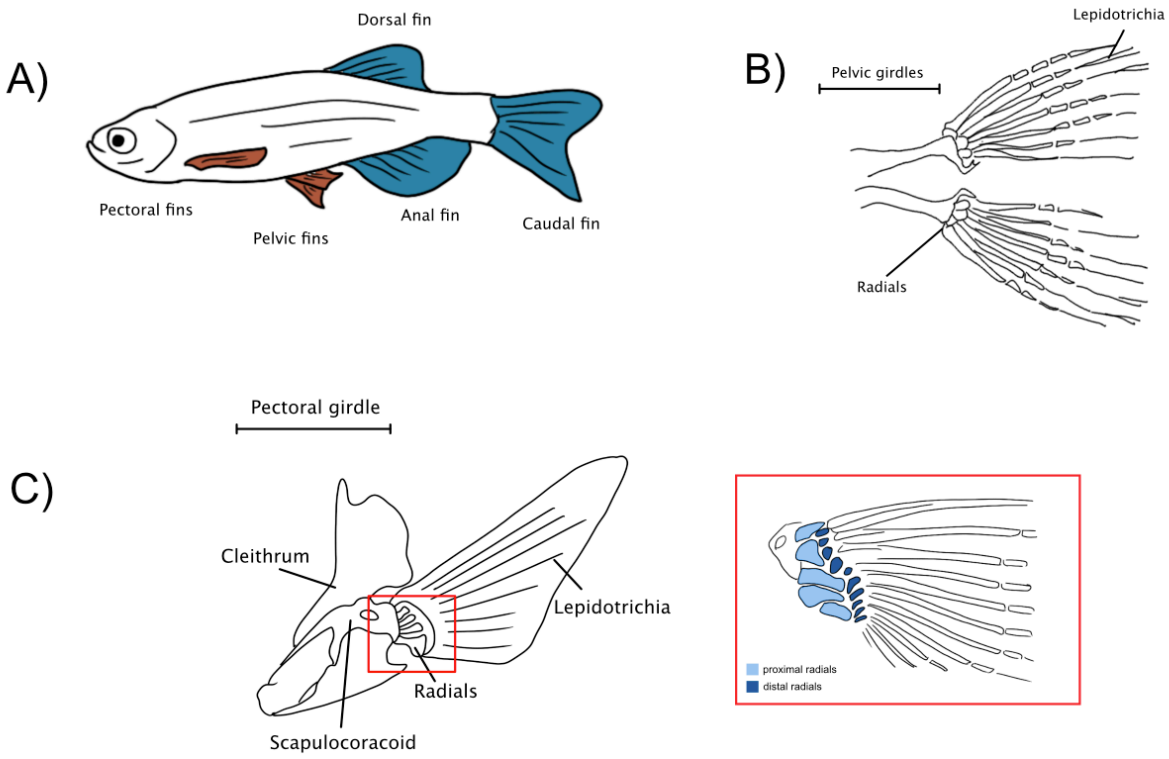

Figure 1.1 - Pectoral and pelvic fins.

(A) The paired fins (in red) and median fins (in blue) of a representative teleost, *Danio rerio.* (B) Skeletal anatomy of pelvic fins and girdle of a generalized teleost. (C) Skeletal anatomy of a pectoral girdle and fin of a generalized teleost. Inset is a dorsomedial view of the radials.

Tetrapod forelimbs and hindlimbs are homologous to the pectoral and pelvic fins, respectively (Clack, 2009; Coates, 1994; Owen, 1849). The fin-to-limb transition within the sarcopterygian lineage resulted in the transformation of the fin radials into the stylopod and zeugopod (humerus, radius/ulna, respectively). In actinopterygians at least, the cell population

that gives rise to both radials and lepidotrichia is homologous to the population in tetrapods that was transformed into the autopod (digits) (Daegwon Ahn & Ho, 2008; Nakamura, Gehrke, Lemberg, Szymaszek, & Shubin, 2016). The tetrapod forelimb and hindlimb data are an essential comparative source to understand actinopterygian fin development. Loss of expression and misexpression experiments in chick and mouse have shed light on the limb initiation regulatory network, which provide fertile testing ground for how fin bud initiation might occur.

In this introduction, I will review the literature surrounding the origin of paired/median fins in evolutionary history. Secondly, I will describe the lateral plate mesoderm and what is known about how the paired fins/limbs are initiated in gnathostomes. Thirdly, I will tour the diversity of the Actinopterygii, mention current key issues in the study of their phylogenetic relationships, and then explore how the pelvic fins have been specialized in different groups. Next, I will return to the pelvic fins in a comparative developmental context and survey what has been studied. Finally, I will present the scope of this thesis and give an overview of the chapters.

1.2 Origin of the paired and median fins

Paired appendages are a defining feature of gnathostomes, the jawed vertebrates. Sister groups hagfish and lamprey (cyclostomes) are jawless, lack paired appendages, and only possess median (dorsal, ventral), unpaired fins. Most of the information concerning the evolution of paired appendages comes from the fossil record. In recent years, the evolution of fin origins has become a constantly shifting landscape due to a surge of new fossil discoveries, re-descriptions, and significant changes in phylogenetic hypotheses. Here I will briefly discuss the

paleontological and developmental evidence surrounding theories of paired fin acquisition, which gives context to how paired fins and median fins relate to one another.

Median fins first appeared in the earliest vertebrates, which lack paired fins (e.g. *Haikouichthyes eracaicunensis* [530 Ma] (Zhang and Hou, 2004)). These vertebrates are characterized by a continuous median fin fold around the dorsal and ventral midlines of the body. The Median Fin Fold Hypothesis proposes that the separate median fins, namely the caudal, dorsal, and anal fins, arose through selective retention and reduction of the continuous median fin fold (Owen, 1849; Stewart, Bonilla, Ho, & Hale, 2019). This hypothesis was derived from the ontogenetic observation that many larval fish first develop a continuous median finfold (Mabee, Crotwell, Bird, & Burke, 2002; Stewart et al., 2019) and this has long informed transformational scenarios. However, the tissue layers that comprise the eventual median fins do not derive from the larval finfold itself; the thin finfold is invaded by paraxial mesoderm and neural crest that give rise to the fin rays (Lee, Thiery, & Carney, 2013; Smith, Hickman, Amanze, Lumsden, & Thorogood, 1994).

It was not until stem gnathostomes that evidence of paired pectoral fins emerged in the fossil record, ranging from ambiguous lateral paired "flaps" in anaspids [e.g. *Rhyncholepis* (Coates, 1994, 2003) and *Cowelepis ritchiei* (Blom, 2008)], to the well-developed, definitive lobed pectoral fins of the osteostracans (e.g. *Waengsjoeaspis*) that importantly, possessed endoskeletal elements (Adrain & Wilson, 1994; Coates, 1994, 2003; Scott & Wilson, 2012) (Figure 1.2). Pelvic fins in the fossil record were first seen in *Parayunnanolepis xitunensis* (413 Ma), an early placoderm and jawed vertebrate (Zhu, Yu, Choo, Wang, & Jia, 2012).

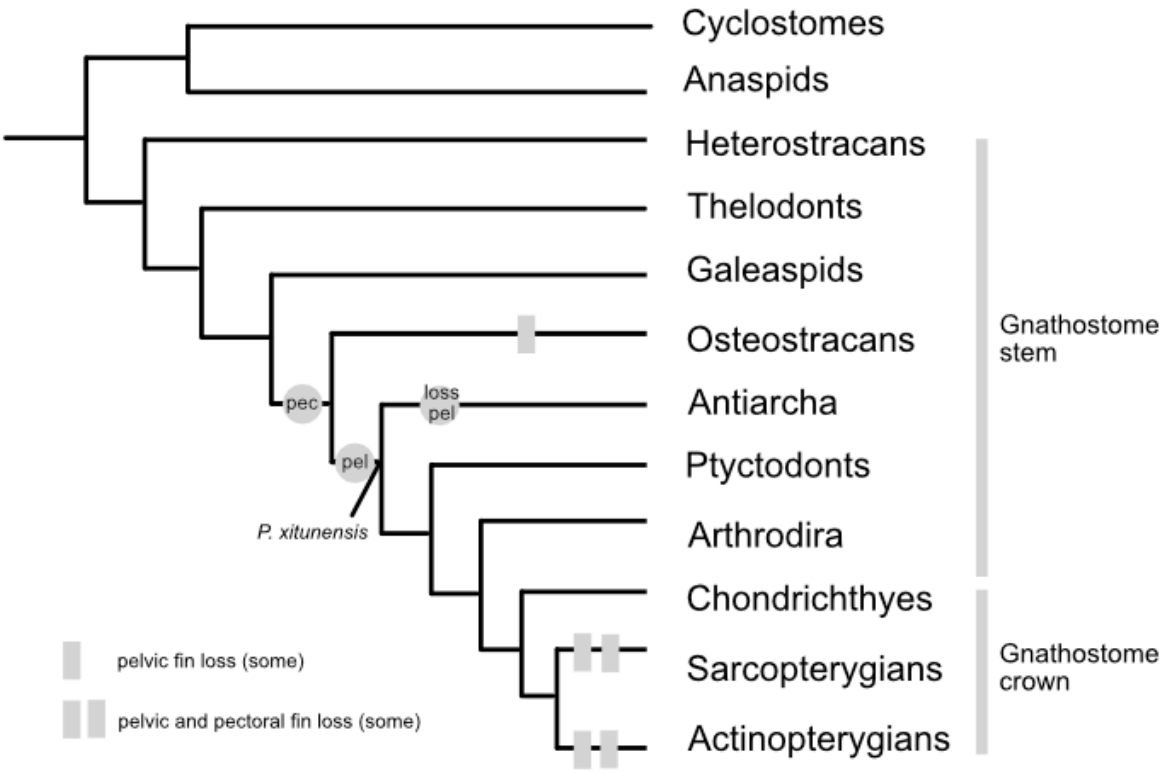

Figure 1.2 - Phylogeny of stem and crown gnathostomes from Miyashita et al. (2018) and proposed sequence of fin evolution.

Pec - Origin of pectoral fins (Coates, 2003) **Pel -** Origin of pelvic fins and jaws (Zhu et al. 2012) **Loss Pel -** Loss of pelvic fins in some antiarchs. Other possibilities are that pelvic fins did not arise until the common ancestor of ptyctodonts and living gnathostomes and that pelvic fins in *Parayunnalolepis* arose independently, or that antiarchs are paraphyletic.

Because median fins evolved first, hypotheses on how the paired appendages evolved often posit that the patterning for median fins was co-opted or transformed into paired fins. The "lateral fin fold" theory hypothesized that an ancestral vertebrate possessed longitudinal, bilateral ventral finfolds that connected with the continuous median finfold (Balfour, 1881; Mivart, 1879; Thacher, 1877a). In this scenario, the elongate lateral fin fold was reduced to the spatially

distinct pectoral and pelvic fins. However, it is limited in the scope of paleontological evidence available, as there is no clear fossil evidence of a specimen with lateral fin folds (although anaspids have been suggested) (Coates, 2003). Historically, fossils such as *Haikouichthys* and *Myllokumingia* that show pairs of long, ventral fins were cited as examples of such a hypothetical ancestor, but recent analyses suggest that without evidence of endoskeletal support, these structures are likely not homologous to the gnathostome paired fins. Furthermore, as the fossil record stands, pectoral fins appeared before pelvic fins, which does not support the idea that both pairs of fins emerged from the lateral fin fold simultaneously.

The gill-arch theory is a competing hypothesis that stems from Gegenbaur's Archipterygium and Owen's vertebrate archetype, the hypothetical primitive fin from the ancestor of jawed vertebrates (Gegenbauer, 1878; Gegenbaur, 1876). Gegenbauer proposed that the branchial arches (gill arches) of stem gnathostomes were transformed into the girdles and fin rays of the pectoral fin and the pelvic fin, with the pelvic fin being translocated posteriorly. This theory suffers from much of the same issues as does the lateral fin fold theory, in that there is no clear fossil evidence of an intermediate form, and that it appears that the pectoral fins were present first (Coates, 2003). Additionally, while the median and paired fins share similar developmental programs (Freitas, Zhang, & Cohn, 2006), lending support to the lateral fin fold theory, it is less apparent how gill arches and paired fins might share the same regulatory programs. Nevertheless, emerging research in skates is showing that gill arches and pectoral fins share an Shh-Fgf feedback loop mechanism for outgrowth, and respond similarly to patterning signals (retinoic acid, Shh) (Gillis, Dahn, & Shubin, 2009). Since the posterior gill arches in skate are derived from both neural crest and lateral plate mesoderm, Sleight and Gillis (2020)

argued that the gill arches and pectoral fins ancestrally arose from a common population of cells that could form either component. The contribution of the same type of tissue to different structures does not necessarily imply a transformational homology between the two structures, however, and the composition of the gill arches in other major lineages will be needed to be examined to ensure this is not merely a chondrichthyan feature.

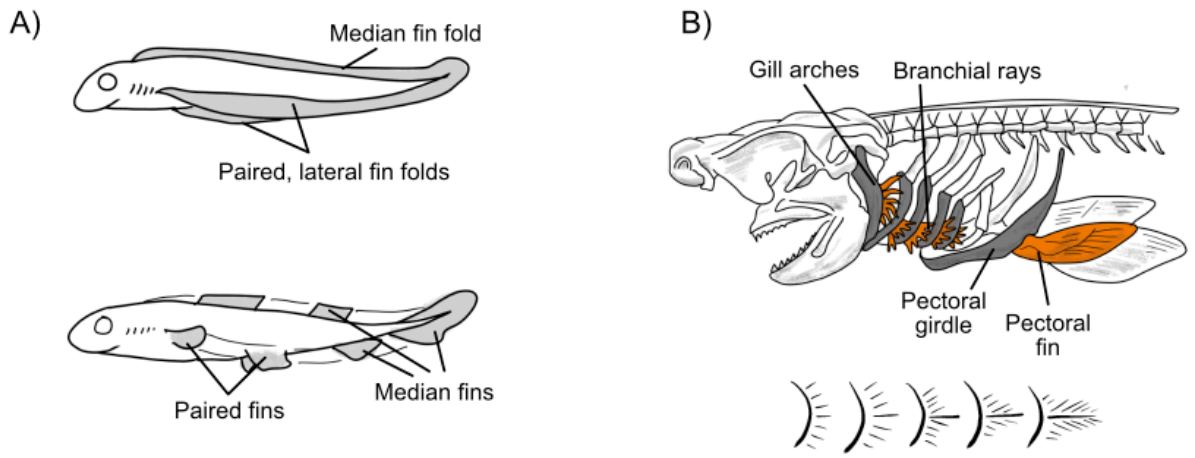

Figure 1.3 - Lateral fin fold and gill arch theories.

(A) Lateral fin fold theory – top illustrates a hypothetical ancestor with paired lateral fin folds, bottom illustrates the basal condition of gnathostomes. (B) Theoretical homologies between the gill arches/pectoral girdle and the brachial rays/pectoral fin from Gegenbaur's gill arch theory in a chondrichthyan. Transformational series below is from gill arch to pectoral fin. Redrawn from (Gegenbaur, 1876).

While pelvic fins were present in the common ancestor of all living gnathostomes, the timing of the origin of pelvic fins relative to the origin of the jaws is still under debate. Both characters are believed to have emerged before the base of the placoderms, an extinct group of jawed stem gnathostomes (Brazeau & Friedman, 2015) (Fig 2), if they are considered to be monophyletic. Prior to Zhu *et al.* (2012)'s re-description of *Parayunnanolepis xitunensis* (413

Ma), the earliest fossil evidence of pelvic fins was found in only a subset of placoderms (Coates, 2003; Trinajstic *et al.*, 2015), which present with unambiguous pelvic girdles and radials. This arrangement meant that pelvic fins did not appear until after the origin of jaws, as all placoderms are jawed. Zhu *et al.* (2012)'s discovery of pelvic girdles within *P. xitunensis,* an early member of the antiarchs, suggested that the appearance of pelvic girdles might have coincided with the origin of jaws instead of occurring afterwards. However, the absence of pelvic structures in all other antiarchs would imply that all other antiarchs secondarily lost pelvic fins, if the antiarchs are indeed a monophyletic group.

1.3 Development of the paired fins

1.3.1 Lateral plate mesoderm

The lateral plate mesoderm (LPM) is a versatile tissue layer that gives rise to multiple structures in gnathostomes. It is thought to form the paired fins in fish and the paired limbs in tetrapods (Ruvinsky & Gibson-Brown, 2000). Additionally, the LPM contributes to the formation of the heart, blood, kidneys, smooth muscle of the gut tube, and the visceral and parietal peritoneum, among other tissues (reviewed in Prummel, Nieuwenhuize, & Mosimann, 2020). The variety of structures and organs that result from LPM differentiation elevate this tissue layer into one of the most fascinating developmental systems in vertebrates.

The LPM derives its name from its location on the lateral edges of the vertebrate embryo after gastrulation is complete. Along the antero-posterior axis, the LPM is further regionalized into the anterior lateral plate mesoderm (ALPM) and the posterior lateral plate mesoderm

(PLPM) (Figure 1.4B). The ALPM contains cardiac precursors that will give rise to the secondary heart field, pharyngeal arches, and pericardial sac, whereas the PLPM is involved in the formation of other tissues such as limb and peritoneum (L. M. F. Mao, Boyle Anderson, & Ho, 2021; Stainier, Lee, & Fishman, 1993). Dorsoventrally, in chick and mouse, the LPM separates into two adjacent sheets, the somatic and the splanchnic layers of the lateral plate mesoderm (Funayama, Sato, Matsumoto, Ogura, & Takahashi, 1999; Meier, 1980) (Figure 1.4A). This splitting proceeds anteroposteriorly, and the split itself forms coelomic cavities known as the pleural cavities, the pericardial cavity, and the peritoneal cavity. The somatic mesoderm develops into the parietal peritoneum, a layer of mesothelium that lines the body wall and contributes to the limb buds. The splanchnic mesoderm becomes the visceral peritoneum, which lines the organs, and contains smooth muscle progenitors (Gays et al., 2017). In teleosts, the bilateral sheets of somatic and splanchnic mesoderm have yet to be observed. Instead, it appears that in zebrafish, these two tissue layers emerge from a common pool of lateral plate mesoderm cells and migrate in distinct streams towards their destinations (Gays et al., 2017; Prummel et al., 2022). For zebrafish PLPM, these cells migrate ventrally from the bilateral dorsal "stripes" underneath the epithelium and encase the yolk and developing gut tube (movements of the somatic mesoderm and splanchnic mesoderm, respectively).

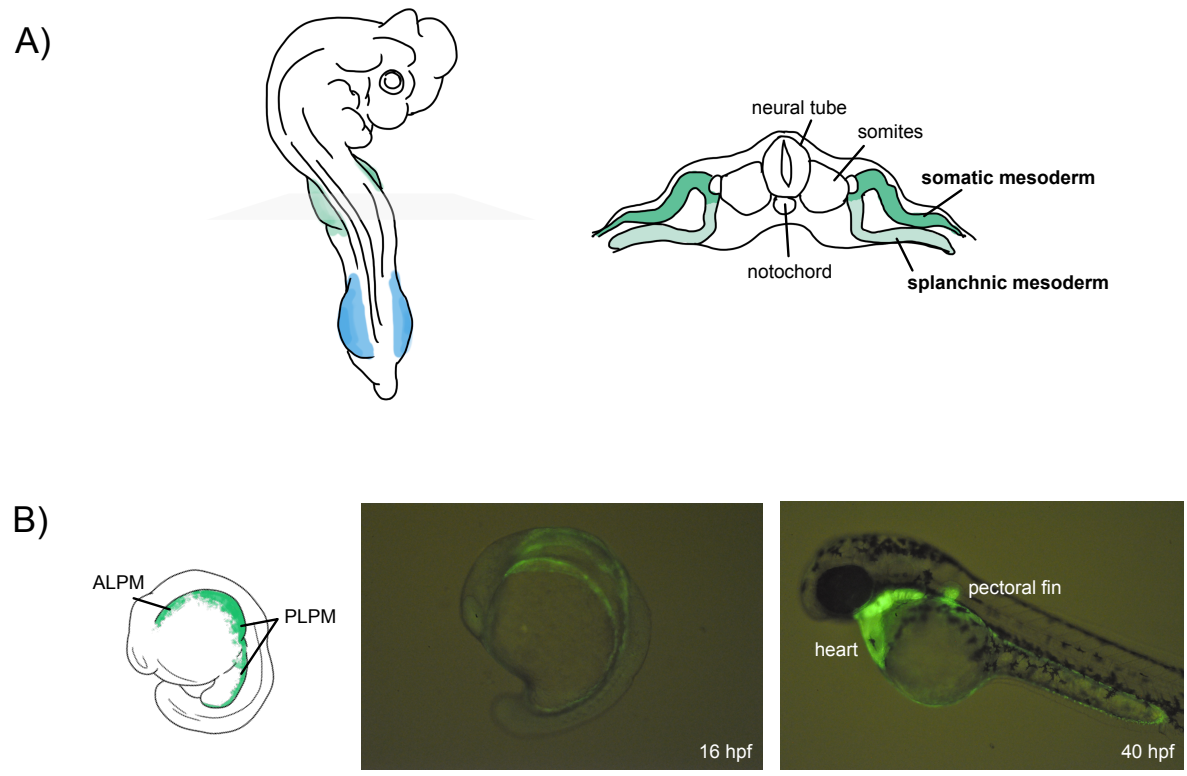

Figure 1.4 - Lateral plate mesoderm in chick and zebrafish.

(A) Chick embryo at limb bud stage with cross section at the forelimb bud level (green). Hindlimb buds in blue. The lateral plate mesoderm has split into two layers. The somatic mesoderm will give rise to the limb buds, and the splanchnic mesoderm will develop into the visceral peritoneum. (B) Zebrafish embryos at 16 hpf (left diagram, middle) and 40 hpf (right). Diagram depicts the distribution of LPM in the embryo, in green. Photos depict *Tg(hand2:EGFP),* a line that marks LPM+ cells. The zebrafish LPM is divided into the ALPM (anterior lateral plate mesoderm) that includes the future secondary heart field, and the PLPM (posterior lateral plate mesoderm) that forms other tissues such as limb and peritoneum. The LPM is undivided into separate somatic/splanchnic layers at 16 hpf and is located in bilateral dorsal stripes. At 40 hpf, the LPM contributes to the heart and pectoral fin, as well as more posterior structures.

In the forelimb in chick and mouse, an epithelial-to-mesenchymal transition (EMT) is associated with initiating limb bud formation (Gros & Tabin, 2014). The somatopleure (somatic mesoderm overlain with ectoderm) in the limb field immediately prior to the limb bud stage has been shown to be more epithelial than mesenchymal in nature, as it is characterized by epithelial molecular markers polarized to the apical end of the cells (Gros & Tabin, 2014). The authors show that limb field cells must undergo EMT for an ectodermal Fgf signal to be established and promote cell proliferation in the bud. Contrary to the idea that cell proliferation marks the onset of limb initiation, Gros and Tabin demonstrate that a mesenchymal population of cells must be generated at the outset. They finally propose that *TBX5* (a T-box transcription factor) and *FGF10* regulate the EMT process through a yet undescribed mechanism, as knockout *Tbx5-/-* and *Fgf10-/-* mice lack defined EMT characteristics in their limb fields. Indeed, previous experiments have shown that in the forelimb, *Tbx5* is necessary for initiation of the limb bud. In mouse and chick, the *Tbx5* conditional knockout lacks forelimbs, though a reduced bud briefly forms in chick (Agarwal et al., 2003; Rallis, 2003; Takeuchi, 2003) (Figure 1.6B).

In zebrafish, where Tbx5 has duplicated, loss of function of *tbx5a* produces fish without pectoral fins (Garrity, Childs and Fishman, 2002; Ahn *et al.*, 2002) (Figure 1.6B). Work from our lab has shown that *tbx5a* marks pectoral fin field cells and that a subset of these cells is activated by *tbx5a* to start expressing *fgf24*, which acts as a convergence cue for migratory *tbx5a*+ cells to form a fin bud (Q. Mao, Stinnett, & Ho, 2015) (Figure 1.5). In the absence of either *tbx5a* or *fgf24,* the cells in the limb field migrate laterally and fail to converge or form a fin bud (Draper, Stock, & Kimmel, 2003). *fgf24* appears to be zebrafish-specific, as it is not

involved in the induction pathway in mouse and chick (Mercader, 2007). Knockout of *fgf24* will produce zebrafish that are unable to form pectoral fin buds (Mao et al. 2015). Finally, research from our lab has shown that the role of *tbx5b* is to control the mediolateral extent of migration, whereas *tbx5a* primarily controls the anteroposterior convergence of the limb field (Boyle-Anderson, Mao, & Ho, 2022).

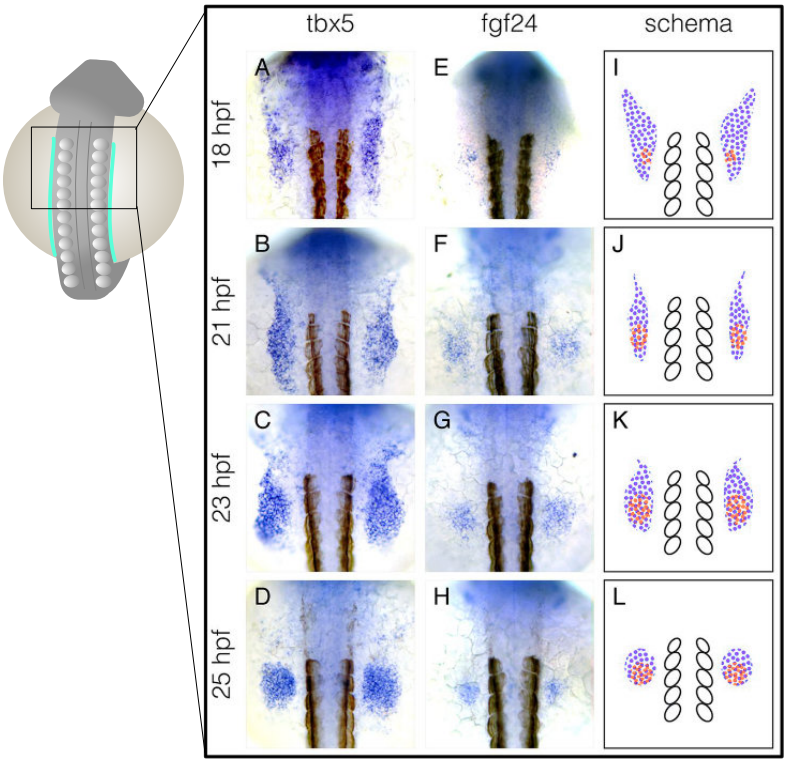

Figure 1.5 - Expression pattern of tbx5 and fgf24 during pectoral fin formation.
Dorsal view of embryos showing the fin field (marked by *tbx5a*) and the subset of cells expressing *fgf24*. The fin field coalesces into a fin bud with *fgf24* acting as a convergence cue. Modified from (Q. Mao et al., 2015).

In summary, in teleosts and tetrapods, it appears that a mesenchymal population of cells is responsible for limb bud initiation. In tetrapods, these mesenchymal cells are generated from localized EMT, whereas in zebrafish, these cells converge from an actively migrating lateral

plate mesoderm. I hypothesize the tetrapod condition is primitive to gnathostomes (see Chapter 5). *Tbx5* is indispensable for all species for the forelimb/pectoral fin to form, and *Tbx5* eventually activates *Fgf10* to promote outgrowth, with *fgf24* acting as an intermediate in zebrafish.

1.3.2 Pelvic fin and hindlimb development

There is strong consensus that the pelvic fins are serially homologous to the pectoral fins (Gegenbaur, 1876; Owen, 1849; I Ruvinsky & Gibson-Brown, 2000; Thacher, 1877b). Pectoral fins/forelimbs and pelvic fins/hindlimbs share many of the same developmental patterning mechanisms that assign anteropoterior and dorsoventral identity to the bud, and these similarities continue throughout fin/limb outgrowth (reviewed in Tanaka, 2016; Petit, Sears and Ahituv, 2017).

Tetrapod hindlimbs are characterized by EMT, and at the level of tissue development, follows a similar developmental trajectory to the forelimb (Gros & Tabin, 2014). There are key differences between hindlimb and actinopterygian pelvic fin development that make comparisons between the two more nuanced, despite their taxic homology. First, while paired appendage buds appear near simultaneously in tetrapod and chondrichthyan embryos, the pelvic fin buds in actinopterygians can develop weeks after the pectoral fin buds. For instance, in zebrafish, the pectoral fin buds are visible by 30 hours post fertilization (hpf), whereas the pelvic fins only appear after approximately 3 weeks post fertilization. Second, the position of the pelvic fins is

variable among different actinopterygian species, whereas its position is consistent at the trunk-tail boundary in tetrapods and chondrichthyans (to be discussed in more detail later).

Histologically, the initiation of the zebrafish pelvic fin is first seen as a condensation of mesenchymal cells, approximately a few cell layers thick, located ventrally between the hypaxial myotomes and the epithelium of the parietal peritoneum (Grandel & Schulte-Merker, 1998). The number of cells in the pelvic fin bud then increase, though it is not known whether this is caused by proliferation or migration of cells into the bud. An apical ectodermal fold then develops, and the mesenchyme subsequently differentiates into lepidotrichia and radials.

Similar but separate genetic networks control the initiation of forelimbs and hindlimbs. In the chick and mouse hindlimb, *Tbx4* (paralogous to *Tbx5*) is necessary for limb outgrowth, but not for bud initiation. Knockout of *Tbx4* lacks hindlimbs, though a smaller bud does form and then degenerate (Naiche & Papaioannou, 2007; Takeuchi, 2003). Don *et al.* (2016) showed that *tbx4* knockout zebrafish mutants will also form a pelvic fin bud, but the bud fails to form an apical ectodermal ridge (AER) and degenerates. This suggests that if pelvic fin development includes a fin field convergence factor, *tbx4* does not activate it (such as how *fgf24* is activated by *tbx5a* in the pectoral fin field) because fin buds still form in its absence.

Pitx1 (paired like homeodomain 1) is another gene that might be involved in pelvic fin bud convergence. While *Pitx1* is not necessary for bud initiation in mouse, as *Pitx1* knockouts will form small and deformed hindlimbs, the deletion of a *Pitx1*-specific enhancer and the concurrent absence of *Pitx1* expression appears to be responsible for pelvic loss in freshwater

sticklebacks (Chan et al., 2010; Cole, Tanaka, Prescott, & Tickle, 2003; Shapiro et al., 2004). It is worth considering whether *Pitx1* might act as a positional cue. In chick and mouse, *Pitx1* is expressed in the prospective hindlimb region before a limb bud forms (Lanctôt, Lamolet, & Drouin, 1997; Logan, Simon, & Tabin, 1998). *pitx1* is also expressed in the prospective pelvic region in marine sticklebacks, which will continue to develop pelvic spines, but not in the same region in freshwater stickleback, which do not develop pelvic spines (Shapiro et al. 2004). *Pitx1* might act as an upstream regulator of central hindlimb patterning genes. Studies in mouse show that *Pitx1* binds to *Tbx4* enhancer elements and to *HoxC10* and *HoxC11*, genes that mark the position of the hindlimb on the body axis (Infante, Park, Mihala, Kingsley, & Menke, 2013; Jain et al., 2018; Nemec, Jain, Sung, Pastinen, & Drouin, 2017). To date, there has been no description of the gene expression profile of *pitx1* expression in zebrafish that focuses on the prospective pelvic fin region in late stages.

After the limb bud is initiated, regardless of whether it is the forelimb or hindlimb, zebrafish, mouse, and chick employ *Fgf8* and *Fgf10* to establish the apical ectodermal ridge (AER) and maintain proliferation and outgrowth of the limb/fin bud (reviewed in Petit, Sears and Ahituv, 2017) (Figure 1.6A). A summary table of all the experiments mentioned in 1.3.2 and 1.3.3 can be found in Appendix B.

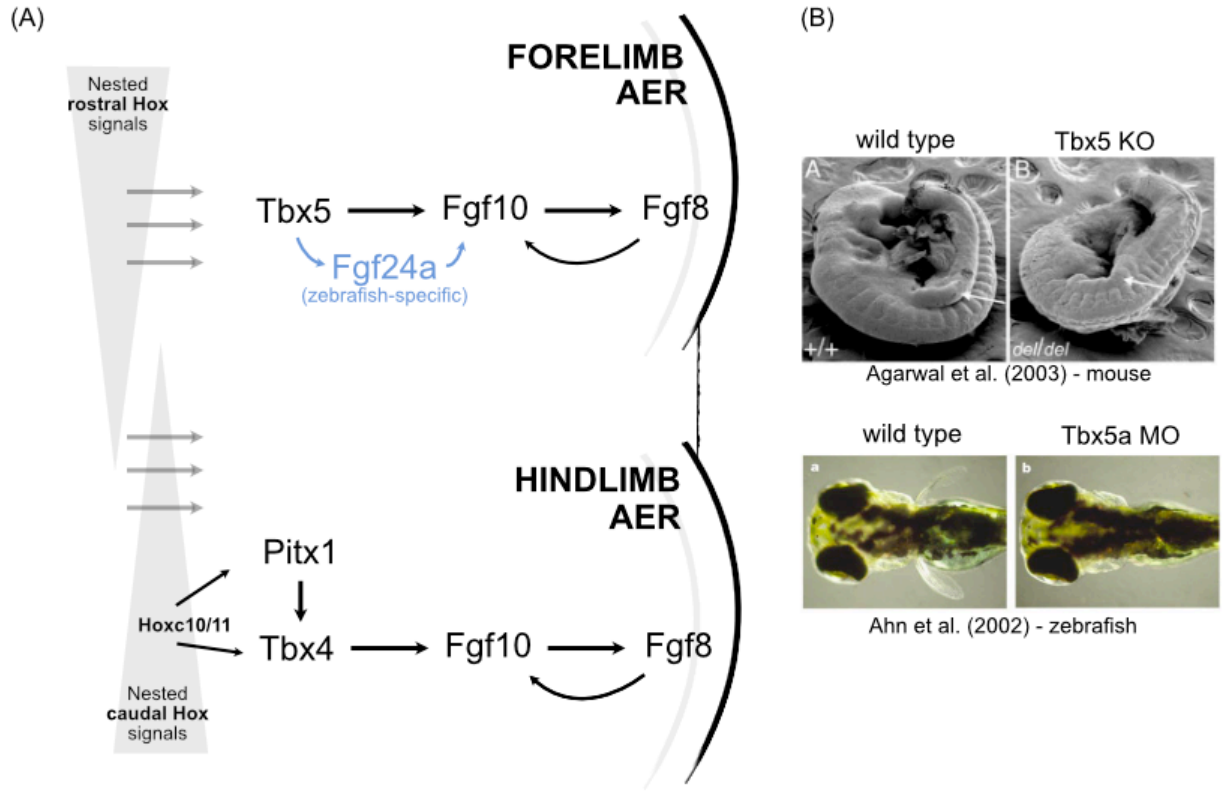

Figure 1.6 - Diagram of the forelimb and hindlimb initiation pathways.

(A) Nested Hox signals activate T-box genes, which then activate an Fgf cascade. (B) Phenotypes of *Tbx5* mutants in mouse and zebrafish. In mouse panels, the white arrows point to the forelimb region.

1.3.3 Forelimb and hindlimb positioning through Hox coding

In tetrapods, the positions of the forelimbs and hindlimbs are conserved with respect to landmarks on the vertebral column. The forelimbs are found at the cervical-thoracic boundary, and the hindlimbs at the lumbar-sacral boundary (Burke, Nelson, Morgan, & Tabin, 1995). This positioning is thought to be delineated by co-linear Hox patterning that activates the correct limb-forming signals and represses other identities (Minguillon et al. 2012; Nishimoto and

Logan 2016). In chick, rostral *HOX4* group genes actively bind to enhancers of *TBX5*, while signals from caudally-expressed *HOX8-10* are known to repress *TBX5* expression (Carolina Minguillon et al., 2012). It is proposed that this combination of Hox expression restricts *TBX5* expression to the appropriate anteroposterior levels to create the forelimb field. The genetic regulatory network that controls hindlimb positioning is less well-known, and is limited to the finding that *Hoxc9* is a transcriptional activator of *Pitx1*, thereby controlling hindlimb identity (Nishimoto and Logan 2016). However, there exist outstanding questions of what represses hindlimb identity in the forelimb field/interlimb regions, and of which other caudal Hox genes might activate hindlimb initiation.

1.3.4 Limb competent zones and revisiting the origin of paired fins

The ability for ectopic limbs to be induced in the interlimb zone has been well-known for several decades. Experiments in chick show that FGF-soaked beads implanted on the lateral flanks of these embryos can produce a forelimb or hindlimb bud, depending on the location of the bead (Cohn, Izpisúa-Belmonte, Abud, Heath, & Tickle, 1995; M. Tanaka et al., 2000). In zebrafish, application of an Fgf-soaked bead within the pectoral fin field can induce migration of cells into a fin bud, consistent with the idea that *fgf24* acts as a convergence cue (Q. Mao et al., 2015; M. Tanaka et al., 2000). However, it is not known whether Fgf-soaked beads implanted in the LPM posterior to the pectoral fin field would produce a pectoral or pelvic fin bud (or a phenotype in between), and whether the result would be timing-dependent is also untested.

Ectopic median fin buds can also be induced in the dorsal midlines of gnathostomes (chick, mouse, and zebrafish) (Abe, Ide, & Tamura, 2007; Tamura, Yonei-Tamura, & Belmonte, 1999; Yonei-Tamura et al., 2008). Because the median and paired fins in gnathostomes share many patterning mechanisms (e.g. Freitas, Zhang and Cohn, 2006), Yonei-Tamura *et al.* (2008) proposed that "competent stripes" - regions that could potentially produce fin outgrowths – were first expressed along the dorsal and ventral midline along the AP axis, then acquired in paired lateral stripes to form the paired fins. Shared competency to respond to an FGF cue is markedly different from the claim that competent stripes were acquired in the lateral plate of early vertebrates, however.

Tbx4 and *Tbx5*, genes that are critical for fin/limb formation and may provide clues for how the pelvic fin evolved in the ancestral gnathostome. Based on phylogenetic analyses of T-box genes in vertebrates (Agulnik et al., 1996; I. Ruvinsky, Oates, Silver, & Ho, 2000; Ilya Ruvinsky, Silver, & Gibson-Brown, 2000)), Ruvinsky and Gibson-Brown (2000) proposed that *Tbx4* and *Tbx5* initially existed as an ancestral cluster (*Tbx4/5*) in jawless vertebrates and subsequently duplicated into *Tbx4* and *Tbx5* around the stem gnathostome base. The authors suggest two situations. The gene duplication might have arisen first - *Tbx4* and *Tbx5* would have been redundantly co-expressed in the first paired, presumably pectoral, fins and the pelvic fins would have arisen through novel *Tbx4* expression in the posterior flank. Or, the fin duplication arose first - the ancestral *Tbx4/5* would have been expressed in the pectoral fins and then was re-expressed in the posterior flank to produce pelvic fins; only after pelvic fins arose would the *Tbx4/5* cluster have duplicated. Regardless of the scenario, Ruvinsky and Gibson-Brown (2000)

speculate that "modifier genes," such as *Pitx1,* acquired new functions to specify pelvic fin/hindlimb identity as separate from pectoral fin/forelimb.

Paired fins might have arisen through new interactions between developmental tissue layers. In gnathostomes, the paired fins/limbs derive from the somatopleure and signaling between the somatic mesoderm and ectoderm is essential for the outgrowth of the limb bud (e.g. the apical ectodermal ridge promoting cell proliferation in the mesodermal mesenchyme). The somatopleure appears to be a gnathostome novelty – in lampreys, the lateral plate mesoderm is sequestered around the endodermal gut tube by a layer of body wall muscle (dermomyotome), thus never making contact with the ectoderm (Tulenko et al., 2013). Stem gnathostomes such as osteostracans, the group with the first endoskeletally-supported pectoral fins, may have been among the first to develop a somatopleure if this were the case. The dermomyotome eventually will invade into the somatopleure after the limb bud is developed to form the limb musculature and hypaxial musculature. These new interactions between the dermomyotome and the lateral plate mesoderm has been termed the "lateral somitic frontier" (Burke & Nowicki, 2003; Julie L Nowicki, Takimoto, & Burke, 2003; Shearman & Burke, 2009). This theory predicts that by entering a different developmental environment (the lateral plate mesoderm), tissues from the dermomyotome become patterned uniquely relative to any uninvested cells, allowing for independent evolution of invested and uninvested cells. While it is certainly true that developmental context is critical for cell fate decisions, the lateral somitic frontier argument lacks focus on the decision point between lateral plate investment and lack thereof.

1.4 Evolution of the paired and median fins in actinopterygians

1.4.1 Phylogenetic overview of the actinopterygians

The actinopterygians are one of the most speciose vertebrate groups with over 31,000 extant species and over 370 extant families (Rabosky et al., 2018) (Figure 1.7). Within this group, the Neopterygii separate out the Acipenseriformes and the Polypteriformes from the rest of the Actinopterygii. Later, Neopterygii is split into the Holostean clade (Amiiformes + Lepisosteiformes) and Teleostei, which comprise 96% of all extant fishes (Nelson, Grande, & Wilson, 2006). Teleosts are characterized by at least 27 anatomical synapomorphies (De Pinna, 1996) and are famous for undergoing a round of whole genome duplication (Amores et al., 1998; Hurley, Hale, & Prince, 2005; Prince, Joly, Ekker, Development, & 1998, 1998; Taylor, Van de Peer, Braasch, & Meyer, 2001). They are also a source of interest for numerous specializations in their jaws, feeding mechanisms, and tail supports (Lauder, 1982, 1989). Within teleosts, branches from Elopocephali (tarpons, eels), Osteoglossomorpha (mooneyes, elephantfishes), and Otomorpha (herrings, catfish, carp, minnows, zebrafish, etc) first emerge, and the rest of the teleosts belong to a subclade named Euteleostei. The earliest diverging branches of Euteleostei include small groups such as Lepidogalaxiiformes (salamanderfish), Protocanthopterygii (pike, salmon), and Stomiatii (smelt), which are sister to the larger clade, Neoteleostei.

Neoteleostei have been long accepted as a monophyletic group based on both morphological and molecular data, though its anatomical synapomorphies are few (Betancur-R et al., 2017; Johnson, 1992; Nelson, Schultze, & Wilson, 2010; Rabosky et al., 2018). The presence

of a retractor dorsalis muscle, a small pharyngeal jaw muscle, is the most prominent synapomorphy (D. Rosen, 1973). The Neoteleostei node is sandwiched between the Acanthomorphan node (the spiny-rayed fish, where over 50% of the species diversity in Actinopterygii lie) and the Teleostean node, which has earned it little recognition. Indeed, Nelson et al. (2006) declines to "provide formal rank" for Neoteleostei in his survey of global fishes.

Within Neoteleostei, there first exist a few small lineages (Ateleopodidae, Aulopiformes, Myctophiformes) which lurk in the deep-water realm, but the rest of Neoteleostei is characterized by the massively speciose Acanthomorpha. Acanthomorphans, as their name suggests, ancestrally share the presence of anterior fin rays in the dorsal fin that have been modified into defensive spines. Acanthomorphans enjoy the widest variation in body shapes among the actinopterygians, occupying morphospaces with differing body depths and lengths, feeding apparatuses, and of course, a wide variety of fin configurations (Friedman et al., 2020; Ghezelayagh et al., 2021; Larouche et al., 2018; Price et al., 2015).

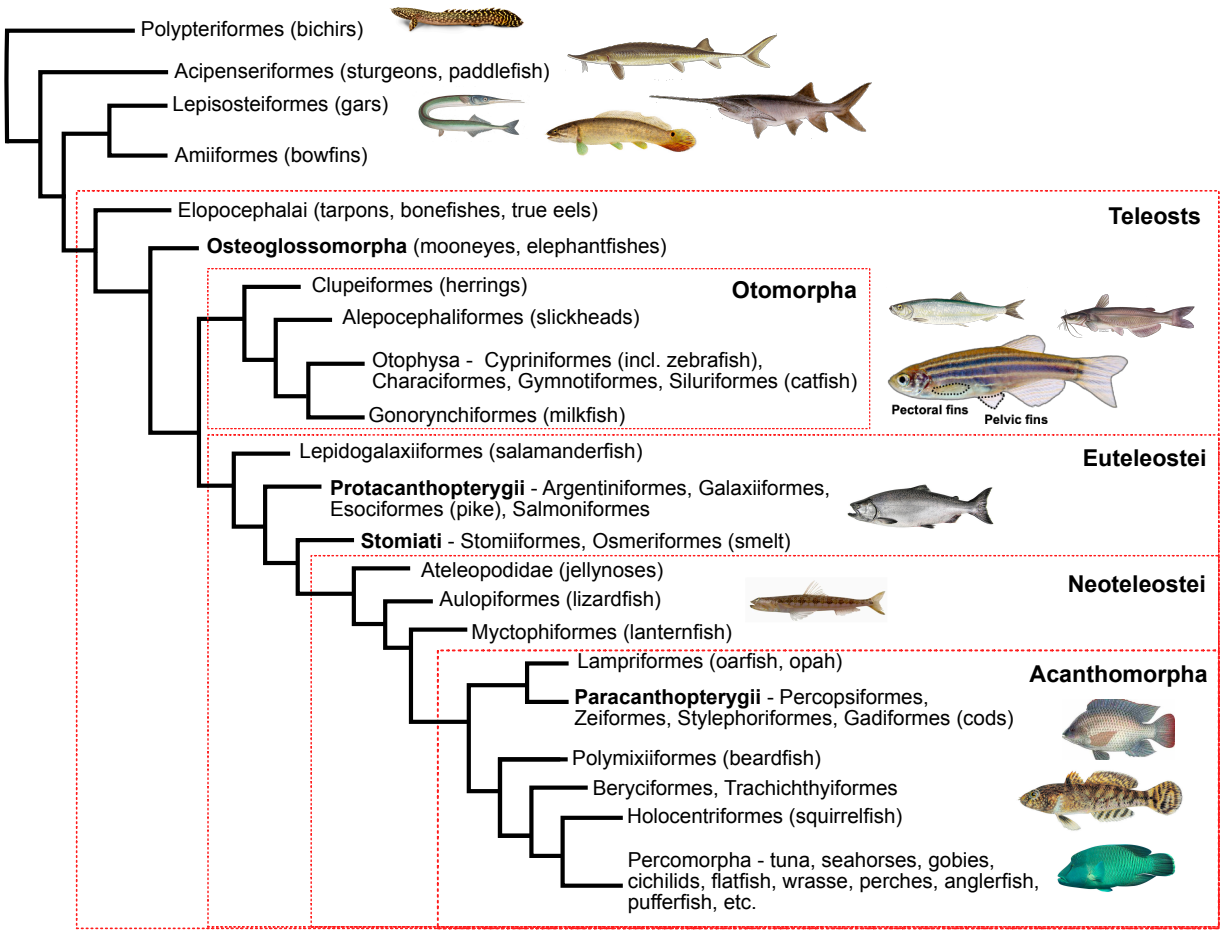

Figure 1.7 - Phylogeny of extant Actinopterygii with major groups outlined.

1.4.2 Timing of actinopterygian diversification and corresponding fossil evidence

Resolving the actinopterygian phylogeny is the last major challenge in resolving the vertebrate tree of life. New methods and tools have been recently applied to work towards resolving issues of fossil placement, morphological and molecular conflict, and long stems. Lack of clarity surrounding the timing of the origin of important clades and the inability to assign fossil species to stems are persistent issues that hinder the interpretation of macroevolutionary patterns, as seen in Chapter 2. For example, molecular phylogenies estimate that the teleost

crown originates in the Permian/Carboniferous (307-283 Ma although with substantially large confidence intervals, Betancur-R et al. 2017; Near et al. 2012) although the first crown teleost, *Elopsomolos*, is from the late Jurassic (Tithonian, 150-145 Ma) (Arratia, 2000; Sallan, 2014). These first fossils in the teleost crown represent a hard minimum (youngest possible age). The disparity between the molecular estimate and the maximumly known fossil evidence creates uncertainty in aligning major innovations at nodes to environmental events. Additionally, an extensive assortment of fossil actinopterygians have not been assigned to stems of extant lineages and instead are grouped in the wastebasket taxon of 'paleoniscids.' This prevents fossil data from being used to time-calibrate deeper nodes and illuminate any stepwise progressions of trait evolution when there are abrupt transitions in morphological forms, e.g. fin positional shifts.

1.4.3 Variation in actinopterygian fin presence/absence and morphologies

Given the wide variety of environments and niches that actinopterygians inhabit, it follows that fin morphology and positioning is richly varied as well. The pectoral and pelvic fins have been frequently lost (26 orders for pelvic, 8 orders for pectoral) and more than 13 orders have subdivided their dorsal fin (Larouche, Zelditch, & Cloutier, 2017). An adipose fin, which is a novel median fin between the dorsal and caudal fin, is a fleshy and large fin that has also been independently acquired in multiple lineages (Larouche et al., 2017; Stewart et al., 2014). As mentioned previously, the positioning of pectoral, pelvic, and dorsal fins is also widely variable, details of which will be explored in the next chapter.

Pelvic fins have been modified repeatedly to suit novel functions in fish, likely because their hydrodynamic function is less important than that of the other fins (Harris, 1938). Memorable examples of unique pelvic fins include the Lophiiform frogfish and batfish, which have modified their pectoral and pelvic fins into stout, pseudo-digited pudgy appendages used for walking on the benthic substrate (Dickson & Pierce, 2018; Pietsch & Grobecker, 1987). Mudskippers similarly use their beefy paired fins for terrestrial locomotion (Kawano & Blob, 2013). Other pelvic fins have been specialized into suction disks for station holding (e.g. lumpfishes, snailfishes, gobies) or even copulatory organs (e.g. phallosthetids) (reviewed in Yamanoue, Setiamarga, and Matsuura 2010). (Figure 1.8)

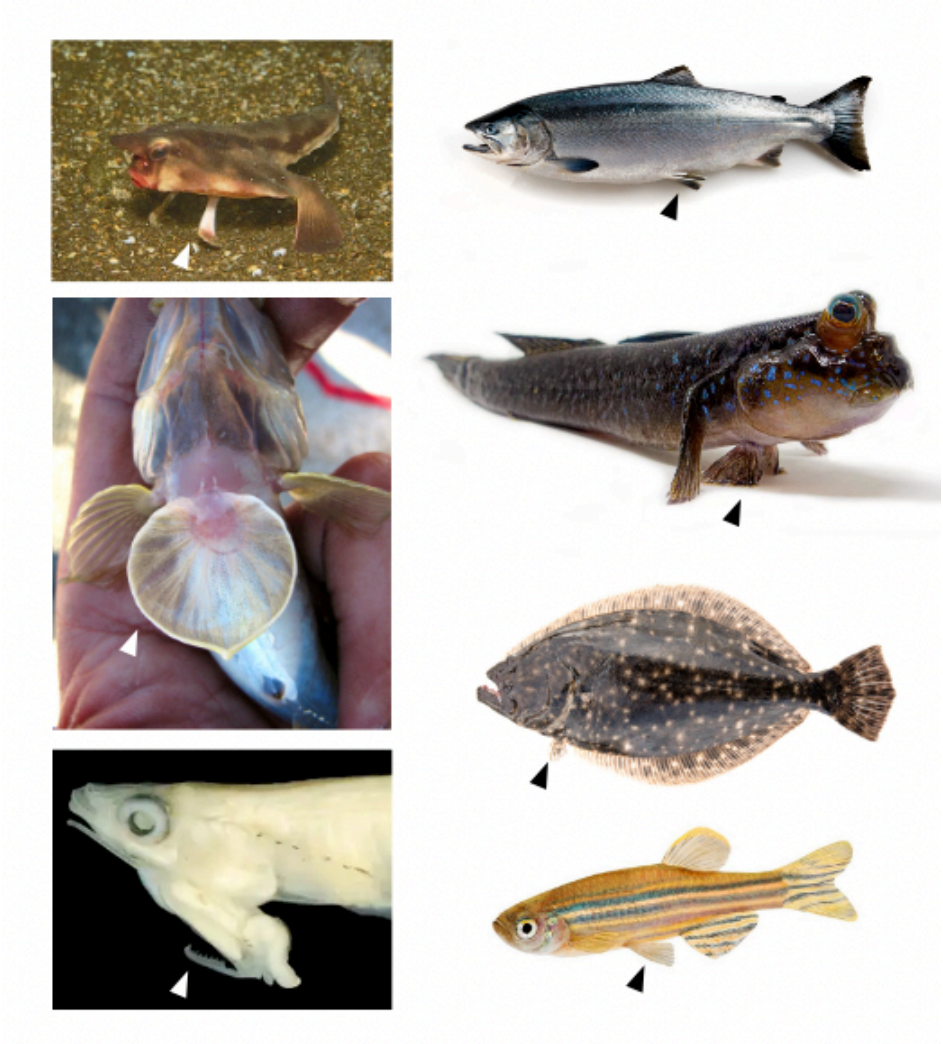

Figure 1.8 - Magnificent diversity of pelvic fin positions and structures.

From top to bottom for each column – red-lipped batfish, goby, priapiumfish, salmon, mudskipper, flounder, zebrafish. Black and white arrowheads point to the pelvic fins. (Alaska Seafood Marketing Institute, 2022; Brittanica, n.d.; Fishbio, 2014; Hutchings Museum Institute, 2022; NC DEQ, n.d.; Shibukawa, Tran, Loi, & Tran, 2012; Sloan Kettering Institute, 2019)

1.4.4 Variation in actinopterygian fin configurations

As mentioned in the Overview and expanded upon later in Chapter 2, a cursory glance at the fin placements in actinopterygians reveals that they are immensely variable. This has not gone unnoticed – Rosen (1982) noted that earlier lineages of actinopterygians possessed more ventral pectoral fins and more posterior pelvic fins, grading to later lineages where there were more dorsally-located pectoral fins and more rostral pelvic fins. However, the precise timing and phylogenetic patterns of these fin shifts have not been described, and the extent of linkage between these two paired fins has not been quantified.

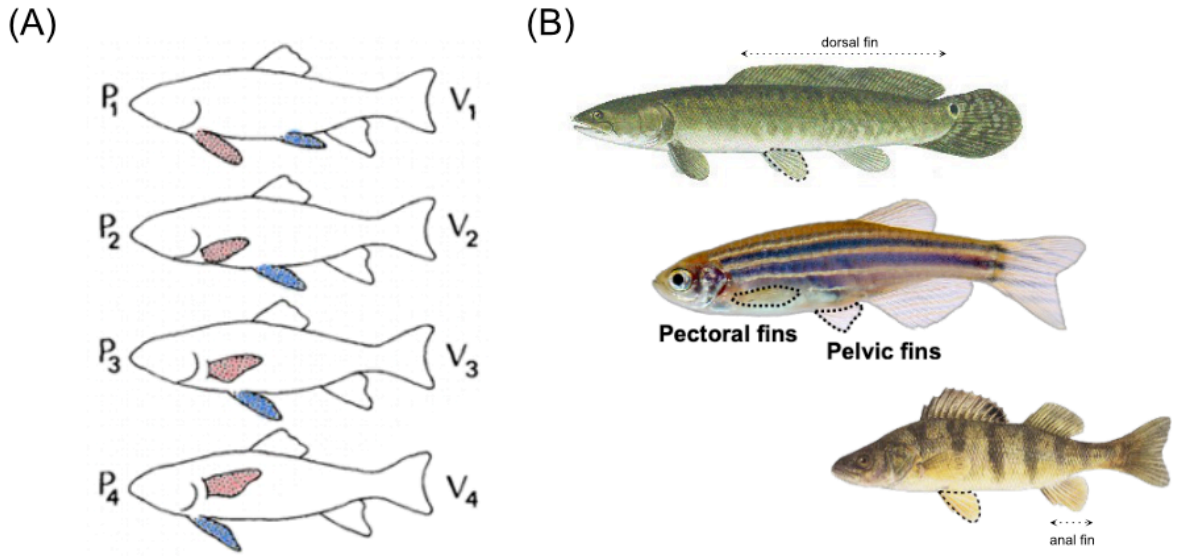

Figure 1.9 - Variation in positions of the paired fins.

A) States of paired fin positions according to Rosen (1982), color-coded here with pectoral fins in red and pelvic fins in blue. P1-P4 are pectoral states, V1-V4 are pelvic states. (B) Examples of positions of pelvic fins (dotted outline) and dorsal and anal fins.

Mabee et al. (2002) noted as well that the dorsal and anal fins were observed to be more in register in fossil actinopterygians. Throughout phylogeny, the anterior and posterior limits of the dorsal fin are extremely fluid, starting anywhere along the trunk. Correspondingly, the total length of the dorsal fin can also be extremely variable. The anterior limit of the anal fin is bound by the anus, but since the anus can shift along the body axis, the anal fin can begin quite close to the head (e.g. flatfish, some laterally compressed fish). The anal fin typically ends at the level of the caudal peduncle.

1.5 Comparative pelvic fin development in actinopterygians

Naturally, it is compelling to uncover the developmental changes that might have underpinned the ability to shift the pelvic fin positions in actinopterygians. Compared to tetrapod limb development, however, the body of work for pelvic fin development in even a model organism such as zebrafish is limited. The pectoral fin field was not well-mapped out until recently (Boyle-Anderson et al., 2022; Q. Mao et al., 2015), and a map for the zebrafish pelvic fin field does not exist – these unanswered questions motivate Ch.3 and Ch.4 of this thesis.

Murata et al. (2010) began to probe at the extent of the pelvic fin field in zebrafish by using DiI injections into the lateral plate mesoderm. The underlying question they addressed was the conflict between the pelvic fin developing at somite level 8-9, and the fact that the anterior limit of Hoxc10, a hindlimb marker, is at somite 13-14. The authors injected DiI at various anteroposterior levels of the LPM at the 16 hpf stage, prior to the yolk extension being formed, in order to trace the movements of the dyed LPM. They found that DiI injected at the somite 13-

14 level resulted in coverage of half the yolk extension by 30 hpf, and sequestering of the DiI at the somite 7 level by the 7 dpf stage (Murata et al., 2010). With these results, the authors posit that allometric growth – as in the somites grow faster posteriorly (trunk-tail protrusion) than does the yolk extension – is responsible for the difference in position from the time period of injection to observation. This is a reasonable conclusion – for instance, the somitic level of the anus changes from somite level 18 to somite level 13-14 between the stages they assayed – but tying these results to the pelvic fin is trickier. Unfortunately, a severe drawback of DiI in rapidly dividing tissue is that its fluorescence diminishes by the time that the pelvic fin forms, 3 weeks later, calling into question whether LPM at somite level 7 was really contributing to the future pelvic fin.

Nevertheless, similar DiI labeling experiments on other actinopterygian species have revealed that the timing of pelvic fin initiation relative to LPM migration varies. In Nile Tilapia (*Oreochromis niloticus*) which produces pelvic fins at a comparatively early 9 dpf, the LPM has not finished migrating ventrally before the bud is produced (Kaneko, Nakatani, Fujimura, & Tanaka, 2014; Murata et al., 2010). In contrast, in medaka (*Oryzias latipes*), the LPM will enclose the body wall a few developmental stages before the pelvic fin bud forms (Kaneko et al., 2014). While the findings from the above studies characterizes the DiI labeled cells as "actively migrating," it is difficult to discern whether these cells are moving as part of the LPM enclosing the yolk ball, or charting an independent path.

1.6 Overview of the thesis

The question of how different actinopterygian species have altered the position of something as fundamental as their paired appendages merges themes of evolutionary constraint, changes to developmental timing as a means of evolution, and untangling cell fate/specification in potentially set-aside cells. In Chapter 2, I will characterize the macroevolutionary patterns of fin configuration in actinopterygians. I show that there is no correlation between pectoral and pelvic fin position until Neoteleostei, where I also recover evidence of a shift in adaptive optima for the paired fins. Here, pelvic fins shift to becoming more rostrally-located, and pectoral fins shift to becoming more dorsally-located. Additionally, I demonstrate that there is a persistent alignment of the anterior limits of the pelvic and dorsal fins, suggesting an unexpected linkage between a median and a paired fin. This linkage appears to have emerged from an ancestral dorsal-anal fin alignment, which we have shown in fossil species.

Chapters 3 and 4 will focus on the development of the pelvic fin and the cells that contribute to the fin field. This careful lineage tracing will be critical for future comparative studies in other species. In Chapter 3, I will show that the pelvic fin field arises from LPM deriving as potentially wide as somite levels 6-11, although most of the cells most likely derive from somite levels 7-10. I have generated a new transgenic line *Tg(hsp:cre-ert2)* that will be widely useful for other lineage tracing studies in the zebrafish field. In Chapter 4, I will test whether specification of the pelvic fin precursor cells is early (embryonic, coincident with pectoral fin specification) or later (larval, around 3 weeks). I use *in situ* hybridizations of known

hindlimb specification genes to show that while these genes are not expressed early, they do appear in the body wall and myotomal septae prior to pelvic fin initiation in larvae. The posterior limits of the hindlimb specification genes in the body wall mirror the precursor pelvic fin field derived from the lineage tracing experiments.

In Chapter 5, I will present a hypothetical model of pelvic fin initiation throughout the 3 weeks of development until pelvic fin stage. I will speculate on how pelvic fin positional lability might have been achieved in actinopterygians compared to sarcopterygians and chondrichthyans. Finally, I will outline future directions and areas of particular interest for this research program.

Chapter 2 - MACROEVOLUTIONARY PATTERNS OF FIN CONFIGURATIONS IN ACTINOPTERYGIAN FISH

2.1 PREFACE

This chapter would not have been possible without the efforts of Elisabeth Incardona (University of Chicago ‘22), who performed much of the data collection, spearheaded the fossil taxon sampling, and conducted the reef analysis herself. Her independent analysis on characters of the pelvic girdle in relation to the pectoral girdle can be found in her senior thesis. I would also like to thank Dr. Samantha Price and Dr. Olivier Larouche for providing the photographs of the species and the reef dataset. Finally, thank you to my committee chair, Dr. Graham Slater, for providing the scripts for the phyloEM and ratematrix analyses, and for feedback on the writing.

2.2 ABSTRACT

Jawed vertebrate paired appendage locations are highly conserved – forelimbs/pectoral fins are ventral, and hindlimbs/pelvic fins are usually present at the posterior of the trunk, near the anus. In contrast, among actinopterygian fishes, pelvic fin position along the anteroposterior axis varies immensely across species, in some cases even forming rostrally to the pectoral fins. Furthermore, it has been posited that such rostral shifts of the pelvic fins are accompanied by a dorsal shift of pectoral fin position. We have investigated whether coordinated shifts in paired fin position necessarily occur in tandem, thus testing the hypothesis that these fin relocations represent an evolutionary constraint or bias.

Surveying 300 actinopterygian families, we searched for a macroevolutionary signal, but our data reject the presence of a correlation ($p=0.08$) between pectoral and pelvic fin positions along antero-posterior and dorso-ventral axes. We next looked for shifts in adaptive optima and found that the optimum of both traits shift concurrently at the base of Neotelostei, a group within Teleostei. These twin adaptive peaks therefore create an illusory correlation (i.e. Felsenstein's "Worst Case Scenario"). We expanded our analysis to explore median fins (a previously proposed module) and found that although there is no correlation between dorsal and anal fin anterior limits, the anterior limits of the dorsal and pelvic fins are consistently in register.

To conclude, the positions of teleost pelvic and pectoral fins (classic serial homologues) are less tightly coupled than previously thought, but the extent to which this is a specialized condition for gnathostomes remains undetermined.

2.3 INTRODUCTION

Tinkering with body plans requires a delicate balance between transformational change and fitness. Such alterations must overcome the impacts of canalization and developmental and functional integration with other systems (Peter & Davidson, 2011; Siegal & Bergman, 2002; Waddington, 1942). Additionally, whether changes are gradual or rapid may reflect the underlying architecture of the evolutionary landscape (Carroll, 2001; Gould & Eldredge, 1972; Theißen, 2009). Actinopterygians, or the ray-finned fish, are renowned for their magnificent diversity in forms seen among this group of over 30,000 species. Variable fin configurations of

both median and paired fins are in part responsible for generating these highly disparate forms. These appendages are fundamental to the gnathostome body plan, and the positioning of these appendages is critical for defining the overall shape and function of the organism.

For sarcopterygians and chondrichthyans, the positions of the paired fins: hindlimbs/pelvic fins and the forelimbs/pectoral fins, are highly conserved. The hindlimbs/pelvic fins are customarily stationed at the posterior of the trunk near the anus, and the forelimbs/pectoral fins appear ventrally, near the head-trunk boundary. There are two major exceptions where the forelimbs/pectoral fins are positioned dorsally – in iniopterygians, an extinct clade of chondrichthyans, and in birds, where the attachment of the humerus to the coracoid is near the dorsum of the trunk. Otherwise, unless the limbs are absent or extremely specialized, it is rare for the positioning of the paired limbs/fins to vary.

In contrast, among the actinopterygian fishes, the position of pelvic fins along the anteroposterior axis varies immensely across species, frequently emerging even rostral to the pectoral fins (Figure 2.1A). Actinopterygian pectoral fins can also be quite variable in position, ranging anywhere from the ventral side (e.g. catfish), to the mid-flank (e.g. wrasse), to near the dorsum (e.g. flying fish). It has been observed by numerous authors (Alexander, 1974; D. E. Rosen, 1982; Tanaka, 2011) that later diverging actinopterygian clades tend to have more rostral pelvic fins, whereas the earliest diverging clades (e.g. Chondrostei, Holostei, early teleosts) have posteriorly positioned pelvic fins nearer to the anus, which is the condition in sarcopterygian and chondrichthyan outgroups. Acanthomorpha, or the spiny-rayed fishes, a clade that contains around 60% of extant actinopterygian diversity (Nelson, Grande, & Wilson, 2006), have been

repeatedly identified as a later-diverging clade exhibiting rostrally-positioned pelvic fins (Alexander, 1974; D. E. Rosen, 1982; Tanaka, 2011). Included in this group are the Percomorpha, or perch-like fish, the largest clade within Acanthomorpha. The presence of a spiny anterior division of the dorsal fin relative to soft rays in the posterior of the fin is a key synapomorphy of Acanthomorpha. Alexander (1974) noted that in the Acanthomorpha, their pectoral fins are often "set high on the body" and that level stopping, or braking without considerable roll/pitch/yaw, is "only achieved by a balance between the forces on the pectoral and pelvic fins" and that this balance is "only possible because of the position of the pelvic fins… immediately ventral to the pectoral fins" (p. 45). Essentially, he suggested that rostral shifts of the pelvic fin are often accompanied by a dorsal shift of pectoral fin position due to a possible biomechanical constraint or bias in the actinopterygian body plan.

The actinopterygian paired fin system therefore offers a compelling opportunity to discover whether constraints result in restricted avenues for body plan evolution. Aside from the biomechanical constraints as suggested by Alexander (1974), one might imagine that there could be further biomechanical constraints due to conflicts in position (e.g. ventral pectoral fins and rostral pelvic fins may collide during swimming) and developmental constraints (perhaps mediated by distribution of lateral plate mesoderm, the tissue layer that gives rise to the paired limbs). We test for a macroevolutionary signature of these constraints by asking whether the pectoral and pelvic fin positions are correlated in actinopterygians; that is, are posteriorly-located pelvic fins always accompanied by ventrally-located pectoral fins, and are rostrally-located pelvic fins always accompanied by dorsally-located pectoral fins? (Figure 2.1B).

To address these questions, we first characterized patterns in pectoral and pelvic fin position across ~600 species of actinopterygians by plotting species across a paired fin morphospace, and then testing for correlation between pectoral and pelvic fin position. Contrary to our expectations, we found that there was no correlation in paired fin position across all actinopterygians. We next looked for shifts in adaptive optima for these two traits and found that a major shift occurred at the base of Neoteleostei. This suggests that a significant release in paired fin positional constraints occurred at this node; we were also able to identify a correlation between paired fin positions specifically within Neotelostei. In addition, we tested for positional symmetry between the median fins and paired fins and found a surprising linkage between the pelvic fins and the anterior limit of the dorsal fin.

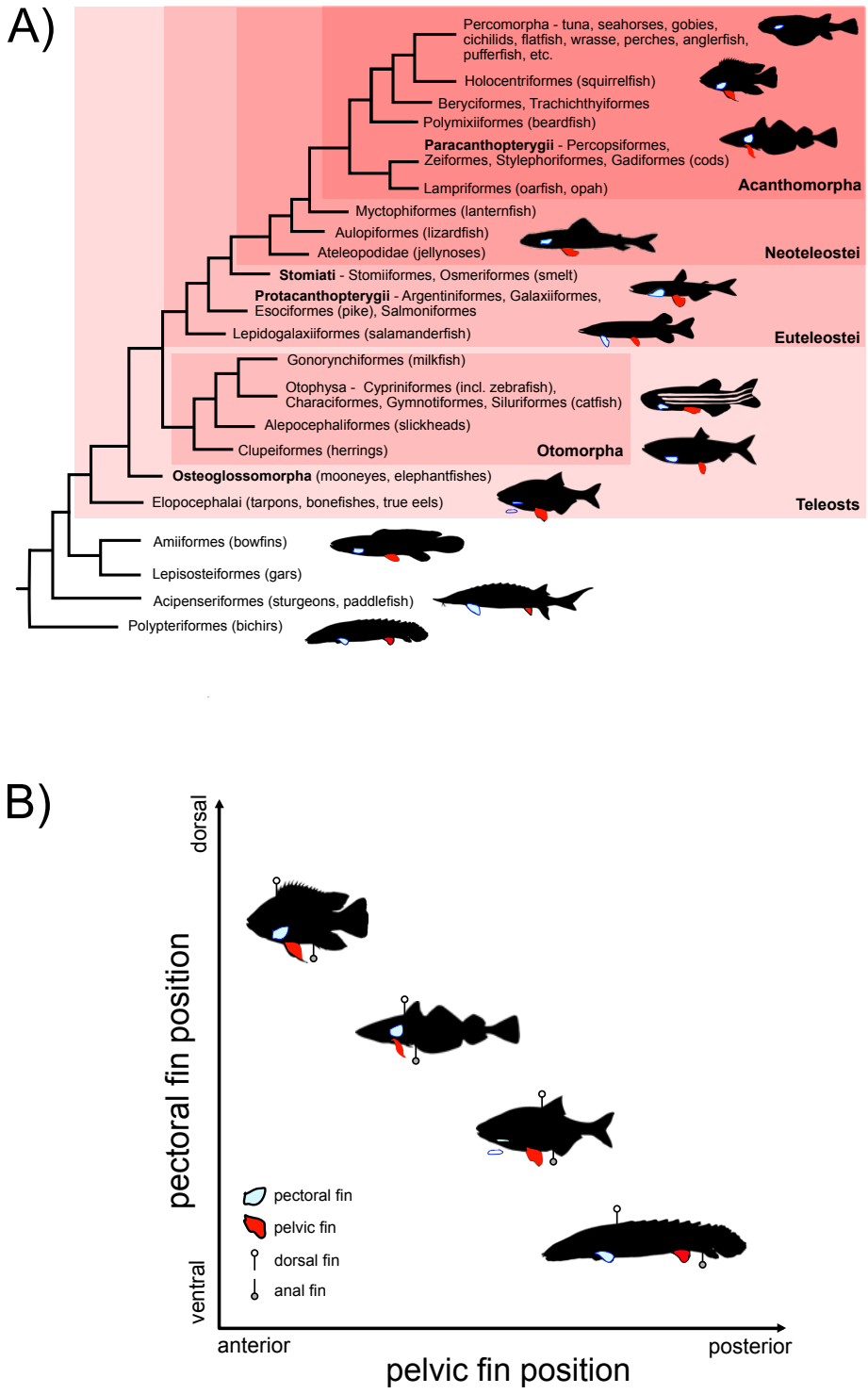

Figure 2.1 - Actinopterygian phylogeny and the paired fin morphospace.

(A) Actinopterygian phylogeny with major groups annotated. (B) Pectoral vs. Pelvic fin position morphospace, with species falling along a hypothetical correlation line.

2.4 METHODS AND MATERIALS

2.4.1 Taxon sampling

We sampled extant 598 species which represented 301 (61%) actinopterygian families (Rabosky et al., 2018). To ensure maximum phylogenetic coverage, we selected 2 phylogenetically distant species per family using the phylogeny from Rabosky et al. (2018). Specimen photographs were primarily derived from the dataset of Price et al. (2019) and online museum databases (Appendix A). A total of 78 fossil species were drawn from the Paleozoic (n=45) and Mesozoic (n=33) eras, and their reconstructions were mostly used to mitigate for compression/distortion (Appendix A).

2.4.2 Quantifying fin position

To capture the positions of the features that we measured, we employed the geomorph package (Adams & Otárola-Castillo, 2013) to record the X and Y coordinates of each feature. Although geomorph is meant to collect landmarks for geometric morphometrics, we only used it here for collecting absolute positions on an image. In total, 21 points were collected, with 12 of them used for quantifying each fin's position. The descriptions of the relevant features can be found in Figure 2.2.

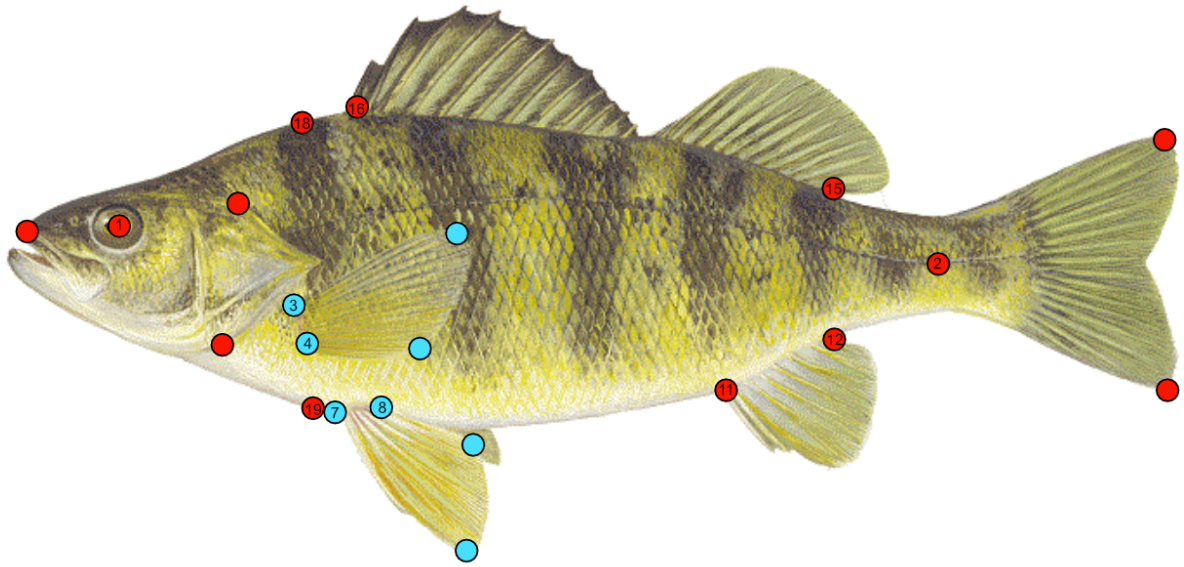

Figure 2.2 - Features collected on each specimen

Bright blue for features related to the paired fins, red for everything else. Numbered features were used for quantification of fin positions. (1) Orbit (2) Caudal peduncle (3) Dorsal-most insertion of pectoral fin (4) Ventral-most insertion of pectoral fin (7) Anterior-most insertion of pelvic fin (8) Posterior-most insertion of pelvic fin (11) Anterior-most insertion of anal fin (12) Posterior-most insertion of anal fin (15) Posterior-most insertion of dorsal fin (16) Anterior-most insertion of dorsal fin (18) Dorsal-most point of body at AP level of pectoral fin (19) Ventral-most point of body at AP level of pectoral fin.

Pectoral fin position was quantified as the ratio of the height of the pectoral fin insertion compared to the overall body depth at the anteroposterior level of the pectoral fin (Figure 2.3A). Pelvic fin position was quantified as the ratio of the length from the orbit to the anteroposterior level of the pelvic fin compared to the overall length from the orbit to the peduncle (Figure 2.3B). This method accounts for any tilt in the photographs and normalizes for body size. The positional symmetry between the dorsal and pelvic fins and the dorsal and anal fins was calculated by quantifying the angle formed between the anteroposterior body axis (as formed by

points marked by the eye and peduncle) and the line connecting the fins (as formed by their landmarks) (Figure 2.3C, 2.3D).

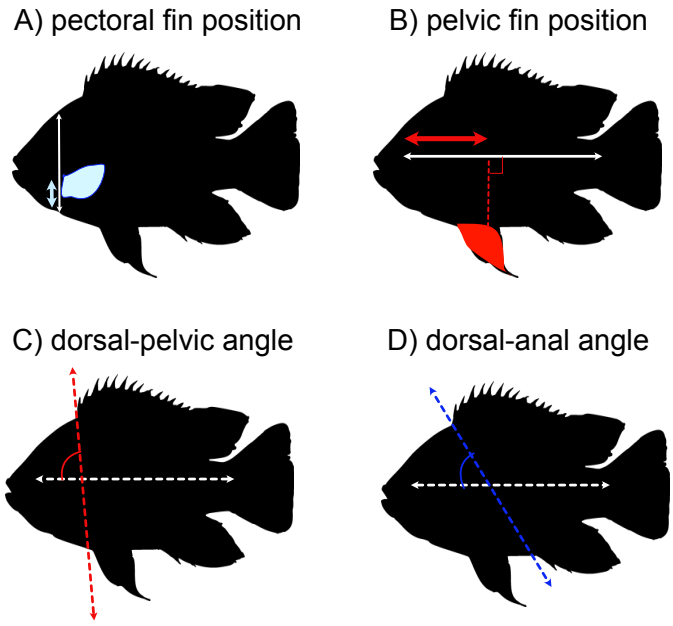

Figure 2.3 - Quantifying fin positions

Schematics of how (A) pectoral fin position, (B) pelvic fin position, (C) dorsal-pelvic angle, and (D) dorsal-anal angle were quantified.

To verify that our two-species-per-family sample was sufficiently representative (of each family), we undertook a proof-of-concept study using Acanthuridae (surgeonfish) with the dataset from George & Westneat (2021). We measured pectoral and pelvic fin position for ~40 species of surgeonfish and compared the range of these values to the 2-species average for Acanthuridae derived from the main photo dataset, which does not include the George & Westneat (2021) dataset (Supplemental Figure S2.1). Since the range of the 40-species Acanthuridae set was well-constrained and was close to the 2-species average, we felt confident

that 2-species sampling was sufficient to represent each family for measuring pectoral and pelvic fin position.

For paired fin analyses, we excluded families where pectoral or pelvic fins were absent. For median fin analysis, we excluded families where the pelvic fins, dorsal fin, or anal fin were absent. This kept the pool of species used in analyses consistent when comparing fin positions. For quality control, we double-checked the species for which their positional values fell outside 2 standard deviations from the overall mean and re-landmarked if needed.

Reef-association data was sourced from Larouche et al. (2020), who had collected and quality-checked reef-association information from FishBase (Froese and Pauly 2020, Boettiger et al. 2012). Reef-association is defined as "spending all or part of life among or around rocks in 0-100 m depth" in the database.

2.4.3 Visualization using phylomorphospace and contMap

We visualized the position of each family on a two-dimensional phylomorphospace consisting of pelvic fin position on one axis, and pectoral fin position on the other axis. Plotting was done with the function *phylomorphospace* in the phytools package (Revell 2012); the input tree was derived from the fishtree package (Chang et al. 2019, Rabosky et al. 2018).

The history of each character trait (pelvic position, pectoral position, dorsal/pelvic angle, dorsal/anal angle) for each family were visualized through the *contmap* function in phytools. For

each fin, the range of values was rescaled to (0,1) to ensure consistency in values. Calculations of ancestral states at nodes was performed using the *fastAnc()* function from phytools, which estimates the maximum likelihood ancestral state at each node.

2.4.4 Regime detection using PhyloEM

To differentiate whether shifts in paired fin positions occurred repeatedly in multiple clades or was the result of one ancestral shift, we used the package phyloEM to detect shifts, or breakpoints in trait optima on trees (Bastide et al. 2018). PhyloEM uses an Expectation Maximization approach to identify the location and magnitude of shifts, according to an Ornstein Uhlenbeck model of phenotypic evolution. It also incorporates data on potential covariation between traits when it infers evolutionary rate matrices, generating a rate matrix that simultaneously models both traits (at the expense of assuming that all traits have the same speed α.

2.4.5 Testing for correlation between pectoral and pelvic fin position

We tested whether there exists a correlation between pectoral and pelvic fin position with phylogenetic least squares (PGLS) and the ratematrix package (Caetano and Harmon 2017a, b), which is based on Bayesian Markov Chain Monte Carlo (MCMC) methods. For PGLS, we used the *gls* function in the nlme package (Pinheiro et al. 2021) to test whether pelvic position was driving pectoral position (pectoral ~ pelvic). We tested both a Brownian model correlation structure and a model where lambda was estimated, then compared Akaike Information Criterion (AIC) scores for all models.

To evaluate whether the evolutionary correlations between pelvic and pectoral fin position evolve across actinopterygian phylogeny, we fitted single and multi-regime models using the Ratematrix package. Ratematrix estimates the posterior distributions for rates of trait evolution and the amount of evolutionary correlation among these traits. The estimation can be divided into different regimes to see if there are significant differences in how traits evolve relative to each other in different groups. Here, we estimated the evolutionary rate matrices for the total dataset, and then again with the dataset divided into Neoteleost and non-Neoteleost regimes (based on results from the PhyloEM method). For all runs, we defined the priors as such: the root priors were given a normal distribution centered around the arithmetic mean of the trait and a standard deviation of 2 times the original standard deviation. The priors around the density of standard deviations was given a log-normal prior. Each chain was run for 1 million generations each with the first 10% of each run discarded as burn-in and every 100^{th} sample was retained. The chains were merged and checked for convergence by verifying that the scale reduction factor was 1 and estimated sample size (ESS) was greater than 200.

To compare regimes against each other, we used the methods from Ovaskainen et al. (2008) to test whether the rate matrices were significantly different from each other. The output of Ovaskainen's test reports the probability that the rate matrices are significantly different from one another (see Slater and Friscia 2019 for a more detailed explanation). We then compared the eccentricities and rate of dispersion into multivariate space of the rate matrices using their relative standard deviation of eigenvalues (rSDE) (Haber, 2016; Van Valen, 1974). Eccentricity (ranging from 0 to 1) characterizes the extent of the regime's dispersion into multivariate space

and is therefore indicative of how strongly each trait constrains the other. Scripts for these tests were taken from Slater and Friscia (2019).

2.4.6 Testing for reef-associated correlations to fin positions

The *phylANOVA()* function from the phytools package (Revell, 2012) was used to test whether the mean paired fin positions in reef-associated and non-reef-associated fish were significantly different. This function also corrected for phylogenetic relatedness using the Rabosky et al. (2018) backbone. The null distribution was simulated against a Brownian motion model 1000 times.

2.5 RESULTS

2.5.1 Phylomorphospace of paired fin positions

To explore the distribution of paired fin configurations in Actinopterygii, we plotted each family on a pectoral/pelvic fin phylomorphospace and color-coded each family by its membership in different large clades (Figure 2.4). We found a striking difference in morphospace occupation between Acanthomorpha, Neoteleostei, and other groups. Whereas most groups – even speciose ones such as Otomorpha – remained clustered within the lower right quadrant of the morphospace (posteriorly located pelvic fin, ventrally located pectoral fin), Acanthomorpha/Neoteleosts are mostly centered in an area indicating a rostrally shifted pelvic fin, and dorsally shifted pectoral fin. This striking visual difference in mean positioning of

Neoteleosts in contrast to the rest of actinopterygians strongly corroborated the breakpoint recovered in the phyloEM analysis, described next.

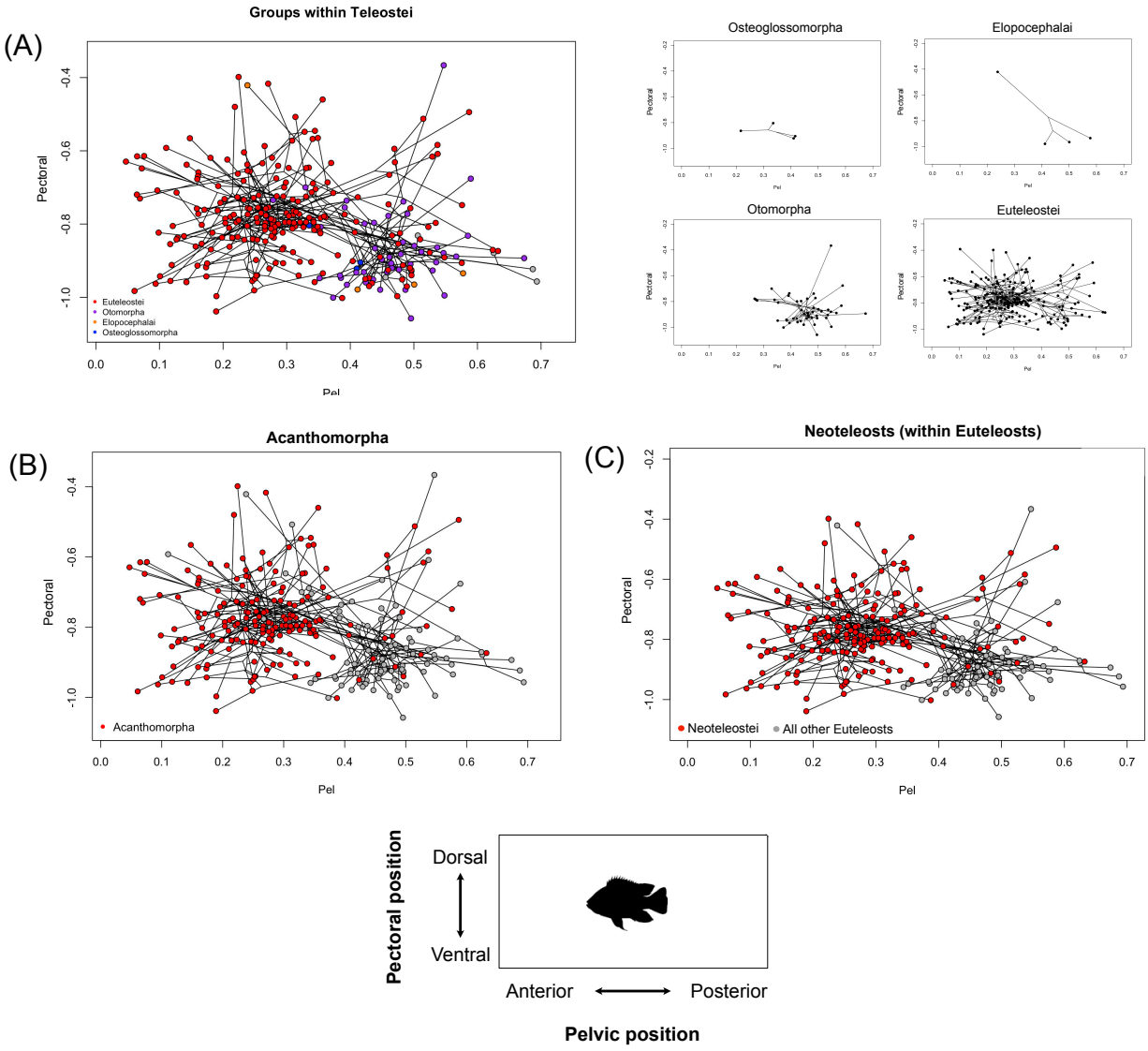

Figure 2.4 - Phylomorphospace occupation of the major clades within Actinopterygii.

Phylomorphospace occupation of the major clades within Actinopterygii. (A) Groups within Teleostei, left panel. Right panels are of smaller groups, shown alone. (B) Acanthomorphs (red) against all other actinopterygians (gray). (C) Neoteleosts (red) against all other Euteleosts (gray). Bottom panel to help interpret axes. See Figure 2.1 for tree reference.

2.5.2 Shifts in adaptive optima in pectoral and pelvic fin position

We estimated that there are 7 shifts in pelvic and pectoral fin position in the actinopterygian phylogeny (Figure 2.5, Supplementary Figure S2.2). Two shifts towards a more rostral pelvic fin/more dorsal pectoral fin were found in non-Neoteleosts : one in Halosauridae (halosaurs, eel-shaped deep-sea fish) and the other in Gasteropelecidae (hatchetfish). Of note, we found that one major shift towards a more rostral pelvic fin and a more dorsal pectoral fin occurred at the base of Neoteleostei. Within Neoteleostei, a reversal towards a more posterior pelvic fin/ventral pectoral fin was found in Cyprinodontiformes (toothcarps), and a reversal towards a more posterior pelvic fin was found in Beloniformes (needlefish and relatives), which kept their pectoral fins high. In the dorsoventrally flattened clade Lophiidae (goosefish), we also found evidence of a shift – Lophiidae pectoral fins were extremely ventrally-located and its pelvic fins were quite anterior. Finally, in Pleuronectiformes, a clade of flatfish, the pelvic fins were in a jugular position.

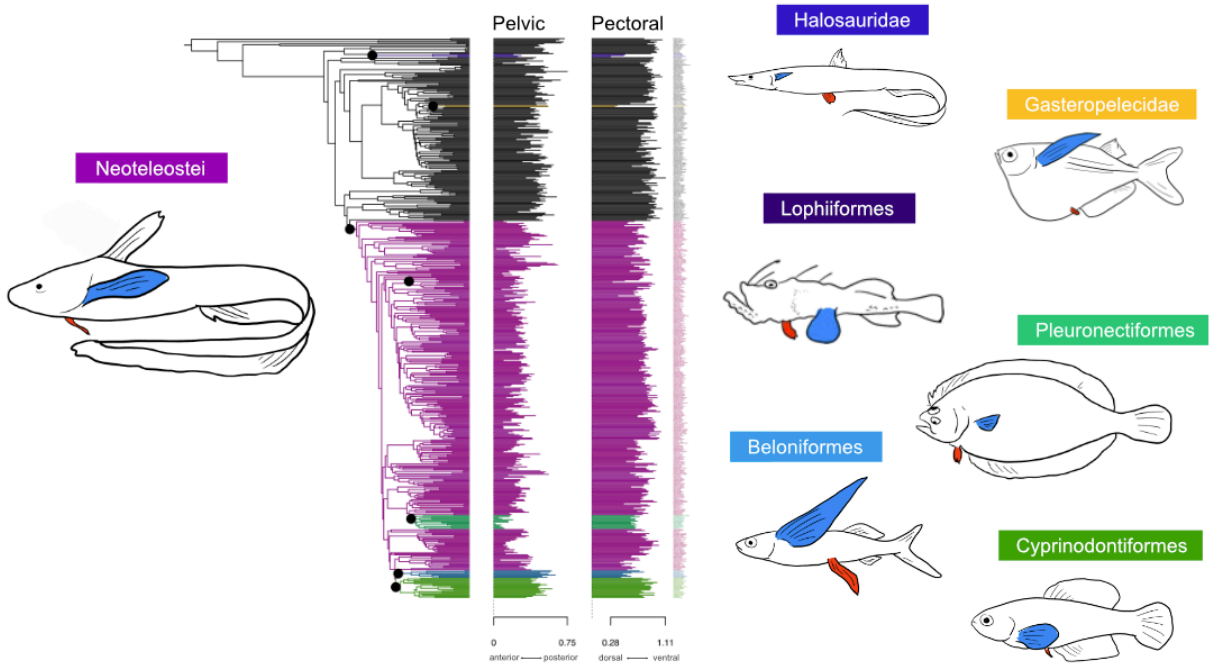

Figure 2.5 - PhyloEM results for pectoral and pelvic fin shifts.

PhyloEM results, with black dots showing the shifts in adaptive optima on the phylogeny. Halosauridae (indigo), Gasteropelecidae (yellow), Lophiiformes (dark violet), Pleuronectiformes (seafoam green), Beloniformes (blue), Cyprinodontiformes (green). Neoteleostei (purple). Pectoral fins (blue) and pelvic fins (red) are shown on representative fish.

2.5.3 Correlation between paired fin positions seen only in Neoteleosts

We initially found little support for a correlation between pectoral and pelvic fin position in actinopterygians. We first visually explored the data (Figure 2.6) using the contMap function and discovered that there was no consistent pattern – neither negative nor positive correlation – when there were shifts in either fin's position on the actinopterygian phylogeny. Additionally, we noticed a shift in both pelvic and pectoral fin position at the base of Neoteleostei, corroborating the results found using the phyloEM methodology.

Using RateMatrix, we reject the presence of a correlation in the total dataset (p=0.97). We further subsetted the data into Neoteleosts and Non-Neoteleosts regimes to investigate whether either of these might individually show a correlation. The Non-Neoteleost subset still shows no correlation (p=0.12), but the Neoteleost does show a significant negative correlation between pectoral and pelvic fin position (p=0.03). Given that we found that these two groups occupy different areas of the pectoral/pelvic fin morphospace and are demarcated by a regime shift, we next asked whether there are fundamental differences in the evolution of these traits between these two groups.

	p	r
Entire dataset	0.97	-0.08
Non-Neoteleosts only	0.12	-0.08
Neoteleosts only	**0.03**	-0.06

Table 2.1 - Testing for correlation between pectoral and pelvic fin position using RateMatrix
Only Neoteleosts show a correlation between pectoral and pelvic fin position.

	P(Ψd(A,B) > 0)	PP(rSDE)	PP(disp)
Neoteleost vs. Non-Neoteleost	0.03	0.90	0.98

Table 2.2 - Pairwise comparisons between the 2x2 R matrices of Neoteleosts and Non-Neoteleosts.

Pairwise comparisons between the 2x2 R matrices of Neoteleosts and Non-Neoteleosts. P(Ψd(A,B) > 0 represents the probability that the matrices represent different distributions. PP(rSDE) represents the probability that Neoteleosts have a higher eccentricity than Non-Neoteleosts. PP(disp) is the probability that Neoteleosts are evolving at a higher rate of multivariate dispersion.

To test whether the evolutionary rate matrices R in Neoteleosts and Non-Neoteleosts can be differentiated from one another, we employed Ovaskanien et al.'s (2008) test and found that they represent different distributions ($P(\Psi d(A,B) > 0) = 0.03$) (Table 2.1).

We found that the R-matrices of Non-Neoteleosts (rSDE = 0.24) are significantly more eccentric (Posterior Probability [PP] = 0.90) than that of Neoteleosts (rSDE = 0.10) (Table 2.2). Visualization of these matrices (Figure 2.7) shows that non-Neoteleosts not only show a higher eccentricity, but that their principal vectors are oriented in the direction of pectoral fin position, suggesting that they diversify predominantly on the pectoral fin axis (Figure 2.7). In comparison, the lower eccentricity of the Neoteleosts are suggestive that they can evolve more freely in the direction of either pectoral or pelvic fin position. Finally, the rate of multivariate dispersion for Neoteleosts is greater than Non-Neoteleosts (PP = 0.98), indicating that Neoteleosts are evolving into different areas of the morphospace at a significantly higher rate than Non-Neoteleosts (Table 2.2).

In summary, we found that the nature of the correlation between pectoral and pelvic fin position is fundamentally different between Non-Neoteleosts and Neoteleosts, and that this is likely due to a release from constraints in pelvic fin position evident in Non-Neoteleosts.

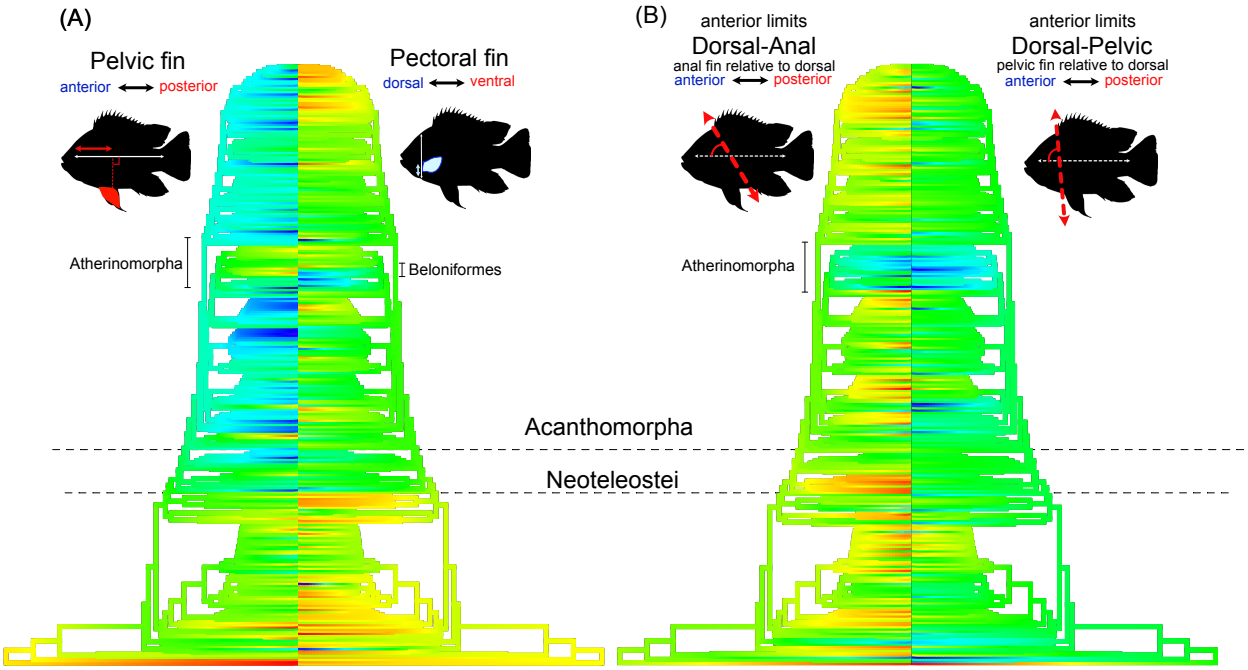

Figure 2.6 - ContMap of fin positions.

(A) ContMap of pelvic fin vs. pectoral fin position, showing little correlation between the two traits. Warmer colors = more posterior pelvic, more ventral pectoral. (B) ContMap of the anterior limits of the dorsal-anal and dorsal-pelvic fin symmetry, showing both no correlation and no major transitions. Warmer colors = anal fin is more posterior relative to dorsal fin, pelvic fin is more posterior relative to dorsal fin.

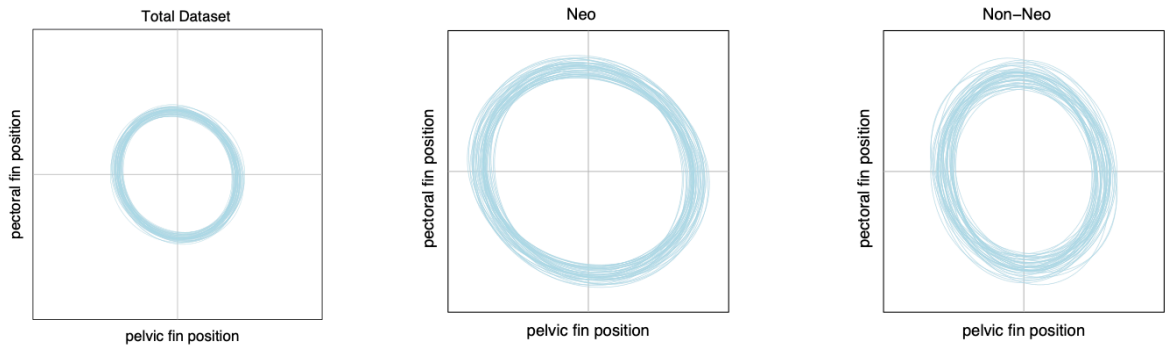

Figure 2.7 - 2x2 Rate Matrices

2x2 rate matrices showing the evolutionary covariances between pectoral fin position and pelvic fin position in the (A) total dataset (B) Neoteleosts only (C) Non-Neoteleosts only. The eccentricity of the ellipses are indicative of correlation (more eccentric = more correlated); we do not find much eccentricity in the total dataset or Non-Neoteleosts. The vertical orientation of the Non-Neoteleost ellipse suggests that Non-Neoteleosts can evolve more freely along the pectoral fin axis than the pelvic fin axis.

2.5.4 Paleozoic and Mesozoic fossil actinopterygians are constrained in the pelvic/pectoral morphospace

To investigate whether fossil species encompassed the same range of phenotypes as extant species, we projected extinct actinopterygian species into our pectoral/pelvic morphospace. Fossil species (n=71) from the Paleozoic and Mesozoic cluster distinctly in the ventral pectoral/posterior pelvic fin area of the morphospace, overlapping with Non-Neoteleosts. Outstandingly notable exceptions to the cluster include *Dorypterus,* an anomalous Permian genus (Gill, 1925; Hancock & Howse, 1870; Westoll, 1941) with an extremely anterior pelvic fin, and three species of *Sinosaurichthys* (Wu et al., 2011), which have dorsally-located pectoral fins.

Binning by geologic time, the fin positions of the fossil species have remained generally constant, with much greater variation seen in extant species, though the mean position of the pelvic fin has shifted anteriorly in extant species (Supplemental Figure S2.3).

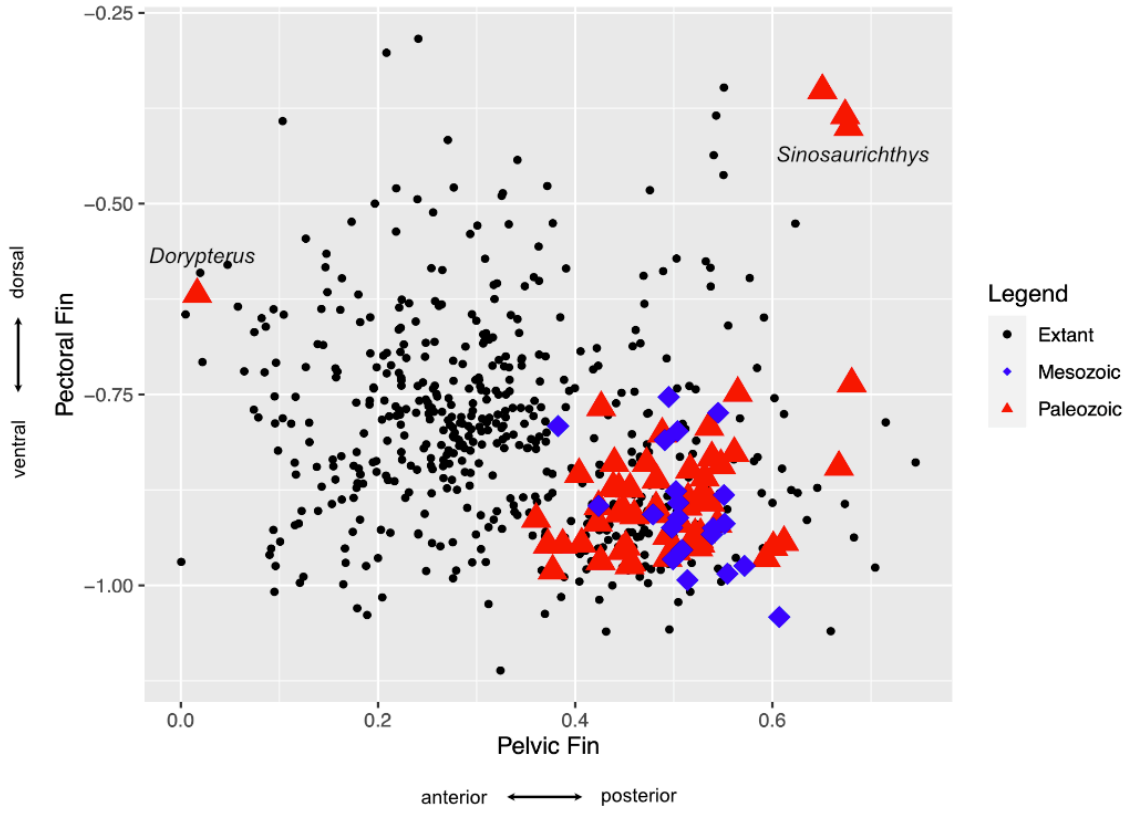

Figure 2.8 - Morphospace of pelvic vs pectoral fin position with fossil data projected on top.

Morphospace of pelvic vs. pectoral fin position with fossil data projected on top. Extant = black dots, Mesozoic = blue triangles, Paleozoic = red triangles. Except for *Dorypterus* and *Sinosaurichthys*, the fossils universally have posterior pelvic fins and ventral pectoral fins.

2.5.5 Positional symmetry between the anterior limits of the dorsal and pelvic fins

We next examined the possibility of positional symmetry between the dorsal and anal fins, and the dorsal and pelvic fins. Using our metric, if two fins are positioned symmetrically on the anteroposterior axis, we expect that the angle formed between them relative to the anteroposterior axis should be close to 90 degrees.

To determine whether there were any shifts in adaptive optima in extant actinopterygians, we ran phyloEM on the dorsal-pelvic and dorsal-anal angles and recovered no shifts for any of the traits (Supplementary Figure S2.4). Additionally, when visualizing the distribution of these traits via contMap (Figure 2.6), we saw little change in trait values throughout the tree. There was a slight posteriorizing of the dorsal fin relative to both the pelvic and anal fin in Atheriniformes/Beloniformes, but the magnitude of this posteriorizing was not significant enough to be detected by the phyloEM method. Estimation of the ancestral state of dorsal-anal symmetry and pelvic-dorsal symmetry at the extant actinopterygian root yielded values of 52 degrees and 91 degrees, respectively. This indicates that the dorsal fin was ancestrally anterior to the anal fin in extant actinopterygians, and that the dorsal fin was in register with the pelvic fin.

We found a pronounced discontinuity in these traits between Devonian-Triassic and Jurassic-Recent fish. Devonian-Triassic fish have dorsal fins that are more posterior relative to the pelvic fin, while Jurassic-Recent fish essentially have their dorsal and pelvic fins in register. Meanwhile, the dorsal fin is slightly anterior to the anal fin in Devonian-Triassic fish, but

becomes profoundly more anterior relative to the anal fin in the Jurassic-Recent groups. Given that the pelvic and pectoral fin absolute positions remain mostly the same (posteriorly-located pelvic, ventrally-located pectoral) in our fossil dataset (Figure 2.9, Supplemental Table S2.1), this indicates that changes to the anterior limit of the dorsal fin was driving the sudden discontinuity.

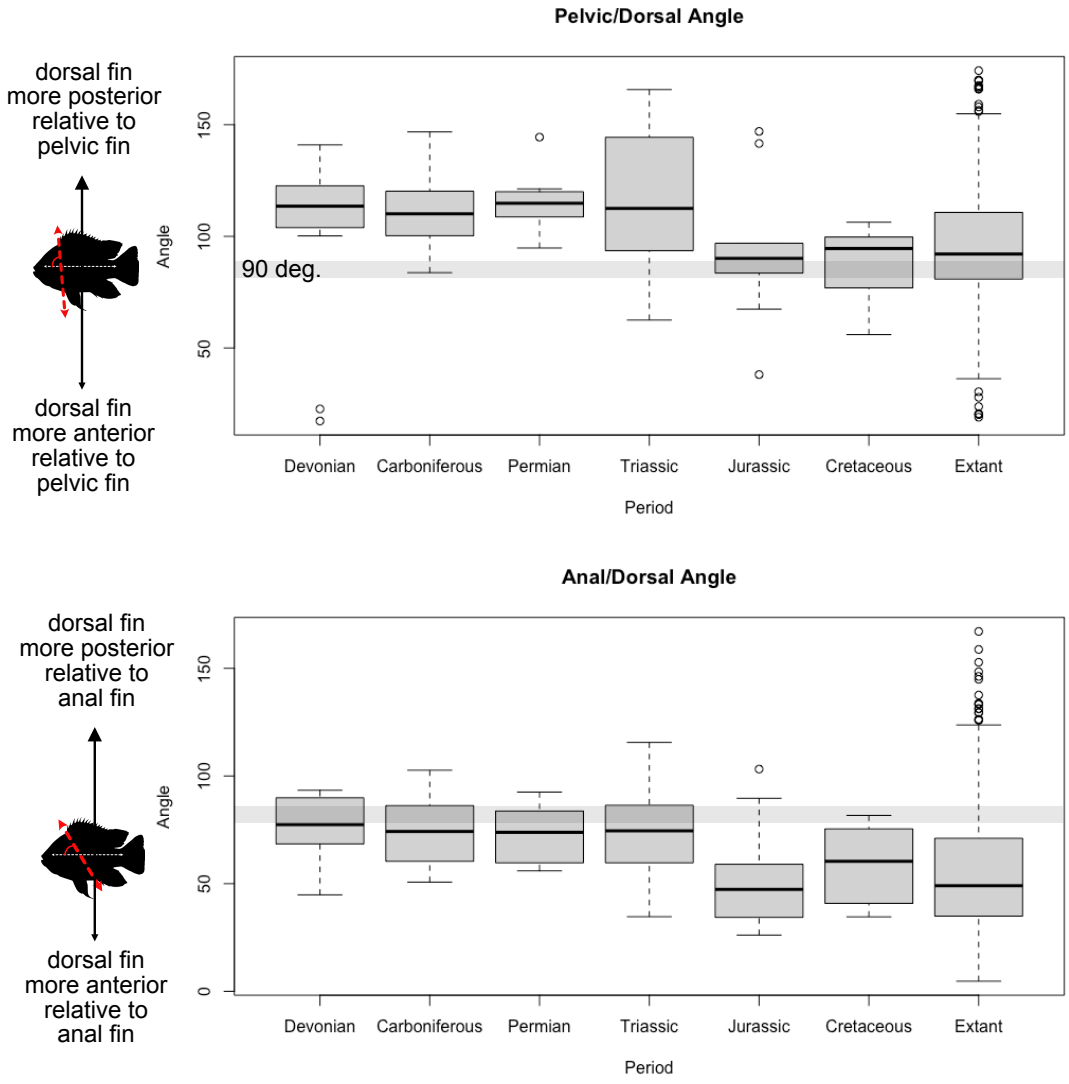

Figure 2.9 - Changes to Pelvic/Dorsal and Anal/Dorsal angle by geologic periods. Major shifts in these features occur in the Jurassic, which begins to resemble the extant condition.

2.5.6 Pelvic and pectoral fin position is not correlated with reef-association

We explored whether selective pressures may be constraining position by testing whether reef environments might be associated with a particular fin configuration. Specifically, we hypothesized that due to the need to navigate tighter physical surroundings, fish living in reef habitats might need to have greater maneuverability. A classic dynamically unstable body plan has been posited to be laterally compressed with dorsally-positioned pectoral fins to combat roll, and more ventrally-positioned pelvic fins to act as "brakes" (Alexander 1996, Standen 2008). Using the dataset from Larouche et al. (2020) that classified species as either reef-associated or not, we find that there is no correlation in either pectoral or pelvic fin position based on their reef-association ($p=0.95$ pectoral fin, $p=0.35$ pelvic fin; Supplemental Figure S2.5, Supplemental Table S2.2).

2.6 DISCUSSION

Within a phylomorphospace of pectoral/pelvic fin position, we demonstrated that living groups of Non-Neoteleosts occupy much of the same area of the morphospace (posterior pelvic, ventral pectoral), whereas Neoteleosts are more diffusely scattered but centered in a space with more rostral pelvic and dorsal pectoral fins. We tested whether there was a significant correlation between pectoral and pelvic fin position and find that there is none across all actinopterygians. Given that there was no correlation in fin position, we looked for shifts in adaptive optima of these two traits, or places in the phylogeny where the optimal trait value (for fin position) would differ from the ancestral state. Groups centering around different optima may create the illusion

of a correlation, as characterized in Felsenstein's "worst case scenario" (Felsenstein, 1985). We predicted that any shifts, if such existed, would occur at the base of Acanthomorpha due to its rich history of being used as an example of the fin positional shifts (Alexander, 1974; D. E. Rosen, 1982; Mikiko Tanaka, 2011). Instead, to our surprise, we found that the adaptive optimum of these two traits concurrently shift at the base of Neoteleostei, a lesser-discussed, but more inclusive, group within Teleostei that encompasses Acanthomorpha and other groups. Furthermore, we found that within Neoteleostei (but not within Non-Neoteleostei), there exists a correlation between pectoral and pelvic fin position. Therefore, correlations between pectoral and pelvic fin position appear to be set-dependent in Actinoptergyii. In summary, we identified Neotelostei as the node where a major innovation in pelvic/pectoral fin repositioning occurred.

Alexander (1974) linked the rostrally-positioned pelvic fin and dorsally-positioned pectoral fin morphotype to deep-bodied forms, suggesting that this combination makes acanthopterygians more maneuverable. Since then, several authors have promoted the idea that increased evolvability of pelvic fin positioning has acted as a "release" for teleost evolution and a key innovation that facilitated the diversification of behaviors and habitats in teleosts (Mikiko Tanaka, 2011; Yamanoue et al., 2010). It has recently been shown that certain attributes such as a deeper body and narrower/shallower caudal peduncles are associated with reefs, a habitat that presumably selects for greater maneuverability (Larouche et al., 2020). Therefore, we were interested to test whether the rostral-pelvic/dorsal-pectoral form was more predominantly found in reef teleosts, predicting that this would be case if this form was correlated with enhanced maneuverability. However, using the Larouche et al. (2020) classification of reef-association in

tandem with our dataset, we found that there is no correlation between reef-association and either paired fin position.

We further explored positional relationships involving the dorsal and anal fins. Mabee et al. (2002) speculated that dorsal and anal fins are linked together within a "dorsal and anal fin positioning module" that is primitive to actinopterygians and possibly a gnathostome characteristic, citing symmetry between the anterior limits of the dorsal and anal fin in Paleozoic (e.g. *Cheirolepis*) and Recent actinopterygians (e.g. *Polyodon*). Mabee and colleagues posit that decoupling of this module allowed dorsal-anal symmetry to be broken in many actinopterygian groups. They further speculate that a "First Dorsal Fin Module" was a key innovation in Acanthomorpha, and therefore a new developmental condition. According to the authors, the spinous anterior portion of dorsal fins in many acanthomorphans represents a duplication and subsequent divergence from the plesiomorphic, single dorsal fin module, and that this "new first dorsal fin" is positionally released, in some sense, from the anal fin and thus often positioned far anteriorly (e.g. cod, frogfishes).

To test if this scenario is supported, we predicted that we should (1) recover dorsal-anal symmetry as the primitive state for extant actinopterygians and (2) detect a shift in the adaptive optimum in dorsal-anal fin symmetry at the base of Acanthomorpha. Here, we found that while Paleozoic actinopterygians have dorsal and anal fins that are closer in register than in Mesozoic and in extant actinopterygians, but we found little evidence for complete dorsal-anal symmetry as the primitive state. Additionally, we did not detect any shifts in the adaptive optima for dorsal-anal symmetry within extant actinopterygians. Instead, we discovered a surprising positional

symmetry between the anterior limits of the dorsal and pelvic fins dating from Mesozoic species, suggesting an unexpected linkage between the positions of a paired and median fin.

In this discussion, we will first review our findings in the context of modularity. Then, we will explore how developmental and functional constraints may have influenced the macroevolutionary patterns that we have uncovered. Finally, we will unpack the shifts in adaptive optima in the context of habitat and ecology.

2.6.1 Modularity in the paired and median fins

Modules can be useful frameworks for testing evolutionary questions if they are set with meaningful boundaries. The purpose of delimiting modules is usually to (1) purport that the module in question can undergo change more or less easily than the rest of the modules in the organism, or to (2) assert that the components of a module are fixed together in some way, and therefore if/when change occurs, it will affect all components in some way. Both of these require understanding that some process/function must underlie the components in module. Covariation is frequently an indicator of modularity and is an important first step to identifying modules (e.g. Goswami & Polly, 2010).

Modularity has frequently been invoked as an explanatory mechanism for macroevolutionary patterns and rates in the paired and median fins of actinopterygians (Mabee et al. 2002, Larouche et al, 2017, 2018). Previous work has already assembled evidence that there are elements of covariation among these fins. Using presence/absence data from extinct and extant fish, Larouche et al. (2017) found non-independence between pectoral/pelvic and

dorsal/anal fins (i.e. species with absent pectoral fins were more likely to have absent pelvic fins, and the same for dorsal/anal fins). A further study from Larouche et al. (2018) used geometric morphometrics of body shape and fin positioning in 58 actinopterygian species and found that together, the fins inserted along the trunk (pectoral, pelvic, dorsal, and anal) are more tightly coupled than the rest of the body.

Our work continues exploring covariation in fin positioning by focusing in on the relationships between individual fins, which is a necessary step to uncovering the processes that might underpin the linkage between these fins. We interpret our result, that pectoral/pelvic positional correlation is unique to Neoteleostei, to mean that a potential paired fin positioning module is present in Neoteleosts but not Non-Neoteleosts. We acknowledge that there is more variance in paired fin positions in the Neoteleostei than in the Non-Neoteleosts, and thus the potential presence of a module does not necessarily imply tight constraint.

We suggest that there is no dorsal-anal fin positioning module because the dorsal and anal fin anterior limits are not in register in either fossil or extant species, at least as seen in our data. We also find no support for the presence of a "First Dorsal Fin Module" as there are no shifts in adaptive optima that would indicate a sudden duplication (and anteriorization) of the dorsal fin. It is compelling, however, to unexpectedly discover that a paired fin (pelvic fin) and median fin (dorsal fin) are constantly in positional register in our Mesozoic and extant dataset. Furthermore, there appears to be a dramatic shift from an uncoordinated pelvic-dorsal fin to an aligned pelvic-dorsal fin between the Paleozoic and the Mesozoic datasets, respectively, though we currently have not placed these species on the actinopterygian phylogeny. Without a

phylogenetic framework for the fossil species, we are unable to determine taxonomically where this shift occurred due to difficulty in setting taxa on stems, and further lines of work may opt to carefully characterize the evolution of these traits.

In summary, while we do not support a median fin module consisting of the dorsal and anal fins, we propose that at some point in actinopterygian evolution, a new linkage between the dorsal and pelvic fins anterior limits emerged and has remained stable since.

2.6.2 Constraints on fin positioning

There are surprisingly few shifts in fin positioning given the long history and morphological diversity of actinopterygians – just 2 in Non-Neoteleosts, and only 4 in Neoteleosts. In half of these shifts, they are concomitant with striking changes to their body plans - dorsoventrally narrowing in Gasteropelecidae (hatchetfish), and flattening in Lophiidae (goosefish) and Pleuronectiformes (flatfish). In Halosauridae, Beloniformes (needlefish and relatives), and Cyprinidontiformes (toothed carp) however, they retain a general, fusiform body shape in their pre-caudal region. This suggests that there may be constraints, either functionally selective or developmental, that prevent frequent shifts in paired fin positioning, and that this constraint may have been released in Neoteleosts.

Little is known about how the pathways and regulatory networks that govern how the fins are positioned in development, both anteroposterior and dorsoventrally. Furthermore, signals for patterning and induction are mostly described in tetrapod paired limb systems (Petit et al., 2017),

leaving open questions of whether these signals are shared in actinopterygian fish.

(i) Anteroposterior and dorsoventral positioning in development

In ray-finned fish, the pelvic fin bud often develops significantly later (days to weeks) than the pectoral fin bud. For example, in zebrafish, the pectoral fin arises at 48 hours post fertilization, but the pelvic fin bud only emerges at 3 weeks post fertilization. Therefore, it is an outstanding question whether the pelvic fin precursor cells are specified early in development, during the same time as the pectoral fin, or whether there is a redeployment of Hox patterning of the lateral plate mesoderm-derived tissues at 3 weeks. It is tempting to speculate that this decoupling in timing has allowed for shifts in pelvic fin position unique to ray-finned fish.

It is generally accepted that the paired fins arise from the lateral plate mesoderm, a transient embryonic tissue layer that also gives rise to limbs, the circulatory system and heart field, and the visceral/parietal peritoneum (Nishimoto and Logan 2016, Prummel et al. 2020). Regionalization of the lateral plate mesoderm along the anteroposterior axis is likely coordinated through Hox patterning – for example in the forelimb, rostral Hox expression is associated with forelimb bud initiation while potentially repressing hindlimb factors (Cohn et al., 1995; Petit et al., 2017).

In tetrapods, the forelimb and hindlimb buds are initiated at roughly the same time, and correspondingly, there is collinear Hox expression throughout the lateral plate mesoderm to coordinate this process (Minguillon et al., 2012). It is possible that by delaying the formation of the pelvic fin, actinopterygians can modify Hox patterning of the LPM without disrupting

important processes during embryogenesis. Nevertheless, while most actinopterygians have delayed pelvic fin initiation, extremely rostrally-shifted pelvic fins are only first seen in Neoteleosts. This implies that further developmental constraints may have been released in Neoteleosts – perhaps changes to the mobility and migration of the lateral plate mesoderm cell type – and further comparative developmental work is needed.

Factors that control the dorsoventral positioning of the pectoral fin have not been explored, especially as the final position of the pectoral fin is not stable until post-metamorphosis, following allometric growth – the aspect ratio of larval fish is rarely the same of that of the adult. In addition, because the pectoral girdle articulates with the skull, shifting the position of the pectoral fin might require modifying the shape of the girdle and its articulation points.

The dorsal and anal fins arise within a transient median fin fold that encircles the larval fish. Although they appear as condensations between the two epithelial layers of the fin fold, fin mesenchyme is mostly derived from trunk paraxial mesoderm (Freitas et al. 2006, Lee et al. 2013). The anteroposterior positioning of the dorsal fins is not well studied in actinopterygians, but is likely mediated through nested HoxD patterning as in catshark where Hoxd9-13 are activated sequentially in the prospective dorsal fins (Freitas et al. 2006). Elements of HoxD combinatorial expression appear to be conserved in cichlid, catfish, and flatfish to mark the site of the dorsal fin (Chen, Liu, Yao, Gao, & Bao, 2017; Höch, Schneider, Kickuth, Meyer, & Woltering, 2021). How the anal fin is positioned remains to be determined, however, its anterior limit is almost always immediately posterior to the anus.

Recent work on the specification between the spinous (anterior) and soft ray (posterior) domains of acanthomorph fish does not support the idea that the "First Dorsal Fin Module" was a duplication of the ancestral dorsal fin (Höch et al., 2021). The authors identified a BMP (bone morphogenetic proteins)-gremlin-shh signaling network that modulates the boundary of the spinous and soft ray domains in cichlid (an acanthomorph) and find that the same network is found throughout the catfish dorsal fin (a non-acanthomorph). They proposed that the spinous portion of the fin arose through expansion of anterior identity and exaptation of the anterior signals into a new spinous identity. If a "First Dorsal Fin Module" arose due to duplication, we would expect to find two sets of the BMP-gremlin-shh expression pattern, with one set in the first dorsal fin and one set in the second dorsal fin.

In summary, since the development of the pelvic and dorsal fins is quite distinct given that they are formed from different embryonic tissue layers (somitic mesoderm vs. lateral plate mesoderm), it is surprising that their positions are so coordinated. The introduction of a rostrally shifted pelvic fin induced the anterior limit of the dorsal fin to also shift rostrally. Further studies that investigate the developmental mechanisms behind fin positioning may uncover a shared responsiveness to a common positioning signal, or if no common signal is found, find that these separate positioning mechanisms tend to evolve together.

(ii) Constraints due to maneuverability and stability

Our analysis shows that dorsally-positioned pectoral fins first arose at the base of Neoteloestei, which include lineages such as the Ateleopodidae (jellynoses) and Aulopiformes

(lizardfishes). While their pectoral fins are quite dorsally located, their overall body shape is elongate, suggesting that the ability to shift pectoral fins dorsally preceded deep-bodied forms in Neoteleostei. Within Neotelostei, deep-bodied forms only appear within Acanthomorpha, and this body shape is correlated with the presence of spines on the dorsal and anal fins, potentially to dissuade predation (Price et al., 2015).

Fish with more dorsally-positioned pectoral fin are often accompanied by a vertically oriented fin insertion base (E. G. Drucker & Lauder, 2002). In contrast, species with more ventral pectoral fins tend to have a more horizontal orientation of their fin insertion base (e.g. sturgeons). More dorsally-positioned pectoral fins are positioned closer to the center of mass in these deep-bodied, laterally-compressed fish than if they were positioned ventrally (Alexander, 1974; Eliot G. Drucker & Lauder, 2001). Importantly, it is thought that this higher position confers the ability for a deep-bodied fish to remain level during steady state swimming (Blake, 2004; Webb & Fairchild, 2001). This begs the question – can fish with deep-bodied forms possess ventral pectoral fins, or would the resulting fin configuration be too unstable? We are unaware of any examples of this configuration and support previous hypotheses that having a deep-bodied form constrains pectoral fin position to a more dorsal position. In the Cyprinidontiformes reversal to a more ventral pectoral fin, it is notable that the order does not possess any deep-bodied forms. In extinct deep-bodied forms such as *Chirodus* and *Platysomus,* the pectoral fins are not ventrally placed, even though the pelvic fins are near the anus. On the other hand, elongate body forms have evolved multiple times in Acanthomorpha and in these lineages, they have frequently retained a dorsal pectoral fin (e.g. Beloniformes), suggesting that body shape is constraining fin position, and not the other way around.

Propulsion through oscillation of the median and paired fins (MPF) is one of the major methods that fish use for locomotion, as opposed to whole body/caudal fin propulsion. Species that employ MPF swimming tend to have deeper, more laterally compressed bodies (Friedman, Price, & Wainwright, 2021) than those that rely mostly on undulation. A logical next step would be to investigate whether MPF swimmers are more likely to have dorsally-shifted pectoral fins in order to test the link between the position of the pectoral fin and its importance in generating propulsive force. In sturgeon, where the pectoral fin is ventrally located, it mainly acts to stabilize the fish instead of generating any lift (Wilga & Lauder, 1999).

The function of pelvic fins for steady state swimming and maneuvering remains a wide-open field for further investigation. Just a few studies have been performed. Using the rainbow trout (*Oncorhynchus mykiss*) as a model, Standen (2008, 2010) found that its posteriorly-positioned pelvic fins actively oscillated during swimming and maneuvers, and that they produce powered corrective forces that damp body oscillations. Digital particle image velocimetry (DPIV) studies revealed that pelvic fins slow the flow along the ventral side of the trout, influencing how the anal fin interacts with water flow (Standen 2010). The data from Standen (2008, 2010) suggest that the pectoral, pelvic, and anal fins might be functionally interlinked to channel water flow along the body axis to each other.

With the exception of Amiiform and Gymnotiform swimming, the dorsal and anal fins are generally not the sole source of propulsive force (Sfakiotakis, Lane, & Davies, 1999). Instead, their role is likely related to providing balancing forces during steady state swimming

(Standen & Lauder, 2005, 2007). It has also been shown that the dorsal fin and anal fins cooperate functionally to stabilize the fish from forces generated by each other, and that the position of these fins relative to the center of mass will modulate the directions of torques generated (Standen & Lauder, 2007).

Given that we found a consistent linkage between the anterior limit of the dorsal fin and the anteroposterior position of the pelvic fin, we speculate that this is a response to a biomechanical constraint in balancing lateral forces. The posterior limits of the dorsal and anal fin have tended to stay in register throughout actinopterygian evolution (Supplemental Figure S2.6), suggesting that remaining in register is important enough not to be discarded. However, detailed studies on the flows and forces generated by each fin relative to another will be required to test this hypothesis. Additionally, if dorsal-anal symmetry was more prevalent in fossil fish, it would be interesting to explore how this affected their mode of swimming.

The kinematics of fish swimming, maneuverability, and stability is an entire field of study, with multiple other factors adding complexity to the story. The shape of the pectoral fins and the stiffness of the fin rays, for example, play a surprisingly large role in controlling the mode of swimming in fishes (Aiello, King, & Hale, 2014; Du, Tissandier, & Larsson, 2019; Feilich, 2016). All of these factors make assigning broad macroevolutionary trends difficult, as each lineage of fish have unique combinations of traits that produce different outcomes.

2.6.3 Reef association

While reef-associated fish may have more laterally compressed bodies and narrower caudal peduncles (Larouche et al. 2020), there appears to be no effect on paired fin positioning. There could be several explanations behind these results – first, it is possible that phylogenetic constraints are a larger contributing factor to body shape than ecological pressures. Our analyses for paired fin shifts revealed that they are uncommon throughout actinopterygian phylogeny, only occurring 7 times. Second, it may be the case that the classic maneuverable paired fin arrangement of dorsally-located pectorals and rostrally-located pelvics is far less critical than traits such as lateral compression or narrower caudal peduncles.

2.6.4 Characterization of regime shifts

In the two shifts in Non-Neoteleosts, Halosauridae and Gasteropelecidae, the pectoral fins are shifted dorsally while the pelvic fins are mostly still posterior. Halosauridae are benthic, deep-sea fish with very elongate tails, and any specialization of the pectoral fins has not been described (Nelson et al., 2006). Gasteropelecidae, or the freshwater hatchetfishes, have extremely deep bodies with elongated pectoral fins, though the depth of the body is mostly due to an elongated ventral keel (Nelson et al., 2006). These fish are known to jump out of the water, so it is likely that a dorsally-located pectoral fin may be an adaptation to this behavior, as in flying fishes.

Within Neoteleostei, the Lophiidae are the first group to exhibit a reversal of their pectoral fins back to a ventral location. Surprisingly, the pelvic fins in this group remain fairly anterior, creating the possibility of a collision. However, these benthic fish have drastically modified their pectoral fins into muscular, fleshy "limbs" that allow them to walk over the substrate and have laterally displaced these fins (Dickson & Pierce, 2018) whereas the pelvic fins appear to be used more for balance and mechanosensation. Future studies may discover whether fish with substrate locomotion tend to have more ventral pectoral fins.

The Pleuronectiformes within the Neotelostei were singled out by phyloEM for having extremely jugular pelvic fins. These flatfishes locomote through benthic "walking" with their elongate dorsal and anal fins (Fox, Gibb, Summers, & Bemis, 2018), so it may be advantageous to shunt the pelvic fins rostrally and compress the thoracic region to ensure that the anal fin is as long as possible.

The Beloniformes and Cyprinidontiformes have reversed their pelvic fins into a more posterior location, but while the pectoral fins in Beloniformes are still mostly dorsally-shifted, the Cyprinidontiformes have reversed their pectoral fins into a ventral location. The Beloniformes include the flying fishes which use their pectoral fins for gliding – here, it may be more functionally advantageous to retain a dorsally-shifted pectoral fin. It is unclear whether the pelvic fins have any specialized function in the Cyprinidontiformes, but some species of this family (Poeciliidae) have modified anal fins (gonopodium) for internal fertilization in males. It is possible that the pelvic fin may play some role in copulation by being closer to the cloaca, as is the case of the pelvic claspers in male chondrichthyans.

2.6.5 Discontinuity in dorsal/pelvic and dorsal/anal fin relative positions between the Triassic and Jurassic periods

Additionally, we found that there was a sudden discontinuity in the position of the dorsal fin relative to the pelvic and anal fins at the Triassic-Jurassic boundary for our fossil dataset. Before the Jurassic, the anterior limit of the dorsal fin was posterior to the pelvic fins; starting in the Jurassic, the dorsal and pelvic fins appear to be aligned and in register. While further work is needed to determine whether this was a clade-specific change, our results show that the overall fin configurations of fish radically shifted between the Triassic and Jurassic. That is, these data characterize the T-J boundary as the hard minimum age that this morphological change occurred.

We hypothesize that an increase in the relative abundance of modern, teleost-like forms is likely driving the change in the Jurassic. Though molecular estimates place the crown teleost node in the Permian (despite the earliest fossil crown teleost being known from only the late Jurassic), only in the Jurassic and Cretaceous do most modern clades originate and radiate. This is corroborated by the fact that the Jurassic and Cretaceous trait values are close to the mean values of extant species.

Finally, we note that there is substantially more variation trait values for the extant species than in the fossil species. This is surely influenced by preservational bias and because the number of extant species sampled vastly outnumbers the number of fossils available. We predict

that sampling fossil species in the Cenozoic, where fossil species are closer to or in crown groups, would yield a larger range of variation as well.

2.7 CONCLUSIONS

We have shown that the positions of the paired fins of actinopterygian fish simultaneously underwent an abrupt change at the base of Neoteleostei, a previously under-noticed clade. This movement towards a more rostral pelvic fin and dorsal pectoral fin appears to have only occurred once to underpin a new, generalized shape for large groups such as Acanthomorpha within Neotelostei. Furthermore, any reversals to this shift in adaptive optima appear to be unique to monophyletic groups. Future avenues of research should investigate whether these discontinuities are reflective of extant bias because the fossil data is currently unavailable. Finally, we have discovered a previously unrecognized link between the positions of the pelvic fins and the dorsal fin that was first detectable in the Jurassic and remained stable throughout extant actinopterygians. Exploring the developmental and functional constraints that might elucidate the processes behind these patterns will be important to understanding these data, as well as provide further examples of how body plan evolution is influenced by underlying factors.

Supplemental Figures

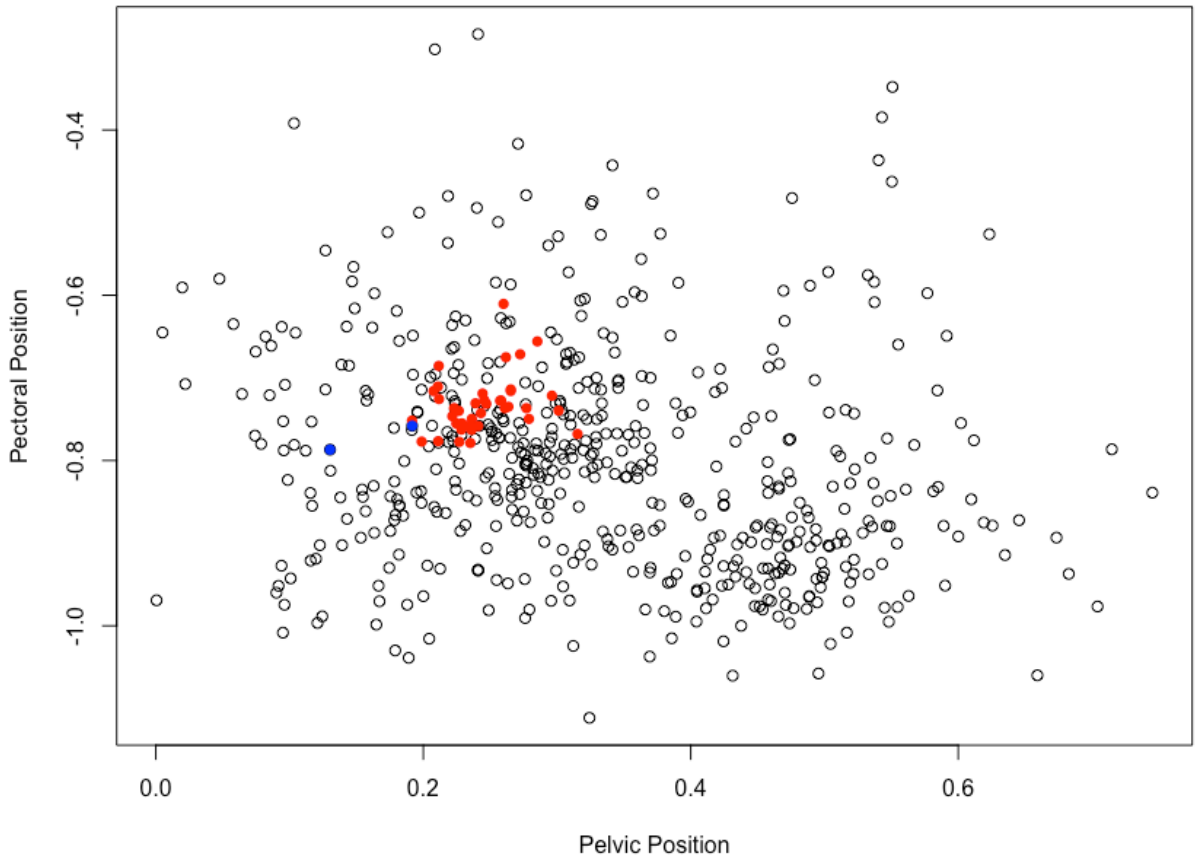

Supplemental Figure 2.1 - Acanthothuridae test.

Red dots are from the George & Westneat (2021) dataset; blue dots are samples from the main photo dataset. Hollow black dots represent the total extant dataset.

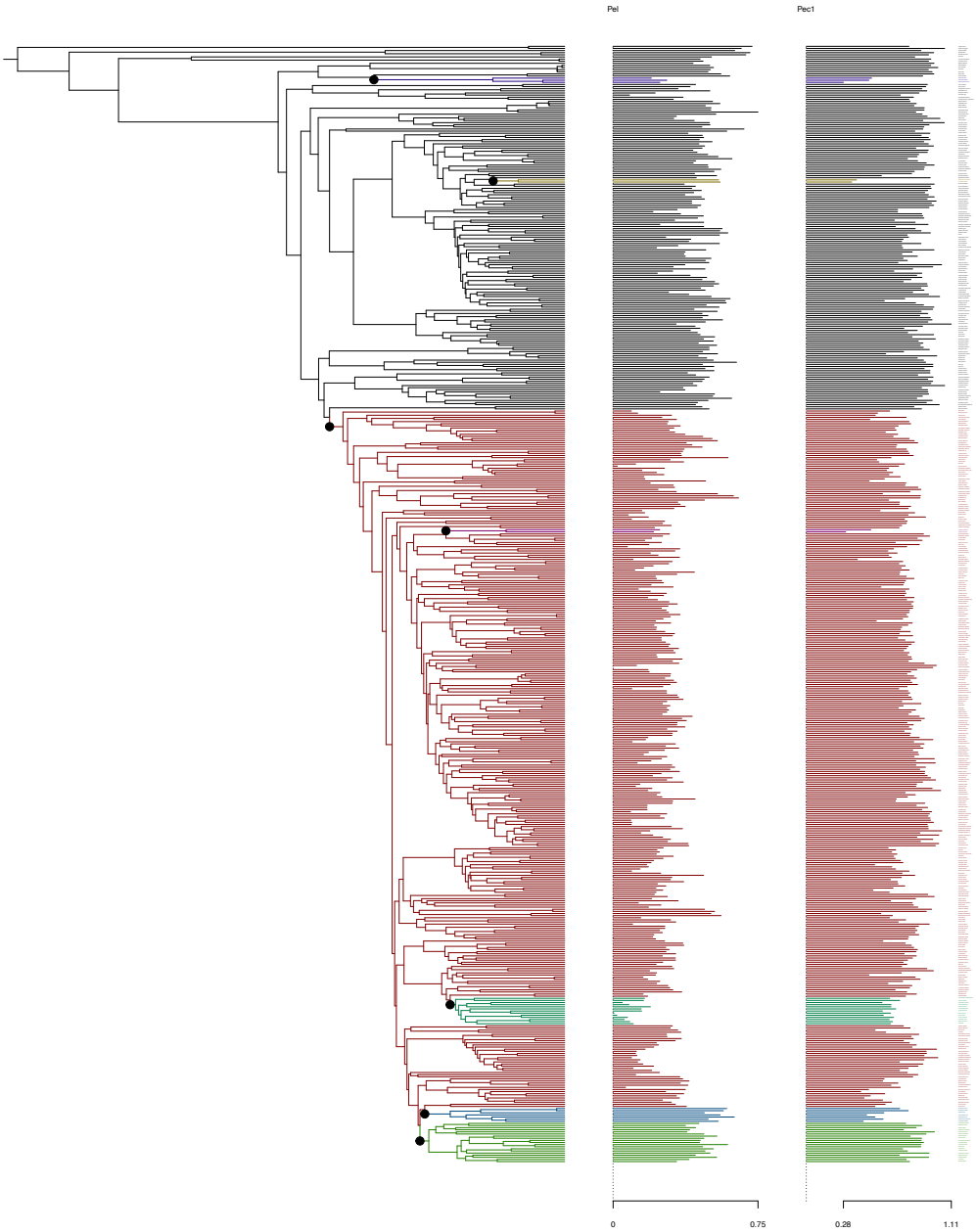

Supplemental Figure 2.2 - Higher resolution view of phyloEM results for pectoral and pelvic fin position.

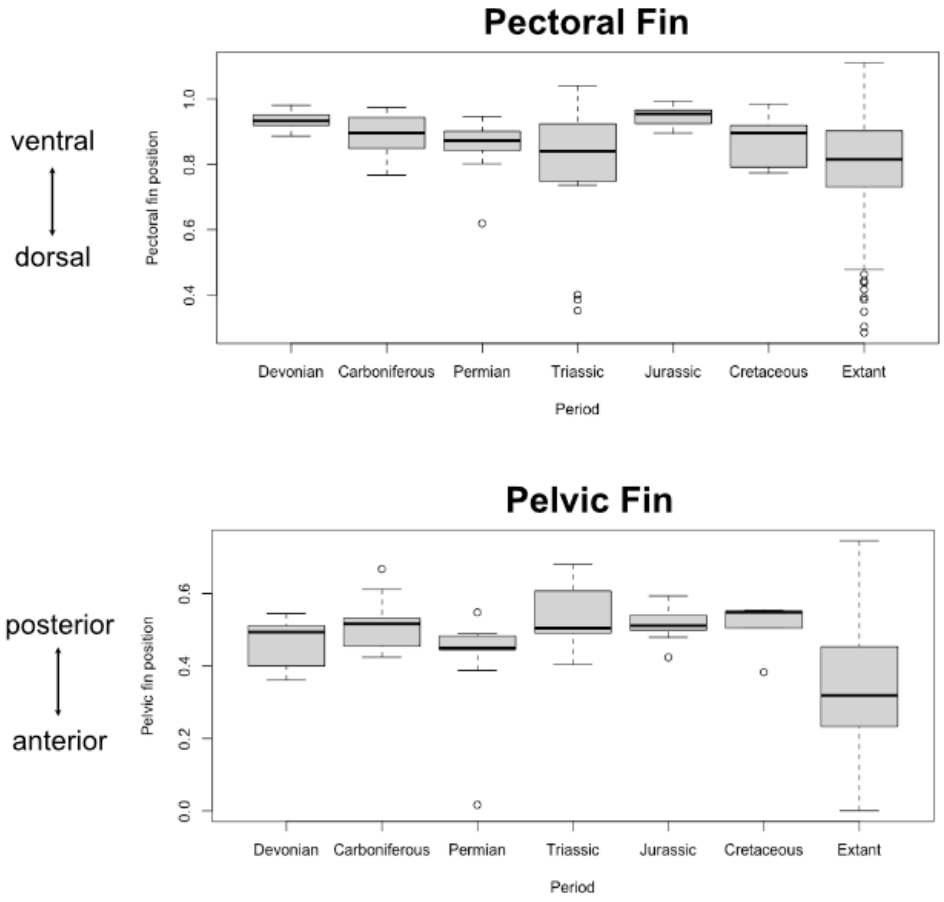

Supplemental Figure 2.3 - Pelvic and pectoral fin position remain stable in fossil groups but are more variable in extant groups.

The mean of pelvic fin position has shifted to a more anterior position in extant groups.

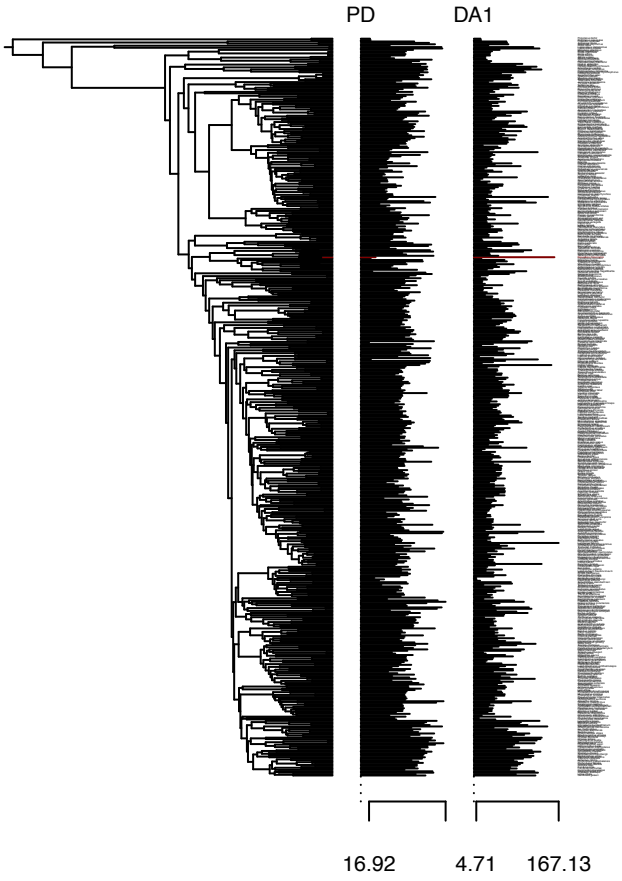

Supplemental Figure 2.4 - No shits in adaptive optima recovered for PD (pelvic-dorsal angle) and DA1 (dorsal-anal angle) using the phyloEM package.

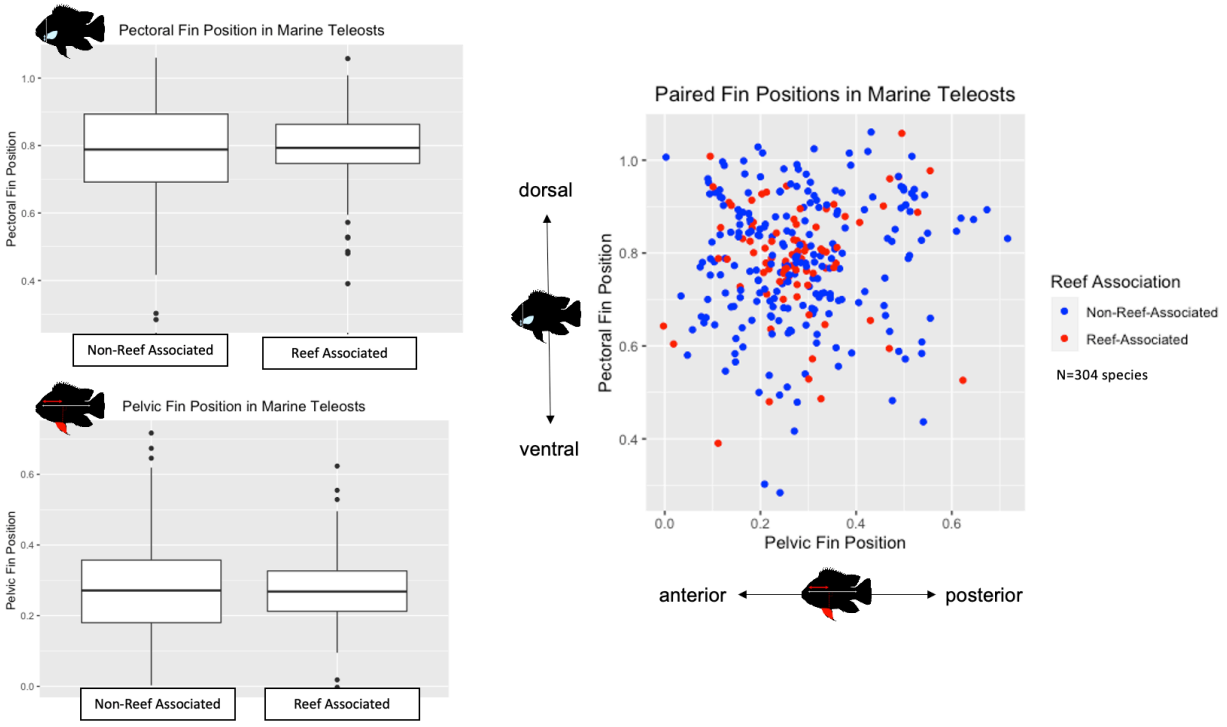

Supplemental Figure 2.5 - No correlation due to reef association.

Left panels: boxplots for each fin position, groups defined by reef-association or non-reef-association. Right panels: morphospace of pectoral and pelvic fin position color-coded by reef-association status. (Plots generated by E. Incardona.)

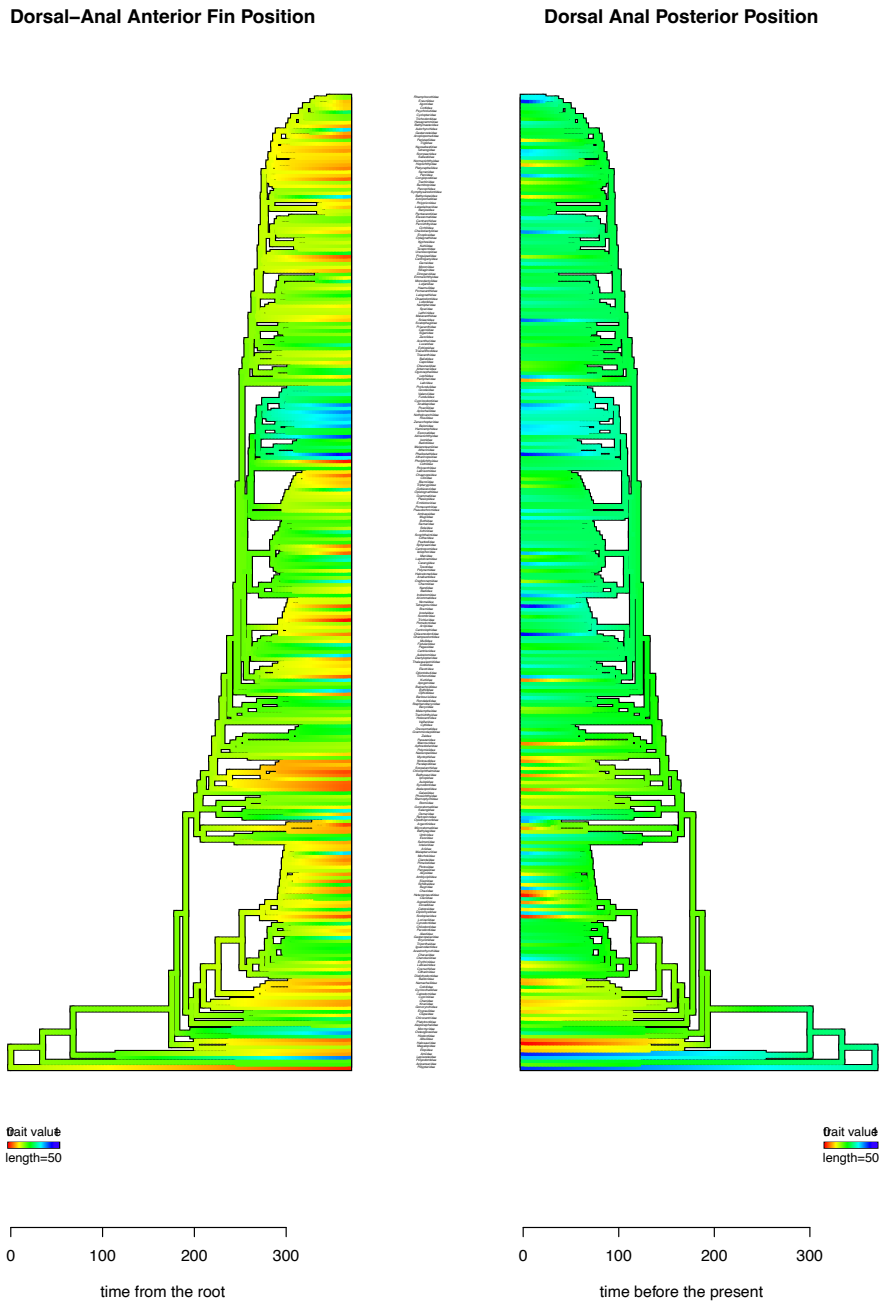

Supplemental Figure 2.6 - Comparing DA1 and DA2.

Comparing the anterior limits of the dorsal fin and anal fin, and the posterior limits of the dorsal fin and anal fin. Warmer colors indicate that the edge of the dorsal fin is anterior to the edge of the anal fin; colder colors indicate the edge of the dorsal fin is posterior to the edge of the anal fin. Green indicates that the two boundaries are in register. The posterior limits of the dorsal and anal fin have remained relatively constant.

	Paleozoic	**Mesozoic**	**Extant**
Pectoral Position	0.90 (n=62)	0.88 (n=21)	0.71 (n=588)
Pelvic Position	0.49 (n=58)	0.50 (n=21)	0.32 (n=538)
Pelvic/Dorsal Angle	114 (n=58)	93 (n=21)	92 (n=537)
Dorsal/Anal Angle	74 (n=62)	59 (n=21)	48 (n=585)

Supplemental Table 2.1 – Mean values for each group (no phylogenetic correction).

	p	F-value
Pectoral fin	0.95	0.0034
Pelvic fin	0.35	1.138

Supplemental Table 2.2 - Testing for significant differences in mean fin positions in reef-associated and non-reef associated fish.

dF=1 between groups, dF=299 within groups, total dF=300 for both tests. (Values generated by E. Incardona)

Chapter 3 - LINEAGE TRACING OF POSTERIOR LATERAL PLATE MESODERM REVEALS EXTENT OF PELVIC FIN PRECURSORS

3.1 PREFACE

I am thankful for the contributions of several people for this chapter: Dr. Christian Mosimann (University of Colorado, Anschutz Medical Campus) and Dr. Karin Prummel (EMBL Heidelberg) for providing the lightsheet timelapses of the *Et(hand2:eGFP)* fish. Eric Yuan (undergraduate, University of Chicago ’24) courageously wrote new scripts to account for tricky embryo growth and performed the cell tracking analysis. Maryam Bolouri (undergraduate, University of Chicago ’22) took a first stab at the confocal timelapses and was integral for performing initial cell tracking. Adam Kuuspalu helped with taking many of the photos during larval development of the laser-labeled fish and was essential for keeping them alive in the facility. And thank you to my committee member, Dr. Timothy Sanders, for guiding me through the Gateway cloning and providing reagents to generate the *Tg(hsp:cre-ert2)* line.

3.2 ABSTRACT

The pelvic fin buds in zebrafish emerge late relative to other vertebrate model embryos, almost 3 weeks after the pectoral fin buds appear. The source of the pelvic fin precursor cells has not been uncovered, and where these cells are located during these 3 weeks of development has not been examined. Using the *Et(hand2:eGFP)* line that marks lateral plate mesoderm, I identified two candidate cell populations within the posterior lateral plate mesoderm (PLPM) that might contribute to the pelvic fin buds. I fate-mapped the movements of these two cell

populations during embryogenesis and found that one cell population migrates ventrally over the yolk extension without much anteroposterior movement, and another cell population populates the pre-anal fin fold as fibroblasts. Next, I generated a *Tg(hsp:cre-ert2)* line that when crossed with *Tg(ubi:switch),* allows for permanent cell labeling when cells are heat-shocked. By labeling cells from both populations, I found that the cells overlying the yolk extension (future parietal peritoneum) contribute to the pelvic fin buds, while the pre-anal fin fold cells do not. Furthermore, cells from the somite levels of 6-11 can comprise the pelvic fin bud, though there is evidence that these cells are mostly from somite levels 7-11. This study is the first to delimit the boundaries of the pelvic fin precursor cells and experimentally demonstrate that they arise from the PLPM.

3.3 INTRODUCTION

In a sense, the posterior lateral plate mesoderm (PLPM) behind somite 5 is the final frontier for our lab. From head to tail – L. Mao et al. (2021) fate-mapped the anterior lateral plate mesoderm (ALPM) and its contribution to the secondary heart field, pharyngeal arches, and pericardial sac. In the pectoral fin region, Q. Mao et al. (2015) and Boyle-Anderson et al. (2022) fate-mapped the PLPM from somite levels 1-5 to show how fin field cells coalesce into a pectoral fin bud. Here, I have attempted to perform fate-mapping on the last stretch of PLPM from somite levels 6-14 to assess its contribution to the pelvic fin and other tissues. Outside studies that have been published during my time in the lab have helped inform my fate-mapping strategy. Gays et al. (2017) showed that some cells from the PLPM will give rise to the smooth muscle surrounding the gut tube. Prummel et al. (2022) time-lapsed the embryonic PLPM to

ascertain its contribution to the visceral and parietal peritoneum. These data have allowed me to distinguish these fates from my target structure, the larval pelvic fin buds.

In zebrafish, the PLPM from somite levels 6-14 primarily rests in bilateral stripes on the yolk extension, or hindyolk, a cylindrical tube jutting out posteriorly from the yolk ball and stopping at the anus (Figure 3.1A). The yolk extension is a synapomorphy of the Cypriniformes (including zebrafish), but also has arisen independently in a few lineages within Characiformes (characins) and Anguilliformes (eels) (Virta & Cooper, 2009). The gut tube develops along the dorsal midline of the yolk extension. The yolk extension thins during the first week of embryonic development as the yolk is resorbed, and completely disappears by the end of the first week. Meanwhile, the ventral midline of the yolk extension is graced by the pre-anal fin fold at 2 dpf, a transient median structure that is lost after the pelvic fins develop (~8.5 mm SL, or around 5-6 weeks post fertilization). This structure has received some prior interest in the lab – a line named the "Lewis" mutant developed a curious median fin within the pre-anal fin fold at the expense of the size of the pelvic fins (Qiyan Mao, 2013). The "Lewis" phenotype prompted questions of whether the pelvic fins might receive contribution from the pre-anal fin fold, or whether they arose exclusively from the PLPM.

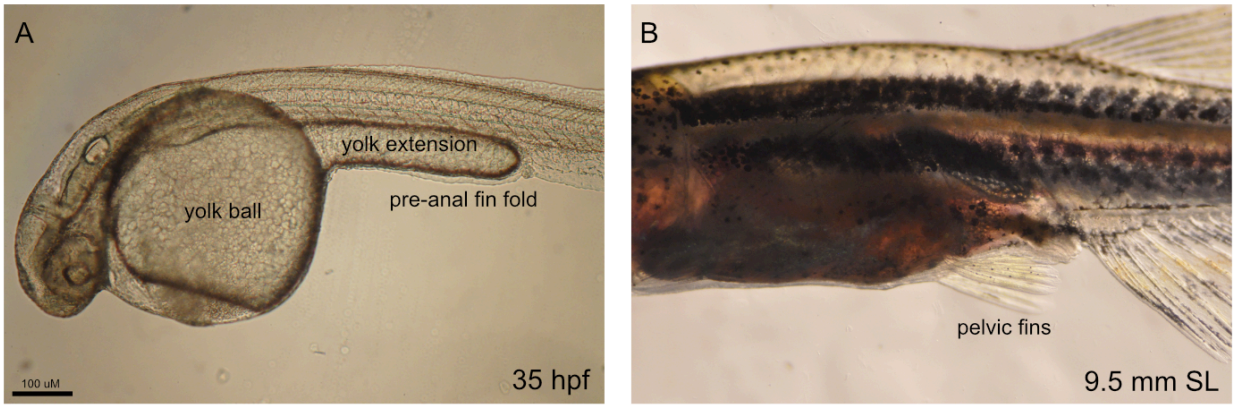

Figure 3.1 - Embryonic and larval structures related to the pelvic fin.

(A) 35 hpf embryo showing yolk ball, yolk extension, and pre-anal fin fold. (B) 9.5 mm SL larva (around 4 weeks old) with pelvic fins. Scale bar is 100 μM.

Late larval structures in zebrafish are much less frequently studied than embryonic ones because there has not been an easy method to perform targeted long-term lineage tracing. Creating transgenic lines with tissue-specific enhancers is usually the route that many researchers need to take in order to follow cells past embryonic stages. Photoconversion of fluorescent proteins (such as Kaede) labeling and lipophilic dye injections are most effective in the first week of development. In order to follow cells up to 3 weeks of development, which is when the pelvic fins appear, I needed to create a new system to allow me to perform long-term lineage tracing. This culminated in the creation of the novel *Tg(hsp:cre-ert2)* line.

Using this labeling system as well as important tools for embryonic fate-mapping, the goals of this chapter were twofold: (1) Determine which structure, pre-anal fin fold or peritoneum, gives rise to pelvic fin precursors (2) Determine the extent of the anteroposterior boundaries of the pelvic fin precursors.

3.4 RESULTS

3.4.1 Observations of the posterior lateral plate mesoderm with the *Et(hand2:eGFP)ch2* line shows two potential cell populations for the pelvic fin precursors

The enhancer trap line *Et(hand2:eGFP)ch2* previously generated from (Q. Mao et al., 2015) labels hand2:eGFP expressing cells, which are representative of lateral plate mesoderm. Hand2 is a transcription factor that is associated with the development of the pectoral fins, heart, and peritoneal structures. Fish from this line were observed over their embryonic and larval development to gain a sense of the tissue layers to which the LPM would contribute. I was particularly interested in whether the pelvic fin buds would contain hand2:eGFP expressing cells, as that would confirm LPM contribution to the pelvic fin.

From 12 – 24 hpf (Figure 3.2 Ai-Cii), hand2:eGFP expressing cells resided in bilateral dorsal stripes on either side of the midline, ending at the posterior limit of the yolk/yolk extension (if formed). The stripes became thinner as they extended posteriorly. As the yolk extension developed (Figure 3.2 Di-Eii, 24-30 hpf), hand2:eGFP expressing cells appeared to begin migrating ventrally (arrows in Figure 3.2). Filopodia (an isolated single leading edge per cell) pointed ventrally were observed. While there did not seem to be any anterior-to-posterior (or vice versa) directional progression of development, the more posterior portions of the yolk extension were covered in hand2:eGFP expressing cells earlier than the more anterior portions, likely because the yolk extension tapered posteriorly and was thinner towards the rear.

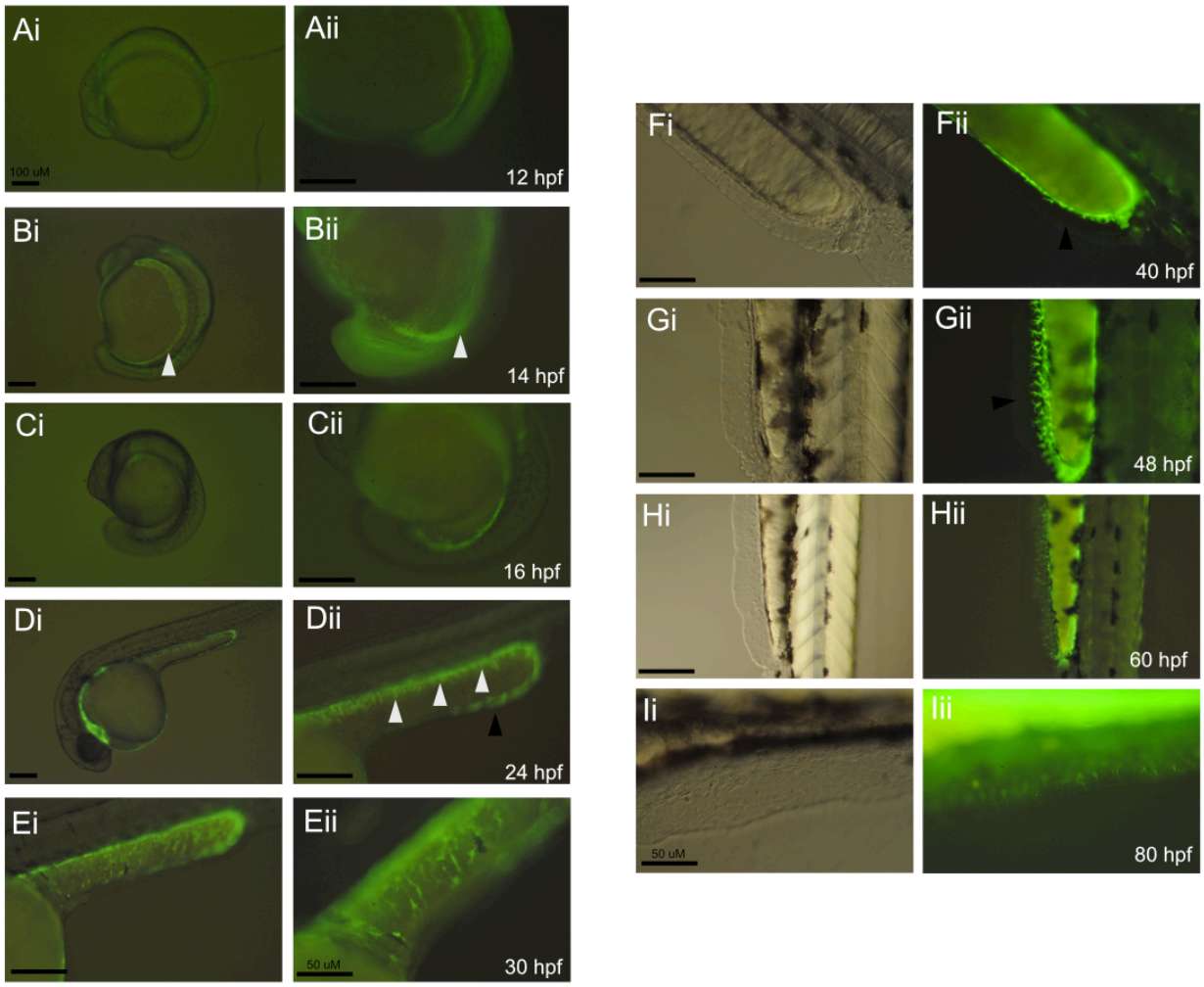

Figure 3.2 - Observations of *Et(hand2:eGFP)ch2* from 12 hpf – 80 hpf in the posterior lateral plate mesoderm.

(Ai-Eii) hand2:eGFP expressing cells appeared to cover the yolk extension throughout development and displayed filopodia. Right panels are higher magnifications. Lateral view, anterior to the left. (Fi-Iii) As the pre-anal fin fold grew outwards, hand2:eGFP expressing cells appeared to invade the fin fold and migrate outwards. Left panels are bright field images. Fi-Hii are lateral views, anterior to the top. Ii-Iii are lateral views, anterior to the left. White arrows = bilateral dorsal stripes, black arrows = midline cells. Scale bar is 100 μM unless otherwise noted.

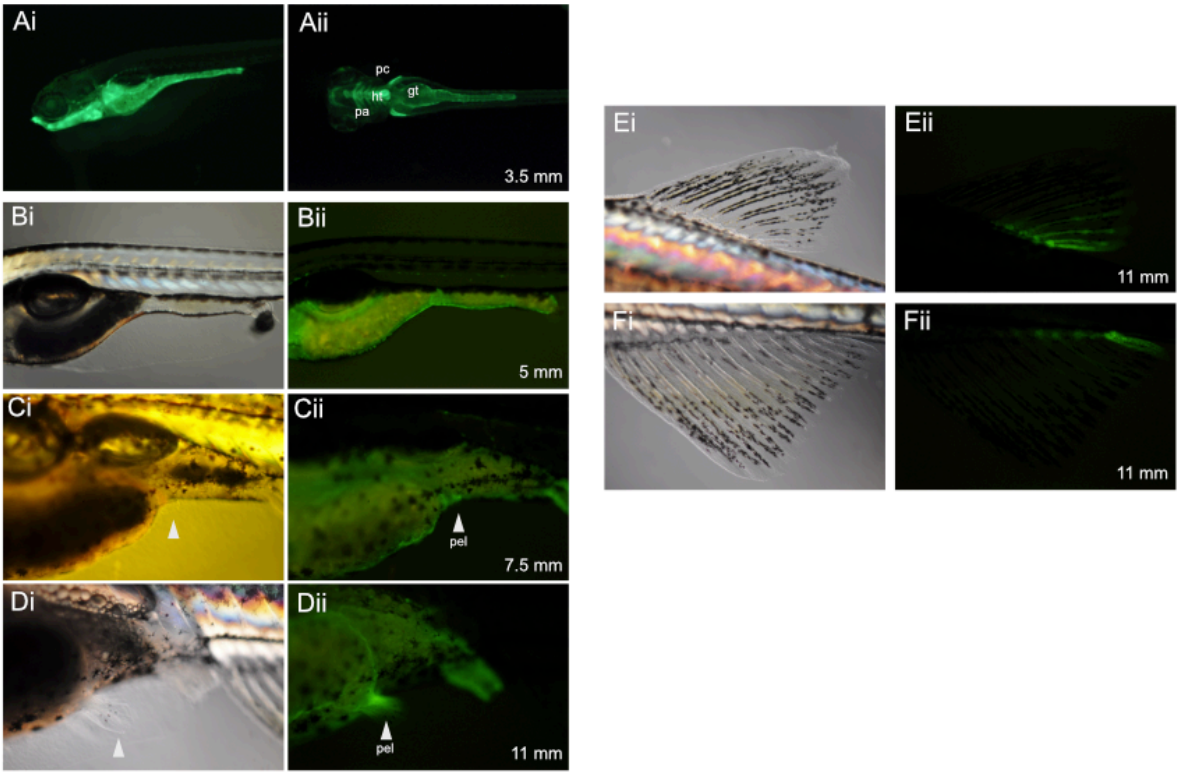

Figure 3.3 - Observations of *Et(hand2:eGFP)ch2* during larval stages, 3.5 mm – 11 mm (approximately 6 dpf – 1 month post fertilization).

(Ai-Aii) hand2:eGFP expressing cells were also incorporated into the pharyngeal arches (pa), pectoral fin (pc), heart tube (ht), and gut tube (gt). (Bi-Bii) Prior to pelvic fin bud formation, hand2:eGFP expressing cells were most visible in the gut tube and appeared striated. (Ci-Dii) Hand2 was not expressed in the initial pelvic fin bud, but was expressed in the growing pelvic fin, most strongly at its posterior half. (Ei-Eii) hand2:eGFP expressing cells were expressed in the posterior rays of the dorsal fin. (Fi-Fii) hand2:eGFP expressing cells were expressed in the posterior-most rays of the anal fin. Lateral views, anterior is to the left.

Meanwhile, at the ventral midline, a group of hand2:eGFP expressing cells appeared to be moving anteriorly (Figure 3.2 Dii) and covered the entire ventral midline of the yolk extension by 48 hpf. Once the pre-anal fin fold began growing outwards, these hand2:eGFP expressing cells appeared to migrate into the fin fold in tandem. The outward growth was

completed around 80 hpf (Figure 3.2 Ii-Iii), after which the Hand2 begin to fade, suggesting that Hand2 was not being expressed as strongly.

In larval fish, hand2:eGFP expressing cells were predominantly located around the gut tube, comprising the smooth muscle and visceral peritoneum (Figure 3.3 Aii-Dii). These cells also contributed to the pharyngeal arches, heart tube, and pectoral fins, as previously described (L. M. F. Mao et al., 2021; Q. Mao et al., 2015). Surprisingly, Hand2 was not expressed in the initial pelvic fin bud itself though it appeared to have stronger expression in the body wall adjacent to the pelvic fin (Figure 3.3 Ci-Cii). Once the pelvic fins were more developed, Hand2 was expressed throughout the fin, most strongly in the posterior half (Figure 3.3 Di-Dii). I also noted hand2:eGFP expression in the posterior rays of the dorsal and anal fins (Figure 3.3 Ei-Fii).

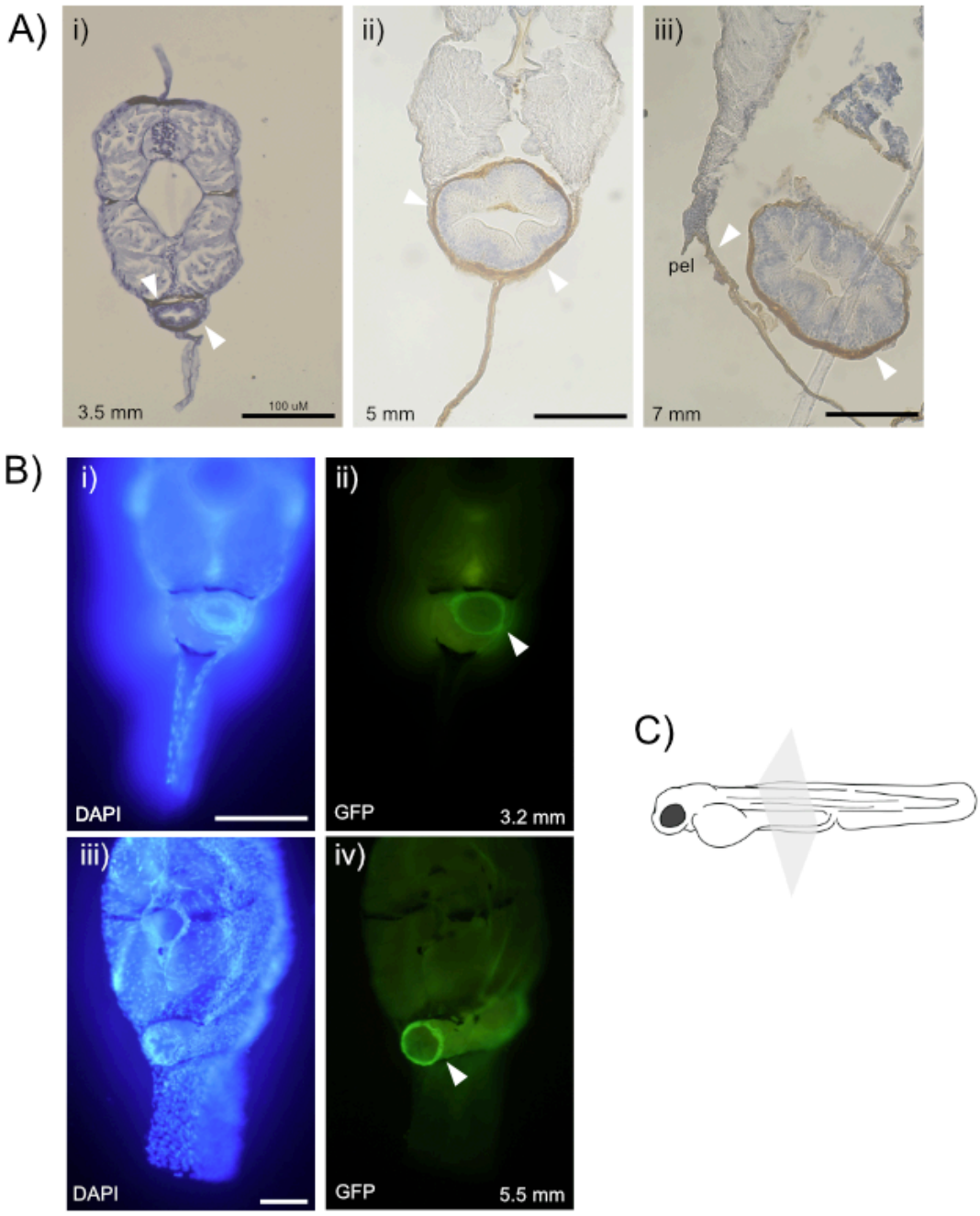

Figure 3.4 - Histology and antibody staining (anti-GFP) of the *Et(hand2:eGFP)ch2* line showed strong expression around the gut tube.

(Ai-iii) DAB staining of hemotoxylin-stained paraffin sections (8 µm sections), arrowheads pointing to DAB-stained gut lining and DAB-stained body wall (parietal peritoneum). Pelvic fin = pel. (Bi-iv) DAPI and Anti-GFP stains of vibratome sections (250 µm), arrowheads pointing to gut tube. Transverse views, dorsal to the top. (C) Approximate sectioning plane. Scale bars are 100 µM.

To localize the expression patterns of hand2:eGFP expressing cells more precisely, I sectioned larvae from the *Et(hand2:eGFP)ch2* line and performed anti-GFP antibody staining to reveal the distribution of hand2:eGFP expressing cells (Figure 3.4). The growth series from 3.2 mm – 7 mm in the paraffin sections (Figure 3.4A) showed a strong band of Hand2 expression (DAB staining, brown) around the gut tube, as well as a weaker signal in the parietal peritoneum lining the inside of the body wall. As seen from the whole mount staining, there were only a few cells with Hand2 expression in the early pelvic fin bud (Figure 3.4 Aiii). Vibratome sectioning produced thicker sections, which allowed me to clearly visualize the gut tube being lined with hand2:eGFP expressing cells (labeled with a GFP Alexa Fluor 488 secondary antibody) (Figure 3.4B).

In summary, my embryonic observations illustrated that there are two structures that contain LPM cells – the cells overlying the yolk extension, and the cells that invaded the pre-anal fin fold. In the larval observations, I found that the lining of the gut tube and the lining of the body wall (visceral and parietal peritoneum) were hand2:eGFP expressing and likely LPM-derived. To connect the embryonic expression data to the larval expression data, I next turned to observe Kaede lineage tracing to unpack the embryonic cell populations.

3.4.2 Cells from the dorsal LPM do not contribute to the pre-anal fin fold

I was interested to know whether the cells that ended up in the pre-anal fin fold were derived from the same population of cells as the bilateral dorsal stripes. To test this, I used Kaede-based lineage tracing. Kaede is a photoconvertible protein that will permanently change

from GFP to RFP upon activation by UV light. Kaede mRNA was injected into single-cell embryos and photoconverted at various timepoints to trace the movements of target cell populations. First, I converted cells at 18 hpf prior to the ventral migration of the bilateral dorsal stripes. Cells starting from the dorsal stripes, regardless of initial anteroposterior position along the yolk extension, never entered the pre-anal fin fold (Figure 3.5B, N=0/10 individuals had cells in the pre-anal fin fold). To determine the origin of the cells in the pre-anal fin fold, I converted cells along the ventral midline of the yolk extension and found that they indeed entered the fin fold (Figure 3.5B, N=8/13 individuals had cells in the pre-anal fin fold). These fin fold cells had the same cellular morphology – with a directed filopodium per cell - as the hand2:eGFP expressing cells seen in our previous observations (Figure 3.2 Fi-Ii). I was interested to see how early I could photoconvert these fin fold cells, and found that by converting the posterior-most region of a 12 hpf embryo, I was able to exclusively label these fin fold cells (Figure 3.5A).

To summarize, there are two separate populations of the hand2:eGFP expressing cells in the hindyolk area of the embryonic zebrafish – one that lies in bilateral dorsal stripes and encloses the yolk extension, and one that lies on the ventral midline, migrates anteriorly, and then invades the pre-anal fin fold.

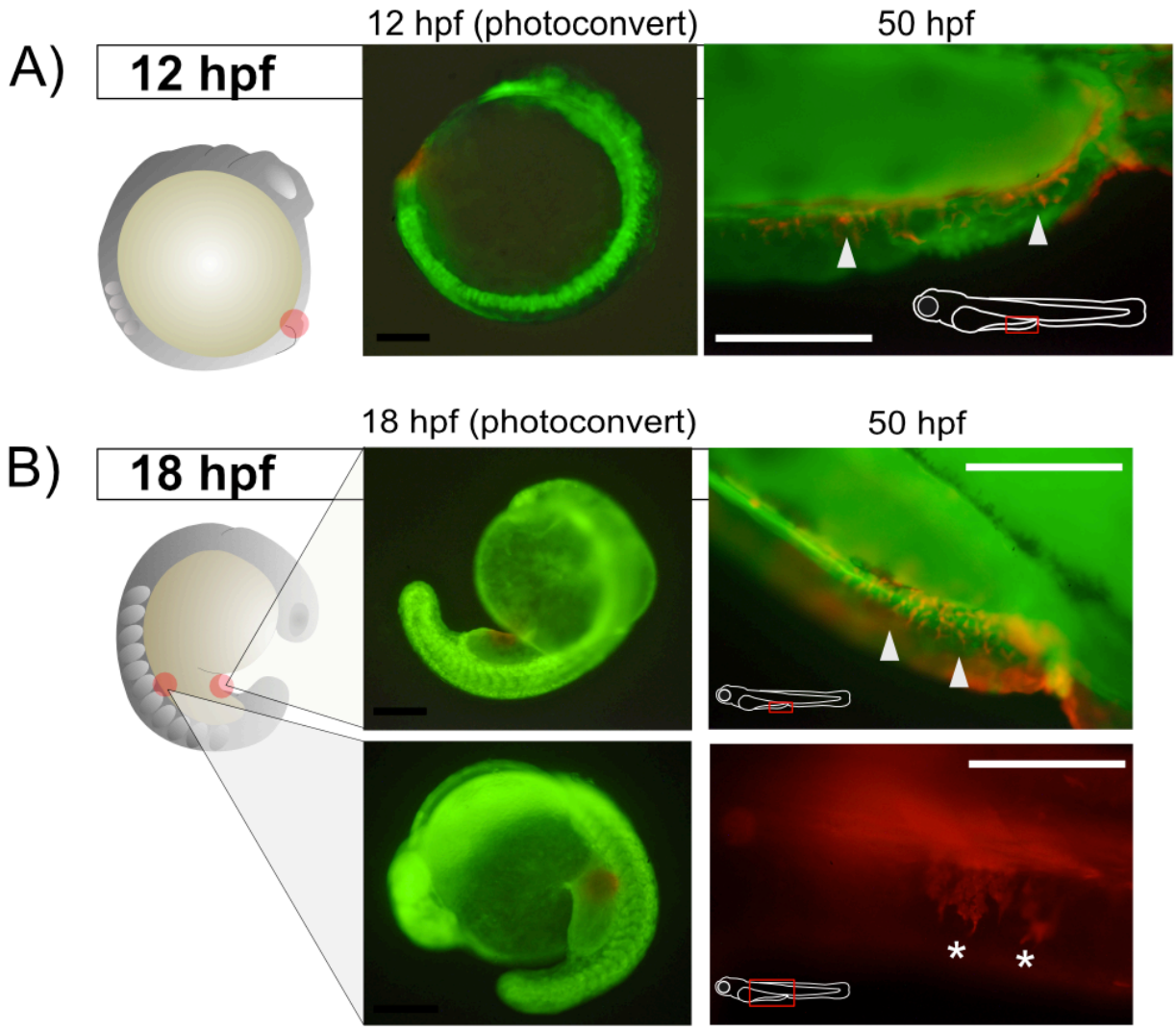

Figure 3.5 – Kaede lineage tracing experiments.

(A) The fibroblasts (white arrowheads) in the pre-anal fin fold were derived from a spot of mesoderm that is anterior and ventral to the tailbud at 12 hpf. (B) Cells from the ventral midline gave rise to the fibroblasts in the pre-anal fin fold (white arrowheads) while cells from the bilateral dorsal stripes encased the yolk extension (white asterisks) and never gave rise to pre-anal fin fold fibroblasts. Scale bar is 100 μM.

3.4.3 Cells from the dorsal LPM stripes migrate ventrally without significant anteroposterior movement

In order to visualize the cell movements of the ventrally-migrating bilateral dorsal stripes of LPM, I turned to confocal timelapsing of the *Et(hand2:eGFP)ch2* line. For the first three timelapses, I began imaging when the hand2:eGFP expressing cells began migrating, around 25-30 hpf (Figure 3.6A-C). Images were taken approximately every 14 minutes and then processed in FIJI to reveal the maximum intensity projection at each timepoint. Cells at the leading edge of the LPM stripes appeared to extend a single filopodia ventrally, followed by squeezing their cell bodies downward into the filopodium. Meanwhile, cells at the ventral midline could be seen crawling anteriorly (Figure 3.6A, C, yellow arrowheads). A later timelapse started at 35 hpf (Figure 3.6D) showed the yolk extension already mostly covered in hand2:eGFP expressing cells. Cells were still migrating ventrally in the last remaining uncovered distance to the ventral midline. Dorsal to the leading edge of the LPM, cells appeared to have much less directionality and their edges were in contact with each other, overall giving the impression that the LPM became more sheet-like than in earlier timepoints.

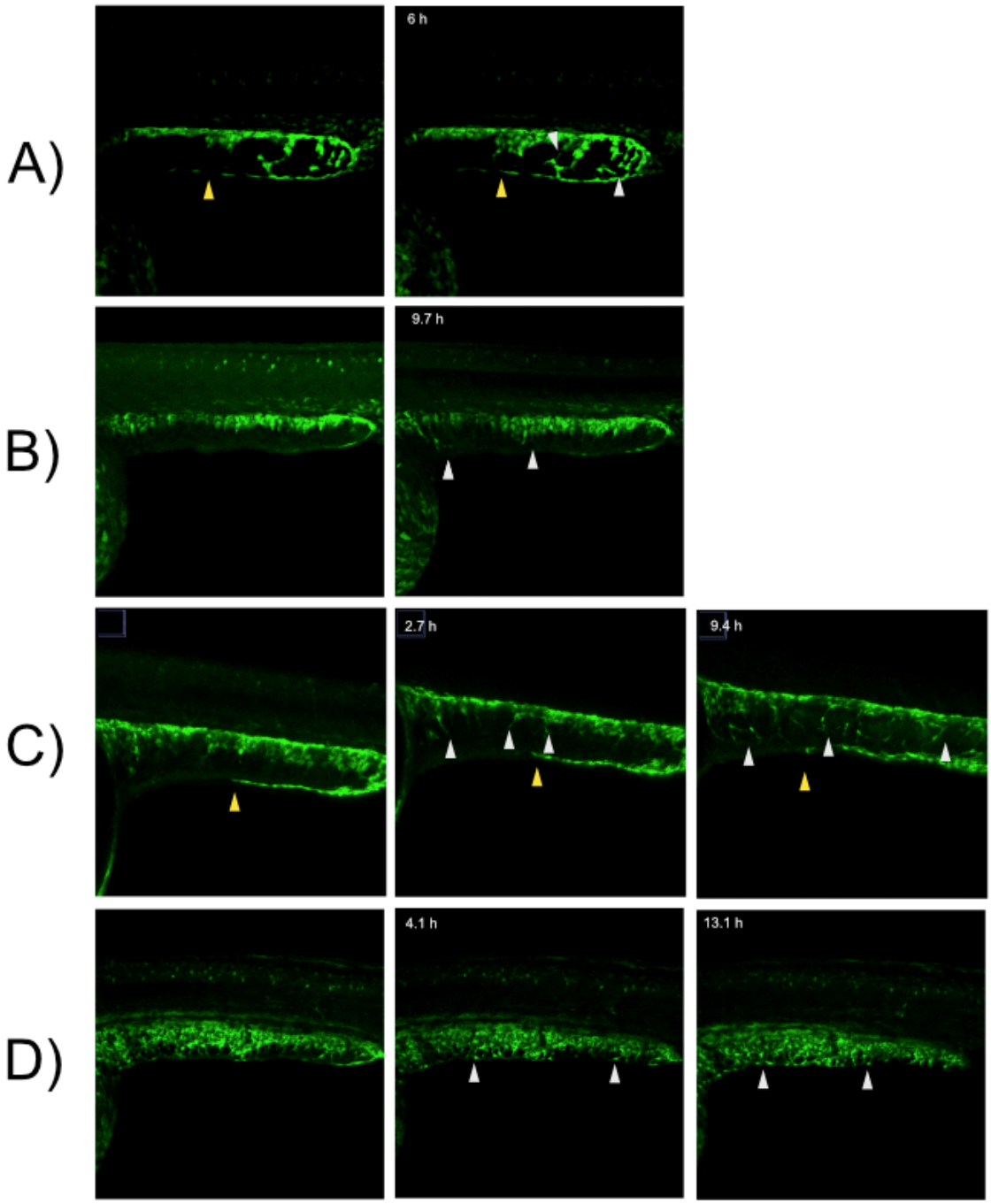

Figure 3.6 – Stills from confocal timelapses of the *Et(hand2:eGFP)ch2* line – four separate timelapses (A-D).

(A-C) Timelapses began around 25-30 hpf. (D) Timelapse began around 35 hpf. Time elapsed between frames is shown in the upper left hand corner of each frame. White arrowheads point to cells extending filopodia, yellow arrowheads point to the anterior extent of the ventral midline cells. (For timelapses B and D, the z-stack did not image deep enough to capture the ventral midline cells).

These confocal timelapses suggested that the bilateral dorsal LPM stripes were migrating ventrally without much anteroposterior movement. Because the ventral midline cell population migrated anteriorly before the dorsal LPM population reached the midline itself, it supported my previous findings that the ventral midline cells did not derive from the bilateral dorsal stripe population. However, a major drawback of the confocal was that it did not allow me to image for more than 12-13 hours at a time. This proved problematic as I was not able to capture the entire migration of the dorsal LPM cells. A collaboration was formed between our lab and that of K. Prummel from C. Mosimann's research group, where they generously shared their lightsheet data of a Hand2 reporter line *TgBAC(hand2:EGFP)*^{pd24} (Kikuchi et al., 2011). This lightsheet data was later published in (Prummel et al., 2022). Eric Yuan, an undergraduate, performed the cell tracking, developed an algorithm for correcting for growth and tilt (described in the methods chapter), and modified the R package CellTrackingEBA from (Boyle-Anderson et al., 2022) to accommodate this new type of data.

Around 45 cells were tracked across the yolk extension between 23 hpf and 65 hpf. The AP movement of these cells was plotted against time (Figure 3.7A). Cells were rarely able to be tracked for the entire time period (to be discussed in this chapter's discussion section), but for the portion of time that they were being tracked, they did not deviate substantially in AP position. Corroborating this finding, a plot of starting vs. final AP position of these cells indicated that there is little change in AP position (Figure 3.7B). For ML movement, we found that cells were migrating with the greatest speed between 23-44 hpf (Figure 3.7C) and then largely remained at

the same ML position for the remainder of the timelapse. In summary, (1) there was little AP movement of cells (2) most ML movement was between 23-44 hpf.

The combination of the confocal and lightsheet timelapses of hand2:eGFP reporter lines allow me to draw two conclusions: (1) the dorsal bilateral stripes and ventral midline cells are two separate populations and do not derive from one another, and (2) the dorsal bilateral LPM cells migrate ventrally over the yolk extension without significant AP movement. The second conclusion, in particular, is critical as it allows the labeling of cells at 2 or 3 DPF at a particular somite level with the understanding that the cell will likely not migrate to other AP levels. This forms the basis for my laser-mediated heat shock labeling technique, described next, that will allow me to label cells permanently.

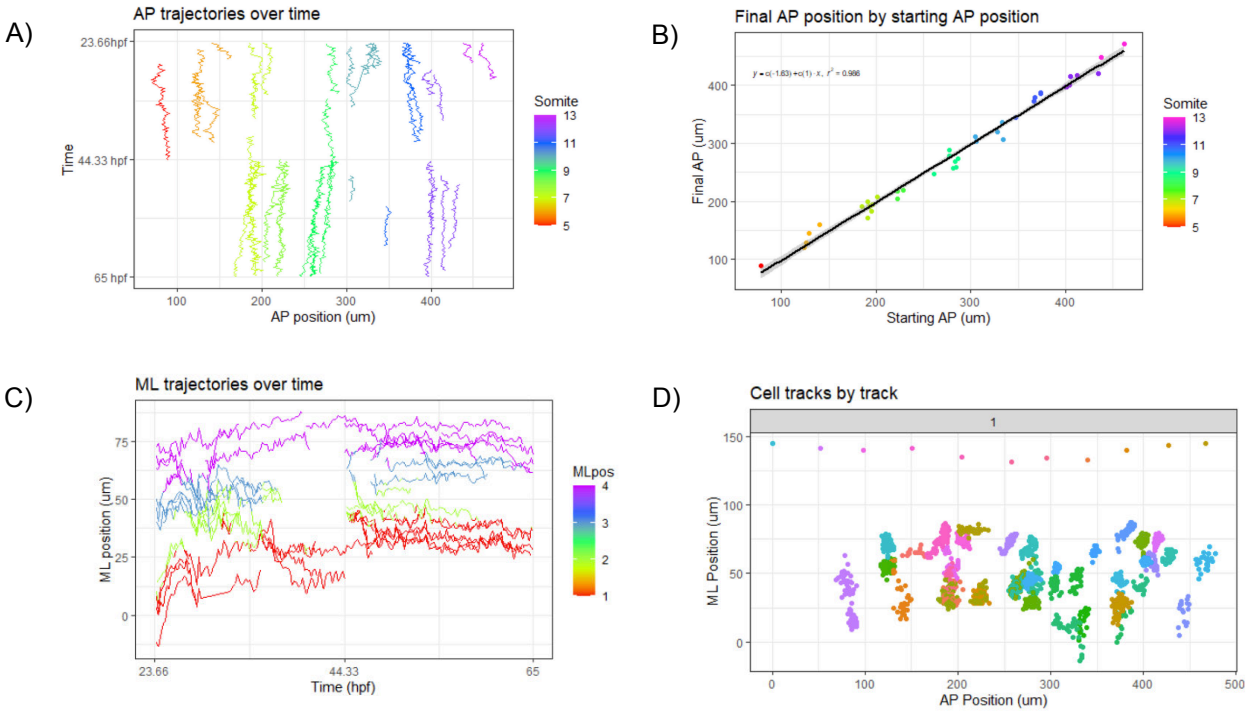

Figure 3.7 - Cell tracking of hand2:eGFP expressing cells from lightsheet data.

AP position ranges from 0-500 µm, with lower numbers more anterior. ML position ranges from 0 to 100 µm, with lower numbers more medial. (A) Cell tracks, color-coded by somite, plotted with AP position by time. Cells were migrating without significant change in AP position. (B) Final AP position by starting AP position of cell tracks (C) ML trajectories over time, color coded into quartiles, with purple being the most lateral. (D) Cell tracks by track to show overall movements in two dimensions, with each individual track color-coded with its own color. Data and graphs generated by Eric Yuan. Code was modified from (Boyle-Anderson et al., 2022).

3.4.4 Generation of the Tg(hsp70:cre-ert2) line

Because Kaede mRNA degrades after 3-4 DPF, I required a labeling technique that would allow me to track cells for up to 3-4 weeks post fertilization. DiI labeling was attempted, but with the rapid rate of cell divison in the growing larva, its fluorescence became too faint to follow after one week. I generated the *Tg(hsp70:cre-ert2)* line, that when crossed with the *Tg(ubi:switch)* line (Mosimann et al., 2011) (Figure 3.8A), would allow me to label a group of selected cells using an infrared laser. After generation of the line and screening (see Methods chapter), F2 founders were identified by ensuring that global heat shock labeled all cells consistently, and that there was limited ectopic, uninduced fluorescence (Figure 3.8B).

With the infrared laser, I was able to successfully induce Cre-ERT2 expression in a ubi:switch background in many different tissue types (Figure 3.9A-C). I showed that brain tissue, caudal fin mesenchyme, lateral plate mesoderm in the parietal peritoneum, and epithelial cells in the pre-anal fin fold can be labeled and tracked for over one month post fertilization. While I did notice some ectopic, uninduced, especially in muscle cells, these cells are usually distinguishable from laser-induced cells as they did not appear in discrete clones.

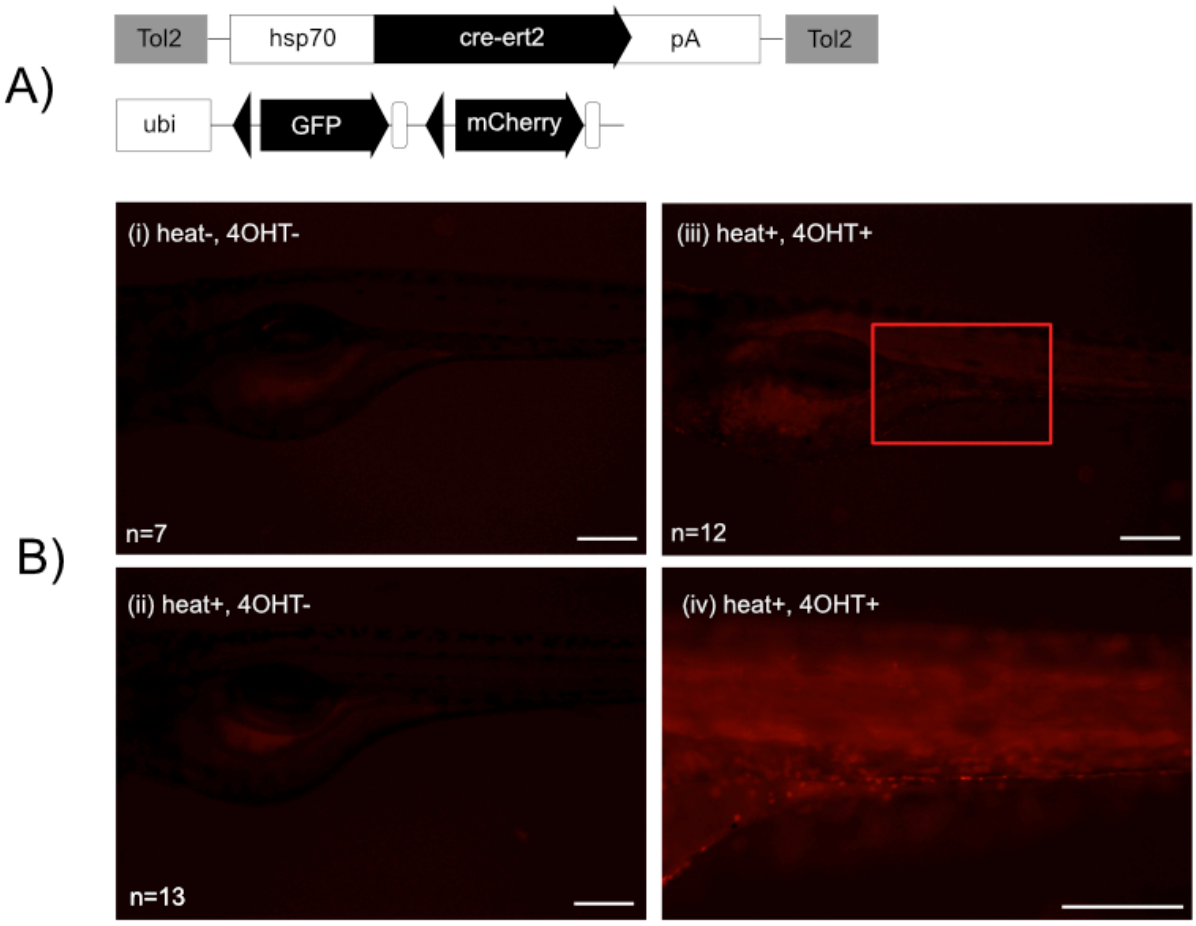

Figure 3.8 - Constructs of the *Tg(hsp70:cre-ert2)* and *Tg(ubi:switch)* (Mosimann et al., 2011) line and testing of the progeny between the lines.

(A) Construct diagrams (B) Successful global heat shock testing of an F2 founder of the line – (i-ii) controls, (iii-iv) application of both heat shock and tamoxifen. Scale bar is 100 μM.

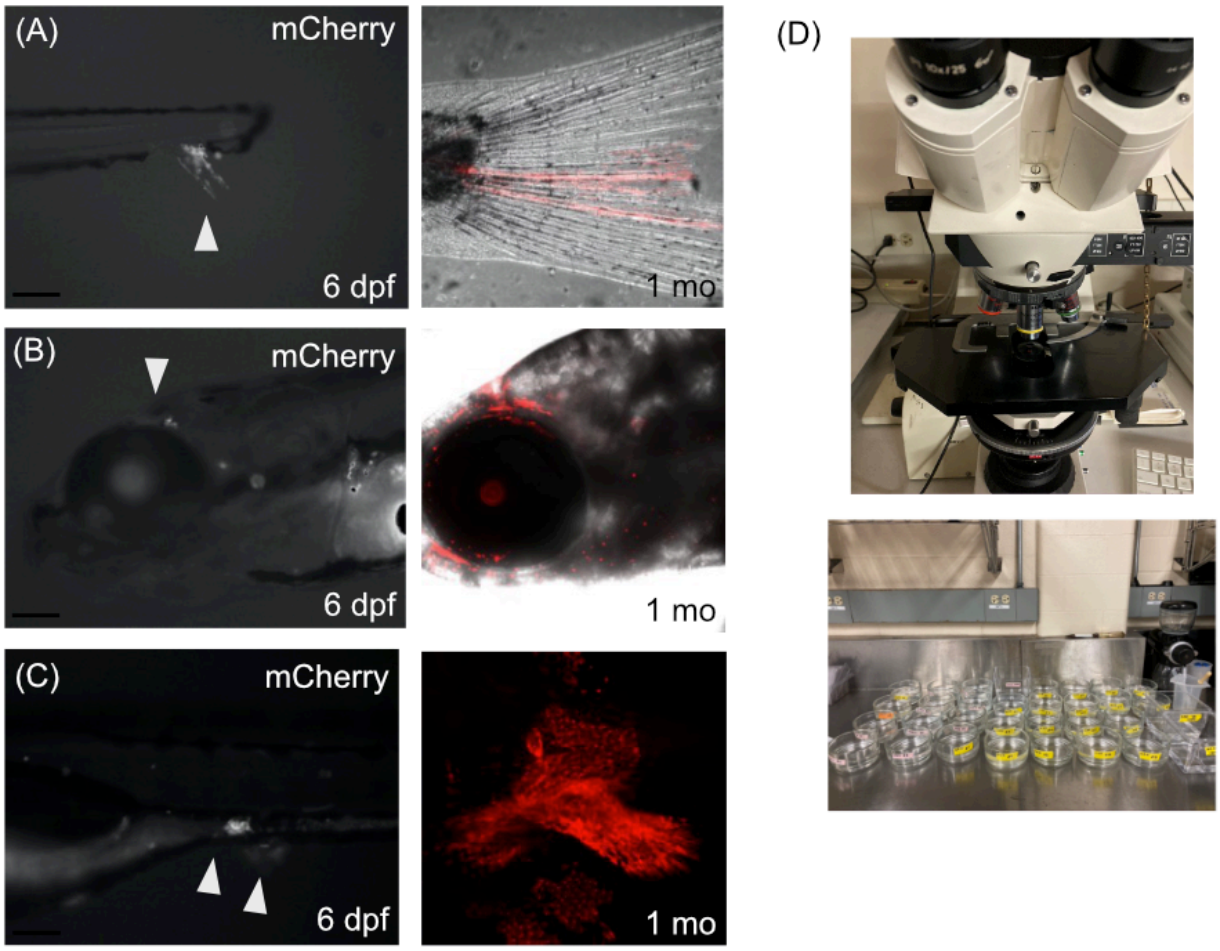

Figure 3.9 - Examples of the infrared laser-mediated heat shock technique.

In A-C, the first column is expression of mCherry a few days after the laser heat shock, and the second column is mCherry expression after 1 month. (A) Labeling of the caudal fin (B) Labeling of brain cells (C) Labeling of the parietal peritoneum over the yolk extension and pre-anal fin fold, leading to expression in the developing pelvic fin and pre-anal fin fold at 1 month post fertilization. (D) Laser set up (described in Methods chapter) and individual housing of fish. Scale bar is 100 μM.

3.4.5 Neural crest was not labeled in the heat shock activation experiments

To rule out the possibility that neural crest was being labeled with the infrared laser, the transgenic line *Tg(sox10(7.2):mRFP)vu234Tg* (Kucenas et al., 2008) was examined throughout larval development. *Tg(sox10(7.2):mRFP)* is used as a reporter line for neural crest (Chimal-Monroy et al., 2003; Rocha, Singh, Ahsan, Beiriger, & Prince, 2020). At 2 DPF, there was no *sox10* expression in the yolk or yolk extension, indicating that this area (red box, Figure 3.10A) is free from neural crest. Larvae were further followed from 3.5 mm to 8 mm, upon pelvic fin development, and there continued to be little *sox10*-expressing neural crest in the ventral regions barring pigment cells (Figure 3.10B-F). At 8mm SL, there is *sox10* expressed in the endoskeletal pelvic girdle, which was likely related to chondrogenic activities (Figure 3.10E-F).

Next, I examined the pelvic fin rays in an individual in which the heat-shocked, labeled cells had been incorporated into the pelvic fin. I found that labeled cells formed solid cores of the fin rays (Figure 3.10G-L), whereas neural crest cells are known to only lie on the surface of the rays (Lee, Thiery, et al., 2013). Confocal slices of the fin rays showed that the labeled cells indeed form solid rods, as they could be seen in successive slices (Figure 3.10I-L). Therefore, the laser-labeled cells are likely not neural crest.

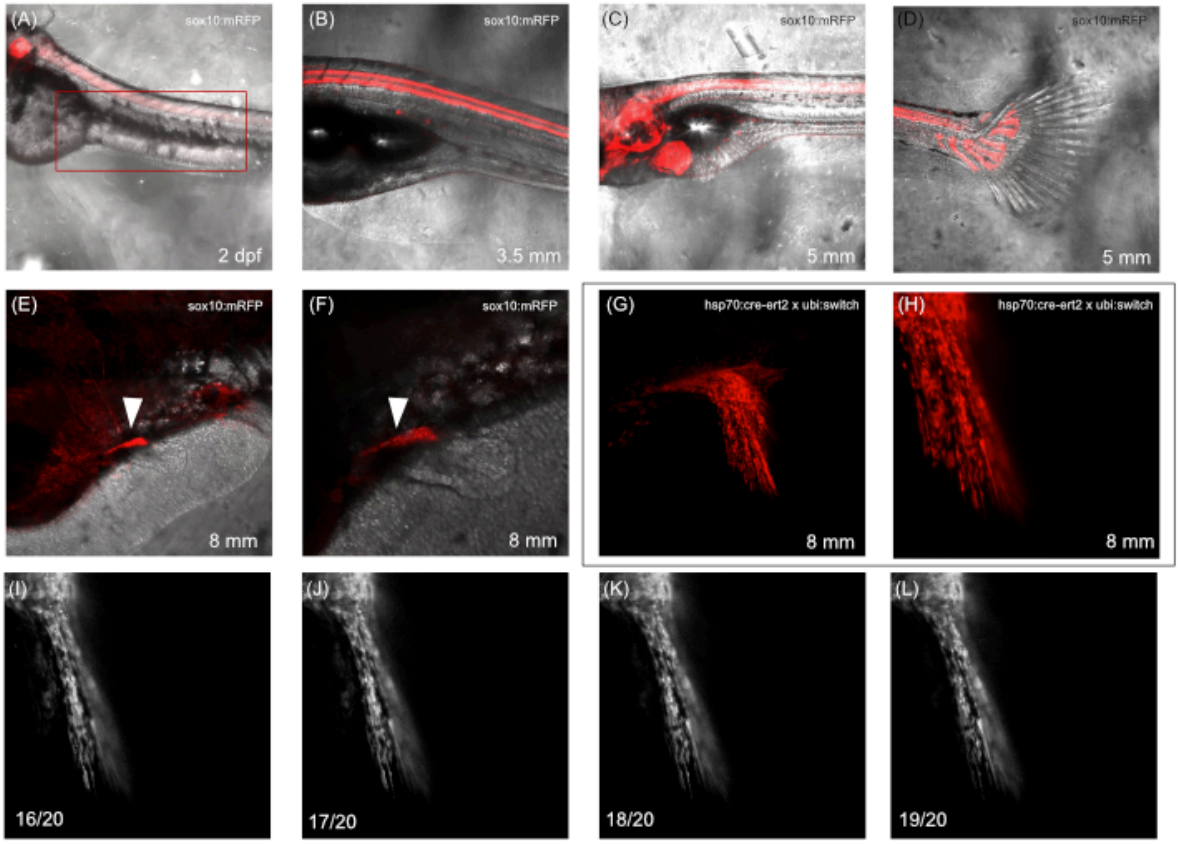

Figure 3.10 – Expression of the *Tg(sox10(7.2):mRFP)vu234Tg* line (A-F) and distribution of labeled cells in the heatshock system (G-L).

(A) Embryonic expression of *sox10* revealed no neural crest present in the yolk extension (B-D) Limited neural crest in the ventral body wall, excepting pigment cells (E-F) *sox10* was expressed in the pelvic girdle (white arrowheads) but not the fin itself, F is increased magnification (G-H) Labeled cells in the pelvic fin rays of the heat shock line constituted solid rods of the fin rays. H is increased magnification of G. (I-L) Successive confocal slices of H, showing that the labeled cells were at the core of the fin rays and not lining the outside of each ray. Numbers at bottom left represent the slice level.

3.4.6 Cells from the pre-anal fin fold do not migrate out of the pre-anal fin fold into the pelvic fin

To determine whether cells in the pre-anal fin fold migrate out and form the pelvic fin bud, I labeled cells in the pre-anal fin fold at 3 DPF. Examples of this labeling can be seen in Figure 3.11. For all individuals in which we exclusively labeled pre-anal fin fold cells (n=9/9) and raised to pelvic fin stage, there were no cells within the pelvic fin that were labeled (Figure 3.11A-B). Furthermore, in numerous individuals where the pre-anal fin fold was labeled alongside the body wall, cells clearly showed the same distribution and arrangement throughout the individual's development (Figure 3.11C). I did not find any evidence of pre-anal fin fold cells with a migratory morphology (i.e. directional filopodia).

3.4.7 Cells from the parietal peritoneum from somite levels 6-11 contribute to the pelvic fin bud

As the pre-anal fin fold was ruled out as the repository for pelvic fin precursor cells, I next turned to the future parietal peritoneum as the other possible source. At 2-3 DPF, I aimed the infrared laser at the LPM cells covering the yolk extension. These cells were at the level of somites 6-14. Clone size was variable depending on laser power and mounting, so I classified these into "small" (equal or lesser than 2 somite lengths, approximately less than 50 cells) and "large" (larger than 2 somite lengths, approximately greater than 50 cells).

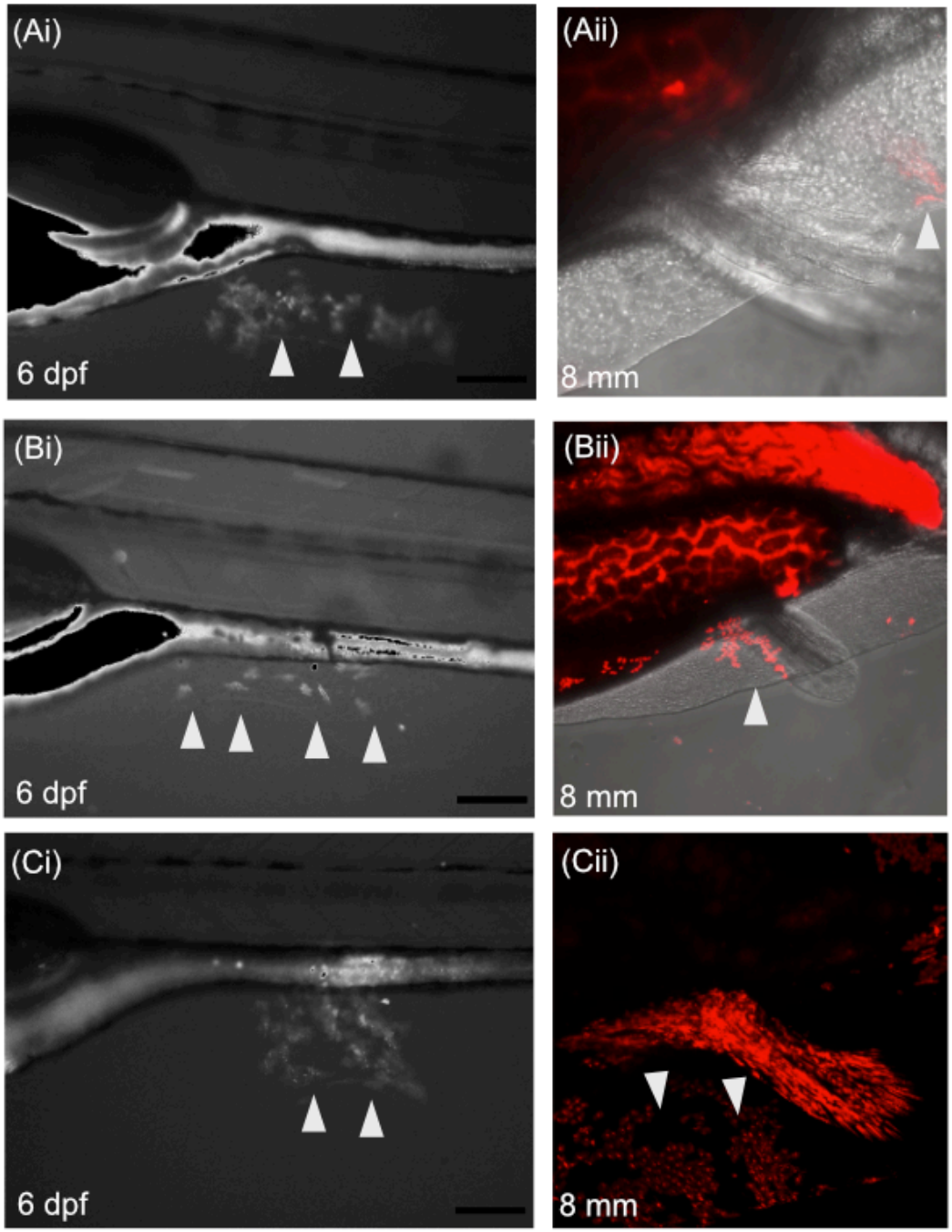

Figure 3.11 - Cells in the pre-anal fin fold do not give rise to the pelvic fin.

Individuals were from a *Tg(hsp70:cre-ert2) x ubi:switch* background and treated with an infrared laser. (Ai, Bi) Conversion of pre-anal fin fold cells, observed at 6 dpf (white arrowheads) (Aii, Bii) Resulting individual without labeled cells in the pelvic fin, but with continued labeling in the regressing pre-anal fin fold (white arrowheads). (Ci-Cii) Incidental labeling of pre-anal fin fold

revealed that cells are static and do not migrate, as they were labeled in the same pattern from 6 dpf to 8 mm (white arrowheads). Scale bar is 100 μM.

Somite level (most anterior)	Total individuals	Total # with pelvic fin fate	2 dpf # pelvic fin fate	3 dpf # pelvic fin fate	Total % with pelvic fin fate	Small clones only
6	9	1	1	0	11%	0%
7	16	1	0	1	6%	6%
8	21	3	0	3	14%	14%
9	19	5	2	3	26%	21%
10	18	2	0	2	11%	11%
11	10	2	0	2	20%	20%
12	3	0	0	-	0%	0%
13	4	0	0	-	0%	0%
14	5	0	0	-	0%	0%

Table 3.1 - Frequency of pelvic fin fate based on somite level of conversion over the yolk extension. The 2 dpf and 3 dpf columns indicate the time at which the individual was heat shocked. Small clones are defined as <2 somite widths in the initial labeling.

A total of 105 individuals survived to the pelvic fin stage, out of 316 total individuals. Of these 105 individuals, I was able to label cells that reached pelvic fin fate from somite levels 6-11 (Table 3.1). I propose that these boundaries represent the anteroposterior extent of the pelvic fin precursors in the parietal peritoneum. To account for imprecision based on the size of the initial conversion (e.g. individuals coded as starting from somite 6 may have labeled cells reaching to somite 9, as the somite coding was based on the most anterior somite), I filtered the data so that only individuals with small clones (<2 somite-lengths) were considered. I found that anteroposterior boundaries of the pelvic fin precursor cells shrunk to somite levels 7-11, and the distribution of frequency of conversion became more bell-shaped, with its peak at somite levels 8-10. A complete list of the somite-level range labeling associated with each individual can be

found in Appendix B.

I noted a difference in pelvic fin conversion fate between individuals converted at 2 DPF and 3 DPF, despite approximately the same total number of individuals (2 DPF = 55, 3 DPF = 50 individuals). The 2 DPF condition seemed to have fewer individuals with pelvic fin fate. Since the LPM is migrating ventrally around this time, I hypothesized that I might not be reaching the precursor cells at 2 DPF. For instance, if the laser were aimed at the dorsoventral center of the yolk extension, it may miss dorsal cells that have yet to migrate ventrally. I categorized the data into where the laser was aimed dorsally (using labeling of the myomeres as a proxy) and centrally. In all 2 DPF fish where the pelvic fin was eventually labeled, the laser was aimed dorsally. In 3 DPF fish, there was approximately the same chance of achieving pelvic fin fate regardless of a dorsal or central conversion.

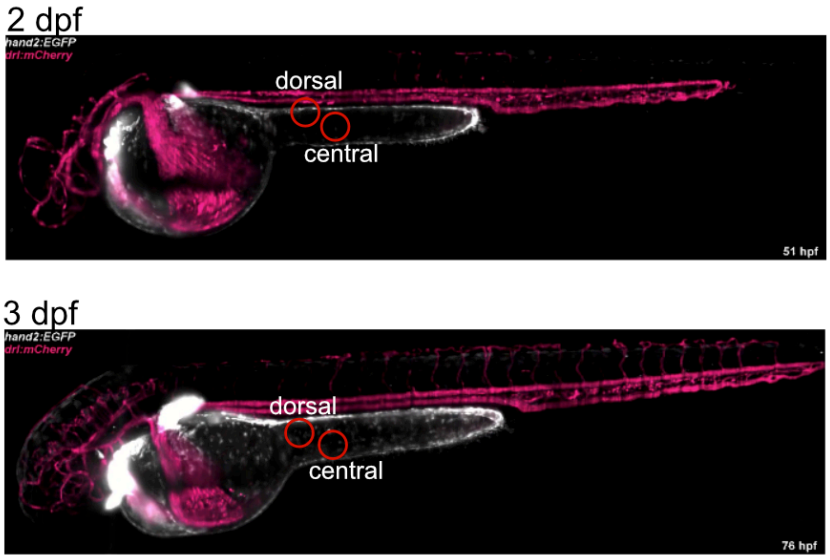

Figure 3.12 - Dorsal vs. central conversion locations at 2 DPF and 3 DPF.

Note that central conversions at 2 DPF may miss cells that have yet migrate ventrally. Stills taken from lightsheet data from Prummel et al. (2022).

total

Somite level	Percent with gut	Percent with myomeres	Percent with pelvic fin muscle	Percent with epithelium	Percent with preAFF
6	89%	44%	0%	44%	22%
7	94%	31%	0%	56%	81%
8	100%	43%	5%	43%	62%
9	100%	42%	21%	21%	68%
10	100%	50%	6%	44%	72%
11	90%	40%	0%	30%	70%
12	100%	33%	0%	33%	67%
13	100%	100%	0%	25%	25%
14	80%	40%	0%	20%	40%

3 dpf

Somite level	Percent with gut	Percent with myomeres	Percent with pelvic fin muscle	Percent with epithelium	Percent with preAFF
6	75%	25%	0%	0%	25%
7	67%	17%	0%	50%	67%
8	67%	27%	0%	27%	60%
9	79%	21%	14%	7%	71%
10	50%	50%	13%	25%	75%
11	67%	33%	0%	67%	67%

2 dpf

Somite level	Percent with gut	Percent with myomeres	Percent with pelvic fin muscle	Percent with epithelium	Percent with preAFF
6	60%	60%	0%	80%	20%
7	80%	40%	0%	60%	90%
8	50%	83%	17%	83%	67%
9	80%	100%	40%	60%	60%
10	60%	50%	0%	60%	70%
11	57%	43%	0%	14%	71%
12	100%	33%	0%	33%	67%
13	75%	100%	0%	25%	25%
14	40%	40%	0%	20%	40%

Table 3.2 - Frequency of labeling other tissue types based on somite level. Separated into total data, then filtered by 3 DPF conversions and 2 DPF conversions. preAFF = pre-anal fin fold.

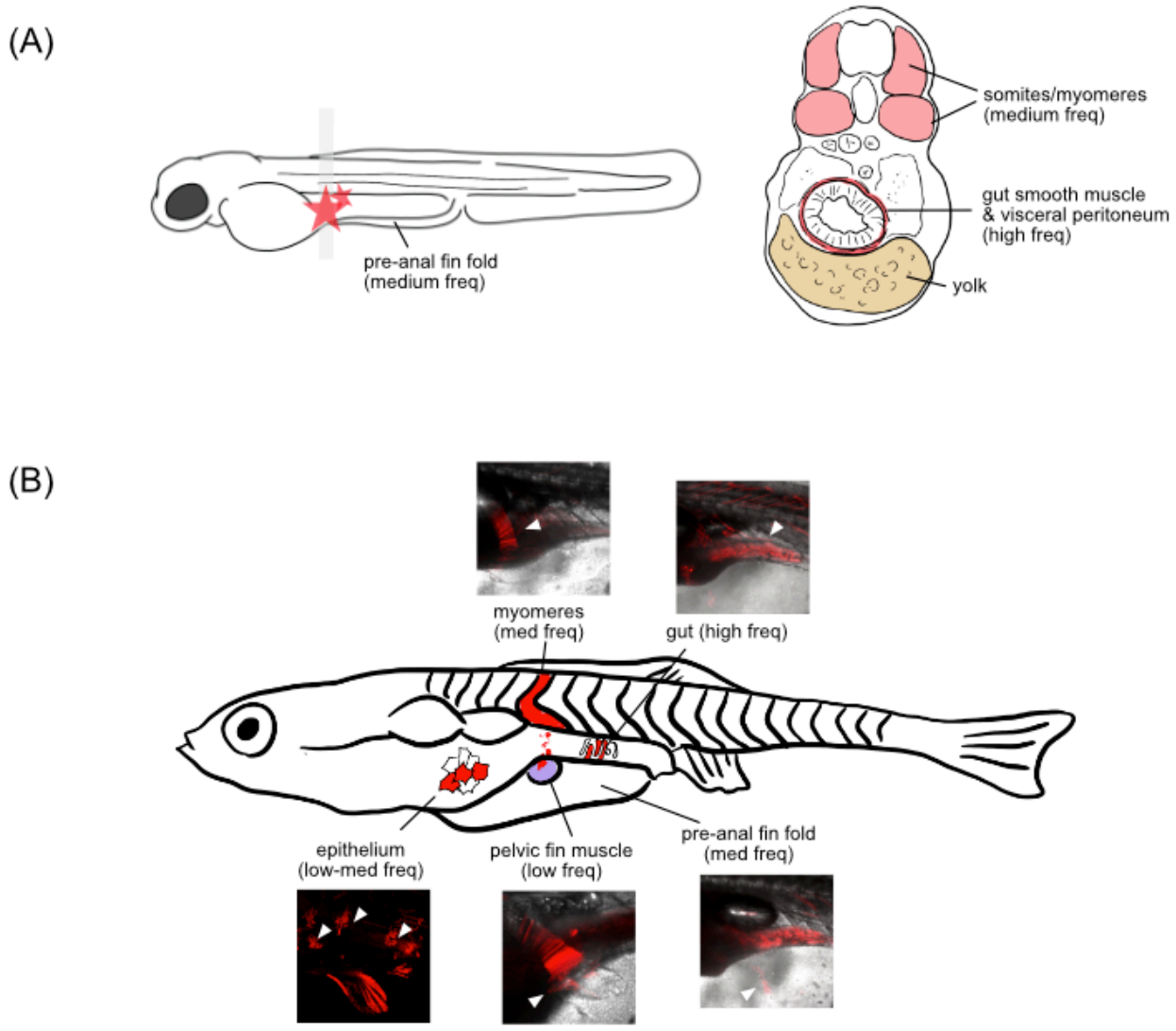

Figure 3.13 - Tissues other than the lateral plate mesoderm were frequently labeled.

Tissues are labeled here with their approximate frequency according to Table 3.2. (A) 3 dpf embryo. Red stars represent a potential labeling spot – note how the laser path may include other tissues. Right panel represents transverse section at labeling location, showing structures that were also frequently labeled. (B) Larval fish at pelvic fin stage with photos of labeled tissues (arrowheads).

It is inevitable that other tissues are also labeled. The somites (myomeres) are dorsally adjacent to the yolk extension, the pre-anal fin fold is ventrally adjacent to the yolk extension, the smooth muscles of the gut and visceral peritoneum arise from the same bilateral stripe population as the parietal peritoneum (Gays et al., 2017; Prummel et al., 2022), and the epithelium overlies the lateral plate mesoderm (Figure 3.13A). Gut tissue was the most frequently labeled, followed by myomeres, epithelium, and then the occasional pelvic fin musculature (Figure 3.13). Pelvic fin musculature arose when the somites 8-9 were labeled, and the myomeres that develop from these particular somites are known to contribute migratory muscle precursors to the pelvic fin (Cole et al., 2011) (Appendix B).

3.5 DISCUSSION

In this chapter, I have shown that the pelvic fin precursors arise from within somite levels 6-11 of the parietal peritoneum. When considering only small clones, I refined the precursor space to somite levels 7-11. Cells from the parietal peritoneum migrate ventrally down the yolk extension without notable anteroposterior displacement. Additionally, I have shown that the pre-anal fin fold is populated by hand2:eGFP expressing cells that are separate from those that will comprise the parietal peritoneum, and that these pre-anal fin fold cells will not contribute to the future pelvic fin.

3.5.1 Comparisons to previous studies

This work expands upon previous attempts at tracking the movements of the LPM over the yolk extension to determine the location of the pelvic fin precursors in zebrafish. As described in Chapter 1, Murata et al. (2010) used DiI injections in the LPM to trace its movements (Figure 3.14). Their findings can be summarized as (1) DiI-injected LPM at one somite level at 16 hpf will expand to cover multiple somite levels as the yolk extension forms (2) due to allometric growth, what was once somite level 14 becomes somite level 8 over the span of development (3) cells from somite levels 13-14 will be sequestered at somite level 7-8 and be incorporated into the pelvic fin bud. The scope of this thesis does not include testing findings 1-2, but personal observations deem this plausible – it can be imagined that the initial DiI spot is lengthened anteroposteriorly during the yolk extension, and then migrates ventrally at 30 hpf. However, the sequestration of the DiI labeled cells into one constrained area that is happening at 5 dpf is puzzling, as this implies active migration of DiI-labeled cells into one region. I do not find evidence of convergence during heat shock labeling between 2 dpf and 6 dpf (clones of cells remain the same size, if not expanding slightly as cells divide). One possible explanation for the pattern seen in Murata et al. (2010) is that DiI fluorescence may be fading by 5 dpf, as rapid cell division can dilute fluorescent signal.

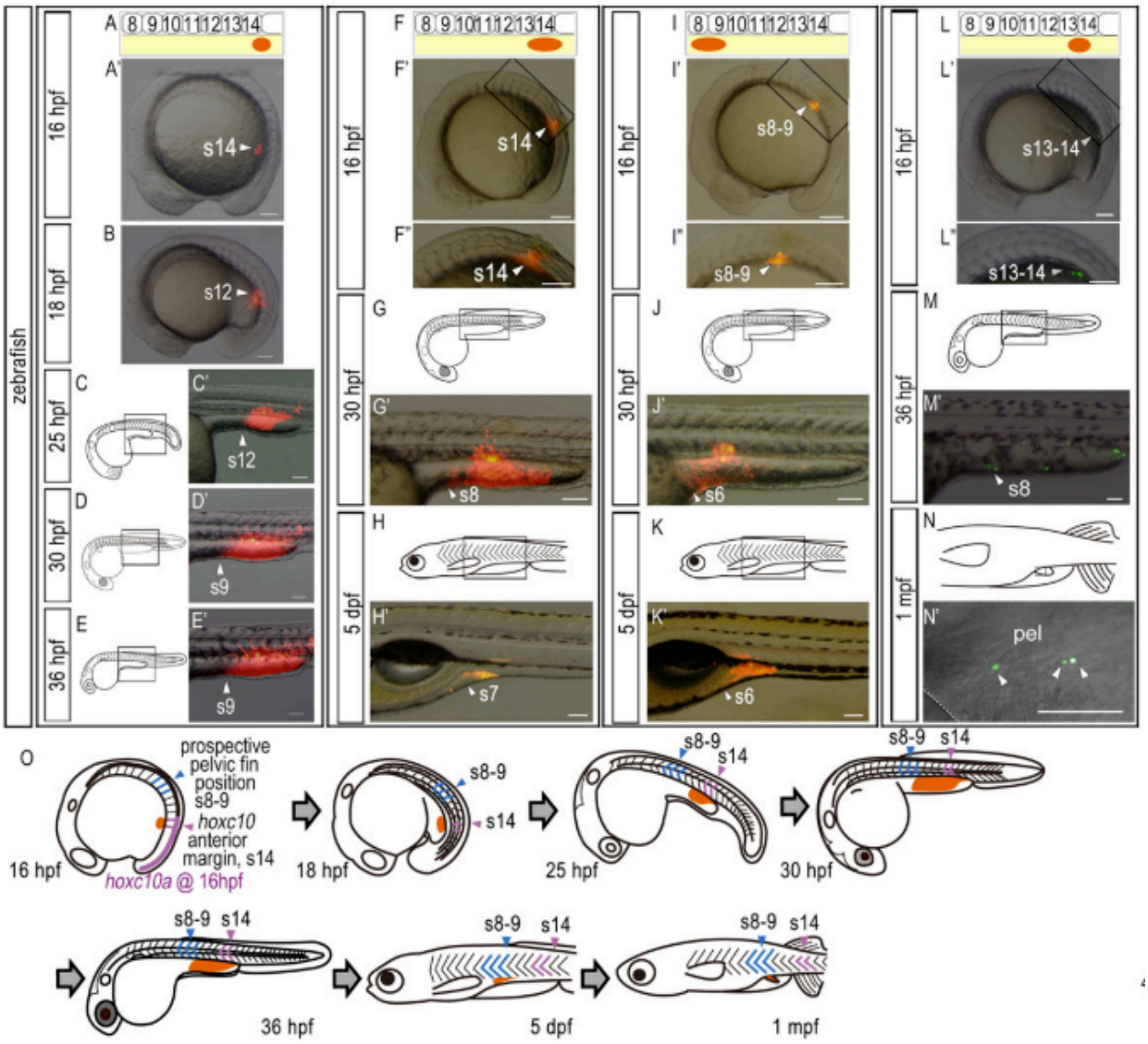

Figure 3.14 - From Murata et al. (2010).

Columns represent various locations of DiI injections (orange) and the resulting distribution of DiI over development. DiI injections at somite level 14 appear to spread to the posterior half of the hindyolk (A-E). DiI injections at somite level 13-14 cover hindyolk and become "sequestered" at 5 dpf at somite level 7 (F-H). DiI injections at somite levels 8-9 become "sequestered" at 5 dpf at somite level 6 (I-K). Quantum dot application at somite 13-14 can be traced to the pelvic fin bud at 1 month, but are also seen in various parts of the hindyolk at 36 hpf (L-N). The bottom diagrams represent Murata et al. (2010)'s model for their DiI experiments.

Importantly, the study from Murata et al. (2010) suggests that only cells from somite levels 7-8 at 5 dpf will give rise to the pelvic fin. In contrast, I found that at 6 dpf, cells from somite levels 6-11 have the potential to be pelvic fin precursors. Not only do my findings expand the boundaries of the pelvic precursors, but they also raise the possibility that because there is such a large potential precursor field, pelvic fin cells may not actually be specified until later in larval development. Murata et al. (2010) connects the somite 13-14 level with the anterior boundary of *hoxc10a* expression since the anterior expression boundaries of the Hox10 paralog group is thought to correlate with hindlimb position in tetrapods. However, if the pelvic fin precursors are not located at an exact boundary but over a swath of the yolk extension, then the anterior boundary of *hoxc10a* may not demarcate the pelvic fin precursor cells in the embryo.

3.5.2 Embryonic LPM movements: limitations of the study

Recent work from Prummel et al. (2022) shows that the lateral plate mesoderm is fated to become the visceral peritoneum and the parietal peritoneum in zebrafish, and that Hand2 is a marker of these tissue layers. My work expanded upon the lightsheet imaging that the authors performed and characterized the migration dynamics at a cellular level. While hand2:eGFP expressing cells over the yolk extension generally migrate ventrally with little anteroposterior movement, there are areas that could merit further clarification. First, it has been shown that during pelvic fin initiation, only a small number of cells appear to be involved (Grandel & Schulte-Merker, 1998). If the specification of the pelvic fin cells occurs early, during embryogenesis, it is possible that there are only a handful of precursor pelvic fin cells migrating ventrally over the yolk extension. Furthermore, it is a possibility that these cells may not have

been included in our sampling. These cells might have a different migration trajectory than the rest of the parietal peritoneum, for example, converging and therefore having significant anteroposterior movement. I do not find evidence of this with visual observations, but I acknowledge it as a possibility.

Second, I note that the cell tracking was performed on a transgenic line, and therefore relied on the expression of hand2:eGFP expressing cells. This is reflected in the data, where hand2:eGFP expressing cells could not be followed for the duration of the timelapse (Figure 3.7A). There are two possible reasons for this: one, the expression of Hand2 in these cells waned, and these cells could not be tracked. Alternatively, it is possible that the cells that fade are splanchnic mesodermal cells migrating medially towards the developing gut tube, and went beyond the imaging boundaries. To differentiate between these scenarios, future lightsheet imaging of the Hand2 reporter line should use a double transgenic with a nuclear marker (e.g. H2A:mCherry).

3.5.3 Movements of yolk extension LPM cells compared to secondary heart field and pectoral LPM

A major difference between the ALPM of the secondary heart field (anterior to somite 1) and the PLPM of the pectoral fin field (somite levels 1-5) is that the pectoral fin field is spatiotopic, whereas the secondary heart field field is not (Boyle-Anderson et al., 2022; L. M. F. Mao et al., 2021; Q. Mao et al., 2015). That is, the more anterior parts of the LPM contribute to the more anterior parts of the pectoral fin, and the more posterior parts of the LPM contribute to

the more posterior parts of the pectoral fin (e.g. position in the pectoral fin is dependent on initial position in the LPM). In contrast, migration in the secondary heart field field is more random, and the cell types are not segregated by AP position.

Here, at somite levels 6-14, I found that the formation of the parietal peritoneum is spatiotopic, as cells migrate ventrally without much AP movement. There is limited evidence that the pelvic fin bud could be spatiotopic as well. In an individual where LPM was labeled at somite 11, the posterior boundary of the precursors, only the posteriormost corner of the pelvic fin bud contained labeled cells (Figure 3.15). However, in all other cases where cells were found in the pelvic fin, there was no regionalization of the cells within the bud. Instead, the entirety of the pelvic fin bud was usually populated with labeled cells.

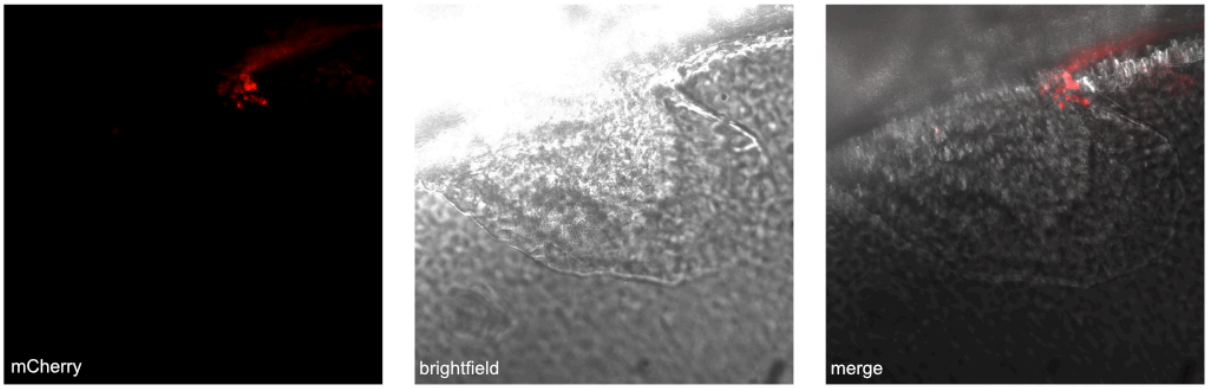

Figure 3.15 - Labeling of cells at the somite 11 level at 2 DPF led to a contribution of cells to the posterior portion of the pelvic fin only in this individual (n=1).
Individual was imaged at 8 mm SL. Anterior to the left, ventral to the bottom of the images.

This thus presents an interesting question – how are cells spanning as anteriorly as somite level 6, and as posteriorly as somite level 11, all potentially contributing to the pelvic fin bud,

which is at somite levels 8-9? It is especially perplexing given that we have shown there is little AP movement during the embryonic formation of the parietal peritoneum, the tissue layer that will contain the precursor pelvic fin cells.

The period of growth between 6 dpf and 3 weeks for zebrafish is rife with anatomical change. The anterior swim bladder buds off and inflates, the gut tube widens and loops, and gonads fill the body cavity. For the body cavity to accommodate these additional structures, the body cavity bulges ventrally, as seen in Figure 3.16. This necessarily requires some remodeling of the epithelium and the parietal peritoneum that lines it, as they will need to expand ventrally.

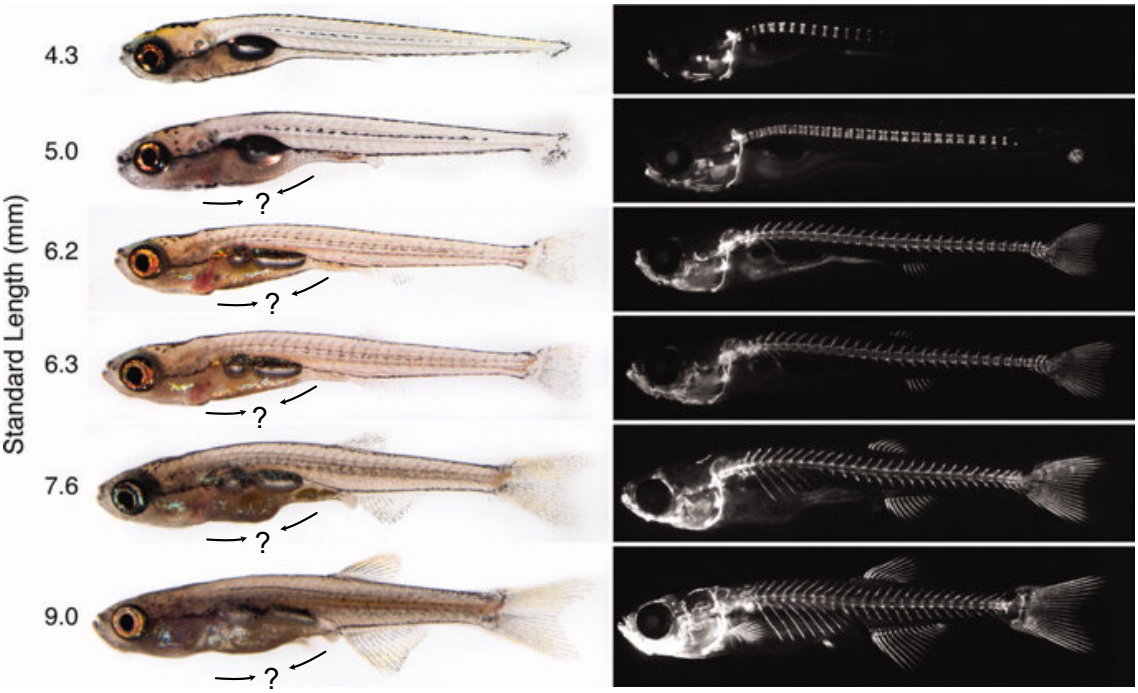

Figure 3.16 - Stages of zebrafish larvae from Parichy et al. (2009).

Arrows and question marks in brightfield images have been added to show possible differential growth of the body cavity, and therefore anteroposterior compaction.

It is tempting to speculate that as the body cavity expands ventrally, differential growth "pulls" in the body cavity at its most ventral point (~somite 5). Indeed, some form of anteroposterior contraction is occurring, as the somite-level of the anus shifts from somite 16-17 at 6 dpf, to somite levels 13-14 at pelvic fin stage (~7 mm SL). This anteroposterior contraction could account for why there is such a large initial field from somite levels 6-11 – the most posterior portions of the body wall could be compacted, resulting in a concentration of cells near the prospective pelvic fin region (somite level 8-9).

I have not observed any evidence of active migration of labeled cells in the parietal peritoneum. Instead, the clone of cells retained its shape as a coherent group. Additionally, preliminary observations showed that clones of cells tend to shift towards the future ventral-most portion of the body wall, somite level 6, during larval growth (Figure 3.17). Cells that were posterior to somite level 6 tended to shift anteriorly, and cells around somite level 6 remained at that somite level. (We did not label cells anterior to somite 6, though that would be the logical next step to test this hypothesis.) This mechanism of differential growth may explain why labeled cells as far as somite level 11 can be "pulled" into the prospective pelvic fin area.

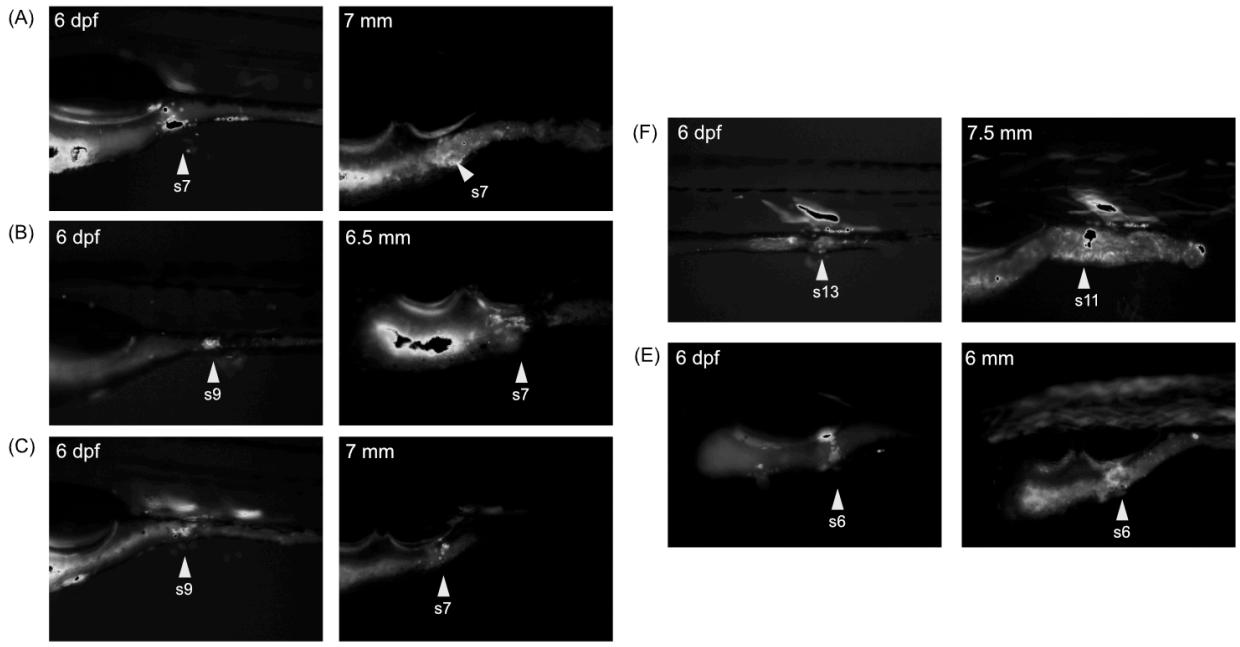

Figure 3.17 - Comparison of initial labeling position and position after a few weeks of larval growth (6-7 mm SL) shows clones being "pulled" towards somite 6.

There is little evidence of active migration as the circular clone shape remains much the same. Anterior to the left, dorsal to the top.

3.5.4 Contribution of LPM to the pre-anal fin fold, a median structure

I was surprised to find that the LPM, or at least hand2:eGFP expressing cells, contributed to the pre-anal fin fold. These cells appeared to originate from a small area just anterior and ventral to Kupffer's vesicle at 12 hpf, which to my knowledge, has not been formally described. This area was also just adjacent to the blastopore at 12 hpf. It is possible that this was a population of mesodermal cells that have not joined the rest of the lateral plate mesoderm in migrating dorsally, and have remained near the opening of the blastopore. However, the tailbud region is a site of diverse movements (Kanki & Ho, 1997) and we await detailed single-cell labeling to determine the origin of these potentially "leftover" mesodermal cells.

Median structures are comprised of paraxial mesoderm, not lateral plate mesoderm, derivates, so the finding that LPM is likely developing into a median finfold bucked this general rule. I will explore how this finding affects our views of limb/fin competency in Chapter 5.

3.5.5 Neural crest vs. mesoderm contribution to the pelvic fins

My finding that neural crest does not contribute to the pelvic fin bud corroborates the finding that neural crest does not contribute to the trunk exoskeleton (Lee, Knapik, Thiery, & Carney, 2013; Lee, Thiery, et al., 2013; Shimada et al., 2013). Due to the multipotent nature and diverse cell lineage types of neural crest, it had been previously thought that this tissue layer also contributed to fin mesenchyme and the bony fin rays (see Lee, Knapik, et al. 2013 for a review). Instead, in zebrafish, neural crest appears to have almost no contribution to the mesenchyme of the median fins (dorsal, caudal, anal) and the pectoral fins. Paraxial mesoderm is responsible for generating the mesenchyme for median fins, and the lateral plate mesoderm is the exclusive contributor for the mesodermal portion of the pectoral fin rays.

I add strong evidence that the pelvic fin mesenchyme is also not derived from neural crest. There was no *sox10* (neural crest marker) in the migrating parietal peritoneum between 24-60 hpf, and we see no evidence of *sox10* in the pelvic fin bud mesenchyme. *sox10* was present in the region of the developing pelvic girdle, where it is likely associated with chondrogenesis. Overall, this implies that changes to the position of the pelvic fin in actinopterygians is mediated through novel developmental changes (see Chapter 5 for a discussion) in the lateral plate mesoderm, asserting its status as another flexible and evolvable tissue type.

3.5.6 – Future directions to define the pelvic fin field more precisely

Individuals were labeled at 2 or 3 DPF, however in theory, these fish could also be labeled at any stage in development when the cells can be accessed by the laser. Adding in data points where the labeling occurred at perhaps 1-2 weeks post fertilization could help refine the pelvic fin field, as there might be less ectopic labeling (any ectopically labeled cells labeled early would contribute to a greater proportion of cells later on).

A drawback of the *Tg(hsp:cre-ert2)* x ubi:switch system described in this chapter was that it was not restricted to non-LPM tissues. Although this is advantageous for other applications, as this feature permits its use outside of LPM studies, its wide labeling made screening for LPM-labeled individuals very time-consuming and challenging. One more targeted approach would be to generate a LPM-specific driver of loxP-GFP-loxP-mCherry, such has *a Tg(hand2:switch)* or *Tg(prrx1:switch).* These would still be coupled with the *Tg(hsp:cre-ert2)* line to allow for spatial control.

Chapter 4 - EVIDENCE FOR LATE SPECIFICATION OF PELVIC FIN FATE

4.1 PREFACE

This chapter benefited greatly from the work of Maryam Bolouri (undergraduate, Univeristy of Chicago ’22) who along with the ever-present Adam Kuuspalu, helped refine the larval *in situ* hybridization protocol during her time as a Katen Scholar. Many thanks as well to Dr. Timothy Sanders who provided the elusive recipe for “Solution X,” which allowed me to clear the specimens and clearly visualize the staining patterns.

4.2 ABSTRACT

The pelvic fins develop at 3 weeks post fertilization, but when its precursor cells are specified to become pelvic fin is unknown. In tetrapods, hindlimb specification is marked by expression of *Tbx4* and *Pitx1* in the lateral plate mesoderm. As such, I sought to characterize expression of these candidate ‘hindlimb’ genes in zebrafish throughout embryonic and larval development. I found no detectable expression of *tbx4, pitx1,* and *fgf24* during embryogenesis (0-3 dpf) over the lateral plate mesoderm, suggesting that pelvic fin specification probably does not occur at this time. However, *tbx4, pitx1,* and *fgf24* were detected in the body wall in the prospective pelvic fin region approximately 1-2 weeks before pelvic fin initiation, as well as in the pelvic fin buds themselves. Along with expression of posterior Hox genes such as *hoxc10, hoxc9,* and *hoxd9* in the body wall as well, these results suggest that pelvic fin specification occurs late, perhaps just prior to pelvic fin initiation. Lastly, to my surprise, I discovered

expression of candidate 'hindlimb' genes in the myoseptae in the prospective pelvic fin region, which provides a springboard for new research questions on how the myoseptae might be involved in pelvic fin initiation.

4.3 INTRODUCTION

Two types of comparisons can be made with the zebrafish pelvic fin: (1) comparing the zebrafish pelvic fin to the tetrapod hindlimb (2) comparing the zebrafish pelvic fin to the pectoral fin. In the first case, similarities and differences arise from a shared history in the ancestral osteichthyan pelvic fin. Comparisons between the pelvic and pectoral fins emerge within the context of a potential serial homology between these two fins, between which an ancestral developmental program may have been reiterated.

The tetrapod forelimb and the zebrafish pectoral fin are characterized by a conserved suite of gene expression patterns during their initiation and outgrowth. Similarly, the expression patterns of a conserved group of genes are diagnostic of tetrapod hindlimb initiation. As mentioned in Chapter 1, *Tbx5* and *Tbx4*, paralogs of each other, are markers of forelimb and hindlimb identity, respectively. Together with *Tbx4, Pitx1* is an important indicator of hindlimb identity and necessary for normal initiation. For both limbs, an *fgf* cascade (*Fgf10, Fgf8*) is activated during bud outgrowth. In summary, in the scope of limb specification, the T-box genes and *Pitx1* are the clearest markers that the field has for limb identity.

There are a few differences in the gene expression patterns for the zebrafish pectoral fin, but largely the overall trajectory is the same. Due to a whole genome duplication event unique to teleosts, zebrafish possess two Tbx5 copies, *tbx5a* and *tbx5b*, which are both expressed in the pectoral fin field and have roles in ensuring that the fin field cells properly converge into a fin bud (Dae-gwon Ahn et al., 2002; Boyle-Anderson et al., 2022; Q. Mao et al., 2015). A copy of *tbx4* has been lost in zebrafish. Another important difference is the inclusion of *fgf24a* at the beginning of the *fgf* cascade, which is directly activated by *tbx5a*. *fgf24a* appears to be necessary for pectoral fin bud formation. Aside from gene expression patterns, additional comparisons between fins/limbs and fins/fins can be derived from the timing of the limb bud initiation. While the forelimbs and hindlimbs of tetrapods appear at similar times, the pelvic fin in zebrafish (and many other actinopterygians) develop weeks after the pectoral fin. In Chapter 3, I reported that the zebrafish pelvic fin precursors can be found between somite levels 6-11 in the parietal peritoneum. However, an outstanding question that remained was whether these precursor cells were specified to be pelvic fin at the same time as the pectoral fin such as the case in tetrapods, or whether they were specified later in development, perhaps closer to the time of pelvic fin initiation. In this chapter, I examine the expression patterns of candidate hindlimb genes, paying particular attention to the somite level 6-11 region in the parietal peritoneum, to determine if pelvic fin specification was likely early or late. If specification is early, I predicted that there should be earlier expression of these hindlimb genes in the pelvic fin precursor region. If specification is late, then these genes should only be expressed immediately prior to pelvic fin initiation.

Limb induction in tetrapods is also associated with an epithelial-to-mesenchymal transition (EMT), where cells undergo morphological change as they become more migratory (Gros & Tabin, 2014; Ocaña et al., 2012). Therefore, the outgrowth of a tetrapod limb bud is not due solely to localized proliferation – it is also attributed to converging movements of limb field cells. The LPM at the level of the pectoral fin is already in a migratory state when the fin bud forms (Q. Mao et al., 2015; Ocaña et al., 2012), and overexpression of EMT-associated proteins such as *prrx1a* will produce an invasive phenotype where LPM cells migrate into extraembryonic tissues (Ocaña et al., 2012). Because the parietal peritoneum is more epithelial in nature than mesenchymal by the time the pelvic fin appears, I hypothesized that the pelvic fin precursor cells undergo EMT to converge into a bud, as is the case in tetrapods. Common markers of EMT can be found in the expression patterns of N-cadherin and E-cadherin, which are upregulated and downregulated respectively during this process ("cadherin switch") (Loh et al., 2019; Scarpa et al., 2015).

4.4 RESULTS

4.4.1 Absence of candidate 'hindlimb' gene expression suggests specification is probably not early

If specification of the pelvic fin field is early, then I would expect to find expression of the candidate 'hindlimb' genes during embryogenesis. However, I found no detectable expression of candidate 'hindlimb' genes *tbx4* and *pitx1* in the lateral plate mesoderm during this period. There was also no expression *of fgf8a, fgf10a*, or *fgf24,* genes involved in the pectoral fin

fgf cascade, in the LPM over the yolk extension. I detected expression of *fgf8a, fgf10a, and fgf24* in the ventral midline of the yolk extension, and then later in the fibroblasts of the pre-anal fin fold, indicating that the absence of detectable expression over the yolk extension was not due to sensitivity issues. Therefore, while the pectoral fin field is specified during embryogenesis, the pelvic fin field is likely not.

4.4.2 Expression of *tbx4, pitx1,* and *fgf24* in the parietal peritoneum immediately prior to pelvic fin bud initiation suggest late specification

Next, I examined the expression of the same candidate 'hindlimb' genes throughout larval development. I found expression of *tbx4, pitx1,* and *fgf24* in the parietal peritoneum well prior to pelvic fin stage (starting at 4-5 mm SL) (Figure 4.2). The staining for these genes tended to intensify as specimens reached closer to pelvic fin stage (6 mm), especially in the prospective pelvic fin location. These transcripts were all detected in the pelvic fin bud. Additionally, these genes were frequently detected in the vertical myoseptae roughly between somites 7-12. *fgf10* was not expressed until immediately prior to pelvic fin stage (6 mm), and its expression in the parietal peritoneum was much more restricted to the prospective pelvic fin location. It is later expressed in the apical ectodermal ridge of the pelvic fin (Figure 4.3C). *fgf8a* was not present in the body wall but was expressed in the pelvic fin bud (Figure 4.2). Neither gene was expressed in the vertical myoseptae.

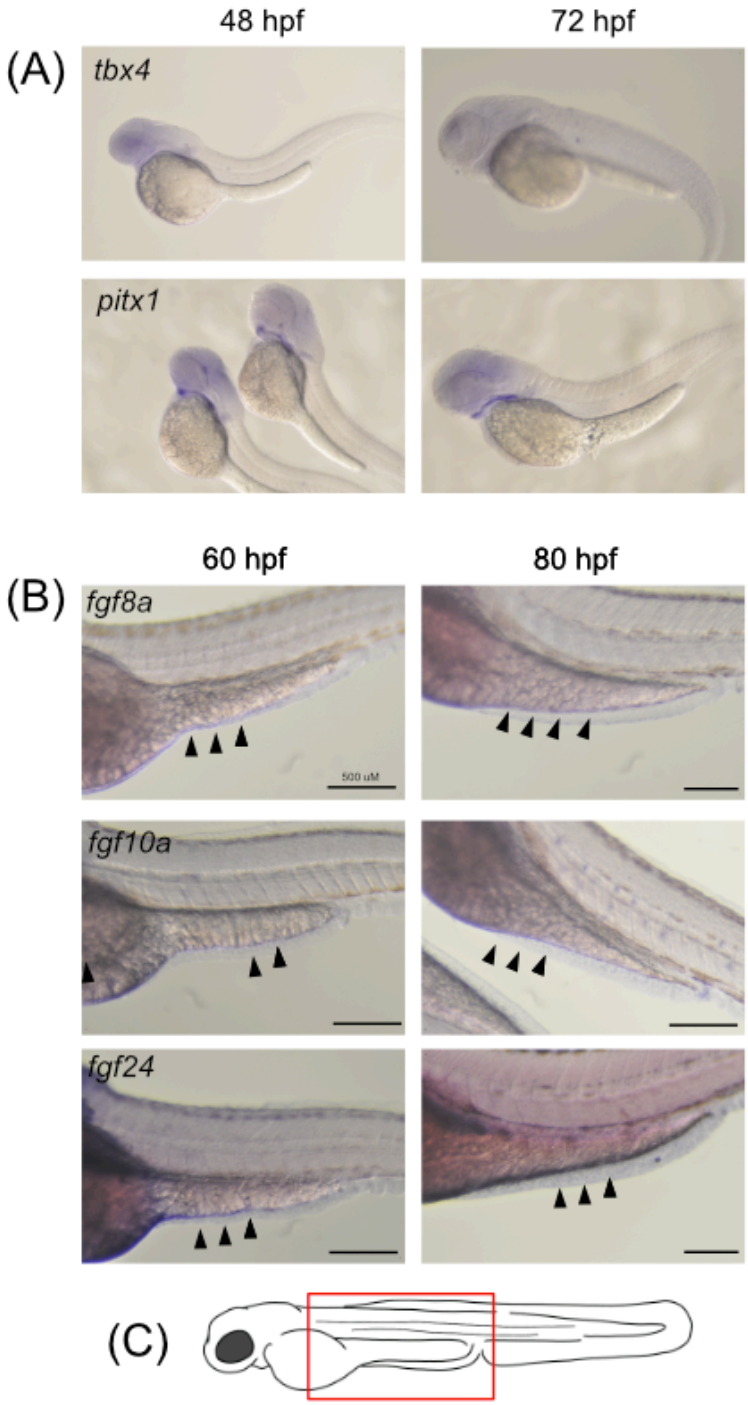

Figure 4.1 - Expression patterns of candidate hindlimb genes from 2-5 dpf.

Lateral views. Anterior to the left, dorsal to the top of the page. (A) No detectable expression of *tbx4* and *pitx1* over the yolk extension. (B) No expression of *fgf* genes over the yolk extension, however there is expression in the ventral midline and in the pre-anal fin fold (black arrowheads). (C) Red box indicates the location of photos from (B). Scale bars are 500 uM.

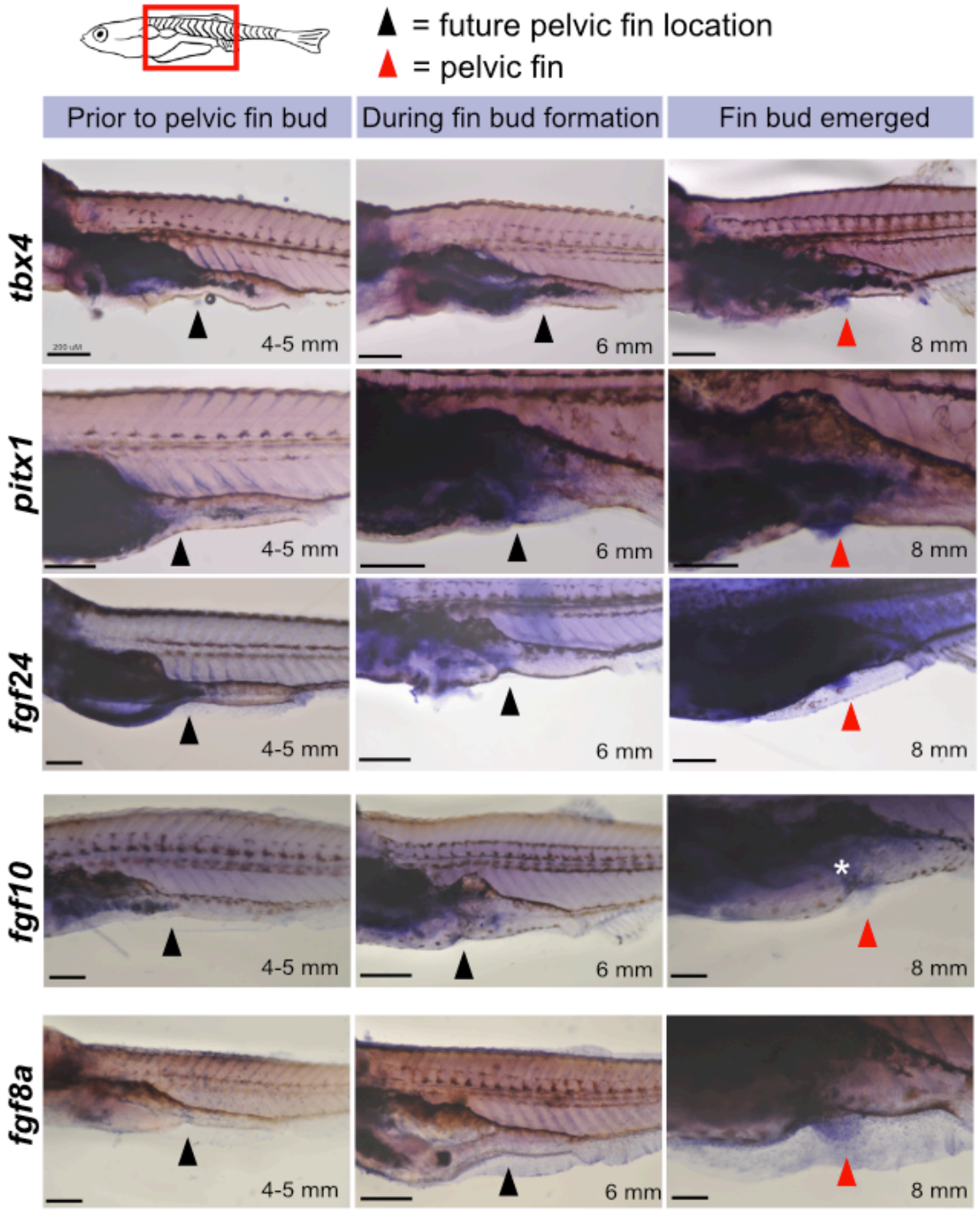

Figure 4.2 - Expression of candidate 'hindlimb' genes during larval development.

Black arrowheads point to prospective pelvic fin location; red arrowheads to the pelvic fin buds. White asterisk in fgf10 8 mm panel represents an example of 'localized' expression. Lateral view, anterior to the left, dorsal to the top.

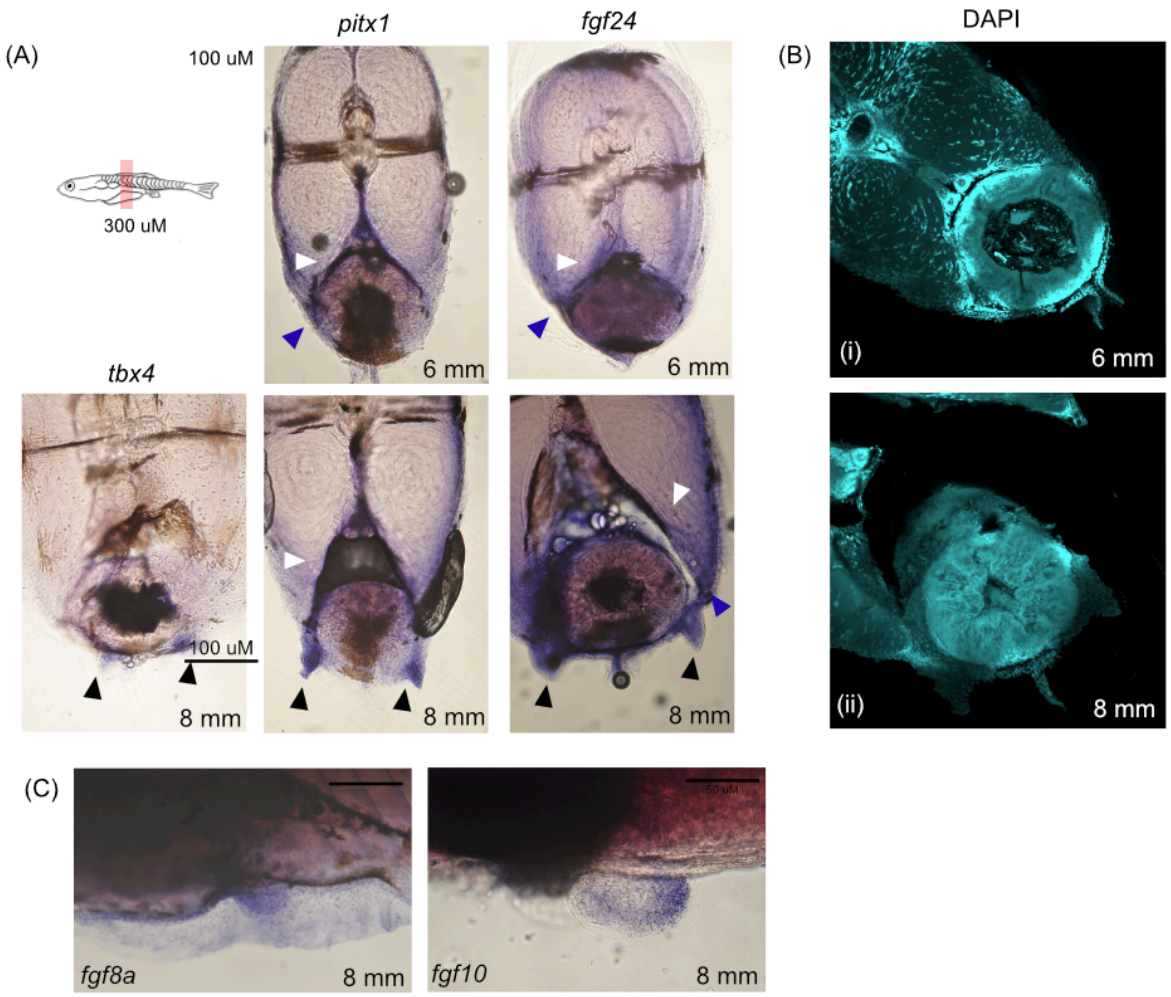

Figure 4.3 - Vibratome sections

(A) Vibratome sections of whole mount in situ larvae. White arrowheads point to myoseptal staining. Purple arrowheads point to staining within the parietal peritoneum. Black arrowheads point to pelvic fin buds. 6 mm is prior to pelvic fin initiation, 8 mm is after pelvic fin initiation. (B) Vibratome sections of DAPI-stained larvae – (i) 6 mm (ii) 8 mm. Scale bar is 100 uM unless otherwise noted.

I performed vibratome sectioning of these whole mounts to verify that the staining was present at the parietal peritoneal layer. I was able to verify this for *pitx1* and *fgf24* (a section of *tbx4* at 6 mm SL is needed). For all genes, I confirmed expression in the pelvic fin buds. Because the precipitate in the *in situ* hybridization reaction along with any residual digestive matter may

obscure tissue morphologies, I stained these sections with DAPI to visualize the nuclei (Figure 4.3B). This confirmed that there were cells present in the parietal peritoneum regions that were stained, and that it was not merely deposited/trapped precipitate. Control sections where there was no antibody included in the reaction also verified the actual presence of gene expression staining (Figure 4.3CA). In total, these results suggest that pelvic fin specification occurs during the larval phase.

4.4.3 Caudal Hox genes are co-expressed with candidate hindlimb genes

Because pelvic fin gene expression appeared to be late, I next investigated expression of Hox genes, as they may be involved in patterning the LPM and activating hindlimb-specific genes. Hox genes are primarily active during the early patterning stages of embryogenesis, so it would be surprising if they were activated in larval stages. As a preliminary exercise, I chose caudal Hox genes *Hoxc9, Hoxc10,* and *Hoxd9,* particularly as they have been known to interact with *Pitx1* and *Tbx4* in mouse (Infante et al., 2013). The expression of these genes mirrored that of *tbx4, pitx1,* and *fgf24* – within the parietal peritoneum, myosepta, and pelvic fin buds (Figure 4.4A). As a control, I performed in situ hybridization with rostral Hox genes *hoxc4* and *hoxc6* to ensure that not all Hox genes were activated. I did not see expression of these genes within the parietal peritoneum or the pelvic fin buds. As anticipated, *hoxc4* and *hoxc6* were mostly expressed in rostral tissues (brain, anterior swim bladder). In total, these results indicate that Hox expression is still active during larval phases and may be continuing to pattern the body axis.

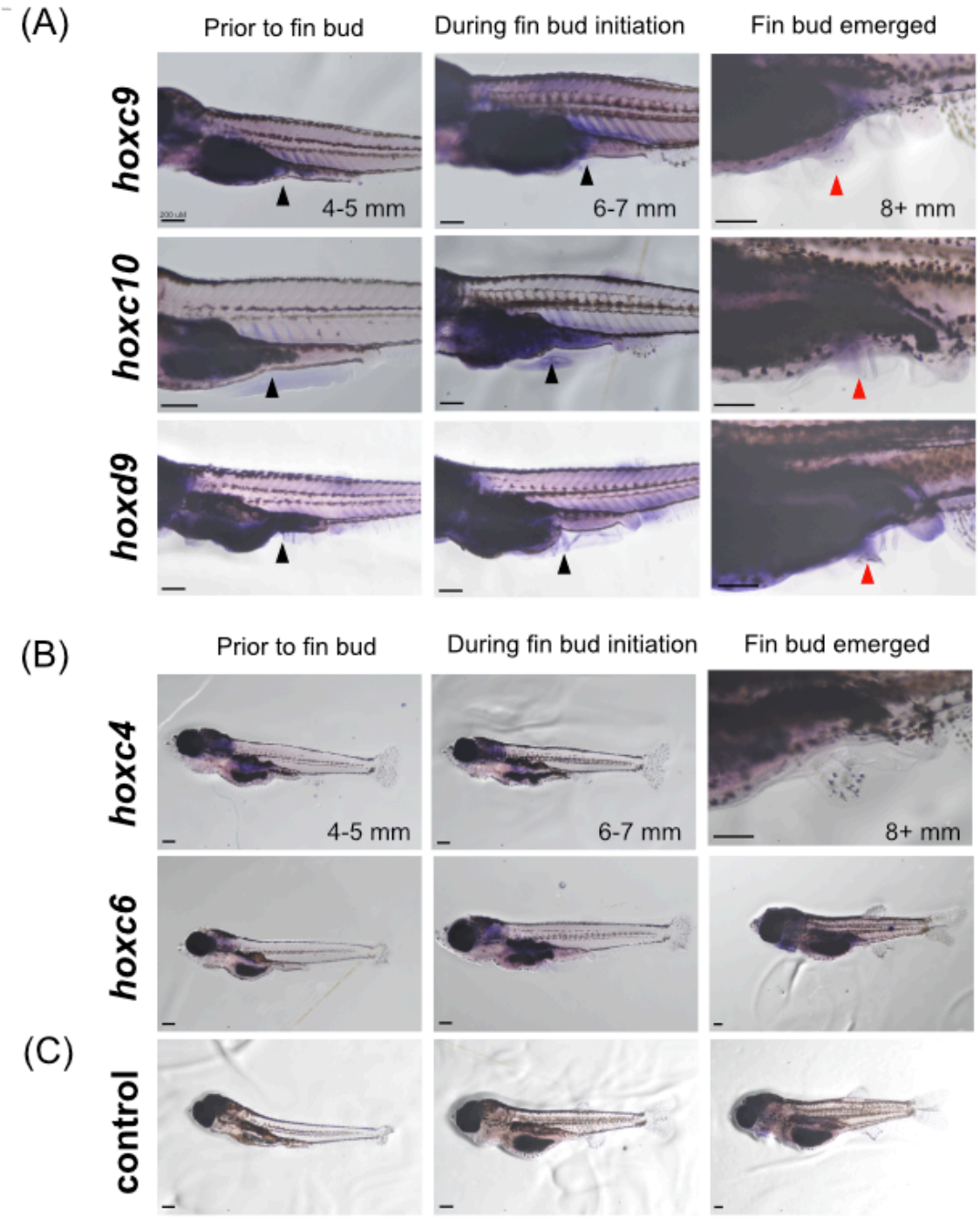

Figure 4.4 - Whole mount in situ hybridization of larvae

(A) caudal and (B) rostral Hox genes and (C) no primary antibody control. Lateral view, anterior to the left. Black arrowheads point to prospective pelvic fin location, red arrowheads point to pelvic fin buds. Scale bar is 200 uM.

4.4.4 Preliminary evidence of EMT in the parietal peritoneum

Finally, I investigated the possibility that pelvic fin initiation may be associated with EMT, as previously described in tetrapod limbs (Gros & Tabin, 2014). I stained for expression of *twist1b*, whose ortholog *TWIST1* has been linked to chick limb EMT (Newton, Williams, Major, & Smith, 2022) (Figure 4.5A). Again, I found *twist1b* co-expressed with *pitx1, tbx4,* and *fgf24* in the parietal peritoneum of the prospective pelvic fin location, the myosepta at the prospective pelvic fin level, and within the pelvic fin bud (Figure 4.5A, starting at 4-5 mm SL). *twist1b* is also expressed at the base of the median fins, where somite-derived mesenchymal cells are known to invade at those stages (Lee, Knapik, et al., 2013).

Next, I performed antibody staining for Cdh1 (E-cadherin) and Cdh2 (N-cadherin) to discern whether there was a signature of a "cadherin switch." If this were observed, there would be downregulation of Cdh1 and upregulation of Cdh2. I did not find evidence of this in these preliminary data. Levels of both Cdh1 and Cdh2 appeared to remain the same at the base of the pelvic fin bud (n=6 Cdh1 specimens observed, n=9 Cdh2 specimens observed). There were a few noticeable differences between the two expression patterns – Cdh1 was more punctate, perhaps vesicularized within the cells, and was expressed in the entire pelvic fin bud at 7 mm. Cdh2 was localized in the cell junctions and was more commonly restricted to the base of the pelvic fin bud, instead of being present throughout. These two expression patterns remained the same throughout different stages. In total, these initial experiments do not seem to support changes in Cdh1 and Cdh2 levels that might have indicated EMT processes.

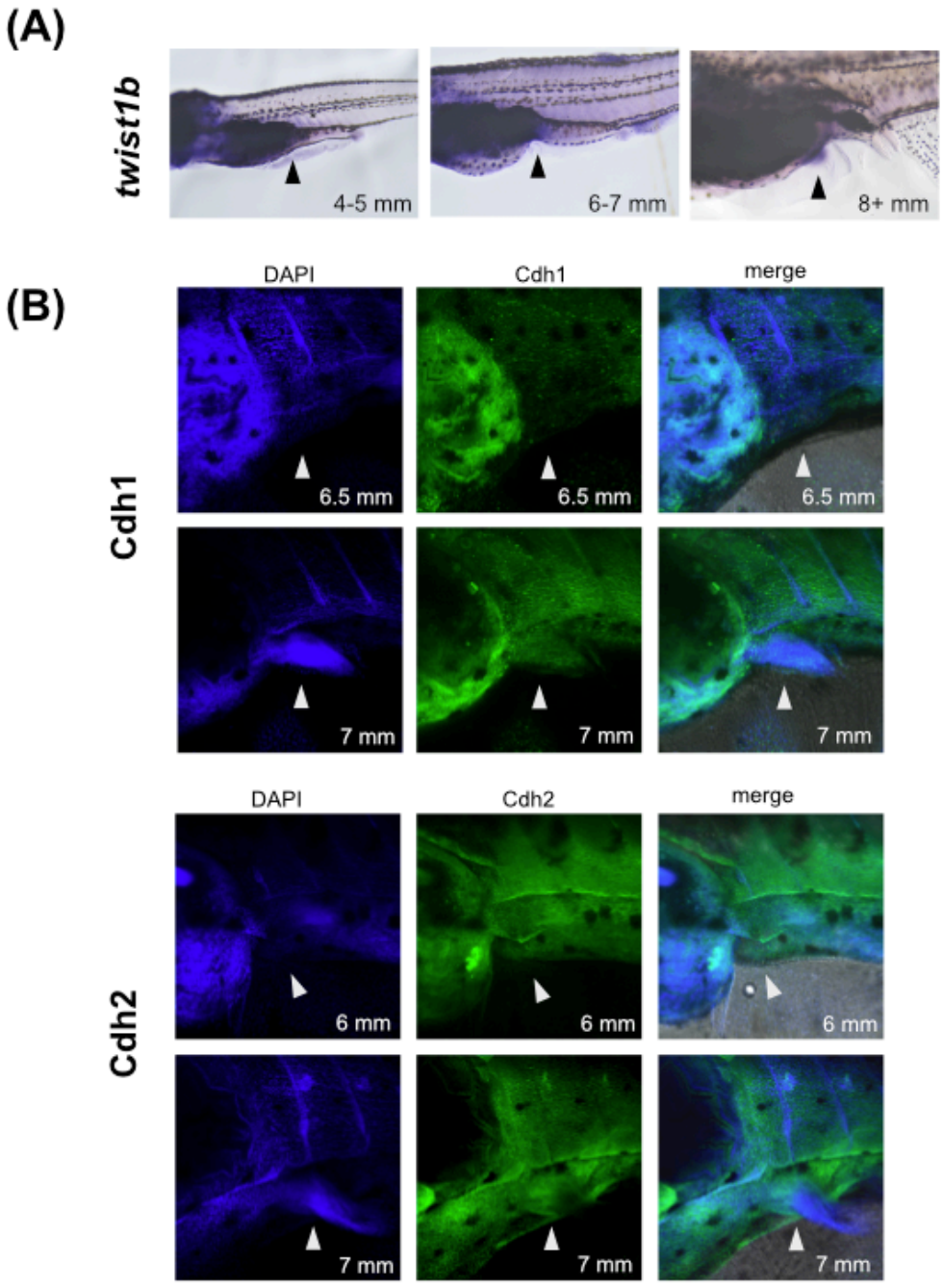

Figure 4.5 - Staining for markers of EMT

(A) Whole mount in situ hybridization of *twist1b* in larvae. Lateral view. Anterior to the left, dorsal to the top. (B) Antibody staining of Cdh1 (E-cadherin) and Cdh2 (N-cadherin) at 6 mm and 7 mm stages. White arrowheads point to prospective pelvic fin location (6-6.5 mm) and pelvic fin buds (7 mm).

4.4.5 Quantifying the extent of anteroposterior expression of candidate ‘hindlimb’ genes

I was interested in quantifying the extent of the anterior and posterior boundaries of the candidate ‘hindlimb’ gene expression domains, both in the myosepta, and in the body wall. Particularly, I asked whether the areas of gene expression would overlap with the fate mapping field as discovered in Chapter 3. If cells arose from a region that both was known to contribute to the fin and expressed classic ‘hindlimb’ genes, this would strengthen their status as potential pelvic fin field cells.

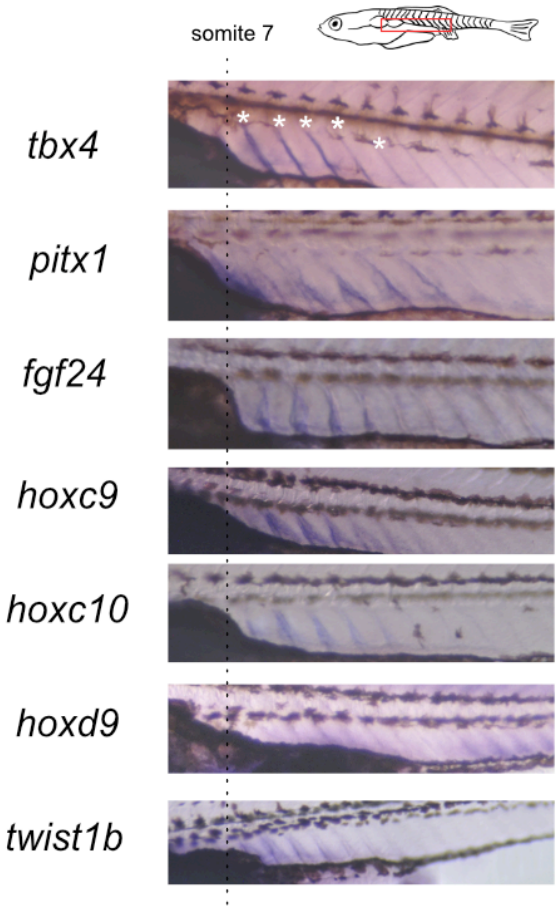

Figure 4.6 - Comparisons of myoseptal expression in representative individuals.

Red inset box shows location of the images, which is the ventral compartment of the myomeres. Asterisks in the first panel (*tbx4*) show myoseptal staining.

For all candidate genes, the expression in the vertical myosepta began at somite 7, which is the posterior boundary of the swim bladder. Expression continued posteriorly to varying degrees, but for all genes, terminates by somite level 11 (Figure 4.7). In most cases, there was a decrease in staining intensity as it progresses posteriorly. This staining appeared to be restricted to the ventral section of the myosepta below the level of the notochord. Staining in the dorsal-most section of the vertical myosepta was occasionally observed, but was inconsistent. Examples of this staining can be found in the Appendix B.

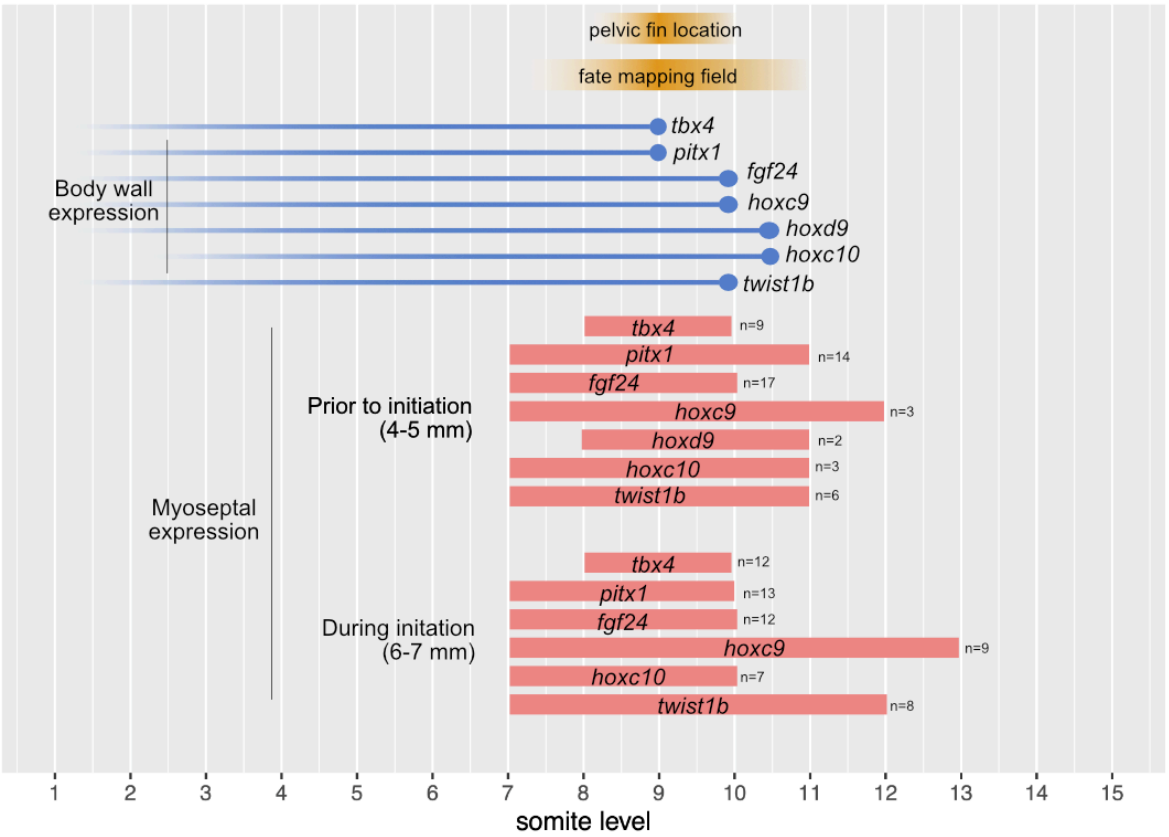

Figure 4.7 - Candidate 'hindlimb' gene expression in the body wall and myosepta compared to the pelvic fin location and fate mapping field.

The posterior boundary of the body wall expression data was averaged from all individual specimens for each gene. The boundaries of the myoseptal expression were calculated by averaging the anterior boundary and posterior boundary separately.

The anterior boundaries for the genes assayed began at somite levels 1-2 and terminated between somite levels 9-11 in general (Figure 4.7). In the younger larvae (4-5 mm SL), I noticed that the staining in the parietal peritoneum was more diffuse, and it was not until 6 mm SL that I observed more intense, "localized" staining in the parietal peritoneum of the prospective pelvic fin area (Table 4.1). The localized staining tended to be in the shape of a vertical band around 1-2 somite lengths (e.g. Figure 4.2, *fgf10*at 8 mm for a very clear example – white asterisk in image). The localized staining was always present after the pelvic fin bud formed.

	4 mm	**5 mm**	**5.5 mm**	**6 mm**	**6.5 mm**	**7 mm**	**7.5 mm**	**8 mm**	**9 mm**
fgf24	0/3	0/14		1/8		3/4	1/1		
hoxc10	0/1	0/2		1/5		2/2		1/1	
hoxc9		1/3		1/6	1/2	1/1			
hoxd9		0/1	0/1			2/2		1/1	
pitx1		0/14		4/11		1/2		2/2	
tbx4	0/1	0/9		8/12		6/6			1/1
twist1b	0/5	0/5	0/1	4/4	1/2	4/4	1/1	4/4	1/1

Table 4.1 - For each gene and stage (standard length), the two numbers represent the number of "localized" staining (first number) / number of total individuals assayed (second number).

4.5 DISCUSSION

The absence of candidate hindlimb gene expression during embryogenesis and its presence during the larval stage suggests that pelvic fin specification is late, not early, relative to the condition in tetrapods (summarized in Figure 4.8). Expression of *tbx4, pitx1,* and *fgf24* in the body wall precedes the appearance of the pelvic fin bud itself, indicating that they may mark the pelvic fin field. Additionally, I unexpectedly discovered expression of these candidate hindlimb genes in the myosepta surrounding the prospective pelvic fin bud. This is all accompanied by preliminary evidence that there may be EMT associated with the pelvic fin bud formation. In this discussion, I will consider the implications and limitations of the expression data as it relates to (a) specification of the pelvic fin field (b) potential for long-distance signaling through the myosepta and (c) possibility of EMT driving pelvic fin bud formation.

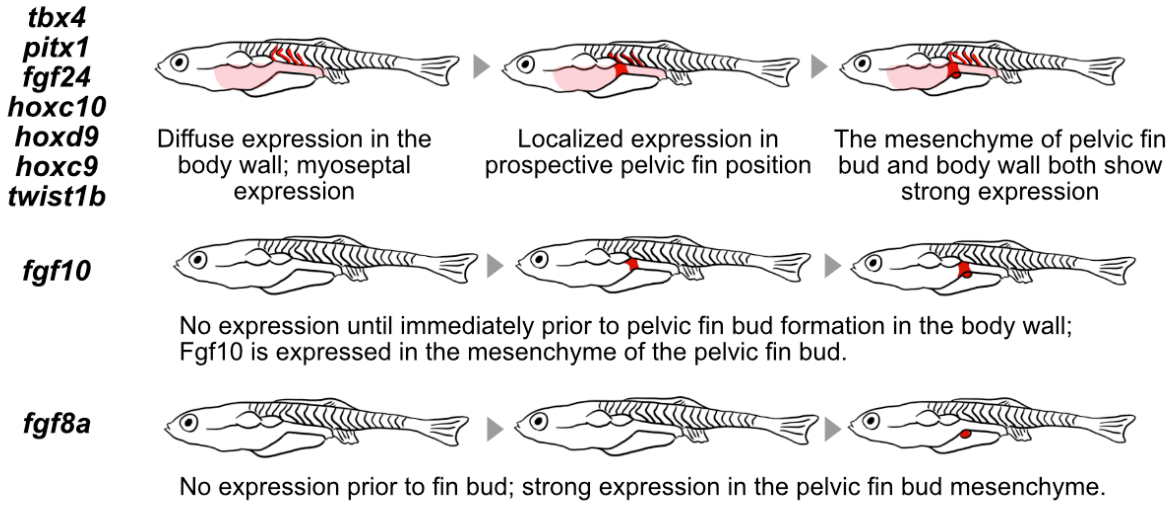

Figure 4.8 - Expression patterns of genes assayed in this chapter can be grouped into three categories. Most are first diffusely expressed in the body wall, then display strong localization.

4.5.1 Specification of the pelvic fin field

To reiterate, I define a fin field as the population of cells that will contribute to the fin bud. Specification is strictly defined as "capable of differentiating autonomously when placed in a neutral environment with respect to the developmental pathway – commitment is still capable of being reversed" (Gilbert, 2000). Here, in the absence of excision experiments, I employ a looser definition of specification. I use *tbx5a* and *tbx4* as indicators of specification (though they may not be responsible for the specification itself) as their expression patterns are correlated with the presence of the fin/limb field (Dae-gwon Ahn et al., 2002; Q. Mao et al., 2015; Carolina Minguillon, Del Buono, & Logan, 2005). That is, I take *tbx4* and *tbx5a* to mark lateral plate mesoderm cells that have been specified to become part of the fin field, and in turn, give rise to the fin bud.

If one accepts *tbx4/5a* as a fin field marker, then its diffuse expression in the body wall as early as 4-5 mm SL may indicate that the fin field spans the range from the first somite to the posterior boundaries indicated in Figure 4.7. However, I noted that the intensity and specificity of staining at the prospective pelvic fin location increased immediately prior to pelvic fin bud formation, at 6 mm SL. There are two possibilities regarding the fin field based on these observations: (1) It is possible that the diffuse expression all along the body parietal peritoneum is unrelated to fin bud initiation, and it is only when the expression is "localized" that the fin field is present. *tbx5a* is not solely expressed in the pectoral fin field, as it is also found in the secondary heart field and other tissues, so it may be the case that *tbx4* is also expressed in other tissues. (2) Alternatively, the fin field is actually as large as the diffuse expression indicates, and

the later-stage narrowed, localized expression represents a refinement of the field that prefigures the imminent bud. This refinement could be the result of active migration of a subset of fin field cells, or the result of that subset of cells receiving fin bud-specific signals. There is certainly precedent for the latter pattern – in pectoral fin development, the "localization" of *tbx5a* expressing cells is due to active convergence of these cells, which physically modifies the boundaries of the fin field (Q. Mao et al., 2015). Alternatively, immediately prior to tetrapod limb bud initiation, Tbx4, Tbx5, and Pitx1 are expressed in broad bands along the LPM and are only restricted in position once the limb bud arises (Agarwal et al., 2003; Nemec et al., 2017; Nishimoto & Logan, 2016a). However, unlike the pectoral fin and tetrapod limb development, the diffuse staining of *tbx4* and *pitx1* remains even after the pelvic fin bud has emerged.

Competency to form a fin bud is different from inclusion in the fin field. While many parts of the lateral plate mesoderm are theoretically competent to form limb/fin buds (Cohn et al., 1995; Yonei-Tamura, Ide, & Tamura, 2005), they are not considered part of the limb/fin field, because cells from that region will not contribute to the limb/fin bud. Therefore, for a region of LPM to be considered as part of the fin field, it must be both competent to form a fin bud, and contribute cells to the fin bud. To differentiate between the scenarios above, one could verify whether the region can produce a fin bud through competency experiments (to be discussed in Chapter 5) – regions that are not fin bud competent in the "diffuse" expression zones cannot be labeled as fin field. Additionally, labeling these regions with the heat shock system described in Chapter 4 at later stages could identify whether cells from these regions are present in the fin bud mesenchyme.

4.5.2 Long-range signaling through the vertical myosepta

The vertical myosepta arise from the somite boundaries and after embryogenesis, lie at the boundaries between the myomeres. They are eventually the site of the myotendinous junctions, which are sheets of connective tissue that link the myomeres and transmit force between them (Rescan, 2019). In teleosts, the myosepta are initially acellular and only contain collagenous matrix, but in larval (15 dpf+) fish, begin to be invaded by fibroblasts (Esteves de Lima et al., 2021). It has been proposed that these fibroblasts arise from the sclerotome, though more precise lineage tracing is needed (Esteves de Lima et al., 2021). Aside from fibroblasts, the vertical myosepta are host to nerves and nerve-associated melanophore stem cells that travel distally out from the center of the fish to the hypodermis (Budi, Patterson, & Parichy, 2011; Parichy & Spiewak, 2015). This raises the possibility that the vertical myosepta might act as a signaling highway for pelvic fin induction. It is unlikely that the pelvic fin precursor cells are derived from cells surrounding the notochord region, as (1) individuals with labeled pelvic fin cells had pelvic fins comprised almost completely of labeled cells, and (2) myotomes were commonly labeled and did not contribute cells to the pelvic fin bud mesenchyme.

Expression of candidate ‘hindlimb’ and posterior Hox genes in the myosepta is quite intriguing, as it suggests that the paraxial mesoderm-derived tissues might play a role in pelvic fin initiation. This has not been proposed before in the literature, especially since the pelvic fins are not in proximity to the myomeres. Paraxial mesoderm has previously been identified as a potential source of limb induction signaling through production of retinoic acid (RA). RA is a vitamin A derivative, the absence of which leads to a phenotype without pectoral fins, among

other developmental defects. In zebrafish, RA signaling from the somitic mesoderm during gastrulation is necessary to specify the pectoral fin precursors (Grandel & Brand, 2011). This signaling pathway traverses the intermediate mesoderm, which lies between the somitic mesoderm and the lateral plate mesoderm during the time of pectoral fin development and activates *tbx5a* expression (Mercader, Fischer, & Neumann, 2006). Additionally, the concentration of RA along the anteroposterior axis is responsible for determining the position of the pectoral fin field (Quintanilla & Ho, 2020). Overall, this suggests that signaling from the paraxial mesoderm has an important role in the induction of the pectoral fin in zebrafish. In mouse, RA signals from the somites are thought to repress FGF expression in the lateral plate mesoderm to demarcate the prospective forelimb field (Cunningham et al., 2013; Zhao & Duester, 2009). However, RA repression of FGFs does not appear to be involved in setting up the hindlimb field, leaving the role of paraxial mesoderm in hindlimb initiation unclear (Zhao & Duester, 2009). Given the differing requirements for the role of RA signaling from the paraxial mesoderm for mouse forelimb and hindlimb induction, it is difficult to speculate whether the zebrafish pelvic fin requires similar RA patterning as the pectoral fin, especially if RA appears to only be critical during gastrulation.

4.5.3 Thyroid hormone as a potential induction signal

It is also entirely possible that pelvic fin induction signals from the paraxial mesoderm, if they exist, are acting independently of RA signaling. Thyroid hormones (TH) are one potential signal that might trigger the onset of induction, an idea that was proposed by Murata et al. (2010). The thyroid hormones thyroxine (T_3) and triiodothyronine (T_4) are critical for normal

hormonal regulation in the adult zebrafish, but most importantly, indispensable for the transition between the larval to juvenile stages (Brown, 1997; Liu, Chan, Liu, Chan, & Chan, 2002; Power et al., 2001; Shkil, Kapitanova, Borisov, Abdissa, & Smirnov, 2012). The process of metamorphosis itself may be mediated by relative changes in the ratio of T_4 to T_3. For zebrafish, the ratio of T_4:T_3 steadily increases until just prior to metamorphosis (approximately 3 weeks post fertilization), after which it drops dramatically (Chang et al., 2012).

Absence/overexposure to thyroid hormones causes developmental defects to be lethal, and larvae do not survive beyond 7 dpf (Liu et al., 2002). In hypothyroid fish where their thyroid gland has been ablated in the larval stage, there is a marked delay in the development of the cranial skeleton, scales, gastrointestinal tract, and quite interestingly, an observed delay in the resorption of the pre-anal fin fold and the appearance of the pelvic fin (Aman, Kim, Saunders, & Parichy, 2021). In another experiment where T_3 was antagonized or exogenously applied, while the absence of T_3 alone did not severely affect pelvic fin development, application of T_3 caused the pelvic fin to not develop at all in both zebrafish and barb (*Labeobarbus intermedius*), another cyprinid (Shkil et al., 2012). Together, these results suggest that the precise rising and falling of the thyroid hormones is critical for initiating pelvic fin development.

To begin to determine the effects of thyroid hormones (THs) on pelvic fin development, in situ hybridizations of the candidate 'hindlimb' genes could be assayed in exogenous T_3 fish, where the pelvic fin failed to form, and in hypothyroid fish from McMeinnan et al. (2014), where the pelvic fin was delayed. The timing of the applications/thyroid ablation will need to be titrated as to avoid lethal effects, but applied early enough to affect pelvic fin development. We would

expect to see a concomitant delay/absence in the expression of these genes compared to the wildtype expression at the same stage if they were downstream targets of THs. Additionally, the expression patterns of thyroid hormone receptors alpha a (*thraa*) and b (*thrab)* and thyroid hormone receptor beta (*thrb)* could be examined to see if they are co-expressed with the candidate 'hindlimb genes, especially in the myosepta. So far, these have only been examined embryonically in the zebrafish and are not expressed in the peritoneum or in the myosepta (Marelli et al., 2016)

Murata et al. (2010) proposed a scenario where the pelvic fin precursor cells were specified early during embryogenesis, and that these cells "remembered their fate" upon metamorphosis through THs. Because our results seem to support the idea that pelvic fin cells are actually specified late, not early, I hypothesize that THs are the inducing signal that specifies the pelvic fin precursor cells and sets off the cascade of the candidate 'hindlimb' genes. That is, THs could activate Hox positioning genes such as *hoxc10*, which could then interact with *tbx4* and *pitx1* to specify the pelvic fin field. THs could also drive EMT by activating *twist1b.* Alternatively, THs could merely be involved in the initiation of pelvic fin bud development, and would be independent of the specification process. If there is no spatiotemporal difference in gene expression of the candidate 'hindlimb' genes in the TH-treated fish, then THs may not be involved in specification. However, if a pelvic fin bud still does not form despite similar gene expression profiles, this suggests that THs are involved in initiation (Figure 4.9).

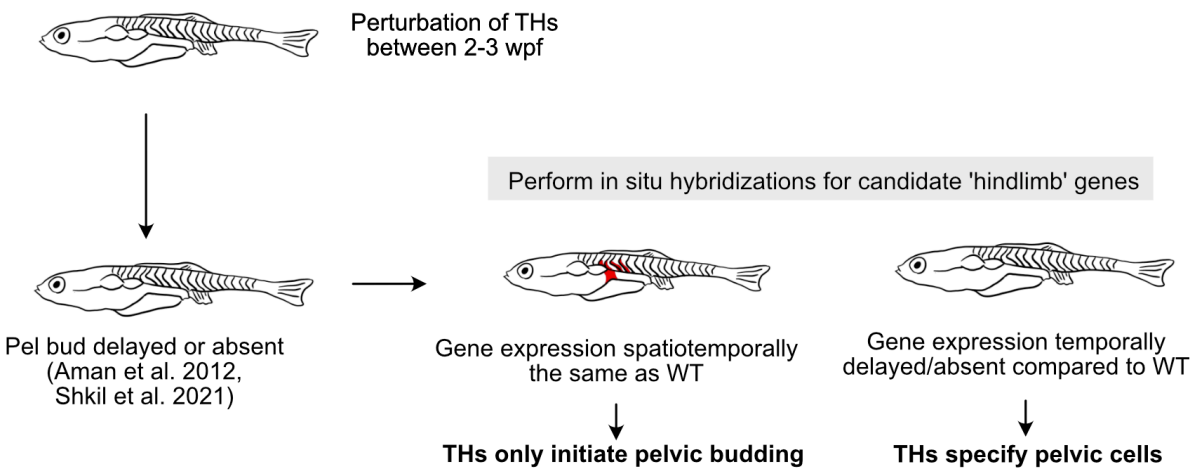

Figure 4.9 - Testing whether THs are involved in pelvic fin field specification.

Overall, the TH system in zebrafish is a complex pathway that has not been described in much of its intricacies and has whole-body effects. Much like how experiments with RA need to consider potential side-effects, future work with THs will need to carefully control for unintended effects.

4.5.4 EMT driving pelvic fin bud formation

The question of whether there is solely localized proliferation or alternatively, migration into the limb bud, has been a central question of limb development. Migration into the fin bud is critical for pectoral fin development, and EMT is observed in association with forelimb/hindlimb development in tetrapods (Gros & Tabin, 2014; Q. Mao et al., 2015). Here, we preliminarily began to explore this question and demonstrated that there is an EMT-associated gene, *twist1b*, co-expressed with candidate 'hindlimb' genes in the prospective pelvic fin area. However, staining for Cdh1 and Cdh2, which are common markers of EMT, was unable to conclusively

determine whether EMT was occurring. Our work was limited to lateral confocal optical slices; future work could perform transverse vibratome sectioning of the pelvic fin bud to more precisely localize cdh1 and cdh2. Other markers for EMT can also be used, as per Gros and Tabin (2014) – we would expect to see F-actin, β-catenin, and atypical protein kinase C (aPKC) at the apical ends of cells, and vitellin and laminin at the basal ends of cells if they are polarized for EMT.

Perturbation of known steps in the EMT process will help illuminate if this is a critical step in pelvic fin budding. Gross and Tabin (2014) electroporated RhoA into the prospective limb region in chick, which immobilizes cell movements by increasing extracellular matrix components. Electroporation in zebrafish at the 2-3 week post fertilization stage is certainly possible, though unconventional (a previous attempt with the electroporation set-up in the Sanders Lab was quite electrifying). Future studies could also generate conditional expression of RhoA by injecting a floxxed ubi:RhoA construct into a hsp:cre-ert2 background and inducing the cells with a heat-shock infrared laser. New approaches that allow for conditional Cre-based gene inactivation through linking cas9-sgRNA of the gene of interest can also elucidate late-stage function (Hans et al., 2021). For example, it is known that *twist1b* is necessary for EMT of pectoral fin field cells and without it, cells fail to migrate (Newton et al., 2022). Knocking out *twist1b* transcription at 2-3 weeks post fertilization, if it is not extremely deleterious, could determine whether pelvic fin cells also require EMT. Linking this system to my spatially-controlled hsp:cre-ert2 approach may allow us to only target the posterior somatopleure if the side-effects are too far-reaching.

Chapter 5 - CONCLUSIONS AND FUTURE DIRECTIONS

5.1 General conclusions

In this dissertation, I have used both a macroevolutionary and developmental perspective to begin to tie together how actinopterygian fish have managed to fundamentally alter their body plans across species, both in timing of formation and positioning of organs. The positions of the paired fins/limbs are comparatively stable in sarcopterygians and chondrichthyans, and these clades exhibit little delay between the appearances of their pectoral fin/forelimb buds and pelvic fin/hindlimb buds. First, I characterized the nature of these alterations over the actinopterygian phylogeny to gain a sense of the lability of these shifts. I investigated whether fin positioning shifts were frequently spotted in independent origins, which would suggest higher lability than if fin shifts were derived from a few events. To determine the extent of entanglement (structural, developmental, or functional) between the fins – if the shifting of one fin necessitates the shifting of the other – I tested for correlation between fin positions.

I have found that the dorsal shift of the pectoral fins and the rostral shift of the pelvic fins occurs together at the Neoteleostei node, a group that has previously received little attention. Furthermore, a correlation between the positions of these two traits was only seen in Neoteleostei, as this positional linkage only occurs once the ability to shift both fins is acquired. Using Bayesian estimation of evolutionary rates, I also found several differences in the macroevolutionary signatures between Neotelostei and Non-Neotelostei. Non-Neoteleosts display slower rates of evolving into different areas of the pectoral-pelvic fin position morphospace and are more constrained in their evolution of pelvic fin position than that of

Neoteleosts. Fossil actinopterygian species are mostly constrained to the Non-Neoteleost area of the morphospace, with ventral pectoral fins and posterior pelvic fins.

I also identified a correlation in the anterior limits of a median fin (dorsal fin) and a paired fin (pelvic fin). This linkage holds true in most extant actinopterygians despite the diversity in pelvic fin/dorsal fin position. Fossil actinopterygian data suggest that the pelvic-dorsal register only begins in the Jurassic, with older species showing a greater anal fin – dorsal fin symmetry. It remains to be determined where phylogenetically this shift occurred, and upcoming studies incorporating new characters into fossil placements should facilitate this task.

The first part of my work described the pattern of fin shifts; the second aimed to uncover the developmental processes that underlaid these changes. A fundamental, basic step was to understand how the pelvic fins develop in one actinopterygian species – I started here with the zebrafish, *Danio rerio*, given its status as a tractable model organism. The overarching questions that I addressed related to the boundaries of where precursor pelvic fin cells could arise from and when they had been specified to become pelvic fin.

To begin the process of tracing precursor pelvic fin cells throughout 3 weeks of development, I characterized the movements of the embryonic LPM through short-term Kaede lineage tracing and analyzing lightsheet timelapses. I found that there are two populations of Hand2:eGFP expressing cells (as a marker of LPM), one that populates the pre-anal fin fold, and another, the future parietal peritoneum, that envelops the yolk extension. In this latter population, the dorsal-to-ventral migratory movements of these cells over the yolk extension are devoid of

much anteroposterior movement. Next, I used a laser heat-shock permanent lineage tracing system and found that the anteroposterior boundaries of LPM that could contribute to the pelvic fin are from somite levels 6-11, at the widest, with evidence for peritoneum at somite levels 7-11 contributing most frequently to the pelvic fin bud.

My results additionally support the idea of late specification of the pelvic fin instead of early specification, as previously hypothesized in the literature. This is supported by the absence of classic hindlimb-associated genes *tbx4* and *pitx1* in the lateral plate mesoderm of the embryo, and the expression of these genes in the body wall of the prospective pelvic fin region immediately prior to pelvic fin initiation. The caudal Hox cluster genes were also found to be co-expressed with the hindlimb-associated genes, perhaps suggesting that re-regionalization of the somatic mesoderm in the body wall was occurring.

5.2 Proposed mechanism of pelvic fin field specification and induction in zebrafish

While further work is needed to support this hypothesis, I will propose here a mechanism for pelvic fin field specification and induction in zebrafish based on my findings from this dissertation. In the 18 hpf embryo, the lateral plate mesoderm is distributed as two, bilateral dorsal stripes. While the pectoral fin field has already been specified (Quintanilla & Ho, 2020), within the first 24 hours of development, the pelvic fin field likely has not yet been set. Throughout the next few days of development, the lateral plate mesoderm divides into two cell populations, the splanchnic and somatic mesoderm, and the somatic mesoderm envelops the body wall. The somatic mesoderm then develops into the parietal peritoneum. (Figure 5.1A)

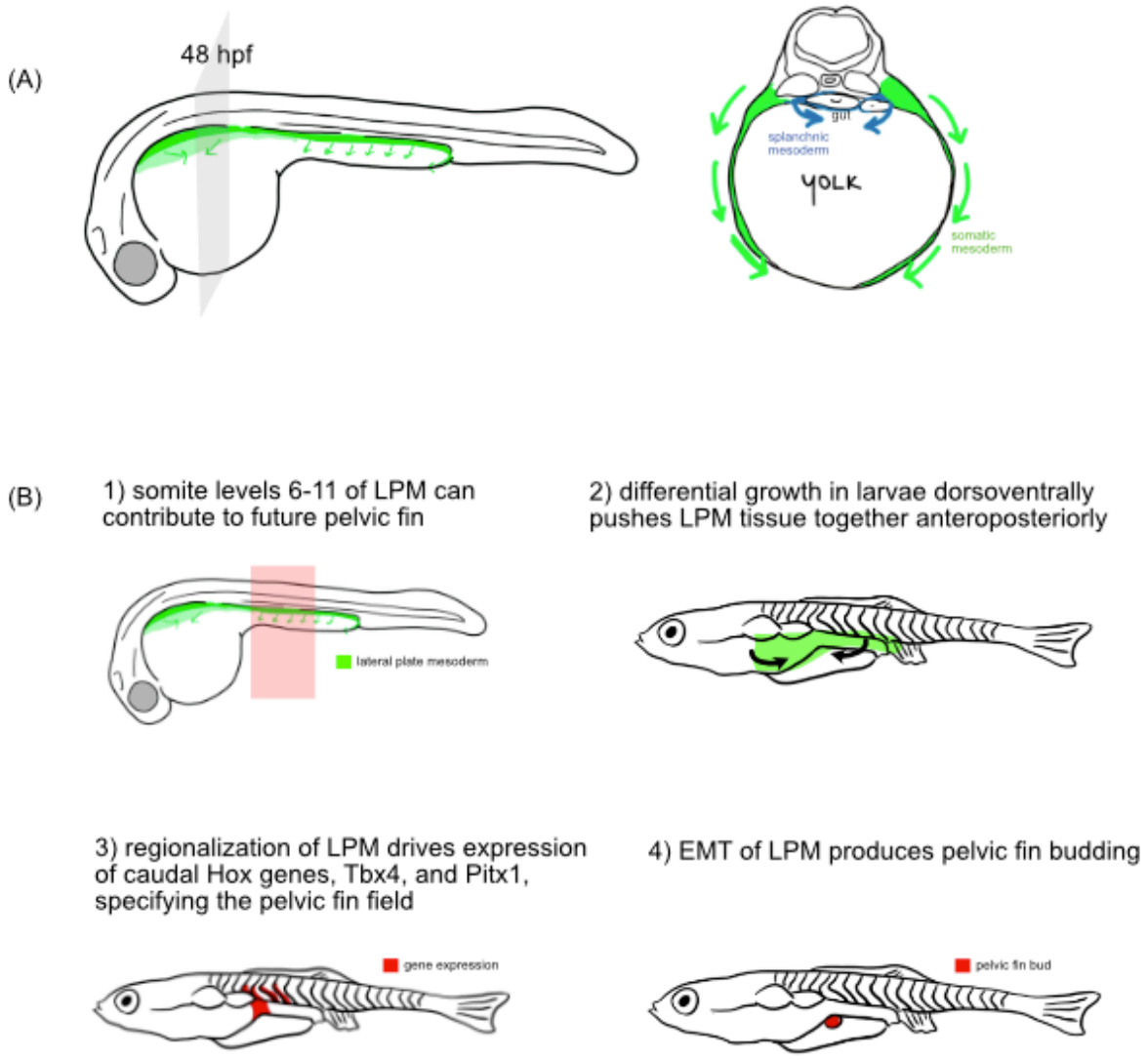

Figure 5.1 - Movements of LPM in zebrafish development

(A) Schematic diagram of a transverse section of a 48 hpf embryo, showing the splanchnic mesoderm (blue) migrating around the endodermal gut tube, and the somatic mesoderm (green) migrating over the yolk and yolk extension. (B) Proposed mechanism for pelvic fin specification and induction.

Starting 2-3 weeks post fertilization, as metamorphosis begins, changes in the levels of thyroid hormones (Liu et al., 2002) potentially trigger the initiation of the pelvic fins, and thus I would expect to see TH-responsive elements in the peritoneum here. The LPM is then possibly regionalized again by the activation of posterior Hox cluster genes and the fin field is specified, which trigger pelvic fin field markers such as *tbx4* and *pitx1*. At 3 weeks post fertilization, EMT signals in the fin field potentially convert the static epithelium of the parietal peritoneum to mesenchymal cells that coalesce into fin buds. The Fgf cascade for outgrowth is initiated, leading the way for future patterning and differentiation of the pelvic fins. (Figure 5.1B)

For the rest of this chapter, I will discuss future directions and outstanding questions generated from this research. These will first be limited to zebrafish pelvic fin development, then expanded to other LPM-associated tissues in the zebrafish. Then, I will use the results from both the evolution and developmental chapters to form a model of how these fins have shifted position in actinopterygians.

5.3 Future directions to investigate zebrafish pelvic fin development

Here, I will summarize the follow-up work proposed in Chapters 4 and 5. There is ample opportunity to more precisely define the cells that contribute to the pelvic fin buds, and this will be most elegantly accomplished through generating new transgenic lines. An LPM-specific switch line used in conjunction with the laser-mediated heat shock system will allow us to determine if LPM is truly the only tissue that contributes to the pelvic fin bud, as well as minimize background expression that commonly interferes with imaging and interpretation.

Secondly, functional studies are the next logical step for ascertaining the timing of specification of the pelvic fin field and determining the role of the genes that were expressed prior to pelvic fin initiation. Conditional, late-stage genetic knockouts of the candidate 'hindlimb' genes will reveal their importance, or potential redundancy, in pelvic fin initiation. Testing the role of thyroid hormone as a possible initiator through blocking/overexposure and assaying whether there is a difference in gene expression afterwards will provide insight into its role in the initiation pathway. Finally, perturbing the EMT pathway and/or quantifying cell proliferation can help elucidate whether this is a necessary process for the fin bud to form.

5.3.2 Competency of the LPM to form fin buds

Testing for tissue competency to form fin buds is an exciting prospect that addresses many of the questions surrounding specification, the extent of the pelvic fin field, and perhaps even the origin of the paired fins themselves. Lateral plate mesoderm transplantation experiments in chick were fundamental to understanding the limb field and the roles of Tbx5, Tbx4, and Pitx1 (J. L. Nowicki & Burke, 2000). Given the thinness of the lateral plate mesoderm (1-2 cell layers thick) and the delicate nature of the yolk sac, these types of transplantation experiments are not as tractable in the zebrafish embryo (though possible, see Ahn et al. 2002). Instead, bead implantation experiments where Fgf-soaked beads are embedded into the overlying epithelium to test for induction of a fin bud are more commonly used (Cohn et al., 1995; Q. Mao et al., 2015).

Implantation of an Fgf-soaked bead over various timepoints can narrow down a window of competency, and implantation over various axial levels can refine or dispute the boundaries of the pelvic fin field. Given the results generated from this thesis, I would expect that competency is not established until 2-3 weeks post fertilization, when we begin to see the expression of posterior Hox genes to possibly regionalize the lateral plate mesoderm. I predict that a fin bud would only be generated within the boundaries of *tbx4* or *pitx1* "localized" gene expression, with the frequency of successful bud outgrowth more likely to be induced nearer somite levels 8-9 (Figure 5.2). The alternative is that buds could also be induced in the "diffuse" expression realms seen in Chapter 4. The sharpness of the boundaries can be measured in frequency of bud induction, but could also be measured by the size of the bud induced. As the beads are much smaller than the larval myomeres (50 μM vs. 200 μM), myomeric boundaries will serve as sufficient resolution for counting position. It is possible that instead of an all-or-nothing switch for bud induction, buds induced near the boundaries could recruit fewer LPM cells and simply begin smaller in size. For all experiments, double staining for *tbx5* and *tbx4* to verify that the bud is pelvic fin in identity will be a necessary closing step.

Would any LPM-derived tissue have the competency to form fin buds if they were located at the right axial levels? Testing the pre-anal fin fold for competency to form a fin bud would yield potentially intriguing results. Again, the pre-anal fin fold is invaded by a population of Hand2:eGFP expressing cells, suggesting that these future fibroblasts are LPM in origin. Importantly, these cells do not derive from the same population that will become parietal peritoneum, as discussed in Chapter 3. Since the pre-anal fin fold is also a layer of epithelium

sandwiching potentially LPM-derived cells, it resembles a form of "somatopleure" which is defined as epithelium overlying somatic mesoderm.

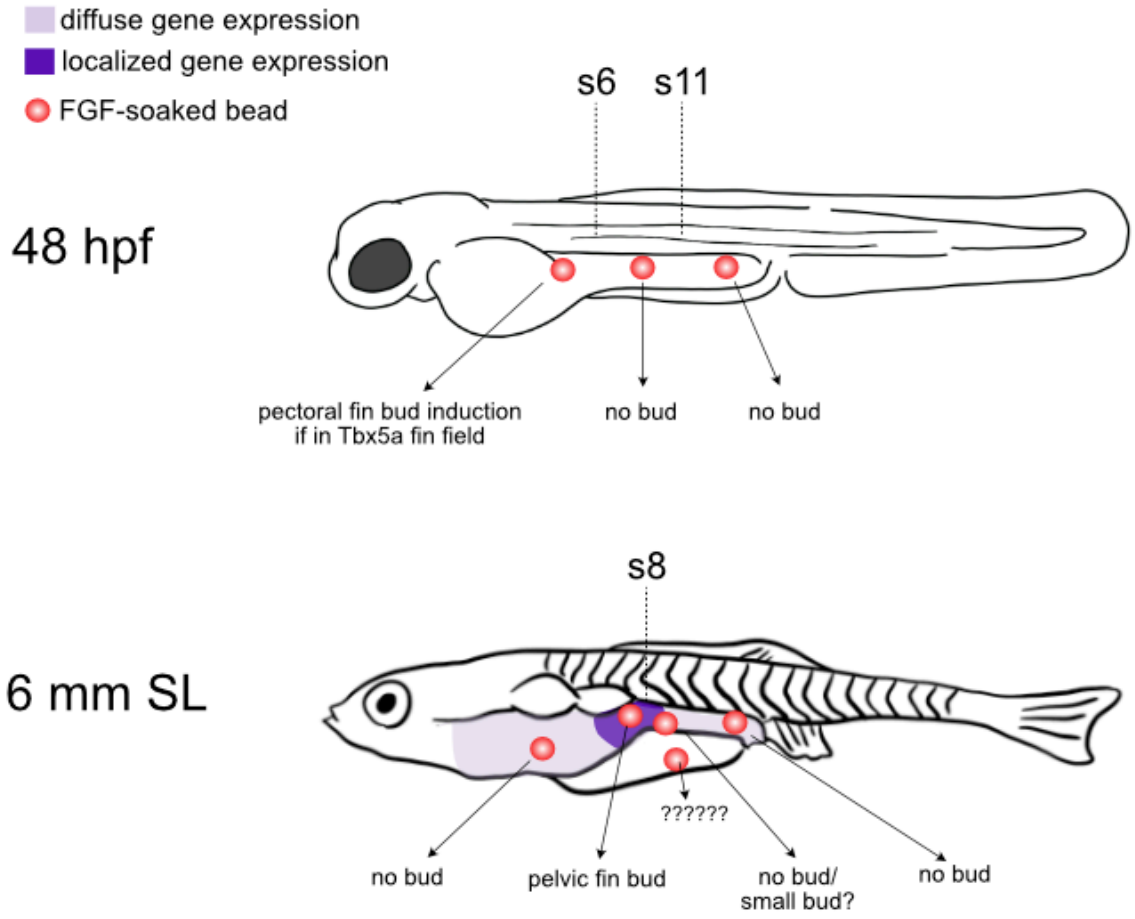

Figure 5.2 - Predictions from Fgf-soaked bead implantation experiments.

The gene expression refers to expression of *tbx4* and *pitx1*, which mark the hindlimb field in tetrapods. If specification is late, then a pelvic fin bud would only be generated at later larval stages.

There is reason to believe that the pre-anal fin fold may be competent tissue, as non-limb forming lateral plate mesoderm has been shown to generate limbs in prior studies. The lateral plate mesoderm splits into the somatic mesoderm (limb-forming parietal peritoneum) and the splanchnic mesoderm (visceral peritoneum). Splanchnic mesoderm, in chick, has been shown to have limb-forming capabilities when transplanted underneath ectoderm in the inter-limb region (Yonei-Tamura et al., 2005). The splanchnic mesoderm appears to already have been regionalized, as splanchnic mesoderm from the wing-level gave rise to forelimb buds, and splanchnic mesoderm from the leg-level gave rise to hindlimb buds. The same experiment has not been replicated in zebrafish given the delicate nature of the somatic/splanchnic mesoderm at embryonic stages.

Most pointedly, fin-like structures have been shown to develop within the pre-anal fin fold. The Lewis fish mutant, previously reported by Q. Mao in her dissertation, generates a single median fin inside the pre-anal fin fold at the level of the pelvic fins (Figure 5.3A). The size of the pelvic fins in these mutants is smaller than that of wild type, suggesting that the Lewis fin might recruit cells that were originally destined for the pelvic fins. Confusingly, the Lewis fin did not express typical markers of pelvic fins – there was no expression of *tbx4*, and no expression of *hand2*, implying that there is no lateral plate mesoderm contribution. In another example, an individual from the heat-shock experiments developed a small bud-like structure within the pre-anal fin fold that appeared to be attracting cells from the nearest myotome (Figure 5.3B). This aberrant bud was at the level of somite 7, anterior to the pelvic fin level, and the pelvic fins of the individual developed normally.

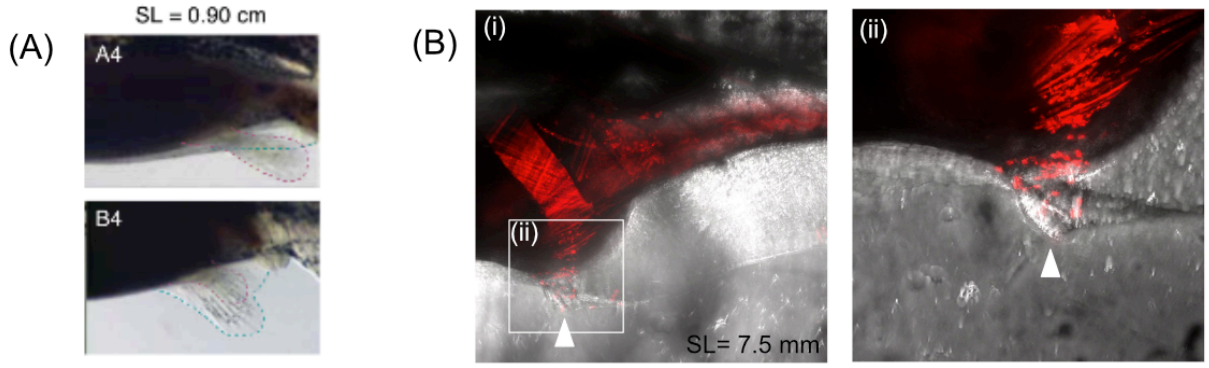

Figure 5.3 - Fin structures within pre-anal fin fold.

(A) A4- wild type, B4- Lewis mutant. Teal dotted line shows pre-anal fin fold, magenta shows pelvic fins. (Qiyan Mao, 2013) (B) Bud-like structure within pre-anal fin fold attracting cells from the nearest myotome.

5.4 Understanding the LPM contribution to the pre-anal fin fold

In addition to the question of fin bud competency, the movement of Hand2:eGFP expressing cells into the pre-anal fin fold crowns it as a fascinating tissue of interest. The larval post-anal fin fold has a similar structure of epithelium sandwiching a layer of invading fibroblast cells, but the fibroblasts derive from the dermomyotome of the somites (Lee, Knapik, et al., 2013). These fibroblasts do not contribute to the bony fin rays in the adult median fins, and instead remain as fibroblasts within the fin webs (Lee, Knapik, et al., 2013). If fibroblasts from the post-anal fin fold are somite-derived, why aren't cells from the pre-anal fin fold also from the somites? Why are these cells derived from Hand2:eGFP expressing cells, which is a marker of LPM cells, instead?

The answer might lie in the anatomy of the zebrafish embryo. While the post-anal fin fold lies adjacent to the somites, the pre-anal fin fold is separated from the somites by the yolk

and yolk extension. If somitic cells were to migrate into the pre-anal fin fold, they would need to traverse across a large distance and interact with the migration of the future parietal peritoneum lateral plate mesoderm cells. The somites/myotomes do not completely envelop the body wall until a few weeks post fertilization, and this is accomplished through a slow myotomal extension process (Windner et al., 2011). (Figure 5.4)

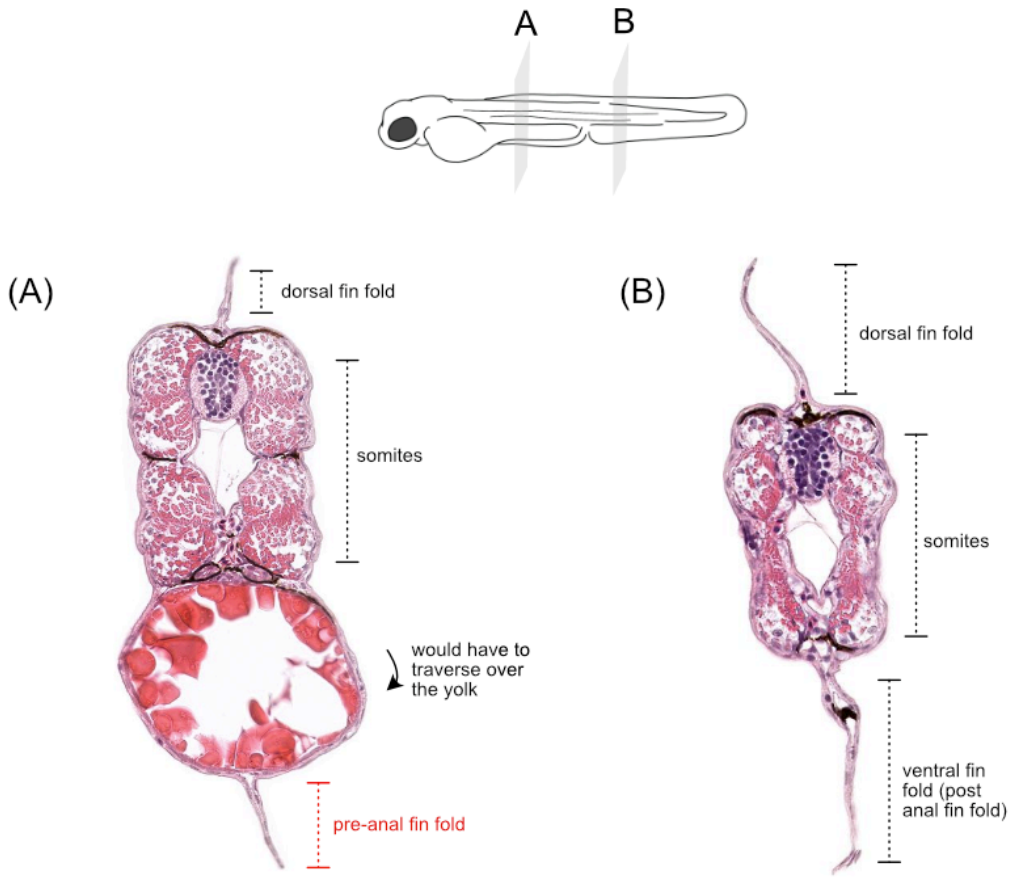

Figure 5.4 - Hemotoxylin-and-eosin-stained sections of a 3 dpf zebrafish embryo.

(A) showing the distance that the paraxial mesoderm cells would have to travel to contribute fibroblasts to the pre-anal fin fold. In contrast, in (B) the paraxial mesoderm cells are immediately adjacent to the continuous dorsal fin fold and the ventral fin fold. Sections are from ("Bio-Atlas - Zebrafish Atlas," 2013).

Another type of cell, migratory muscle precursors (MMPs), delaminate from the dermomyotome of the somites and migrate into the limb buds. In zebrafish, they appear to only arise from somites 1-6 in embryonic stages and migrate into the pectoral fin to give rise to fin musculature (Windner et al., 2011). In zebrafish, MMPs delaminate from myotomes 8-9 to give rise to pelvic fin musculature, but this is only after the myotomes have extended ventrally after some time in development (Cole et al., 2011). The distance traveled by these MMPs is relatively short in comparison to migrating over the yolk. Therefore, while the dermomyotome of these somites have the capacity to contribute migratory cells, the trajectory of these cells appears to be limited to short distances.

Through Kaede lineage tracing, I determined that the source of these Hand2:eGFP expressing cells in the pre-anal fin fold arose from mesodermal cells just anterior to the tailbud (Figure 3.5A) that eventually lie just anterior to the anus. These cells migrate down to the ventral midline and then migrate anteriorly in an almost leader-follower manner, with the leader cell extending filopodia anteriorly and leading a steady chain of fellow Hand2:eGFP expressing cells (Figure 3.6). Based on visual observations from the Prummel et al. (2022) timelapse and static images taken here, these fibroblasts begin invading the pre-anal fin fold as it grows outwards (e.g. the outgrowth of the epithelial layers is in tandem with the outward migration of the fibroblasts). The outgrowth of the pre-anal fin fold usually occurs once the Hand2:eGFP expressing ventral midline fibroblasts reach the anterior limit of the yolk extension. In all of these processes, development proceeds in a surprising posterior-to-anterior fashion, with the posterior-most Hand2:eGFP expressing ventral midline cells invading the pre-anal fin fold first, proving an exception to the typical anterior-to-posterior dogma of development. Thus, not only

do these Hand2:eGFP expressing cells surprisingly contribute to a median fin structure, they also behave in contrast to the normal direction of embryonic development.

The fate of the fibroblasts in the pre-anal fin fold after the fin fold's resorption in the adult form is uncertain, but some clues can be derived from the post-anal fin fold. The post-anal fin fold, which disappears with the emergence of the adult median fins, does not dissolve away via apoptosis, as previously hypothesized (Miyamoto & Abe, 2022). Instead, the epithelial cells of the fin fold shrink dorsoventrally and elongate anteroposteriorly, and then are likely resorbed into the growing body wall (Miyamoto & Abe, 2022). Miyamota and Abe further show that some of the fibroblasts are incorporated into the median fins, but do not contribute to the fin rays themselves. It is possible that the fibroblasts in the pre-anal fin fold are resorbed into the body wall, but through the heat-shock lineage tracing, I have found that they are not incorporated into the pelvic fins. This is likely because while the median fins develop within the post-anal fin fold, the pelvic fins are outgrowths lateral to the pre-anal fin fold, which confers some spatial discontinuity.

Thus, these avenues of further research are of possible interest: (1) What is the nature of the pre-anal fin fold Hand2:eGFP expressing cells? Are they truly LPM? RNA transcriptome analysis assessing for LPM factors would provide insight into this question. Per individual, there are at least 50 fluorescently labeled Hand2:eGFP expressing cells in the pre-anal fin fold. These data can be compared to existing RNA sequencing data from the pectoral fin and the rest of the lateral plate mesoderm to check for similarities (Boyle Anderson & Ho, 2018; Prummel et al., 2022).

(2) What are the leader-follower dynamics in the anteriorly migrating ventral midline cells? Ablation of the pioneer neuron in migrating facial branchiomotor neurons disrupts their early migration into posterior rhombomeres (Wanner & Prince, 2013) – what would occur if the leader cell were ablated in this system? I predict that much like the facial branchiomotor neuron system, early migration might be disrupted, but that later migration would likely rely on another "tract" (perhaps the extending pre-anal fin fold) and could compensate for the loss of the leader cell. Alternatively, the leader cell might not be important to correct migration at all, and migration might not be disrupted if the second-in-line is promoted to a new role.

(3) How is the pre-anal fin fold resorbed into the body wall, if it is at all? Ruling out apoptosis via TUNEL staining would be a straightforward starting point, followed by detailed imaging of the shape of epithelial cells through a cell membrane marker transgenic line. To assess the fate of the fibroblasts, the laser-mediated heat shock system can be used to label them, and individuals can be followed for longer than the current scope of this thesis (>2 months post fertilization). In terms of perturbation of the fibroblasts, I have attempted to ablate and amputate the pre-anal fin fold and have unfortunately encountered why the zebrafish larval fin fold is commonly used as an excellent model for regeneration.

(4) Are there any additional roles for these ventral midline cells besides developing into fibroblasts? As the dorsal stripes of LPM cells migrate ventrally over the yolk extension, how do these cells know how to stop migrating? The ventral midline cells might act as a barrier that informs these dorsal-stripe cells that they have reached the ventral midline. The alternative

scenario is that once the dorsal-stripe cells reach the midline, they encounter the cells on the opposite side of the embryo which acts as the stop signal. However, the ventral midline cells already outline the entire midline of the yolk extension by this point, meaning that the ventral midline cells would be the first to meet the dorsal-stripe cells. In my confocal timelapses, I can see these cells contacting each other through their filopodia (Figure 3.6A). Ablating a few ventral midline cells right before the dorsal-stripe cells reach them might shed insight into the importance of these cells as stop signals; dorsal-stripe cells might mis-migrate to the other side of the yolk extension in the absence of the ventral midline cells.

Furthermore, I have found that the ventral midline cells express *fgfs* (*fgf8a, fgf10a, fgf24*) (Figure 4.1B). Given the role of *fgf24* as a convergence cue in the pectoral fin, it is possible that the ventral midline cells act as a signaling cue to attract the dorsal-stripe LPM cells ventrally, though they cannot be the only factor. The anterior-most dorsal-stripe LPM cells begin migrating ventrally before the ventral midline cells reach that AP level, so there may first be a cue from the dorsal midline encouraging these cells to migrate outwards.

5.5 Comparative evolution and development of pelvic fin positioning

In this section, I will indulge in personal speculation and hypotheses about the developmental changes that might have driven the spectacular diversity of pelvic fin positioning seen in actinopterygians. In my model, there are three events that need to have occurred, listed without any kind of order: (1) decoupling of pectoral and pelvic fin bud initiation, where there is a delay in the specification of the pelvic fin field, (2) splitting of the lateral plate mesoderm into

the somatic and splanchnic layers prior to ventral migration, and (3) the somatic mesoderm acquiring more of a mesenchymal, instead of epithelial, nature.

(1) Decoupling of pectoral and pelvic fin bud initiation

The delay in pelvic fin initiation is a characteristic that is unique to actinopterygians, as the forelimb/pectoral fin and hindlimb/pelvic fin buds in sarcopterygians and chondrichthyans develop much more closely in time. Theoretically, a delay in pelvic fin initiation and/or specification of the pelvic fin field would enable positioning to be more labile. For example, if specification/initiation was early, the pelvic fin field would be fixed posteriorly, as the anterior portion of the LPM would need to be patterned as the pectoral fin field (i.e. *tbx5a* and *tbx4* cannot be expressed in the same cells, as this would lead to confusion over fin identity.) This would necessitate either migration of the LPM rostrally and/or migration of the pelvic fin field cells rostrally within the LPM. However, if specification were delayed relative to pectoral fin bud development, then the parietal peritoneum/somatic mesoderm in the body wall could be patterned without disturbing the placement of the pectoral fins.

Closer inspection of where in phylogeny this delay became more exaggerated reveals that it may have been acquired in either Neopterygi or Teleostei. A pronounced delay is not seen in Polypteriformes, Acipenseriformes, Amiiformes, or Lepisosteiformes (W. W. Ballard & Needham, 1964; William W. Ballard, 1986; Bartsch, Gemballa, & Piotrowskil, 1997; Bemis & Grande, 1992; Long & Ballard, 2001) relative to metamorphosis. In Table 5.1, I have compared the timing of pectoral and pelvic fin bud appearance to the “juvenile” stage, which I have informally defined as roughly corresponding with the complete differentiation of the pectoral fin

(Davis, Shubin, & Force, 2004; Fujimura & Okada, 2007). This is meant to be similar to the "metamorphosis" from larval to juvenile that is more commonly noted in teleost staging literature. As seen in Table 5.1, although there is sometimes a delay in pelvic fin initiation (e.g. *P. senegalus*), relative to the several months that it takes to reach the juvenile stage, the delay is actually not as exaggerated.

Family	**Species**	**Pectoral initiation**	**Pelvic initiation**	**"Juvenile" stage**	**Reference**
Polypteriformes	*Polypterus senegalus*	5 dpf	26 dpf	~90 dpf	Bartsch et al. (1997)
Acipenseriformes	*Polyodon spathula*	11 dpf	13 dpf	52 dpf	Bemis and Grande (1992), Davis et al. (2004)
Amiiformes	*Amia calva*	6 dpf	15 dpf	?	Ballard (1986)
Lepisosteiformes	*Lepisosteus osseus*	5 dpf	6 dpf	~40 days for yolk absorption	Long and Ballard (2001), Dean (1895)
Lepisosteiformes	*Atractosteus tristoechus*	0-3 dah (days after hatching)	4-10 dah	10-18 dah	Comabella et al. (2010)

Table 5.1 - Comparative table for paired fin initiation milestones in early members of Actinopterygii.

Starting in the Neopterygi or Teleostei, we begin to see a longer delay where the pelvic fin initiation is closer in timing to metamorphosis than to the pectoral fin bud initiation. Elopomorphs, the first lineage in Neopterygi and sister to Teleostei, are characterized by an unusual leptocephalic phase where the larvae are large, transparent, and laterally compressed; these leptocephali oddly shrink when metamorphosing into the juvenile stage (Miller, 2009). For this reason, it is difficult to ascribe if the delay began in Neopterygi or Teleostei. Nevertheless,

starting in Osteoglossomorpha, the pectoral fin bud develops rapidly within the first few days, and the pelvic fin bud is more closely tied with metamorphosis (Table 5.2).

Order	**Species**	**Pectoral initiation**	**Pelvic initiation**	**Metamorphosis**	**Reference**
Elopomorpha*	*Megalops cyprinoides*	? but predates pelvic	~30 dpf	~70 dpf	Tsukamoto and Okiyama (1997)
Osteoglossomorpha	*Pollimyrus isidori*	3 dpf	17 dpf	~30 dpf	Diedhiou et al. (2007)
Otomorpha	*Danio rerio*	2 dpf	21 dpf	~30 dpf	Grandel and Merker (1998)
Percomorpha	*Oreochromis niloctus*	~50 hpf	9 dpf	~9 dpf	Fujimara and Okada (2007)

Table 5.2 - Comparative table for paired fin initiation milestones for later members of Actinopterygii.

The sample size in the Tables 5.1 and 5.2 are limited, but I have attempted to assemble a database of pectoral and pelvic fin initiation times, which is described in Appendix C. The outstanding challenge will be to standardize measurements of time (I have used standard length as a proxy) across species. Metamorphosis is used here as a shared, relative timepoint across species, but other milestones such as hatching, flexion, or the development of a particular feature could also be used.

(2) Early splitting of the somatic and splanchnic layers

I hypothesize that the splitting of the somatic and splanchnic layers of the lateral plate mesoderm before their outward migration, as opposed to an initial layer migrating outwards and then splitting, has allowed for the rostral shift in pelvic fin position. In tetrapods, the lateral plate mesoderm first extends outwards, then a coelom forms within the LPM, forming the somatic and splanchnic layers (Funayama et al., 1999; Gilbert, 2000). Once splitting is complete, then the somatopleure (somatic mesoderm + ectoderm) begins to give rise to the limb buds. This appears to be a similar case with sharks (Nelsen, 1953) suggesting that this is a gnathostome synapomorphy. A consequence of extension-first instead of splitting-first is that that the patterning of the somatic and splanchnic layers might be constrained together (Coates & Cohn, 1998). For example, if the LPM is patterned before splitting, then both the somatic and splanchnic layers might retain the same spatial patterning. Such would be the case in chick, where the wing and leg determination occurs at the 13-somite stage, and the complete splitting of the LPM and *TBX4/5* expression occurs simultaneously at the 20-somite stage (Tickle, 2015). Forward shifting of the hindlimb through patterning of the LPM differently might modify the gut regionalization of the smooth muscle and visceral peritoneum (derived from the splanchnic mesoderm). (Figure 5.5)

In contrast, if the LPM splits into its two populations prior to extending outwards, each layer can be regionalized independently. This is seen in zebrafish, where the splanchnic cell population migrates inwards around the endodermal gut tube, and the somatic cell population migrates outwards to encircle the yolk extension (Gays et al., 2017; Prummel et al., 2022). The coelom is formed as the yolk is resorbed. (Figure 5.1A)

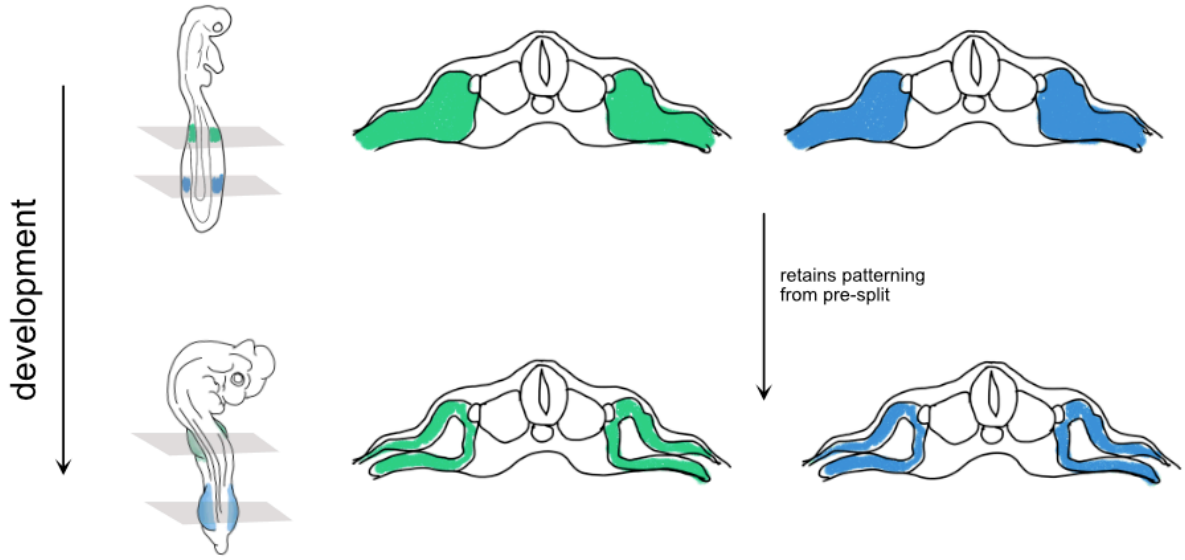

Figure 5.5 - Transverse sections at the forelimb (green) and hindlimb (blue) levels.

An extension-first, split-later formation of the somatic and splanchnic mesoderm layers would mean that the two layers would retain the same patterning as they did pre-split. Example is modeled from a chick embryo.

The earliest lineages of actinopterygians may retain the ancestral state of extend-first, split-later. I believe that holoblastic cleavage in actinopterygians is linked to this condition. Holoblastic cleavage essentially means that the endoderm contains yolk platelets instead of the yolk being a separate mass. Because the endoderm (future gut tube and visceral organs) needs to be enveloped by mesoderm, the lateral plate mesoderm moves as one sheet to encircle the endodermal mass, and forms a coelom within itself. However, with meroblastic cleavage, the embryo lies on top of a separate yolk ball that is not tied with the endoderm. Instead, the LPM is free to split-first into two populations to envelop the endoderm, still lying on top of the yolk ball, and to envelope the yolk, forming the body wall. The resorption of the yolk forms the coelom between the splanchnic and somatic layers. The teleost-specific yolk syncytial layer (YSL) may

likely be an important innovation that facilitated this new form of development; it is a transient extra-embryonic tissue layer that covers the yolk after gastrulation. It is tempting to speculate that the presence of the YSL functions as a center for signaling or protection until the somatic LPM envelops the yolk cell.

This is not to say that all meroblastic cleaving organisms have two separate LPM populations. Chick is famously meroblastic, however, the yolk is not actually incorporated into the body of the chick, and remains a separate sac outside of it. The same is true for chondrichthyans. In contrast, actinopterygians seem to universally absorb their yolk by forming their body walls around it.

In actinopterygians, the Polypteriformes, Acipenseriformes, and the Amiiformes display holoblastic cleavage (Cooper & Virta, 2007) (Figure 5.6B). A scanning electron microscope transverse section of *P. spathula* also appears to show a coelom forming between the primitive LPM, instead of two separate populations (Bemis & Grande, 1992) (Figure 5.6A). Lepisosteiformes have an intermediate form between holoblastic and meroblastic cleavage, with segmented yolk cells, and it appears that the rest of the actinopterygians are meroblastic (Cooper & Virta, 2007). Thus, the early-split of the lateral plate mesoderm into two cell populations may be coincident with Neopterygi or Teleostei.

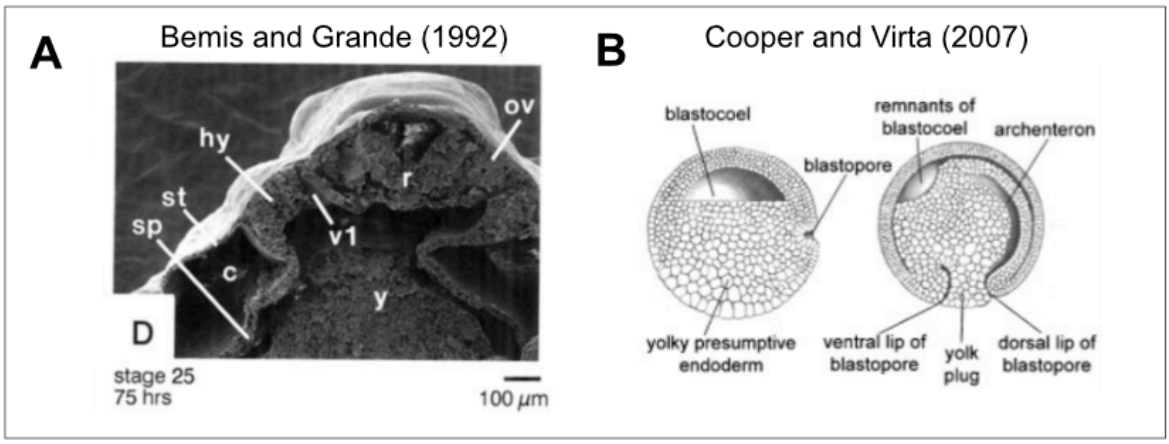

Figure 5.6 - Embryonic LPM in Polyodontiformes and Acipenseriformes

(A) Transverse section of *Polyodon spathula* showing split between somatic mesoderm (st) and splanchnic mesoderm (sp), and the coelom (c) between them. (B) Diagram of holoblastic cleavage of sturgeon, showing the yolky endoderm being enveloped by mesoderm.

(3) Migratory-like instead of epithelial-like LPM may be a characteristic of Teleostei

A feature that appears to be characteristic of tetrapod/non-teleost lateral plate mesoderm is that these cells are quite epithelial in nature, as compared to the mesenchymal, migratory LPM that is seen in zebrafish. For instance, chick LPM actually undergoes a mesenchymal-to-epithelial transition (MET) as the two layers form (Asleh et al., 2022) and is solidly an epithelial sheet by the time the limb buds appear (Gros & Tabin, 2014). An epithelial LPM would be much more rigid, and by nature of being a static epithelial sheet, constrain cells from moving within the LPM or constrain the entire LPM from migrating in a certain direction. In theory, this would limit rostral movement of pelvic fin precursor cells, especially if specification was shifted earlier in some lineages of teleosts.

In the Nile tilapia (jugular pelvic fins) and pufferfish, the LPM appears to be shifting rostrally as a whole based on DiI experimental labeling (Murata et al., 2010; Mikiko Tanaka, Yu, & Kurokawa, 2015). Furthermore, in tilapia, the pelvic fins initiate and bud while the LPM is still in the process of enveloping the yolk (Murata et al., 2010). Many more observations of the LPM cell morphologies will be needed in different lineages, but this data suggest a tenuous connection between a migratory LPM state and the ability to shift fins rostrally.

5.5 Integrative view of actinopterygian fin configuration shifts

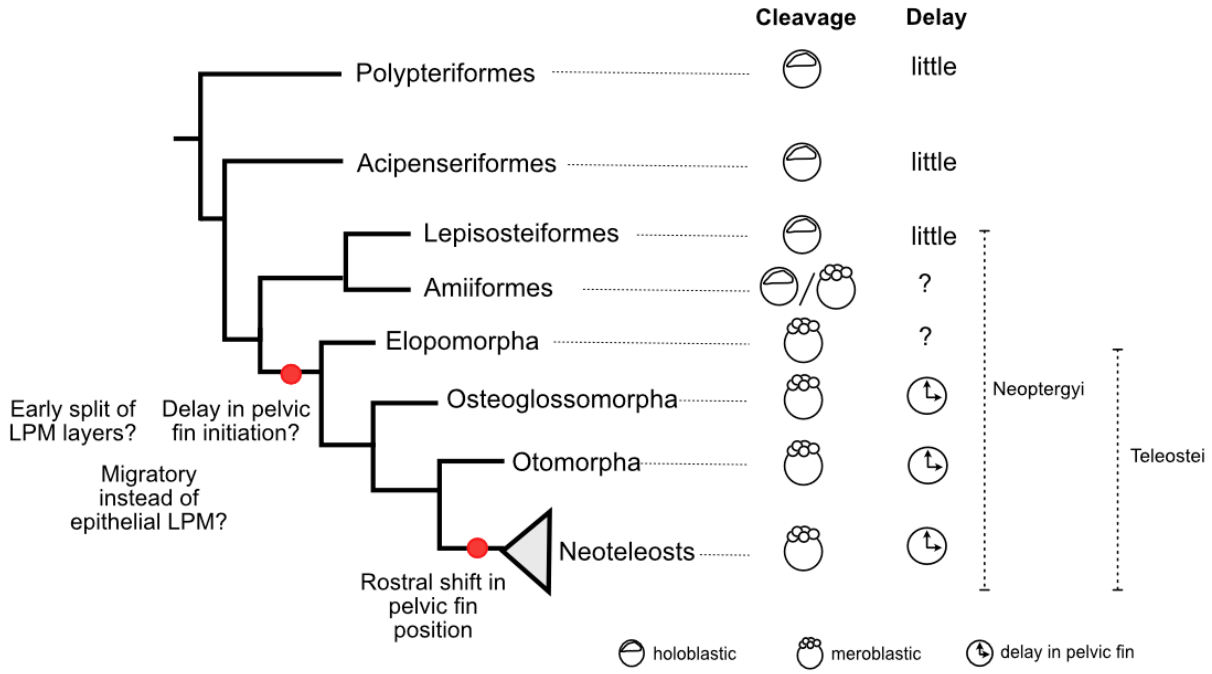

Figure 5.7 - Model of the developmental changes acquired in actinopterygians for the ability to shift pelvic fins rostrally.

From the macroevolutionary analysis, I have found that the Neoteleostei node is when the exaggerated, pronounced shifts in pectoral and pelvic fin position occurred. I hypothesize that

the ability to shift the pelvic fins rostrally was set into motion by changes seen at the base of Neoptergyi/Teleostei – delayed specification of the pelvic fin, a switch to meroblastic cleavage which is facilitated by an early split of the splanchnic and somatic mesoderm cell populations, and conversion to a more mesenchymal instead of epithelial nature of the LPM. (Figure 5.7) If the shift occurred at Neopterygi, this implies there was a reversal at Lepisosteiformes to resemble the ancestral condition. If the shift was at Teleostei, then Amiiformes independently converged on its intermediate cleavage condition. Since both are equally parsimonious, acquiring data on the timing of the delays is necessary for distinguishing the two hypotheses.

The rostral shift of the pelvic fin is accompanied by a dorsal shift of the pectoral fin, and it appears that the pelvic fin does not shift forwards unless the pectoral shifts upwards. This functionally makes sense, as a ventral pectoral fin would collide with a rostrally-shifted pelvic fin. This drives the question – what is contributing to a more dorsal pectoral fin? In most larvae, the pectoral fins are large flaps spanning the whole height of the body. The eventual DV positioning of the pectoral fin in the adult appears to be more mediated by the positioning of the fin radials (endochondral derivative) relative to the cleithrum (dermal skeleton derivative), along with allometric growth of body depth. These are metamorphosis-associated changes, as the adult pectoral fin structure is not stable until that period.

With our extant data, I do not have evidence of one fin position shifting before the other, but it is possible that fossil Neoteleost species might provide evidence of one fin's position driving the other's in the future. Regardless, it appears that the capacity to shift pelvic fins rostrally requires more fundamental shifts in body plan organization and development, so it

follows that this innovation was potentially acquired more ancestrally. I would postulate that the two developmental pathways controlling adult pelvic fin position and pectoral fin position are quite separate, considering that one (pelvic) involves potentially regionalizing the somatic mesoderm, and the other (pectoral) is more related to where the endochondral disc ossifies relative to the cleithrum. Additionally, the finding that Non-Neoteleosts are more constrained in the pelvic fin position axis than are Neoteleosts (Chapter 2) supports the idea that pectoral fin position is inherently more labile. Non-Neoteleosts were more free to evolve along the pectoral fin axis than the pelvic fin axis.

As for the finding that the anterior limits of the dorsal and pelvic fins are almost always in register in extant actinopterygians, I suggest that the dorsal fin is the fin that follows the pelvic fin due to biomechanical constraints. Theoretically, because the larval fin fold encircles the entire dorsal side and post-anal ventral side, and because the dorsal fin is derived from the dermomyotome which also spans the entire length of the dorsal side, the environment and components respectively to create a dorsal fin are not restrictive. It could be possible that the regionalization of the LPM is translated somehow to the axial sclerotome (or perhaps they are derived from the same source), which would inform where the anterior margin of the dorsal fin should develop. In summary, the position of the pelvic fins appear to be more constrained due to their interactions with the pectoral fins, and are more likely to be influencing the position of the dorsal fin than vice versa.

5.6 Key species to investigate next

To begin to test the hypotheses that I have put out in the previous section, I propose that the development of an acipenseriform (sturgeon or paddlefish) and a percomorph with rostral pelvic fins should be prioritized for comparison with zebrafish. (After all, M. Coates would not accept anything less than a three-taxon statement.) The cichlid Nile tilapia as used in previous studies would be a tractable option, or any other substrate-brooding cichlid.

With the acipenseriform, it would be important to verify that the lateral plate does split into two layers through coelom formation – this can be done with a time series of transverse sections. Staining for markers of epithelium, such as proteins that indicate cell polarization, would test the assertion that the acipensereiform LPM layers are more epithelial than mesenchymal. Then, using the forelimb-associated and hindlimb-associated suite of genes, one can test for early or late specification of each fin bud for both the acipenseriform and the percomorph. I predict that the specification for acipenseriform pelvic fins should be relatively close in time to the pectoral fin's specification, given that these buds develop within days of each other. The percomorph condition will likely be late and resemble that of the zebrafish, but if it were early, then this would raise questions about how pelvic fin precursors migrate anteriorly.

Of course, perhaps the most valuable species no longer exist – phylogenetically-placed fossil species are sorely needed to add color to the abrupt shifts in pelvic and pectoral fin position. Without these, we will be missing critical information about the diversity of fin position. Until then, *Dorypterus* – a Permian actinopterygian fish pre-dating the earliest

neotelost, with inexplicably anteriorly placed pelvic fins - will continue to hold its secrets (Hancock & Howse, 1870)

.

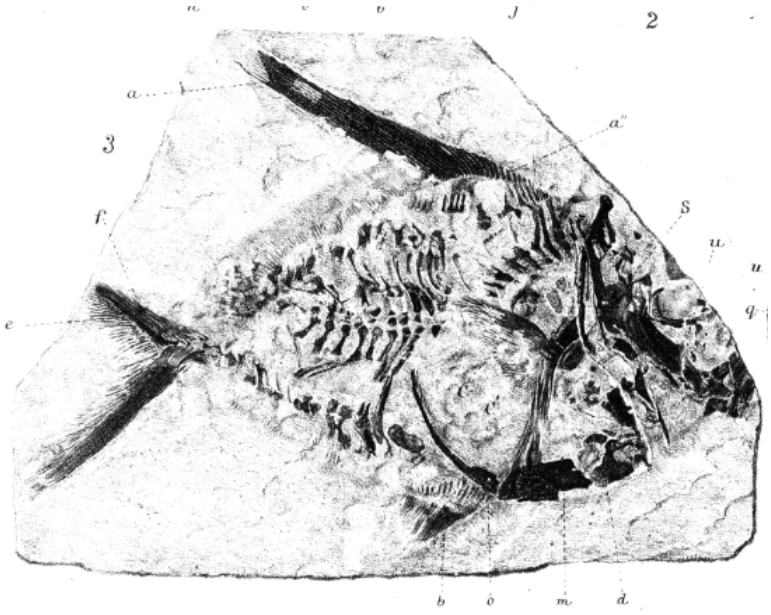

Chapter 6 - MATERIALS AND METHODS

Zebrafish strains and husbandry

Zebrafish were raised according to standard protocol (Westerfield, 2000). The AB wildtype strain was used for all protocols unless otherwise stated. The transgenic lines used were *Tg(hsp70:cre-ert2)* (as generated here), *Et(hand2:eGFP)ch2* (Q. Mao et al., 2015), and *Tg(ubi:switch) (Tg(ubi:loxP-EGFP-loxP-mCherry)*) (Mosimann et al., 2011).

Generation of the *Tg(hsp70:cre-ert2)* line

Tol2 transposon transgenesis (Kwan et al., 2007) was used to create the hsp:cre-ert2 transgenic line. Tg(hsp70:cre-ert2) is a multisite Invitrogen Gateway assembly of p5E-*hsp70* and p3E-polyA from the Tol2kit (Kwan et al., 2007) and pENTR/D_creERt2 (Mosimann et al., 2011) into the destination vector pDestTol2pACryGFP (Berger & Currie, 2013).

32 ng of Tol2 transposase capped mRNA and 32 ng of the transgenic vector were injected into one-cell AB embryos. F0 individuals were screened with an alpha-crystallin:GFP marker and raised into adulthood; almost all injected embryos were positive for the marker (~95%). Adult F0 individuals were outcrossed to AB, and the F1 individuals were screened via global heat shock. Approximately 50% of the F1 individuals were positive for germline transmission. These individuals were outcrossed to AB, and the resulting F2 clutches were tested for germline transmission and leakiness (i.e. extraneous expression of RFP driven by extraneous

Cre-ERT2 activity). F2 lines were established when these conditions were met: at least 50% of the clutch was positive for both the crystallin marker and positive heat shock response (see next section for details); a negative heat shock response was seen for global heat treatment without 4-OHT application, and 4-OHT application without global heat treatment. All lines used for the subsequent laser-mediated heat shock experiments stem from a single F1 individual that produced multiple F2 that met the aforementioned criteria.

Heat shock activation and 4-OHT treatment of the *Tg(hsp70:cre-ert2)* line

To perform long-term lineage tracing, the Tg(hsp70:cre-ert2) line was first crossed with Tg(ubi:switch). Heat-shocking cells with an infrared laser (or immersed at 37C for total-embryo conversion) drove the transcription of the Cre-ERT2 protein, which is tamoxifen (4OHT) dependent for its localization into the nucleus. Immersion of the embryos into 4OHT solution after heat shock drives activity of the Cre-ERT2 protein, which converts heat-shocked cells from GFP-expressing to RFP-expressing.

Global heat shock was used to screen embryos for successful transgenesis of the Tol2 construct. Embryos (48 hpf) were placed into embryo media at 37C for 1 hour, and then transferred into 10 uM of 4-Hydroxytamoxifen (4-OHT, H7904, Sigma, St Louis, MO, USA) overnight following pre-existing protocol (Mosimann et al., 2011).

The XYClone Class 1, 1460 nm, 300 mW infrared laser system (Hamilton Thorne Biosciences) was used to permanently label cells via laser-mediated heat shock activation. The

laser system was coupled with a 20X Zeiss objective. Embryos between 2dpf and 3dpf were mounted in 3% methyl cellulose (155495, MP Biomedicals, Solon, OH, USA) on a depression slide and always positioned so that they were lateral, and their left sides were facing upwards. The power level of the laser (%) and the number of pulses were tailored towards each tissue type. In general, the power % ranged from 20-25% for lateral plate mesoderm, and the number of pulses ranged from 15-25X. Tissues in the tail or pre-anal fin fold were labeled with 15-20% power and 10-15X pulses. Clusters of approximately 10-15 cells were able to be labeled. The embryos were transferred to 10 μM of 4-OHT for at least 2 hours, up to overnight. No difference in expression was seen between short and long 4-OHT treatments. Individuals were checked for Cre activation at 6 dpf, and individuals with the desired labeling (approximately 20% of the embryos) were raised individually in embryo media-filled culture dishes until pelvic fin stage (3-4 weeks post fertilization).

Static imaging and analysis

Confocal images of embryos and larvae were acquired with a Zeiss Inverted Microscope 710 at either 10X or 20X magnification. Fish were mounted in 1% low melting point agarose (Sigma A9414) in embryo medium in a glass-bottom petri dish, which was inverted for mounting (MatTek co. P35G-0-7-C). The resulting Z-stack images were compressed into a maximum intensity projection in Fiji (Schindelin et al., 2012).

All other images were acquired with either a Zeiss Axioplan compound microscope or a Leica MZFLIII dissection microscope. Fish were mounted on a depression slide in 3% methyl cellulose.

Confocal timelapses

*Et(hand2:eGFP)ch2 e*mbryos were imaged on the 10X objective of the confocal using a heated stage with the mounting method described previously. The interval time was 14 minutes and the timelapses ranged from 7-13 hours. Images were exported to Fiji for analysis.

mRNA in situ hybridization and immunochemistry

Protocol step-by-step sheets for mRNA in situ hybridization (embryo, larval) and antibody staining are listed in Appendix D.

DIG-labeled antisense probes were generated from lab stock plasmids for *tbx4, fgf24,* and *fgf8a* (Q. Mao et al., 2015). All other probes were generated from PCR products using 18-21hpf zebrafish cDNA (primer sequences in Table 6.1). The protocols for cDNA synthesis, PCR template generation, and transcription follow those from (Boyle Anderson & Ho, 2018).

The mRNA in situ hybridization protocol followed (Dae-gwon Ahn et al., 2002) for embryo-stage fish. For larvae, the in situ protocol was identical to the embryo protocol with the following modifications:

- Fixation for 3 days instead of 1 day
- Proteinase-K permeabilization at 20 ug/mL for 50 minutes
- Additional 2X SSCT Day 2 wash for 2 hours after the 0.05X SSCT wash
- Additional PBT wash step for a day
- Incubation in clearing solution at 70C, 1 hour, post NBT/BCIP staining

Clearing solution:

- 50% formamide
- 2X SSC
- 1% SDS

For the larvae stained with the Hox probes, the protocol used acetone permeabilization and staining with BM Purple (Cat 11442074001, Roche) following Day 1 of (Vauti, Stegemann, Vögele, & Köster, 2020). The rest of the staining protocol followed the above larvae in situ protocol, with BM Purple substituted for NBT/BCIP.

Whole mount antibody staining for larval specimens was performed with the following protocol. Specimens were fixed for 3 days in 4% PFA (paraformaldehyde, P6148, Sigma) in PBS. They were then permeabilized with acetone for 30 minutes at -20C, or in 20 µg/mL Proteinase-K for 50 minutes. Fish were incubated in blocking solution (Appendix D) for 2 hours at room temperature, then incubated in primary antibody (typically 1:250 or 1:500 in goat serum) at 4C for several days. This was followed by PBT rinses and incubation in blocking solution for 1 hour at room temperature, and then incubation in the secondary antibody (typically 1:2000 in

goat serum) for 1 hour at room temperature or with the DAB substrate kit (SK-4100, Vector Laboratories, Burlingame, CA).

Antibody staining on paraffin sections followed a protocol courtesy of D. Reed (University of Illinois at Chicago), described next. Slides were deparaffinized with histosol and graded into PBS. They were then treated with sodium borohydride and 0.01M citrate buffer. Slides were washed with 0.5% v/v Triton-X100, then 100% MeOH at -20C, and then underwent blocking with 5% goat serum for 1 hour. Incubation in primary antibody (1:250 or 1:500 in goat serum) followed overnight, with each section covered with the antibody and parafilm inside a hydration chamber (airtight container with ddH2O inside). The following day, slides were washed in Triton-X100, ddH2O, and the finally incubated in the secondary antibody (1:2000 in goat serum) or the DAB substrate kit. Sections were finally dehydrated into 100% ethanol and mounted permanently with Permount (SP15-100, Fisher Chemical).

Primary antibodies used were anti-cdh1 (GTX125890, Genetex), anti-cdh2 (GTX125885, Genetex), and anti-gfp (A-6455, Invitrogen). The secondary fluorescent antibodies used were goat anti-rabbit IgG (H+L) Alexa Fluor 488 (A-11008, Invitrogen).

Photoconversion and fate mapping

1290 ng of Kaede mRNA was injected into 1-cell stage embryos and screened at 12-18 hpf for uniform green fluorescence. Kaede+ embryos were then mounted under a bridged coverslip at 12-18hpf and photoconverted in areas of interest – posterior lateral plate mesoderm

over the yolk extension, pre-anal fin fold, and the ventral region immediately anterior to the tailbud. The size of the photoconverted region was controlled by an adjustable pinhole on a 20X objective, and the photoconversion itself was mediated by a 100W W HBO mercury bulb through the DAPI filter on a Zeiss Axioplan microscope. Typically, the size of the photoconverted region encompassed around 20 cells. The embryo underwent photoconversion for approximately 60 seconds and immediately photographed afterwards with a Nikon D5000 camera. Individuals were photographed at various timepoints up until 80hpf.

Cell tracking and trajectory analysis

Cell tracking was performed on lightsheet timelapses shared by K. Prummel from data generated as part of (Prummel et al., 2022). The Fiji plugin MtrackJ was used to manually track Hand2+ (green-fluorescing) cells. To correct for drift and growth, other landmarks were tracked: somite boundaries, non-migrating GFP+ cells outside of the yolk extension, and the ventral-most, anterior-most point of the yolk extension and the ventral-most, posterior-most point of the yolk extension.

To quantify measurements for cell displacement, compaction, scatter, speed, and persistence, the CellTrackingEBA (Boyle-Anderson et al., 2022) package was modified to accommodate our needs for this project. The cell tracking and coding work in R was performed by E. Yuan and is deposited online at the University of Chicago Box.

To correct for whole-embryo translocational drift relative to the microscope lens, movements from non-migrating GFP+ cells outside the yolk extension were subtracted out from the migrating cell tracks. The tracks for each somite boundary were also used to correct for rotational movement of the embryo; a linear regression was calculated for the points in the boundaries to represent the "horizontal" positioning of the embryo. To account for elongation of the yolk extension and changes to its aspect ratio, the ratio between the ventral-most anterior and posterior points of the yolk extension and the first somite boundary tracked (somite 4) was recorded at t=0 and all following x-direction and y-direction cell movements were standardized to this original ratio.

Histology

Paraffin sections of larvae were prepared through the following protocol, courtesy of K. Criswell (University of Oxford) and described here. Specimens were fixed for 3 days in 4% PFA, and sequentially graded into 100% ethanol, Histosol (HS100, National Diagnostics), and then paraffin wax. Specimens were embedded into molds and left to cool overnight. They were then sectioned into 8-12µm sections with an Olympus CUT4060 microtome. After drying, slides were stained with Hemotoxylin (LS-J1045, Vector) and Eosin Y (318906, Sigma) and mounted in Permount.

For vibratome sectioning, fixed specimens were embedded in 4% low melting point agarose in PBT. Specimens were cut transversely between 200-400µm thickness and mounted

with glycerol onto slides. The instrument used was a Vibratome 1000 Plus (IMEB Inc, San Marcos, CA).

Table 6.1 - Primer Sequence Table for in situ hybridization probes

	Forward	Reverse
fgf10a	CAGACACGATCACTACGGACGCTTTAC	TAATACGACTCACTATAGggAGCTTGACTAAATTCGGATGGTAGGAT
fgf10b	GGAAGAACAATAAGCGGCAG	TAA TAC GAC TCA CTA TAG GGT CTC TCT CCT GTC TCT CTC G
fgf16	ACAGGACCACAGCAGATTCG	ATTTAGGTGACACTATAGaaGGCCTCCTCATTTTGGACCA
fgfr1a	gctttgctcagggactcaac	TAATACGACTCACTATAGggtcacctcgatgtgtttcagc
fgfr1a	GTACTCCACTGACCTGACTG	ATTTAGGTGACACTATAGaaGTA CTC CAC TGA CCT GAC TG
fgfr1b	TAATCATGGAGTCGGTGGTG	T AAT ACG ACT CAC TAT AGG GTGC TGA ATG ATG GGA GAT CC
fgfr2	tgacctggtgtcagagatgg	TAATACGACTCACTATAGggccacattaaaaccccaaacg
fgfr2	AGCAATACTCTCCCAGCTTC	ATTTAGGTGACACTATAGaaGGGAGGAATTGATCGGAAGT
fgfrl1a	GATCCTCAGCCTCACATTCA	T AAT ACG ACT CAC TAT AGG GCCT TTA GCA GCA AAC TCC AC
fgfrl1b	CATCGGTGAGTCGTCCTGTAGAG	ATTTAGGTGACACTATAGaaGAG TTG ACC ACA ATA ATG GAG TTC G
fgfrl1b	GGGTGAAGGATGGACGTAAT	ATTTAGGTGACACTATAGaaGAGAGAACAGTCAGGTAGGC
pitx1	GATTAATGCAGCCGTACGAC	TAATACGACTCACTATAGGGCCAAAAGACGGATGCTGTTT

APPENDIX A - SUPPLEMENTARY TABLES FOR CHAPTER 2

Appendix A Table 1 - Complete list of extant species.

Ablennes_hians
Acantharchus_pomotis
Acanthistius_ocellatus
Acanthochaenus_luetkenii
Acanthostracion_quadricornis
Acanthurus_mata
Acestrorhynchus_altus
Acestrorhynchus_falcirostris
Achirus_lineatus
Acipenser_oxyrinchus
Acipenser_sturio
Agamyxis_pectinifrons
Akysis_prashadi
Albula_nemoptera
Albula_vulpes
Aldrovandia_affinis
Aldrovandia_phalacra
Alepocephalus_bairdii
Alloclinus_holderi
Allocyttus_verrucosus
Allotoca_diazi
Ambassis_agassizii
Ambassis_agrammus
Amblyceps_mangois
Amblyopsis_spelaea
Amia_calva
Amissidens_hainesi
Amphichaetodon_melbae
Anabas_testudineus
Anableps_anableps
Anadoras_grypus
Anarchias_seychellensis
Anchoa_hepsetus
Anguilla_anguilla
Anoplopoma_fimbria
Antigonia_rubescens
Apareiodon_piracicabae
Aphanius_mento
Aphredoderus_sayanus
Aphyosemion_loennbergii
Aplocheilus_lineatus
Apogon_indicus
Apsilus_dentatus
Apteronotus_albifrons
Aptocyclus_ventricosus
Arctoscopus_japonicus
Argentina_silus
Argentina_striata
Argyropelecus_hemigymnus
Argyropelecus_lychnus
Ariomma_indicum
Ariomma_melanum
Arnoglossus_laterna
Arnoldichthys_spilopterus
Arripis_georgianus
Arripis_trutta
Aseraggodes_kobensis
Aspasma_minima
Assessor_macneilli
Astyanax_mexicanus
Ateleopus_japonicus
Atheresthes_stomias
Atherinomorus_stipes
Atherinosoma_microstoma
Aulichthys_japonicus
Aulopus_filamentosus
Aulorhynchus_flavidus
Aulostomus_maculatus
Aulostomus_strigosus
Avocettina_infans
Badis_corycaeus
Balistes_capriscus
Banjos_banjos
Barbourisia_rufa
Barbus_lacerta
Bassanago_albescens
Bathyclupea_argentea
Bathygobius_soporator
Bathylagus_euryops
Bathymaster_signatus
Bathypterois_atricolor
Bathysaurus_ferox
Bedotia_geayi
Bellator_militaris
Bembrops_heterurus
Benthalbella_infans
Benthalbella_macropinna
Benthodesmus_simonyi
Beryx_splendens
Betta_fusca
Bidyanus_bidyanus
Bothus_ocellatus
Botia_histrionica
Botia_histrionica
Brachyhypopomus_pinnicaudatus
Brama_brama
Breitensteinia_cessator
Brevoortia_patronus
Brosmophycis_marginata
Brotula_barbata
Brycon_atrocaudatus
Brycon_melanopterus
Bryconops_melanurus
Bunocephalus_coracoideus
Caenotropus_labyrinthicus
Calloplesiops_altivelis
Campylomormyrus_rhynchophorus
Capros_aper
Carnegiella_marthae
cataetyx_rubrirostris
Catostomus_commersonii

Appendix A Table 1, continued

Cebidichthys_violaceus
Centroberyx_gerrardi
Centrogenys_vaigiensis
Centropomus_ensiferus
Centropomus_parallelus
Centropyge_ferrugata
Cepola_macrophthalma
Cepola_schlegelii
Ceratias_holboelli
Ceratoscopelus_maderensis
Cetopsis_coecutiens
Cetostoma_regani
Chaca_bankanensis
Chaenopsis_alepidota
Chaetodipterus_faber
Chaetodon_falcula
Champsodon_atridorsalis
Channa_gachua
Channa_micropeltes
Chanos_chanos
Characidium_fasciatum
Characodon_lateralis
Chaunax_pictus
Chaunax_suttkusi
Cheilodactylus_fuscus
Cheilopogon_exsiliens
Chiasmodon_niger
Chilodus_punctatus
Chiloglanis_niloticus
Chilorhinus_suensonii
Chirocentrus_dorab
Chirostoma_humboldtianum
Chitala_ornata
Chlorophthalmus_agassizi
Chologaster_cornuta
Chondrostoma_nasus
Chrysichthys_nigrodigitatus
Citharinus_citharus
Citharus_linguatula
Clarias_angolensis
Clarias_teijsmanni
Clepticus_parrae
Clupisoma_garua
Cobitis_taenia
Coloconger_cadenati
Compsura_heterura
Congiopodus_peruvianus
Cookeolus_japonicus
Coreoperca_kawamebari
Coryphaenoides_rupestris
Cottunculus_thomsonii
Cottus_bairdii
Crenuchus_spilurus
Cryptacanthodes_maculatus
Cryptopsaras_couesii
Ctenolucius_hujeta
Ctenopoma_acutirostre
Cubiceps_pauciradiatus
Cyclothone_microdon
Cynodon_gibbus
Cyprinodon_macularius
Cyttopsis_cypho
Cyttopsis_rosea
Cyttus_australis
Dactyloptena_peterseni
Dactylopterus_volitans
Dallia_pectoralis
Danio_rerio
Dario_hysginon
Dermogenys_collettei
Dermogenys_pusilla
Deuterodon_parahybae
Diapterus_peruvianus
Diastobranchus_capensis
Dicentrarchus_punctatus
Dinoperca_petersi
Diodon_holocanthus
Diogenichthys_atlanticus
Diplodus_noct
Diplogrammus_goramensis
Diplomystes_nahuelbutaensis
Diplophos_taenia
Distichodus_rostratus
Ditropichthys_storeri
Dolicholagus_longirostris
Dysomma_anguillare
Echiichthys_vipera
Elassoma_okefenokee
Elassoma_zonatum
Eleotris_pisonis
Eleutheronema_tetradactylum
Elops_affinis
Elops_hawaiensis
Elops_machnata
Elops_saurus
Engraulisoma_taeniatum
Enoplosus_armatus
Entelurus_aequoreus
Ephippus_orbis
Epiplatys_chaperi
Erythrocles_schlegelii
Esox_lucius
Esox_niger
Etheostoma_osburni
Eucinostomus_gula
Eumicrotremus_orbis
Eurymen_gyrinus
Fistularia_corneta
Fistularia_petimba
Formosania_lacustre
Forsterygion_lapillum
Fowleria_vaiulae
Fundulus_bermudae
Fundulus_lima
Gadomus_dispar
Galaxias_brevipinnis
Galaxias_zebratus
Galeichthys_peruvianus
Gambusia_geiseri
Gasteropelecus_maculatus
Gasterosteus_aculeatus
Gempylus_serpens.JPG
Glyptothorax_lampris

Appendix A Table 1, continued

Gobiesox_maeandricus
Gobiosoma_chiquita
Gonorynchus_greyi
Grahamichthys_radiata
Gramma_loreto
Grammatostomias_flagellibarba
Grammicolepis_brachiusculus
Graus_nigra
Guavina_guavina
Gymnarchus_niloticus
Gymnelopsis_ochotensis
Gymnocephalus_cernua
Gymnotus_carapo
Gymnotus_coropinae
Gyrinocheilus_aymonieri
Haemulon_plumierii
Halieutichthys_aculeatus
Halosauropsis_macrochir
Harengula_jaguana
Helogenes_marmoratus
Helostoma_temminkii
Hemibarbus_maculatus
Hemiramphus_balao
Hemisorubim_platyrhynchos
Heterocharax_macrolepis
Heteropneustes_fossilis
Heterostichus_rostratus
Hexagrammos_octogrammus
Himantolophus_groenlandicus
Hiodon_alosoides
Hiodon_tergisus
Hippocampus_erectus
Histiopterus_typus
Histrio_histrio
Holtbyrnia_latifrons
Homatula_variegata
Hoplerythrinus_unitaeniatus
Hoplias_microlepis
Hoplichthys_acanthopleurus
Hoplichthys_citrinus
Hoplocharax_goethei
Hoplomyzon_sexpapilostoma
Hoplostethus_crassispinus
Hoplostethus_occidentalis
Hydrocynus_forskahlii
Hydrolycus_armatus
Hypomesus_nipponensis
Hypopomus_artedi
Hypoptopoma_thoracatum
Hyporhamphus_sajori
Hypsagonus_quadricornis
Ichthyococcus_ovatus
Icosteus_aenigmaticus
Ictalurus_punctatus
Ictiobus_bubalus
Iguanodectes_geisleri
Iguanodectes_geisleri
Ijimaia_loppei
Indostomus_paradoxus
Iso_rhothophilus
Jenkinsia_lamprotaenia
Johnius_belangerii
Jordania_zonope
Kajikia_albida
Kali_indica
Kareius_bicoloratus
Kathetostoma_giganteum
Kaupichthys_hyoproroides
Kaupichthys_nuchalis
Kentrocapros_rosapinto
Kryptopterus_macrocephalus
Kuhlia_mugil
Kuhlia_munda
Kurtus_gulliveri
Kyphosus_incisor
Labeo_parvus
Lampris_guttatus
Lateolabrax_japonicus
Latropiscis_purpurissatus
Leiognathus_longispinis
Lepidoblepharon_ophthalmolepis
Lepidocybium_flavobrunneum
Lepidopus_altifrons
Lepidorhombus_boscii
Lepidotrigla_argus
Lepisosteus_osseus
Lepisosteus_platostomus
Lepomis_miniatus
Leptobrama_muelleri
Leptocottus_armatus
Lestidium_atlanticum
Lethrinus_obsoletus
Leuresthes_tenuis
Lignobrycon_myersi
Limia_vittata
Liobagrus_reinii
Liparis_callyodon
Liza_affinis
Lobotes_pacificus
Lobotes_surinamensis
Lophiodes_reticulatus
Lophius_americanus
Lopholatilus_chamaeleonticeps
Lumpenus_fabricii
Lutjanus_campechanus
Luvarus_imperialis
Lycodes_gracilis
Macquaria_colonorum
Macrognathus_zebrinus
Macroramphosus_scolopax
Magnisudis_atlantica
Malacanthus_brevirostris
Malapterurus_beninensis
Malapterurus_electricus
Margariscus_margarita
Marukawichthys_ambulator
Mastacembelus_frenatus
Maulisia_microlepis
Maurolicus_muelleri
Megalops_atlanticus
Melamphaes_polylepis
Melanocetus_johnsonii
Melanocetus_murrayi

Appendix A Table 1, continued

Melanotaenia_duboulayi
Membras_martinica
Mene_maculata
Menidia_menidia
Meuschenia_trachylepis
Micrometrus_minimus
Microspathodon_chrysurus
Monacanthus_ciliatus
Monocirrhus_polyacanthus
Monodactylus_argenteus
Monodactylus_falciformis
Monopterus_albus
Monotaxis_grandoculis
Moringua_edwardsi
Morone_americana
Mugil_curema
Mullus_auratus
Muraenesox_cinereus
Mycteroperca_microlepis
Myripristis_murdjan
Nandus_nandus
Nandus_oxyrhynchus
Nannostomus_beckfordi
Nansenia_longicauda
Naso_thynnoides
Nemacheilus_masyae
Nemadactylus_bergi
Nematolebias_whitei
Nemipterus_zysron
Neocirrhites_armatus
Neoclinus_blanchardi
Neoconger_mucronatus
Neolebias_powelli
Neonesthes_capensis
Neosalanx_brevirostris
Neoscopelus_microchir
Neosebastes_thetidis
Neostethus_bicornis
Niphon_spinosus
Nocomis_leptocephalus
Normanichthys_crockeri
Notesthes_robusta
Notopogon_fernandezianus
Notopterus_notopterus
Noturus_stigmosus
Odontobutis_interrupta
Odontobutis_obscura
Odonus_niger
Ogcocephalus_radiatus
Oligoplites_saurus
Olivaichthys_viedmensis
Oneirodes_acanthias
Ophidion_josephi
Ophioblennius_steindachneri
Opistognathus_aurifrons
Oplegnathus_fasciatus
Oplegnathus_punctatus
Opsanus_tau
Oreochromis_niloticus
Oreoglanis_macropterus
Oryzias_dancena
Oryzias_latipes
Osphronemus_goramy
Osteoglossum_bicirrhosum
Oxyconger_leptognathus
Oxylebius_pictus
Oxyzygonectes_dovii
Pachypanchax_playfairii
Pangasius_nasutus
Pangasius_pangasius
Pangio_muraeniformis
Papyrocranus_afer
Parablennius_marmoreus
Parabotia_fasciata
Paracentropogon_rubripinnis
Paracirrhites_hemistictus
Paraclinus_integripinnis
Parahollardia_lineata
Parailia_pellucida
Parakneria_fortuita
Paraliparis_rosaceus
Parapercis_millepunctata
Parapriacanthus_ransonneti
Parapristipoma_trilineatum
Parascolopsis_eriomma
Parasudis_truculenta
Parauchenoglanis_balayi
Pareques_umbrosus
Parexocoetus_brachypterus
Parodon_hilarii
Parodon_suborbitalis
Parupeneus_barberinus
Pegasus_volitans
Pelteobagrus_ussuriensis
Pempheris_schomburgkii
Peprilus_burti
Percophis_brasiliensis
Peristedion_gracile
Petrocephalus_catostoma
Phanerodon_furcatus
Pholidichthys_leucotaenia
Phyllophryne_scortea
Piabucus_melanostoma
Pimelodus_blochii
Pinguipes_brasilianus
Plagiogeneion_rubiginosum
Plagiopsetta_glossa
Platycephalus_laevigatus
Platydoras_costatus
Plecoglossus_altivelis
Plotosus_canius
Podothecus_accipenserinus
Poecilopsetta_plinthus
Polydactylus_approximans
Polymetme_corythaeola
Polymixia_berndti
Polymixia_japonica
Polyodon_spathula
Polyprion_americanus
Polypterus_bichir
Polypterus_senegalus
Pomacanthus_arcuatus
Pomacentrus_amboinensis

Appendix A Table 1, continued

Pomatomus_saltatrix
Pontinus_rathbuni
Porichthys_notatus
Porochilus_rendahli
Priacanthus_tayenus
Pristigenys_alta
Profundulus_guatemalensis
Profundulus_labialis
Psenes_pellucidus
Psenopsis_anomala
Psettodes_belcheri
Psettodes_erumei
Pseudochromis_bitaeniatus
Pungitius_sinensis
Pyrrhulina_australis
Pythonichthys_asodes
Rachovia_maculipinnis
Ranzania_laevis
Retropinna_retropinna
Retropinna_semoni
Rexea_prometheoides
Rhabdolichops_eastwardi
Rhadinocentrus_ornatus
Rhamphocottus_richardsonii
Rhaphiodon_vulpinus
Rheocles_alaotrensis
Rhynchohyalus_natalensis
Rita_rita
Rondeletia_bicolor
Rondeletia_loricata
Ronquilus_jordani
Sagamichthys_abei
Salangichthys_microdon
Salvelinus_fontinalis
Samariscus_xenicus
Sarda_sarda
Sargocentron_vexillarium
Satyrichthys_laticeps
Saurida_gracilis
Scatophagus_argus
Schedophilus_ovalis
Scleropages_jardinii
Scolecenchelys_gymnota
Scoloplax_distolothrix
Scomberomorus_regalis
Scopelengys_tristis
Scopeloberyx_robustus
Scopelosaurus_harryi
Scophthalmus_aquosus
Scorpaenichthys_marmoratus
Scorpaenodes_xyris
Searsia_koefoedi
Sebastes_capensis
Sebastolobus_macrochir
Secutor_insidiator
Selene_vomer
Selenotoca_multifasciata
Setipinna_taty
Siganus_argenteus
Siganus_uspi
Sillago_asiatica
Sillago_robusta
Silonia_silondia
Silurus_aristotelis
Siniperca_chuatsi
Sinogastromyzon_wui
Sisor_rabdophorus
Solea_solea
Sorsogona_prionota
Species
Sphoeroides_maculatus
Sphyraena_borealis
Sphyraena_guachancho
Spirinchus_thaleichthys
Stenotomus_chrysops
Stereolepis_gigas
Sternarchogiton_preto
Stromateus_fiatola
Sturisoma_festivum
Stylephorus_chordatus
Symphysanodon_berryi
Symphysanodon_octoactinus
Synagrops_bellus
Synagrops_philippinensis
Synchiropus_phaeton
Synodontis_alberti
Synodontis_multipunctatus
Synodus_foetens
Talismania_bifurcata
Taractichthys_steindachneri
Terapon_jarbua
Tetragonurus_cuvieri
Tetrapturus_pfluegeri
Thalassoma_bifasciatum
Thryssa_hamiltonii
Thunnus_atlanticus
Thymallus_arcticus
Toxotes_chatareus
Toxotes_lorentzi
Trachinus_draco
Trachipterus_trachypterus
Triacanthodes_ethiops
Triacanthus_biaculeatus
Trichodon_trichodon
Trichonotus_elegans
Trinectes_maculatus
Triplophos_hemingi
Triportheus_nematurus
Tripterygion_tripteronotum
Umbra_krameri
Uranoscopus_scaber
Valencia_hispanica
Velifer_hypselopterus
Xenolepidichthys_dalgleishi
Xenomystus_nigri
Xiphias_gladius
Zanclus_cornutus
Zaniolepis_frenata
Zaprora_silenus
Zenopsis_conchifer
Zeus_faber
Zu_cristatus

Appendix A Table 2 – Image citations for extant species.

Images for all other species that are not listed below are from the Price dataset (Friedman et al., 2020).

Species	Citation of image source
Acanthostracion_quadricornis	Burgess, G. (n.d.). Photograph of *Acanthostracion quadricornis*. Florida Museum: Discover Fishes. University of Florida. https://www.floridamuseum.ufl.edu/discover-fish/species-profiles/acanthostracion-quadricornis/.
Aldrovandia_phalacra	Orlov, A. (2007). Photograph of *Aldrovandia phalacra*. Fishbase. Fishbase. https://www.fishbase.se/photos/PicturesSummary.php?ID=9012&what=species.
Allotoca_diazi	Artigas Azas, J. M. (2006). Photograph of *Allotoca diazi*. Fishbase. Fishbase. https://www.fishbase.se/photos/PicturesSummary.php?need2save=&tosave=&TRPP=1&id=46442&what=species&personnel=&user_session=&lme=&StartRow=0&TotRec=2&SortBy=iucn.
Amblyceps_mangois	Hosseini, M. A. R. (2006). Photograph of *Amblyceps mangois*. Fishbase. Fishbase. https://www.fishbase.se/photos/PicturesSummary.php?need2save=&tosave=&TRPP=1&id=24792&what=species&personnel=&user_session=&lme=&StartRow=3&TotRec=7&SortBy=iucn.
Anoplopoma_fimbria	Grant, D., M. Gjernes and N. Venables, 1996. A practical guide to the identification of commercial groundfish species of British Columbia. Archipelago Marine Research Ltd., Victoria, BC, Canada. 34 p.
Apsilus_dentatus	Soward, J. (2015). Photograph of *Apsilus dentatus*. Shorefishes of the Greater Caribbean Online Information System. Smithsonian Tropical Research Institute. https://biogeodb.stri.si.edu/caribbean/en/thefishes/species/3681.
Aptocyclus_ventricosus	Senoh, H. (n.d.). Photograph of *Aptocyclus ventricosus*. National Museum of Nature and Science. Kanagawa Prefectual Museum of Natural History. http://mitofish.aori.u-tokyo.ac.jp/images/fishes/Aptocyclus_ventricosus.jpg.
Argentina_silus	Flescher, D. (1997). Photograph of *Argentina silus*. Fishbase. Fishbase. https://www.fishbase.de/photos/PicturesSummary.php?StartRow=1&ID=2700&what=species&TotRec=4.
Argyropelecus_lychnus	Ramjohn, D. D. (1998). Photograph of *Argyropelecus lychnus*. Fishbase. Fishbase. https://www.fishbase.se/photos/PicturesSummary.php?ID=11549&what=species.
Ariomma_indicum	*Ariomma indicum* in Fishes of Australia, accessed 02 Jun 2021, http://136.154.202.208/home/species/741
Assessor_macneilli	Fenner, R. (2001). Photograph of *Assessor macneilli*. Fishbase. Fishbase. https://www.fishbase.se/photos/PicturesSummary.php?need2save=&tosave=&TRPP=1&id=12827&what=species&personnel=&user_session=&lme=&StartRow=0&TotRec=2&SortBy=iucn.

Appendix A Table 2, continued

Ateleopus_japonicus	Naturalis Biodiversity Center. (n.d.). Rmnh.Pisc.D.1410_0. Global Biodiversity Information Forum. GBIF Secretariat. https://api.gbif.org/v1/image/unsafe/https%3A%2F%2Fmedialib.naturalis.nl%2Ffile%2Fid%2FRMNH.PISC.D.1410_a%2Fformat%2Flarge.
Avocettina_infans	Australian National Fish Collection, CSIRO. (2014). Photograph of *Avocettina infans*. Global Biodiveristy Information Facility. GBIF Secretariat. https://www.gbif.org/occurrence/2420021071.
Bassanago_albescens	Bañón-Díaz , R. (2007). Photograph of *Bassanago albescens*. Fishbase. Fishbase. https://www.fishbase.se/photos/PicturesSummary.php?ID=15663&what=species.
Bathyclupea_argentea	Noble, B. (2008). Photograph of *Neobathyclupea argentea*. Fishbase. Fishbase. https://www.fishbase.se/photos/PicturesSummary.php?need2save=&tosave=&TRPP=1&id=46346&what=species&personnel=&user_session=&lme=&StartRow=0&TotRec=2&SortBy=iucn.
Bathylagus_euryops	Orlov, A. (2007). Photograph of *Bathylagus euryops*. Fishbase. Fishbase. https://www.fishbase.se/photos/PicturesSummary.php?StartRow=0&ID=11833&what=species&TotRec=2.
Bembrops_heterurus	Carvalho Filho, A. (2005). Photograph of *Bembrops heterurus*. Fishbase. Fishbase. https://www.fishbase.se/photos/PicturesSummary.php?ID=4934&what=species.
Benthalbella_macropinna	Colombo, G. L. A. (2002). Photograph of *Lagiacrusichthys macropinna*. Fishbase. Fishbase. https://www.fishbase.se/photos/PicturesSummary.php?ID=6975&what=species.
Benthodesmus_simonyi	Maul, G. E. (2009). *Benthodesmus simonyi*, Maderian specimen described in text. . Zoological Society of London. John Wiley & Sons, Inc. https://zslpublications.onlinelibrary.wiley.com/doi/pdfdirect/10.1111/j.1096-3642.1953.tb00162.x.
Botia_histrionica	Janiczak, B. J. (2002). Photograph of *Botia histrionica*. Fishbase. Fishbase. https://www.fishbase.de/photos/PicturesSummary.php?StartRow=2&ID=24691&what=species&TotRec=4.
Brosmophycis_marginata	BOLD Systems. (n.d.). Photograph of *Brosmophycis marginata*. BOLD Systems V3. http://v3.boldsystems.org/index.php/TaxBrowser_Taxonpage?taxid=79412.
Brycon_melanopterus	Lima, F. C. T. (2017). Figure 80. *Brycon melanopterus*, Mzusp 56948, 146.9 mm Sl: Brazil, Amazonas, igarapé da Cachoeira. Global Biodiversity Information Facility. GBIF Secretariat. https://www.gbif.org/species/127620825.
Bryconops_melanurus	Brosse, S., G. Grenouillet, M. Gevrey, K. Khazraie and L. Tudesque, 2011. Small-scale gold mining erodes fish assemblage structure in small neotropical streams. Biodivers Conserv (2011)20:1013-1026.
Caenotropus_labyrinthicus	Venere, Paulo Cesar; Garutti, Valdener.Peixes do Cerrado-Parque Estadual da Serra Azul-Rio Araguaia, MT. São Carlos: RiMa Editora, FAPEMAT, 2011.p.54.

Appendix A Table 2, continued

Carnegiella_marthae	Weitzman, S. H. (2017). *Carnegiella marthae* FIN035446 Slide 35 mm. Smithsonian Institution NMNH Division of Fishes. Smithsonian Institution, NMNH, Fishes. https://ids.si.edu/ids/deliveryService/id/ark:/65665/m3a810b92f00a84fdbbfa5a09bc87b8f42.
Catostomus_commersonii	Scarola, J. F. (1997). Photograph of *Catostomus commersonii*. Fishbase. Fishbase. https://www.fishbase.se/photos/PicturesSummary.php?ID=2965&what=species.
Ceratias_holboelli	Iglesias, S. (n.d.). The Fishes Collection of the Muséum National d'Histoire Naturelle. Muséum National d'Histoire Naturelle. https://api.gbif.org/v1/image/unsafe/http%3A%2F%2Fmediaphoto.mnhn.fr%2Fmedia%2F1406026447359SPLtqrm8BPSy2tZO.
Chaca_bankanensis	Roberts, T.R., 1989. The freshwater fishes of Western Borneo (Kalimantan Barat, Indonesia). Mem. Calif. Acad. Sci. 14:210 p.
Chaetodon_falcula	Randall, J.E., 1997. Randall's tank photos. Collection of 10,000 large-format photos (slides) of dead fishes. Unpublished.
Channa_gachua	Florida Museum of Natural History. (n.d.). Channidae *Channa gachua*. UF FLMNH Ichthyology. https://api.gbif.org/v1/image/unsafe/https%3A%2F%2Fcdn.floridamuseum.ufl.edu%2FFish%2F8e25c954-42d5-4d60-b2e7-59c549768f67.
Cheilodactylus_fuscus	Randall, J.E., 1997. Randall's tank photos. Collection of 10,000 large-format photos (slides) of dead fishes. Unpublished.
Chrysichthys_nigrodigitatus	Klimpel, S. (2003). Photograph of *Chrysichthys nigrodigitatus*. Fishbase. Fishbase. https://www.fishbase.in/photos/PicturesSummary.php?StartRow=0&ID=2440&what=species&TotRec=2.
Coryphaenoides_rupestris	Fabregat, A. G. (2002). Photograph of *Coryphaenoides rupestris*. Fishbase. Fishbase. https://www.fishbase.se/photos/PicturesSummary.php?ID=332&what=species.
Cottunculus_thomsonii	Museum of Comparative Zoology, Harvard University. (n.d.). Mcz:Ich:25869 *Cottunculus torvus*. Museum of Comparative Zoology, Harvard University. https://api.gbif.org/v1/image/unsafe/http%3A%2F%2Fmczbase.mcz.harvard.edu%2Fspecimen_images%2Ffish%2Flarge%2F25869_Cottunculus_torvus84jpeg.jpg.
Cryptopsaras_couesii	Widder, E. (n.d.). A female Triplewart Seadevil, *Cryptopsaras couesii*. Fishes of Australia. Museums Victoria. https://fishesofaustralia.net.au/home/species/3424#summary.
Cyclothone_microdon	Bray, D.J. 2018, *Cyclothone microdon* in Fishes of Australia, accessed 01 Jun 2021, http://136.154.202.208/home/species/3396
Cyttopsis_cypho	Gloerfelt-Tarp, T. and P.J. Kailola, 1984. Trawled fishes of southern Indonesia and northwestern Australia.
Dermogenys_collettei	Florida Museum of Natural History. (n.d.). Hemiramphidae *Dermogenys collettei*. UF FLMNH Ichthyology. https://api.gbif.org/v1/image/unsafe/https%3A%2F%2Fcdn.floridamuseum.ufl.edu%2FFish%2F12ee1aa6-43cc-4d04-85d1-1cd65c45871c.

Appendix A Table 2, continued

Diastobranchus_capensis	Museum of New Zealand. (2009). Photograph of *Diastobranchus capensis,* basketwork eel. Museum of New Zealand. Museum of New Zealand. https://collections.tepapa.govt.nz/object/958596.
Dolicholagus_longirostris	Uyeno, T., K. Matsuura and E. Fujii (eds.), 1983. Fishes trawled off Suriname and French Guiana.
Echiichthys_vipera	Heessen, H. (2006). Photograph of *Echiichthys vipera*. World Register of Marine Species. Flanders Marine Institute. http://www.marinespecies.org/aphia.php?p=image&tid=150630&pic=2625.
Elassoma_okefenokee	Burkhead, N., & Jelks, H. (2013). Photograph of *Elassoma okefenokee*. Fishbase. Fishbase. https://www.fishbase.de/photos/PicturesSummary.php?StartRow=0&ID=3365&what=species&TotRec=2.
Entelurus_aequoreus	Orlov, A. (2007). Photograph of *Entelurus aequoreus*. Fishbase. Fishbase. https://www.fishbase.se/photos/PicturesSummary.php?StartRow=1&ID=67&what=species&TotRec=4.
Fistularia_petimba	Cambraia Duarte, P. M. N. (2001). Photograph of *Fistularia petimba*. Fishbase. Fishbase. https://www.fishbase.se/photos/PicturesSummary.php?StartRow=3&ID=3276&what=species&TotRec=11.
Forsterygion_lapillum	Clements, K. (2001). Photograph of *Forsterygion lapillum*. Fishbase. Fishbase. https://www.fishbase.se/photos/PicturesSummary.php?ID=12940&what=species.
Gadomus_dispar	Bañón-Díaz, R. (2013). Photograph of *Gadomus dispar*. Fishbase. Fishbase. https://www.fishbase.se/photos/PicturesSummary.php?need2save=&tosave=&TRPP=1&id=52175&what=species&personnel=&user_session=&lme=&StartRow=0&TotRec=3&SortBy=iucn.
Gambusia_geiseri	Thomas, C. (2007). Photograph of *Gambusia geiseri*. U.S. Geological Survey: Nonindigenous Aquatic Species. U.S. Department of the Interior. https://nas.er.usgs.gov/queries/factsheet.aspx?SpeciesID=848.
Gempylus_serpens.JPG	Randrihasipara, L. (n.d.). Photograph of *Gempylus serpens*. The fishes collection (IC) of the Muséum national d'Histoire naturelle (MNHN - Paris). MNHN - Museum national d'Histoire naturelle. https://api.gbif.org/v1/image/unsafe/http%3A%2F%2Fmediaphoto.mnhn.fr%2Fmedia%2F1455182534670Rj6Bw0kM99ovevgF.
Gobiesox_maeandricus	prickly_sculpin. (2021). Photograph of *Gobiesox maeandricus*. iNaturalist Research-grade Observations. iNaturalist. https://api.gbif.org/v1/image/unsafe/https%3A%2F%2Fstatic.inaturalist.org%2Fphotos%2F111248143%2Foriginal.jpg%3F1611711864.
Gonorynchus_greyi	Randall, J.E., 1997. Randall's underwater photos. Collection of almost 2,000 underwater photos (slides). Unpublished.
Gymnotus_carapo	Castro, R. M. C. (1998). Photograph of *Gymnotus carapo*. Fishbase. Fishbase. https://www.fishbase.se/photos/PicturesSummary.php?need2save=&tosave=&TRPP=1&id=10915&what=species&personnel=&user_session=&lme=&StartRow=0&TotRec=3&SortBy=iucn.

Appendix A Table 2, continued

Helogenes_marmoratus	Sabaj Pérez, M. H. (2013). Photograph of *Helogenes marmoratus*. Fishbase. Fishbase. https://www.fishbase.de/photos/PicturesSummary.php?need2save=&tosave=&TRPP=1&id=12525&what=species&personnel=&user_session=&lme=&StartRow=1&TotRec=3&SortBy=iucn.
Heterostichus_rostratus	Museum of Comparative Zoology, Harvard University. (n.d.). Mcz:Ich:29891 *Heterostichus rostratus* lateral. Museum of Comparative Zoology, Harvard University. https://api.gbif.org/v1/image/unsafe/http%3A%2F%2Fmczbase.mcz.harvard.edu%2Fspecimen_images%2Ffish%2Flarge%2F29891_Heterostichus_rostratus.jpg.
Hexagrammos_octogrammus	Goff, M. (2014). Photograph of *Hexagrammos octogrammus*. iNaturalist Research-grade Observations. iNaturalist. https://api.gbif.org/v1/image/unsafe/https%3A%2F%2Finaturalist-open-data.s3.amazonaws.com%2Fphotos%2F30513407%2Foriginal.jpg%3F1548141606.
Hoplichthys_acanthopleurus	South African Institute for Aquatic Biodiversity. (n.d.). 2358.Tif. Occurrence records of southern African aquatic biodiversity. https://api.gbif.org/v1/image/unsafe/http%3A%2F%2Fspecify-attachments-saiab.saiab.ac.za%2Foriginals%2F2358.tif.
Hoplichthys_citrinus	McPhee, R., & McGrouther, M. (n.d.). A Lemon Ghost Flathead, *Hoplichthys citrinus*, collected on the Norfolk Ridge during the 2003 Norfanz Expedition. Fishes of Australia. Museums Victoria. https://fishesofaustralia.net.au/home/species/3372.
Hoplocharax_goethei	Hoffmann, P., & Hoffmann, M. (2012). Photograph of *Hoplocharax goethei*. Fishbase. Fishbase. https://www.fishbase.se/photos/PicturesSummary.php?ID=51943&what=species.
Hoplomyzon_sexpapilostoma	Taphorn, D. C. & Lilyestrom, C. G. (n.d.). 97762 *Hoplomyzon sexpapilostoma* l Fz - 22mm Sl. Field Museum of Natural History Zoological Collections. Field Museum of Natural History. https://fm-digital-assets.fieldmuseum.org/652/003/97762_Hoplomyzon_sexpapilostoma_l_FZ.jpg. FMNH 97762 Specimen collected November 13, 1983
Iguanodectes_geisleri	Muséum National d'Histoire Naturelle. (n.d.). Photograph of *Iguanodectes geisleri*. Muséum National d'Histoire Naturelle - Ichthyologie. http://mediaphoto.mnhn.fr/media/1522416433693MFV7DNvaFwJKpfp7.
Iguanodectes_geisleri	Muséum National d'Histoire Naturelle. (n.d.). Photograph of *Iguanodectes geisleri*. Muséum National d'Histoire Naturelle - Ichthyologie. http://mediaphoto.mnhn.fr/media/1522416433693MFV7DNvaFwJKpfp7.
Kajikia_albida	FAO Species Identification Sheet. (n.d.). Drawing of *Kajikia albida*. Florida Museum: Discover Fishes. University of Florida. https://www.floridamuseum.ufl.edu/wp-content/uploads/sites/66/2017/05/Kajikia-albida-02.jpg.
Lepidoblepharon_ophthalmolepis	Shao, K.-T. (1995). Photograph of *Lepidoblepharon ophthalmolepis*. Fishbase. Fishbase. https://www.fishbase.de/photos/PicturesSummary.php?ID=8828&what=species.

Appendix A Table 2, continued

Lepidorhombus_boscii	Sánchez Delgado, F. (2000). Photograph of *Lepidorhombus boscii*. Fishbase. Fishbase. https://www.fishbase.in/photos/PicturesSummary.php?need2save=&tosave=&TRPP=1&id=27&what=species&personnel=&user_session=&lme=&StartRow=-1&TotRec=3&SortBy=iucn.
Liparis_callyodon	The International Barcode of Life Consortium. (n.d.). FHAK075-17 Lateral. International Barcode of Life Project (iBOL) . https://api.gbif.org/v1/image/unsafe/http%3A%2F%2Fwww.boldsystems.org%2Fpics%2FFHAK%2FMAL1114B%2B1501477316.JPG.
Lobotes_pacificus	Robertson, R. (2006). Photograph of *Lobotes pacifica*. Fishbase. Fishbase. https://www.fishbase.se/photos/PicturesSummary.php?ID=60984&what=species.
Lophiodes_reticulatus	Field Museum of Natural History. (n.d.). 77265 *Lophiodes reticulatus*. Field Museum of Natural History (Zoology) Fish Collection. https://api.gbif.org/v1/image/unsafe/http%3A%2F%2Ffm-digital-assets.fieldmuseum.org%2F652%2F096%2F77265_Lophiodes_reticulatus_l_FZ.jpg.
Lopholatilus_chamaeleonticeps	Noble, B. (2014). Photograph of *Lopholatilus chamaeleonticeps*. Fishbase. Fishbase. https://www.fishbase.de/photos/PicturesSummary.php?StartRow=2&ID=362&what=species&TotRec=6.
Monodactylus_argenteus	Randall, J.E., 1997. Randall's tank photos. Collection of 10,000 large-format photos (slides) of dead fishes. Unpublished.
Monopterus_albus	Raredon, S. J. (n.d.). *Monopterus albus* Usnm 376108 photograph 1 of 9 specimens. NMNH Extant Specimen Records. National Museum of Natural History, Smithsonian Institution. https://api.gbif.org/v1/image/unsafe/http%3A%2F%2Fn2t.net%2Fark%3A%2F65665%2Fm3c149d079-0057-4ebe-ae3e-28d42c10b6a2.
Muraenesox_cinereus	Gloerfelt-Tarp, T. and P.J. Kailola, 1984. Trawled fishes of southern Indonesia and northwestern Australia. Australian Development Assistance Bureau, Australia, Directorate General of Fishes, Indonesia, and German Agency for Technical Cooperation, Federal Republic of Germany. 407 p.
Mycteroperca_microlepis	Flescher, D. (1997). Photograph of *Mycteroperca microlepis*. Fishbase. Fishbase. https://www.fishbase.de/photos/PicturesSummary.php?StartRow=0&ID=1212&what=species&TotRec=3.
Nemacheilus_masyae	Ott, G. H. F. (2001). Photograph of *Nemacheilus masyae*. Fishbase. Fishbase. https://www.fishbase.se/photos/PicturesSummary.php?ID=12268&what=species.
Nematolebias_whitei	Sazima, I. (2002). Photograph of *Nematolebias whitei*. Fishbase. Fishbase. https://www.fishbase.in/photos/PicturesSummary.php?ID=11882&what=species.
Nocomis_leptocephalus	Burkhead, N. (2013). Photograph of *Nocomis leptocephalus*. Fishbase. Fishbase. https://www.fishbase.se/photos/PicturesSummary.php?ID=2809&what=species.

Appendix A Table 2, continued

Olivaichthys_viedmensis	Ortubay, S. (n.d.). Photograph of *Diplomystes viedmensis*. Sistema de Información de Biodiversidad de la Administración de Parques Nacionales, Argentina. Administración de Parques Nacionales, Argentina. https://sib.gob.ar/especies/olivaichthys-viedmensis.
Ophioblennius_steindachneri	Allen, G. R. (2006). Photograph of *Ophioblennius steindachneri*. Fishbase. Fishbase. https://www.fishbase.se/photos/PicturesSummary.php?StartRow=0&ID=8300&what=species&TotRec=8.
Oplegnathus_punctatus	Randall, J.E., 1997. Randall's tank photos. Collection of 10,000 large-format photos (slides) of dead fishes. Unpublished.
Oreoglanis_macropterus	ResearchGate. (n.d.). *Oreoglanis macropterus*, Cas 205601, 83.3 mm Sl. ResearchGate. https://www.researchgate.net/figure/Oreoglanis-macropterus-CAS-205601-833-mm-SL-a-dorsal-b-lateral-and-c_fig4_237409700.
Parablennius_marmoreus	Burgess, G. (2017). Photograph of *Parablennius marmoreus*. Florida Museum: Discover Fishes. University of Florida. https://www.floridamuseum.ufl.edu/discover-fish/species-profiles/parablennius-marmoreus/.
Parailia_pellucida	The Trustees of the Natural History Museum, London. (n.d.). 1907.12.1.1942; *Physailia pellucida*; lateral view; Acsi Project image. Natural History Museum, London. Natural History Museum, London. https://www.nhm.ac.uk/services/media-store/asset/db5a318b938563590015a776c99a97c21a802010/contents/preview.
Parapriacanthus_ransonneti	Randall, J.E., 1997. Randall's tank photos. Collection of 10,000 large-format photos (slides) of dead fishes. Unpublished.
Parodon_suborbitalis	Galvis, G., J.I. Mojica and M. Camargo, 1997. Peces del Catatumbo. Asociación Cravo Norte, Santafé de Bogotá, D.C., 188 p.
Pimelodus_blochii	Castro-Lima, F. (2014). Photograph of *Pimelodus blochii*. Fishbase. Fishbase. https://www.fishbase.de/photos/PicturesSummary.php?ID=7556&what=species.
Plagiogeneion_rubiginosum	Yau, B. (2013). Photograph of *Plagiogeneion rubiginosum*. Fishbase. Fishbase. https://www.fishbase.se/photos/PicturesSummary.php?ID=12288&what=species.
Plecoglossus_altivelis	Shao, K.-T. and P.L. Lim, 1991. Fishes of freshwater and estuary. Encyclopedia of field guide in Taiwan.
Pontinus_rathbuni	Uyeno, T., K. Matsuura and E. Fujii (eds.), 1983. Fishes trawled off Suriname and French Guiana. Japan Marine Fishery Resource Research Center, Tokyo, Japan. 519 p.
Porochilus_rendahli	Martin F. Gomon, *Porochilus rendahli* in Fishes of Australia, accessed 01 Jun 2021, http://136.154.202.208/home/species/2768
Profundulus_labialis	Gómez González, A. E. (2016). Fishbase. Fishbase. https://www.fishbase.se/photos/PicturesSummary.php?need2save=&tosave=&TRPP=1&id=49585&what=species&personnel=&user_session=&lme=&StartRow=-1&TotRec=2&SortBy=iucn.

Appendix A Table 2, continued

Rhamphocottus_richardsonii	The International Barcode of Life Consortium. (n.d.). FHAK085-17 Lateral. International Barcode of Life Project (iBOL). https://api.gbif.org/v1/image/unsafe/http%3A%2F%2Fwww.boldsystems.org%2Fpics%2FFHAK%2FMAL1130A%2B1502727438.JPG.
Rhaphiodon_vulpinus	Timm, C. D. (2010). Photograph of *Rhaphiodon vulpinus*. Fishbase. Fishbase. https://www.fishbase.se/photos/PicturesSummary.php?need2save=&tosave=&TRPP=1&id=8697&what=species&personnel=&user_session=&lme=&StartRow=1&TotRec=4&SortBy=iucn.
Rheocles_alaotrensis	Loiselle, P. V. (2009). Photograph of *Rheocles alaotrensis*. Fishbase. Fishbase. https://www.fishbase.de/photos/PicturesSummary.php?need2save=&tosave=&TRPP=1&id=9884&what=species&personnel=&user_session=&lme=&StartRow=-1&TotRec=2&SortBy=iucn.
Samariscus_xenicus	University of Kansas Biodiversity Institute. (n.d.). Photograph of *Samariscus xenicus*. KUBI Ichthyology Tissue Collection. https://api.gbif.org/v1/image/unsafe/http%3A%2F%2Fbiimages.biodiversity.ku.edu%2Fstatic%2FIchthyology%2Foriginals%2Fsp68850128602102260103.att.JPG.
Sarda_sarda	Abdul, N. (2000). Photograph of *Sarda sarda*. Fishbase. Fishbase. https://www.fishbase.se/photos/PicturesSummary.php?StartRow=4&ID=115&what=species&TotRec=8.
Scleropages_jardinii	Sheremetyev, I. (2000). Photograph of *Scleropages jardinii*. Fishbase. Fishbase. https://www.fishbase.in/photos/PicturesSummary.php?StartRow=0&ID=7536&what=species&TotRec=2.
Scomberomorus_regalis	Zúñiga, J. E. G. (2019). Photograph of *Scomberomorus regalis*. iNaturalist. iNaturalist. https://api.gbif.org/v1/image/unsafe/https%3A%2F%2Fstatic.inaturalist.org%2Fphotos%2F37050886%2Foriginal.jpg%3F1556554556.
Scopelosaurus_harryi	GBIF Secretariat. (n.d.). TZFPB408-05 Lateral. Global Biodiversity Information Forum.
Siniperca_chuatsi	Bogutskaya, N. (2000). Photograph of *Siniperca chuatsi*. Fishbase. Fishbase. https://www.fishbase.se/photos/PicturesSummary.php?StartRow=1&ID=28054&what=species&TotRec=3.
Sisor_rabdophorus	Ng, H. H. (n.d.). *Sisor rabdophorus*, Ummz 2440013, 63.8 mm Sl. ResearchGate. ResearchGate. https://www.researchgate.net/figure/Sisor-rabdophorus-UMMZ-2440013-638-mm-SL-Photograph-by-H-H-Ng_fig11_253201010.
Sorsogona_prionota	Randall, J.E., 1997. Randall's tank photos. Collection of 10,000 large-format photos (slides) of dead fishes. Unpublished.
Sphyraena_borealis	Noble, B. (2014). Photograph of *Sphyraena borealis*. Fishbase. Fishbase. https://www.fishbase.de/photos/PicturesSummary.php?StartRow=1&ID=3679&what=species&TotRec=3.

Appendix A Table 2, continued

Spirinchus_thaleichthys	Longfin smelt, 110 mm FL. Photographed on February 14, 2008 at the Tracy Fish Collection Facility, Tracy, CA. Photo by René Reyes, US Bureau of Reclamation.
Synchiropus_phaeton	Bañón, R., Morales, X., Barros-García, D., & De Carlos, A. (2018). Specimen of *Synchiropus phaeton*. ResearchGate. ResearchGate. https://www.researchgate.net/profile/Rafael-Banon/publication/328290543_Northernmost_record_and_new_biological_data_of_the_Phaeton_dragonet_Synchiropus_phaeton_Callionymiformes_Callionymidae_in_the_eastern_Atlantic_Ichthyological_note/links/5be573bba6fdcc3a8dc8f061/Northernmost-record-and-new-biological-data-of-the-Phaeton-dragonet-Synchiropus-phaeton-Callionymiformes-Callionymidae-in-the-eastern-Atlantic-Ichthyological-note.pdf.
Tetrapturus_pfluegeri	Nakamura, I., 1985. FAO species catalogue. Vol. 5. Billfishes of the world. An annotated and illustrated catalogue of marlins, sailfishes, spearfishes and swordfishes known to date.
Thalassoma_bifasciatum	Porcelli, D. (2016). Photograph of *Thalassoma bifasciatum*. iNaturalist Research-grade Observations. iNaturalist. https://api.gbif.org/v1/image/unsafe/https%3A%2F%2Fstatic.inaturalist.org%2Fphotos%2F101916843%2Foriginal.jpg%3F1603648546.
Thunnus_atlanticus	Doray, M. (2005). Photograph of *Thunnus atlanticus*. Fishbase. Fishbase. https://www.fishbase.de/photos/PicturesSummary.php?StartRow=3&ID=144&what=species&TotRec=10.
Uranoscopus_scaber	Dammous, S. (2001). Photograph of *Uranoscopus scaber*. Fishbase. Fishbase. https://www.fishbase.se/photos/PicturesSummary.php?StartRow=2&ID=1779&what=species&TotRec=6.
Xiphias_gladius	Cambraia Duarte, P. M. N. (2001). Photograph of *Xiphias gladius*. Fishbase. Fishbase. https://www.fishbase.de/photos/PicturesSummary.php?StartRow=1&ID=226&what=species&TotRec=9.

Appendix A Table 3 – Citations for images of extinct species and their assignments to periods.

Species	Period	Citation
Acrolepis gigas	Carboniferous	Štamberg, Stanislav. 2013. "Knowledge of the Carboniferous and Permian Actinopterygian Fishes of the Bohemian Massif - 100 Years After Antonín Frič." *Acta Musei Nationalis Pragae Series B Historia Naturalis* 69 no. 3-4: 159-181.
Aeduella blainvillei	Permian	Poplin, Cécile and Didier B. Dutheil. 2005. "Les Aeduellidae (Pisces, Actinopterygii) carbonifères et permiens: systématique et étude phylogénétique préliminaire." *Geodiversitas* 27 no. 1: 17-33.
Aesopichthys erinaceus	Carboniferous	Poplin, Cécile and Richard Lund. 2000. "Two New Deep-Bodied Palaeoniscoid Acinopterygians from Bear Gulch (Montana, USA, Lower Carboniferous)." *Journal of Vertebrate Paleontology* 20 no. 3 (September): 428-449. https://www.jstor.org/stable/4524115.
Aestuarichthys fulcratus	Carboniferous	Gardiner, B. G. 1969. "New Palaeoniscoid Fish from the Witteberg Series of South Africa." *Zoological Journal of Linnean Society* 48 no. 4: 423-452. doi:10.1111/j.1096-3642.1969.tb00722.x.
Allolepidotus nothosomoides	Triassic	Tintori, Andrea and Cristina Lombardo. 1999. "Late Ladinian Fish Faunas from Lombardy (North Italy): Stratigraphy and Paleobiology." In *Mesozoic Fishes 2*, edited by Gloria Arratia and Hans-Peter Schultze, 495-504. München: Verlag Dr. Friedrich Pfeil.
Amblypterus latus	Permian	Štamberg, Stanislav. 2013. "New Data on the Osteology of the Actinopterygian Fish *Amblypterus* and the Relationship Between *Amblypterus* and *Paramblypterus*." *Acta Musei Nationalis Pragae Series B Historia Naturalis* 69 no. 3-4: 183-193.
Anaethelion knorri	Jurassic	Arratia, Gloria. 1996. "Reassessment of the Phylogenetic Relationships of Certain Jurassic Teleosts and Their Implications on Teleostean Phylogeny." In *Mesozoic Fishes*, edited by Gloria Arratia and Günther Viohl, 219-242. München: Verlag Dr. Friedrich Pfeil.
Aspidorhynchus acutirostris	Jurassic	Lambers, Paul. 1992. "On the Ichthyofauna of the Solnhofen Lithographic Limestone (Upper Jurassic, Germany)." Ph.D. diss., University of Groningen.
Australosomus merlei	Triassic	Beltan, Laurence. 1996. "Overview of Systematics, Paleobiology, and Paleoecology of Triassic Fishes of Northwestern Madagascar." In *Mesozoic Fishes*, edited by Gloria Arratia and Günther Viohl, 479-500. München: Verlag Dr. Friedrich Pfeil.
Bobasatrania canadensis	Triassic	Schaeffer, Bobb and Marilyn Mangus. 1976. "An Early Triassic Fish Assemblage from British Columbia." *Bulletin of the American Museum of Natural History* 156 no. 5.

Appendix A Table 3, continued

Bourbonella guilloti	Permian	Poplin, Cécile and Didier B. Dutheil. 2005. "Les Aeduellidae (Pisces, Actinopterygii) carbonifères et permiens: systématique et étude phylogénétique préliminaire." *Geodiversitas* 27 no. 1: 17-33.
Bourbonella hirsuta	Permian	Štamberg, Stanislav. 2013. "Knowledge of the Carboniferous and Permian Actinopterygian Fishes of the Bohemian Massif - 100 Years After Antonín Frič." *Acta Musei Nationalis Pragae Series B Historia Naturalis* 69 no. 3-4: 159-181.
Brookvalia sp	Triassic	Schaeffer, Bobb. 1984. "On the Relationships of the Triassic-Liassic Redfieldiiform Fishes." *American Museum Novitates* no. 2795: 1-18.
Cheirolepis canadensis	Devonian	Pearson, D. Michael and T. Stanley Westoll. 1979. "The Devonian Actinopterygian *Cheirolepis* Agassiz." *Transactions of the Royal Society of Edinburgh* 70: 337-399.
Cheirolepis trailli	Devonian	Pearson, D. Michael and T. Stanley Westoll. 1979. "The Devonian Actinopterygian *Cheirolepis* Agassiz." *Transactions of the Royal Society of Edinburgh* 70: 337-399.
Cuneognathus gardineri	Devonian	Friedman, Matt and Henning Blom. 2006. "A New Actinopterygian from the Famennian of East Greenland and the Interrelationships of Devonian Ray-Finned Fishes." *Journal of Paleontology* 80 no. 6 (November): 1186-1204.
Cyonichthys sp	Triassic	Schaeffer, Bobb. 1984. "On the Relationships of the Triassic-Liassic Redfieldiiform Fishes." *American Museum Novitates* no. 2795: 1-18.
Daedalichthys sp	Triassic	Schaeffer, Bobb. 1984. "On the Relationships of the Triassic-Liassic Redfieldiiform Fishes." *American Museum Novitates* no. 2795: 1-18.
Donnrosenia schaefferi	Devonian	Choo, Brian. 2010. "Revision and Description of the Actinopterygian Fishes of Devonian Eastern Gondwana." PhD diss., The Australian National University.
Dorypterus hoffmanni	Permian	Westoll, T. S. 1941. "The Permian Fishes *Dorypterus* and *Lekanichthys*." *Proceedings of the Zoological Society of London* B111 no. 1-2: 39-58.
Ebenaqua ritchei	Permian	Campbell, K. S. W. and Le Duy Phuoc. 1983. "A Late Permian Actinopterygian from Australia." *Palaeontology* 26 no. 1: 33-70.
Elonichthys krejcii	Carboniferous	Štamberg, Stanislav. 2013. "Knowledge of the Carboniferous and Permian Actinopterygian Fishes of the Bohemian Massif - 100 Years After Antonín Frič." *Acta Musei Nationalis Pragae Series B Historia Naturalis* 69 no. 3-4: 159-181.

Appendix A Table 3, continued

Eosemionotus ceresiensis	Triassic	Bürgin, Toni. 2004. "*Eosemionotus ceresiensis* sp. nov., a New Semionotiform Fish (Actinopterygii, Halecostomi) from the Middle Triassic of Monte San Giorgio (Southern Switzerland)." In *Mesozoic Fishes 3*, edited by Gloria Arratia and Andrea Tintori, 239-251. München: Verlag Dr. Friedrich Pfeil.
Eurynotus crenatus	Carboniferous	Coates, M. I. 1994. "Actinopterygian and Acanthodian Fishes from the Viséan of East Kirkton, West Lothian, Scotland." *Transactions of the Royal Society of Edinburgh: Earth Sciences* 84: 317-327.
Felberia excelsa	Triassic	Lombardo, Cristina and Andrea Tintori. 2004. "New Perleidiforms from the Triassic of the Southern Alps and the Revision of *Serrolepis* from the Triassic of Württemberg (Germany)." In *Mesozoic Fishes 3*, edited by Gloria Arratia and Andrea Tintori, 179-196. München: Verlag Dr. Friedrich Pfeil.
Fouldenia sp	Carboniferous	Sallan, Lauren Cole and Michael I. Coates. 2013. "Styracopterid (Actinopterygii) Ontogeny and the Multiple Origins of Post-Hangenberg Deep-Bodied Fishes." *Zoological Journal of the Linnean Society* 169: 156-199.
Frederichthys musadentatus	Carboniferous	Coates, M. I. 1993. "New Actinopterygian Fish from the Namurian Manse Burn Formation of Bearsden, Scotland." *Palaeontology* 36 no. 1: 123-146.
Fukangichthys longidorsalis	Triassic	Xu, Guang-Hui, Ke-Qin Gao, and John A. Finarelli. 2014. "A Revision of the Middle Triassic Scanilepiform Fish *Fukangichthys longidorsalis* from Xinjiang, China, with Comments on the Phylogeny of the Actinopteri." *Journal of Vertebrate Paleontology* 34 no. 4: 747-759. https://doi.org/10.1080/02724634.2014.837053.
Gogosardina coatesi	Devonian	Choo, Brian, John A. Long, and Katherine Trinajstic. 2009. "A New Genus and Species of Basal Actinopterygian Fish from the Upper Devonian Gogo Formation of Western Australia." *Acta Zoologica* 90 no. s1: 194-210. https://doi.org/10.1111/j.1463-6395.2008.00370.x.
Gonatodus punctatus	Carboniferous	Gardiner, Brian George. 1967. "Further Notes on Palaeoniscoid Fishes with a Classification of the Chondrostei." *Bulletin of the British Museum (Natural History)* 14 no. 5: 143-206.
Haplolepis corrugata	Carboniferous	Lowney, Karen A. 1980. "A Revision of the Family Haplolepidae (Actinopterygii, Paleonisciformes) from Linton, Ohio (Westphalian D, Pennsylvanian)." *Journal of Paleontology* 54 no. 5: 942-953.
Howqualepis rostridens	Devonian	Long, John A. 1988. "New Palaeoniscoid Fishes from the Late Devonian and Early Carboniferous of Victoria." *Memoirs of the Association of Australasian Palaeontologists* 7, no. 7: 1-64.

Appendix A Table 3, continued

Hulettia americana	Jurassic	Schaeffer, Bobb and Colin Patterson. 1984. "Jurassic Fishes from the Western United States, With Comments on Jurassic Fish Distribution." *American Museum Novitates* no. 2796: 1-86.
Kalops diophrys	Carboniferous	Poplin, C. M. and R. Lund. 2002. "Two Carboniferous Fine-Eyed Palaeoniscoids (Pisces, Actinopterygii) from Bear Gulch (USA)." *Journal of Paleontology* 76 no. 6 (November): 1014-1028.
Kalops monophrys	Carboniferous	Poplin, C. M. and R. Lund. 2002. "Two Carboniferous Fine-Eyed Palaeoniscoids (Pisces, Actinopterygii) from Bear Gulch (USA)." *Journal of Paleontology* 76 no. 6 (November): 1014-1028.
Krasnoyarichthys jesseni	Devonian	Prokofiev, Artém M. 2002. "First Finding of an Articulated Actinopterygian Skeleton from the Upper Devonian of Siberia and a Reappraisal of the Family Moythomasiidae Kazantseva, 1971 (Osteichthyes)." *Paleontological Research* 6 no. 3: 321-327.
Lepidotes roxoi	Cretaceous	Gallo, Valéria and Paulo M. Brito. 2004. "An Overview of Brazilian Semionotids." In *Mesozoic Fishes 3*, edited by Gloria Arratia and Andrea Tintori, 253-264. München: Verlag Dr. Friedrich Pfeil.
Leptolepides sprattiformis	Jurassic	Arratia, Gloria. 1996. "Reassessment of the Phylogenetic Relationships of Certain Jurassic Teleosts and Their Implications on Teleostean Phylogeny." In *Mesozoic Fishes*, edited by Gloria Arratia and Günther Viohl, 219-242. München: Verlag Dr. Friedrich Pfeil.
Leptolepis coryphaenoides	Jurassic	Arratia, Gloria. 1996. "Reassessment of the Phylogenetic Relationships of Certain Jurassic Teleosts and Their Implications on Teleostean Phylogeny." In *Mesozoic Fishes*, edited by Gloria Arratia and Günther Viohl, 219-242. München: Verlag Dr. Friedrich Pfeil.
Limnomis delaneyi	Devonian	Daeschler, Edward B. 2000. "An Early Actinopterygian Fish from the Catskill Formation (Late Devonian, Famennian) in Pennsylvania, U.S.A." *Proceedings of the Academy of Natural Sciences of Philadelphia* 150: 181-192.
Luoxiongichthys hyperdorsalis	Triassic	Wen, Wen, Qi-Yue Zhang, Shi-Xue Hu, Chang-Yong Zhou, Tao Xie, Jin-Yuan Huang, Zhong Qiang Chen, and Michael J. Benton. 2012. "A New Basal Actinopterygian Fish from the Anisian (Middle Triassic of Luoping, Yunnan Province, Southwest China." *Acta Palaeontologica Polonica* 57 no. 1: 149-160. http://dx.doi.org/10.4202/app.2010.0089.
Macrosemius rostratus	Jurassic	Lambers, Paul. 1992. "On the Ichthyofauna of the Solnhofen Lithographic Limestone (Upper Jurassic, Germany)." Ph.D. diss., University of Groningen.

Appendix A Table 3, continued

Melanecta anneae	Carboniferous	Coates, M. I. 1998. "Actinopterygians from the Namurian of Bearsden, Scotland, with Comments on Early Actinopterygian Neurocrania." *Zoological Journal of the Linnean Society* 122 no. 1-2: 27-59.
Mentzichthys jubbi	Carboniferous	Gardiner, B. G. 1969. "New Palaeoniscoid Fish from the Witteberg Series of South Africa." *Zoological Journal of Linnean Society* 48 no. 4: 423-452. doi:10.1111/j.1096-3642.1969.tb00722.x.
Microhaplolepis ovoidea	Carboniferous	Lowney, Karen A. 1980. "A Revision of the Family Haplolepidae (Actinopterygii, Paleonisciformes) from Linton, Ohio (Westphalian D, Pennsylvanian)." *Journal of Paleontology* 54 no. 5: 942-953.
Microhaplopeis serrata	Carboniferous	Lowney, Karen A. 1980. "A Revision of the Family Haplolepidae (Actinopterygii, Paleonisciformes) from Linton, Ohio (Westphalian D, Pennsylvanian)." *Journal of Paleontology* 54 no. 5: 942-953.
Mimia toombsi	Devonian	Gardiner, B. G. 1984. "The Relationships of the Palaeoniscid Fishes, a Review Based on New Specimens of *Mimia* and *Moythomasia* from the Upper Devonian of Western Australia." *Bulletin of the British Museum (Natural History)* 37 no. 4: 173-428.
Moythomasia durgaringa	Devonian	Choo, Brian. 2015. "A New Species of the Devonian Actinopterygian *Moythomasia* from Bergisch Gladbach, Germany, and Fresh Observations on *M. durgaringa* from the Gogo Formation of Western Australia." *Journal of Vertebrate Paleontology* 35 no. 4. https://doi.org/10.1080/02724634.2015.952817.
Moythomasia lineata	Devonian	Choo, Brian. 2015. "A New Species of the Devonian Actinopterygian *Moythomasia* from Bergisch Gladbach, Germany, and Fresh Observations on *M. durgaringa* from the Gogo Formation of Western Australia." *Journal of Vertebrate Paleontology* 35 no. 4. https://doi.org/10.1080/02724634.2015.952817.
Moythomasia nitida	Devonian	Choo, Brian. 2015. "A New Species of the Devonian Actinopterygian *Moythomasia* from Bergisch Gladbach, Germany, and Fresh Observations on *M. durgaringa* from the Gogo Formation of Western Australia." *Journal of Vertebrate Paleontology* 35 no. 4. https://doi.org/10.1080/02724634.2015.952817.
Neslovicella elongata	Permian	Štamberg, Stanislav. 2010. "A New Aeduellid Actinopterygian from the Lower Permian of the Krkonoše Piedmont Basin (Bohemian Massif) and Its Relationship to Other Aeduellidae." *Bulletin of Geosciences* 85 no. 2: 183-198.

Appendix A Table 3, continued

Neslovicella rzehaki	Permian	Štamberg, Stanislav. 2013. "Knowledge of the Carboniferous and Permian Actinopterygian Fishes of the Bohemian Massif - 100 Years After Antonín Frič." *Acta Musei Nationalis Pragae Series B Historia Naturalis* 69 no. 3-4: 159-181.
Notagogus novomundi	Cretaceous	González-Rodríguez, Katia and Víctor-Hugo Reynoso. 2004. "A New *Notagogus* (Macrosemiidae, Halecostomi) Species from the Albian Tlayúa Quarry, Central Mexico." In *Mesozoic Fishes 3*, edited by Gloria Arratia and Andrea Tintori, 265-278. München: Verlag Dr. Friedrich Pfeil.
Orthogonikleithrus leichi	Jurassic	Arratia, Gloria. 1996. "Reassessment of the Phylogenetic Relationships of Certain Jurassic Teleosts and Their Implications on Teleostean Phylogeny." In *Mesozoic Fishes*, edited by Gloria Arratia and Günther Viohl, 219-242. München: Verlag Dr. Friedrich Pfeil.
Parahaplolepis tuberculata	Carboniferous	Lowney, Karen A. 1980. "A Revision of the Family Haplolepidae (Actinopterygii, Paleonisciformes) from Linton, Ohio (Westphalian D, Pennsylvanian)." *Journal of Paleontology* 54 no. 5: 942-953.
Parasemionotus labordei	Triassic	Beltan, Laurence. 1996. "Overview of Systematics, Paleobiology, and Paleoecology of Triassic Fishes of Northwestern Madagascar." In *Mesozoic Fishes*, edited by Gloria Arratia and Günther Viohl, 479-500. München: Verlag Dr. Friedrich Pfeil.
Paratarrassius hibbardi	Carboniferous	Lund, Richard and William G. Melton, Jr. 1982. "A New Actinopterygian Fish from the Mississippian Bear Gulch Limestone of Montana." *Palaeontology* 25 no. 3: 485-498.
Phanerorhynchus armatus	Carboniferous	Gardiner, Brian George. 1967. "Further Notes on Palaeoniscoid Fishes with a Classification of the Chondrostei." *Bulletin of the British Museum (Natural History)* 14 no. 5: 143-206.
Potanichthys xingyiensis	Triassic	Xu, Guang-Hui, Li-Jun Zhao, Ke-Qin Gao, and Fei-Xiang Wu. 2013. "A New Stem-Neopterygian Fish from the Middle Triassic of China Shows the Earliest Over-Water Gliding Strategy of the Vertebrates." *Proceedings of the Royal Society B* 280: 20122261. http://dx.doi.org/10.1098/rspb.2012.2261.
Protohaplolepis scotica	Carboniferous	Lowney, Karen A. 1983. "The Earliest Known (Namurian A, E_1) Haplolepids (Osteichthyes: Actinopterygii)." *Transactions of the Royal Society of Edinburgh: Earth Sciences* 74: 69-78.
Pyritocephalus lineatus	Carboniferous	Lowney, Karen A. 1980. "A Revision of the Family Haplolepidae (Actinopterygii, Paleonisciformes) from Linton, Ohio (Westphalian D, Pennsylvanian)." *Journal of Paleontology* 54 no. 5: 942-953.

Appendix A Table 3, continued

Pyritocephalus sculptus	Carboniferous	Štamberg, Stanislav. 2013. "Knowledge of the Carboniferous and Permian Actinopterygian Fishes of the Bohemian Massif - 100 Years After Antonín Frič." *Acta Musei Nationalis Pragae Series B Historia Naturalis* 69 no. 3-4: 159-181.
Robustichthys luopingensis	Triassic	Xu, Guang-Hui, Li-Jun Zhao, and Michael I. Coates. 2014. "The Oldest Ionoscopiform from China Sheds New Light on the Early Evolution of Halecomorph Fishes." *Biology Letters* 10 no. 5. https://doi.org/10.1098/rsbl.2014.0204.
Rubiesichthys gregalis	Cretaceous	Poyato-Ariza, Francisco José. 1996. "A Revision of *Rubiesichthys gregalis* Wenz 1984 (Ostariophysi, Gonorhynchiformes), from the Early Cretaceous of Spain." In *Mesozoic Fishes*, edited by Gloria Arratia and Günther Viohl, 319-328. München: Verlag Dr. Friedrich Pfeil.
Santanaclupea silvasantosi	Cretaceous	Arratia, Gloria. 1999. "The Monophyly of Teleostei and Stem-Group Teleosts. Consensus and Disagreements." In *Mesozoic Fishes 2*, edited by Gloria Arratia and Hans-Peter Schultze,265-334. München: Verlag Dr. Friedrich Pfeil.
Saurichthys dawaziensis	Triassic	Wu, Feixiang, Yuanlin Sun, Guanghi Xu, Weicheng Hao, Dayong Jiang, and Zuoyu Sun. 2011. "New Saurichthyid Actinopterygian Fishes from the Anisian (Middle Triassic) of Southwestern China." *Acta Palaeontologica Polonica* 56 no. 3: 581-614.
Sceletophorus biserialis	Carboniferous	Štamberg, Stanislav. 2013. "Knowledge of the Carboniferous and Permian Actinopterygian Fishes of the Bohemian Massif - 100 Years After Antonín Frič." *Acta Musei Nationalis Pragae Series B Historia Naturalis* 69 no. 3-4: 159-181.
Sinosaurichthys longimedialis	Triassic	Wu, Feixiang, Yuanlin Sun, Guanghi Xu, Weicheng Hao, Dayong Jiang, and Zuoyu Sun. 2011. "New Saurichthyid Actinopterygian Fishes from the Anisian (Middle Triassic) of Southwestern China." *Acta Palaeontologica Polonica* 56 no. 3: 581-614.
Sinosaurichthys longipectoralis	Triassic	Wu, Feixiang, Yuanlin Sun, Guanghi Xu, Weicheng Hao, Dayong Jiang, and Zuoyu Sun. 2011. "New Saurichthyid Actinopterygian Fishes from the Anisian (Middle Triassic) of Southwestern China." *Acta Palaeontologica Polonica* 56 no. 3: 581-614.
Sinosaurichthys minuta	Triassic	Wu, Feixiang, Yuanlin Sun, Guanghi Xu, Weicheng Hao, Dayong Jiang, and Zuoyu Sun. 2011. "New Saurichthyid Actinopterygian Fishes from the Anisian (Middle Triassic) of Southwestern China." *Acta Palaeontologica Polonica* 56 no. 3: 581-614.

Appendix A Table 3, continued

Sixtelia asiatica	Triassic	Sytchevskaya, Eugenia K. 1999. "Freshwater Fish Fauna from the Triassic of Northern Asia." In *Mesozoic Fishes 2*, edited by Gloria Arratia and Hans-Peter Schultze, 445-468. München: Verlag Dr. Friedrich Pfeil.
Sphaerolepis kounoviensis	Carboniferous	Gardiner, Brian George. 1967. "Further Notes on Palaeoniscoid Fishes with a Classification of the Chondrostei." *Bulletin of the British Museum (Natural History)* 14 no. 5: 143-206.
Stegotrachelus finlayi	Devonian	Finlay, T. M., Arthur Smith Woodward, and Errol Ivor White. 1926. "The Old Red Sandstone of Shetland. Part I. South-Eastern Area. With an Account of the Fossil Fishes of the Old Red Sandstone of the Shetland Islands." *Earth and Environmental Science Transactions of the Royal Society of Edinburgh* 54 no. 3: 553-572.
Stemmatodus rhombus	Cretaceous	Nursall, J. Ralph. 1996. "The Phylogeny of Pycnodont Fishes." In *Mesozoic Fishes*, edited by Gloria Arratia and Günther Viohl, 125-152. München: Verlag Dr. Friedrich Pfeil.
Styracopterus sp	Carboniferous	Sallan, Lauren Cole and Michael I. Coates. 2013. "Styracopterid (Actinopterygii) Ontogeny and the Multiple Origins of Post-Hangenberg Deep-Bodied Fishes." *Zoological Journal of the Linnean Society* 169: 156-199.
Thrissops subovatus	Jurassic	Lambers, Paul. 1992. "On the Ichthyofauna of the Solnhofen Lithographic Limestone (Upper Jurassic, Germany)." Ph.D. diss., University of Groningen.
Todiltia schoewei	Jurassic	Schaeffer, Bobb and Colin Patterson. 1984. "Jurassic Fishes from the Western United States, With Comments on Jurassic Fish Distribution." *American Museum Novitates* no. 2796: 1-86.
Trawdenia planti	Carboniferous	Coates, Michael I. and Kristen Tietjen. 2018. "'This Strange Little Palaeoniscid': A New Early Actinopterygian Genus, and Commentary on Pectoral Fin Conditiion and Function." *Earth and Environmental Science Transactions of the Royal Society of Edinburgh* 109 no. 1-2: 15-31.
Turbomesodon praeclarus	Cretaceous	Poyato-Ariza, Francisco José and Sylvie Wenz. 2004. "The New Pycnodontid Fish Genus *Turbomesodon*, and a Revision of *Macromesodon* Based on New Material from the Lower Cretaceous of Las Hoyas, Cuenca, Spain." In *Mesozoic Fishes 3*, edited by Gloria Arratia and Andrea Tintori, 341-378. München: Verlag Dr. Friedrich Pfeil.
Varasichthys ariasi	Jurassic	Arratia, Gloria. 1996. "Reassessment of the Phylogenetic Relationships of Certain Jurassic Teleosts and Their Implications on Teleostean Phylogeny." In *Mesozoic Fishes*, edited by Gloria Arratia and Günther Viohl, 219-242. München: Verlag Dr. Friedrich Pfeil.

Appendix A Table 3, continued

Varialepis bergi	Permian	Tverdokhlebov, Valentin P., Galina I. Tverdokhlebova, Alla V. Minikh, Mikhail V. Surkov, and Michael J. Benton. 2005. "Upper Permian Vertebrates and Their Sedimentological Context in the South Urals, Russia." *Earth Science Reviews* 69 no. 1-2 (February): 27-77. https://doi.org/10.1016/j.earscirev.2004.07.003.
Whiteia woodwardi	Triassic	Beltan, Laurence. 1996. "Overview of Systematics, Paleobiology, and Paleoecology of Triassic Fishes of Northwestern Madagascar." In *Mesozoic Fishes*, edited by Gloria Arratia and Günther Viohl, 479-500. München: Verlag Dr. Friedrich Pfeil.
Woodichthys bearsdeni	Carboniferous	Coates, M. I. 1998. "Actinopterygians from the Namurian of Bearsden, Scotland, with Comments on Early Actinopterygian Neurocrania." *Zoological Journal of the Linnean Society* 122 no. 1-2: 27-59.

APPENDIX B - ADDITIONAL FIGURES AND TABLES FOR CHAPTERS 3 AND 4

All images surrounding the laser heat shock experiments, in situ hybridizations, histology, Kaede, plasmid constructs, and R scripts are deposited online at the University of Chicago Box.

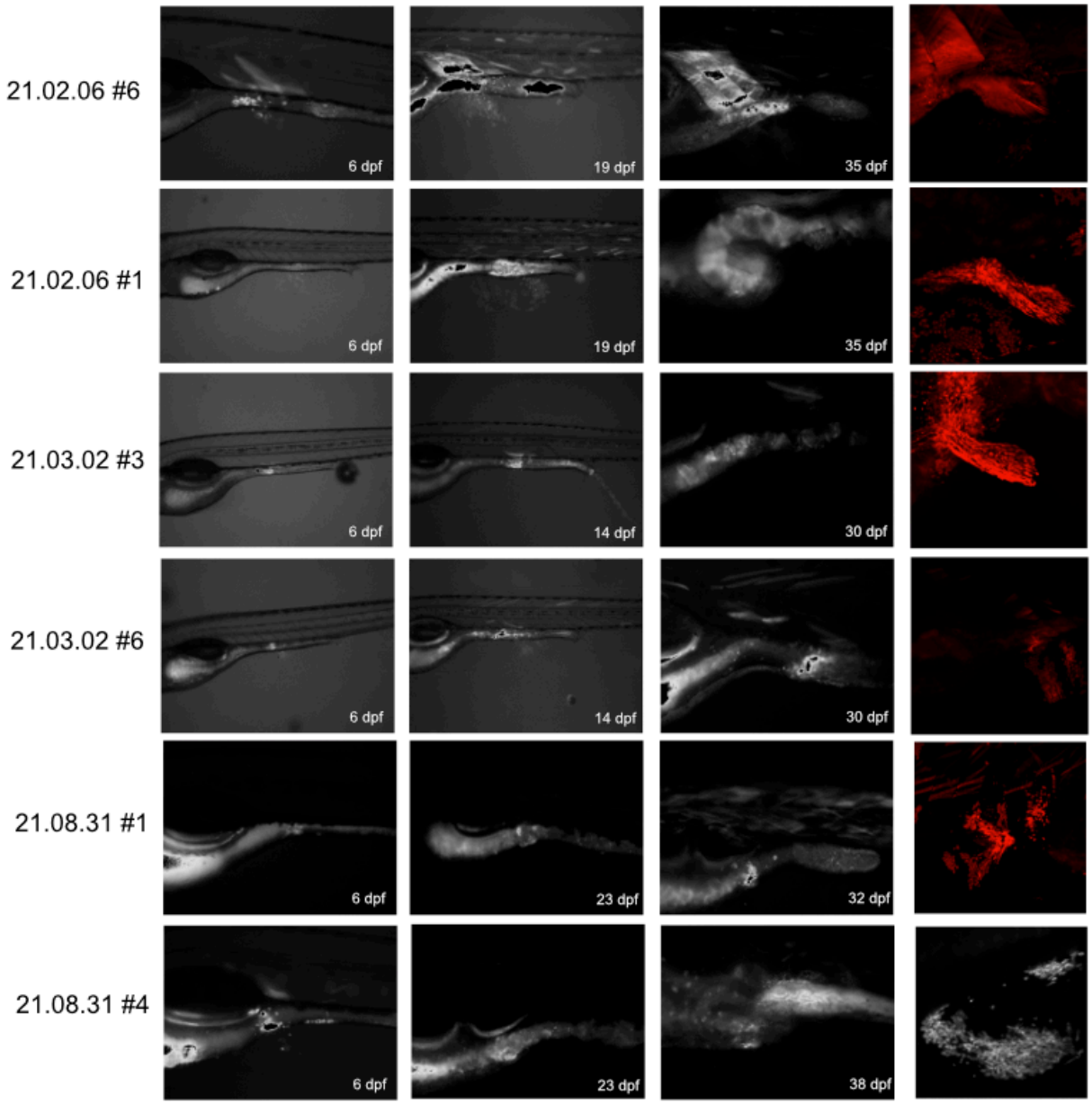

(cont. on next page)

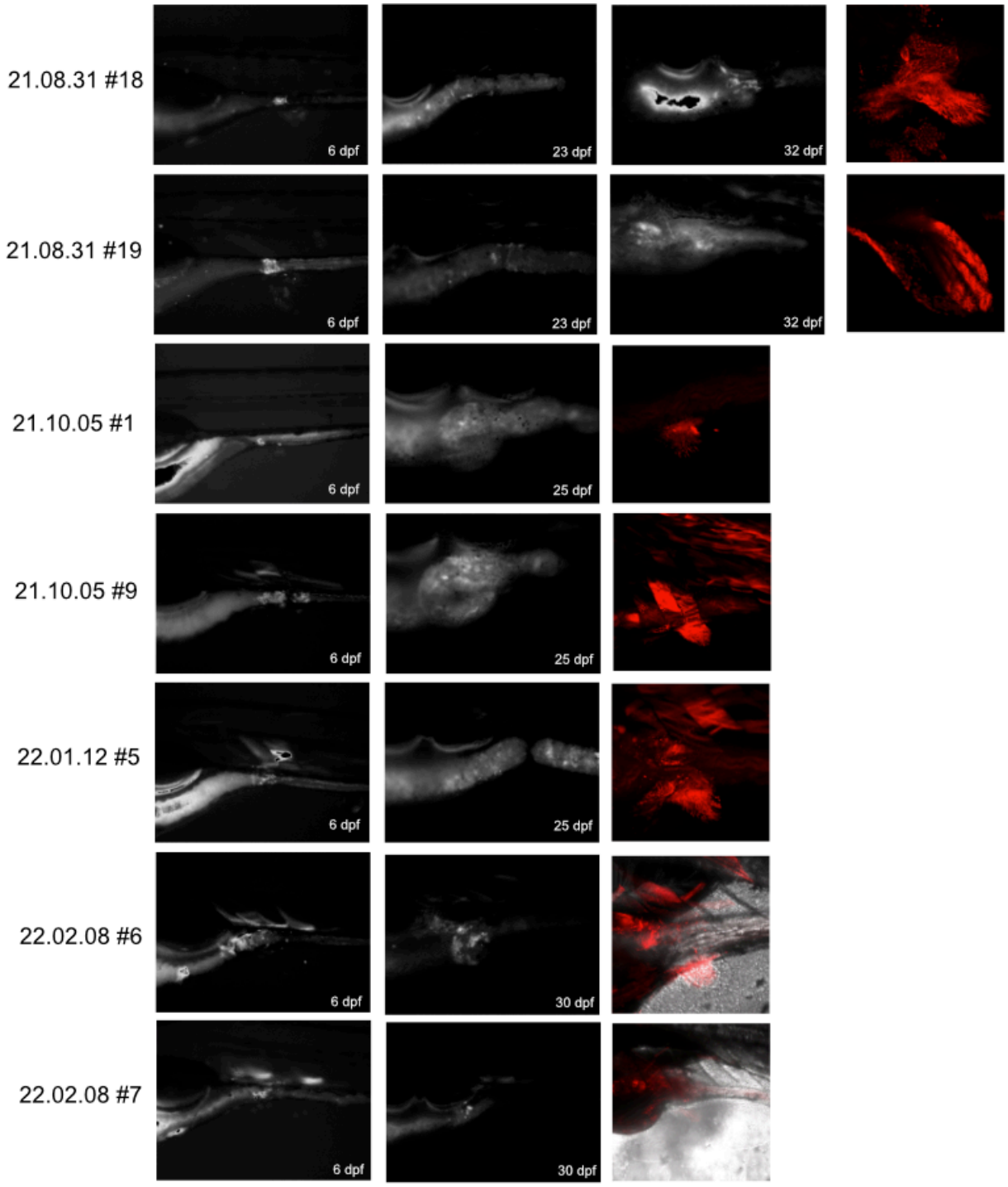

Appendix B Figure 1 - Additional photographs for *Tg(hsp:cre-ert2)* x ubi:switch individuals with pelvic fin mesenchyme fate.

21.08.31 #1 had midline labeling initially, which resulted in a right pelvic fin labeled. Otherwise, all other individuals were labeled on the lateral left side.

Lay Date	ID #	Somite AP first	Somite AP last
1.12.22	5	9	9
2.08.22	**6**	6	9
2.08.22	**7**	9	9
10.5.21	**1**	9	9
10.5.21	**9**	9	11
2.26.21	**1**	11	12
2.5.21	**12**	8	9
3.2.21	**3**	10	10
3.2.21	**6**	11	11
2.26.21	**6**	8	8
8.31.21	**1**	8	8
8.31.21	**4**	7	7
8.31.21	**18**	9	9
8.31.21	**19**	10	10

Appendix B Table 1 – List of *Tg(hsp:cre-ert2)* x ubi:switch individuals with pelvic fin fate and the anteroposterior (AP) range of their cells that were labeled.

Highlighted individuals were counted as “large” clones; all others are “small” clones.

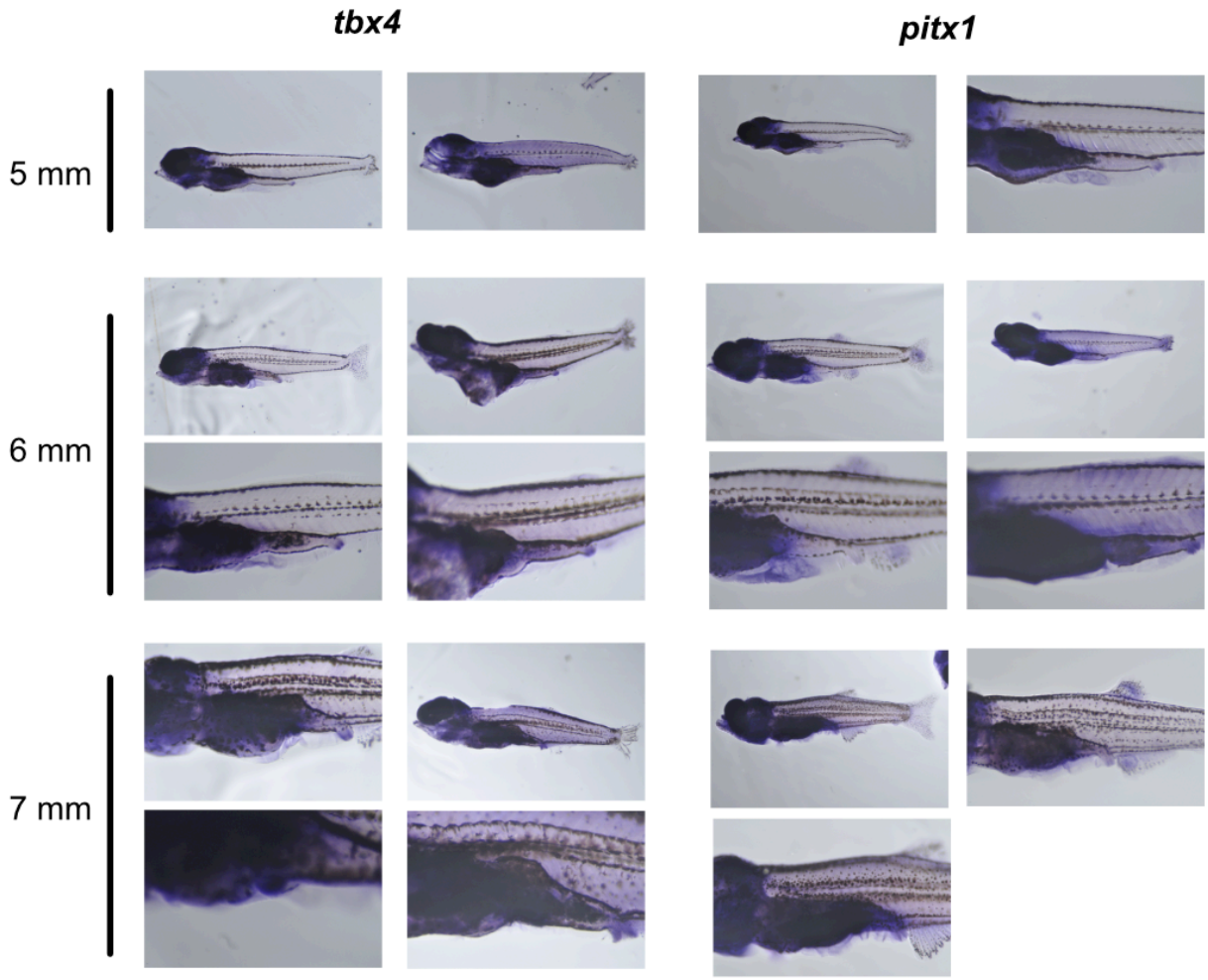

Appendix B Figure 2 - "Light" staining of *tbx4* and *pitx1* larval *in situ* hybridizations with BM Purple instead of NBT/BCIP.

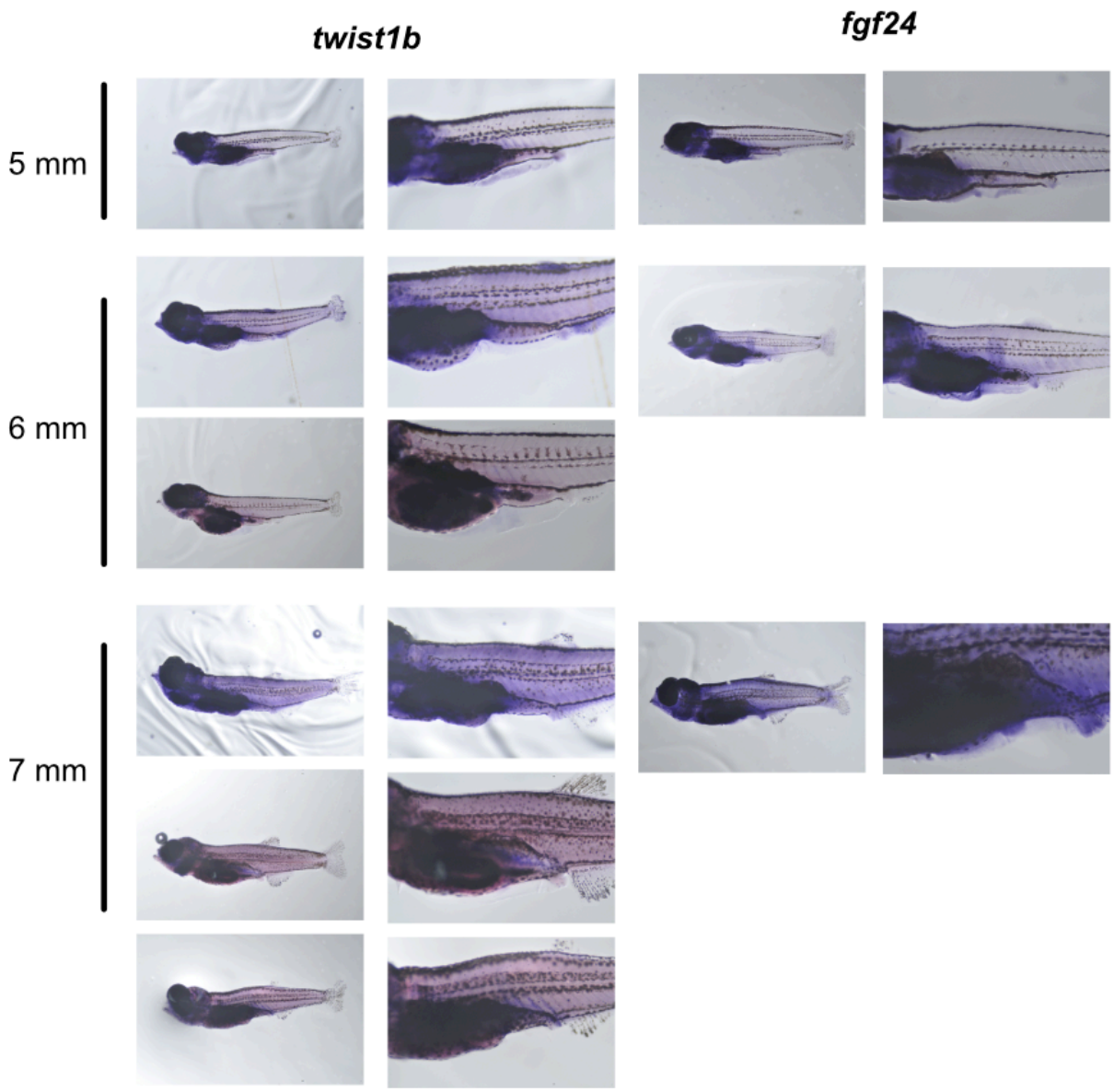

Appendix B Figure 3 – "Light" staining of *twist1b* and *fgf24* with BM Purple.

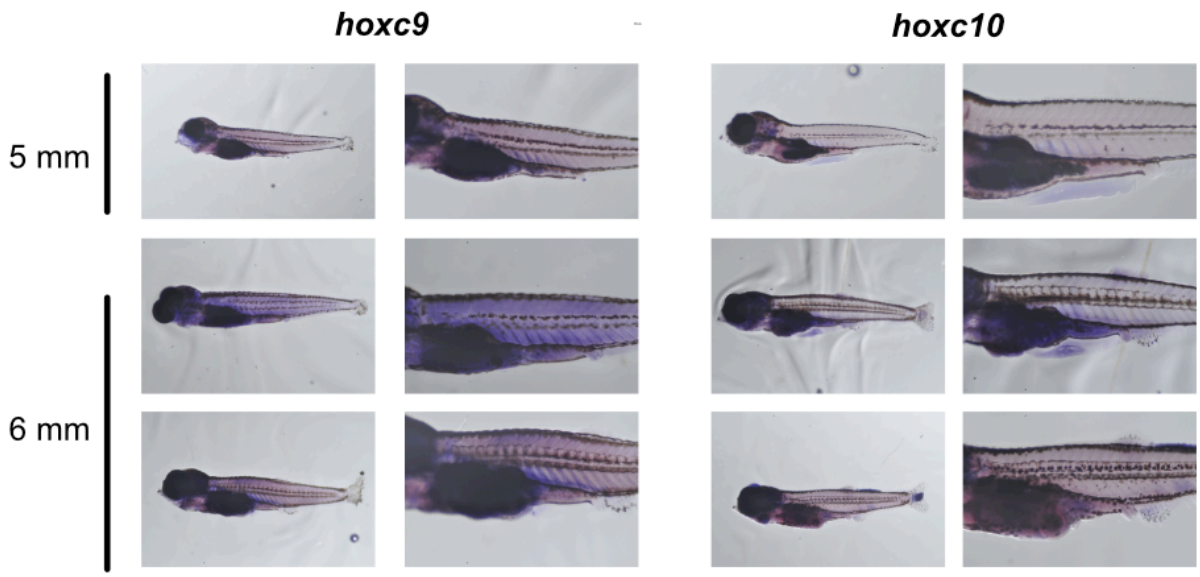

Appendix B Figure 4 - "Light" staining of *hoxc9* and *hoxc10* with BM Purple.

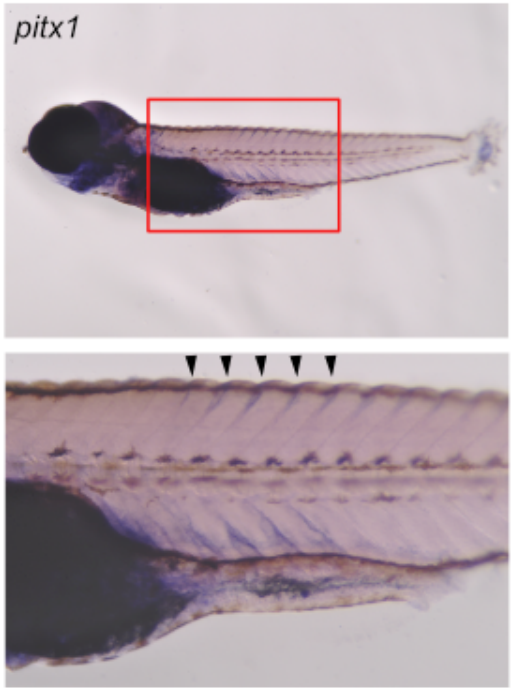

Appendix B Figure 5 - Dorsal myoseptal *pitx1* gene expression (black arrowheads) in a 4-5mm specimen. Second image is an inset of the first.

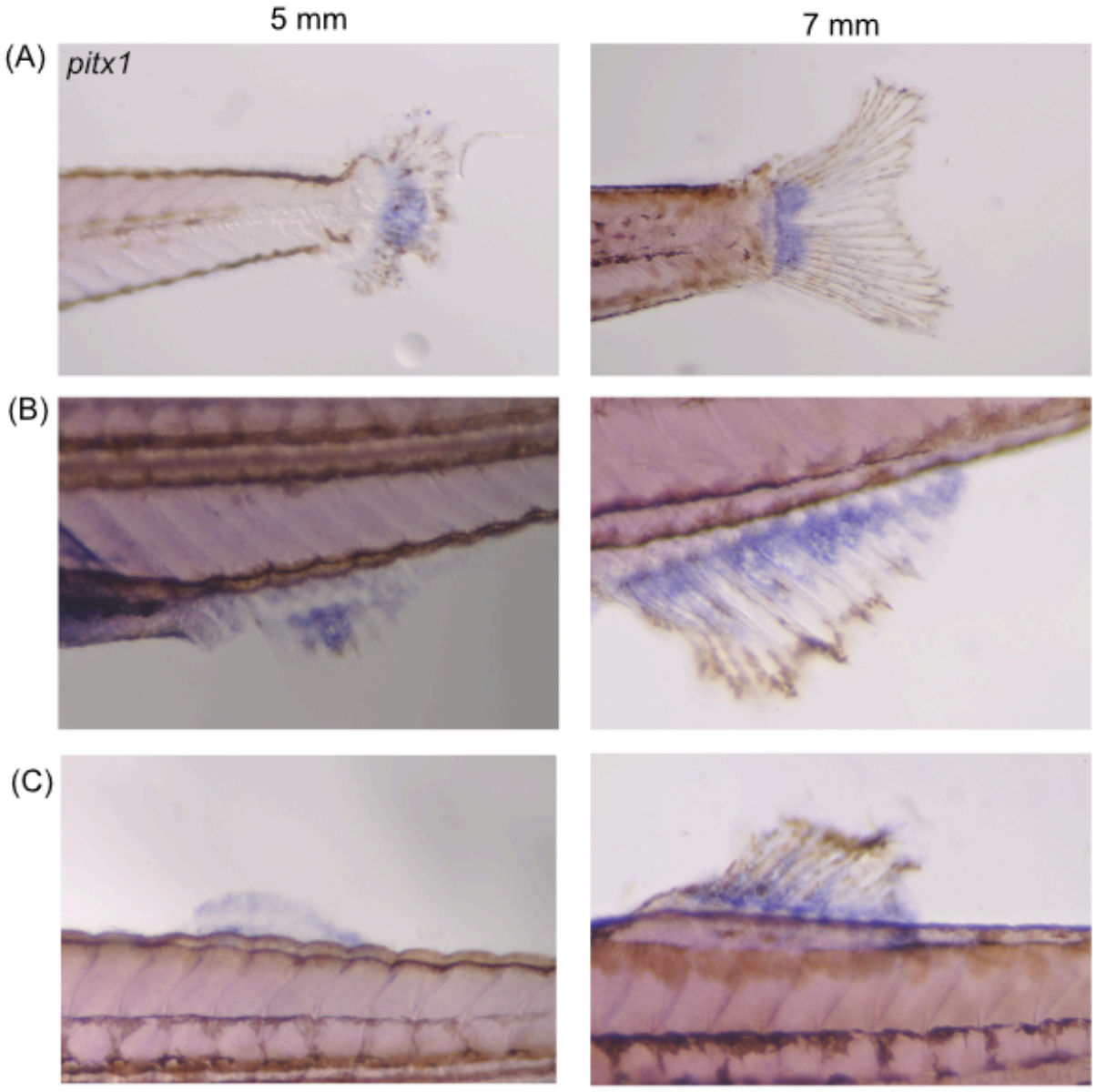

Appendix B Figure 6 – Median fin *pitx1* gene expression. (A) Gene expression in the base of the caudal fin (B) Expression in the proximal region of the anal fin (C) Expression in the dorsal fin anlage, then in the proximal region of the dorsal fin at 7mm.

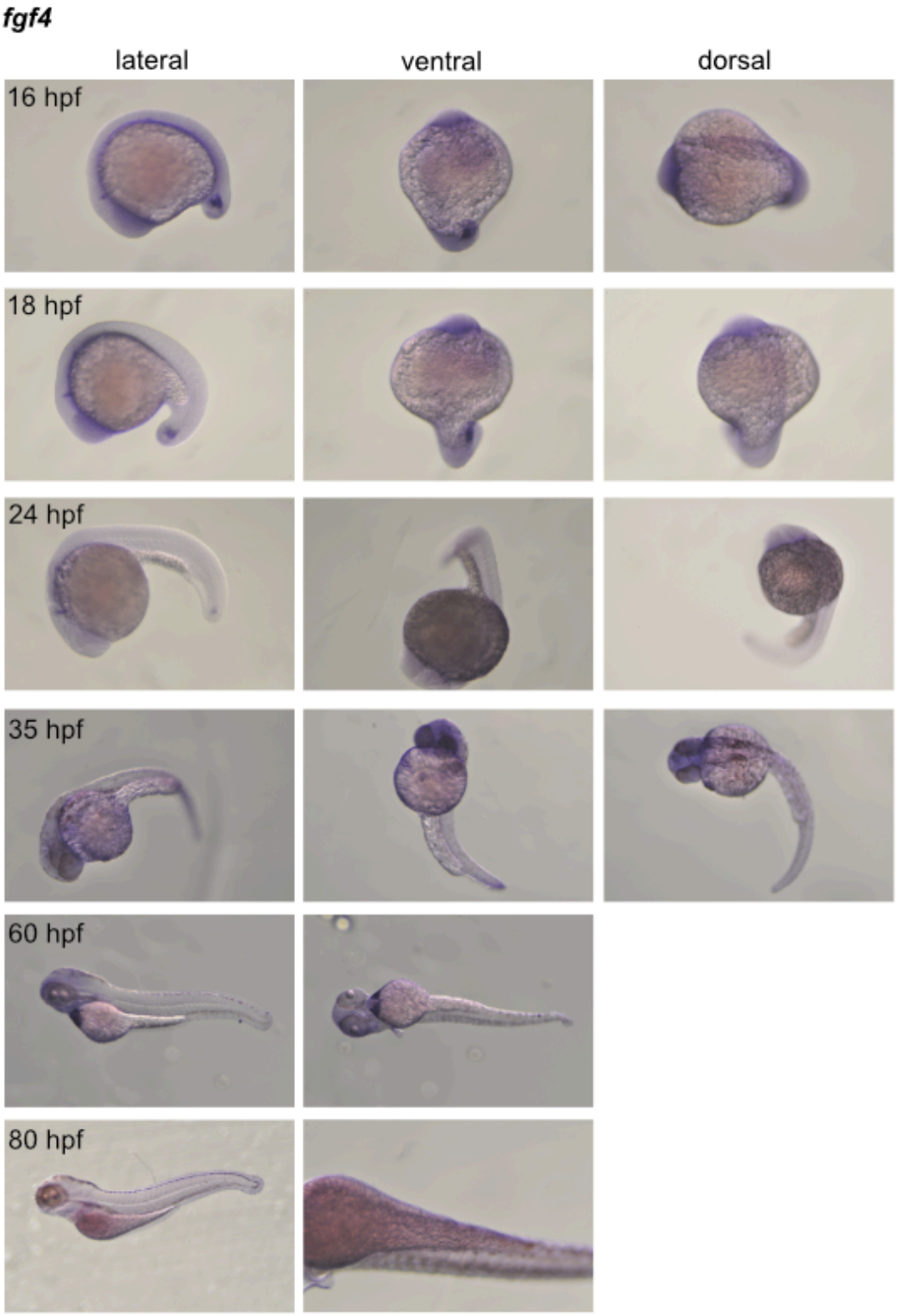

Appendix B Figure 7 – Embryo in situ hybridization of *fgf4*.

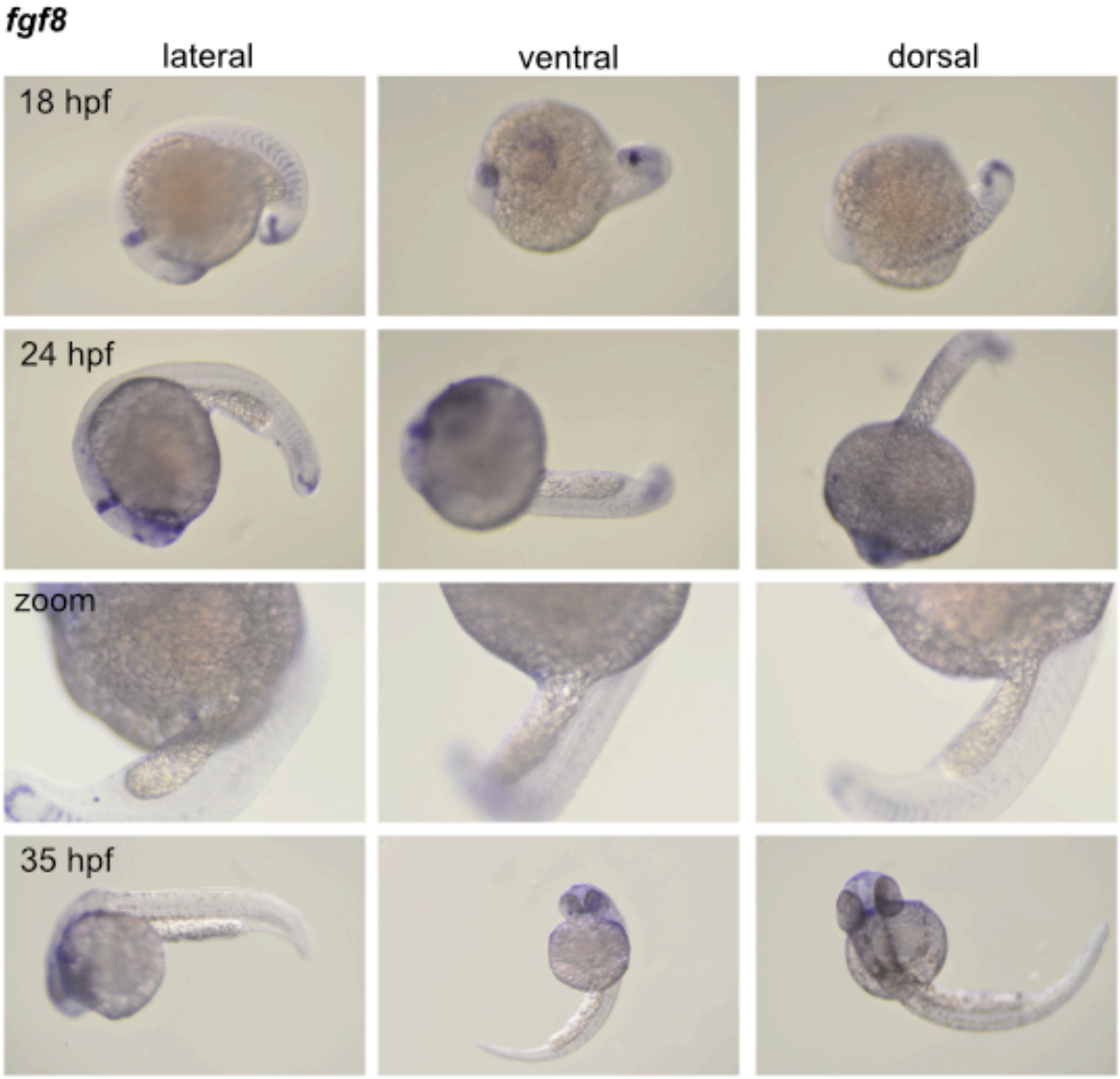

Appendix B Figure 8 – Embryo *in situ* of *fgf8a*.

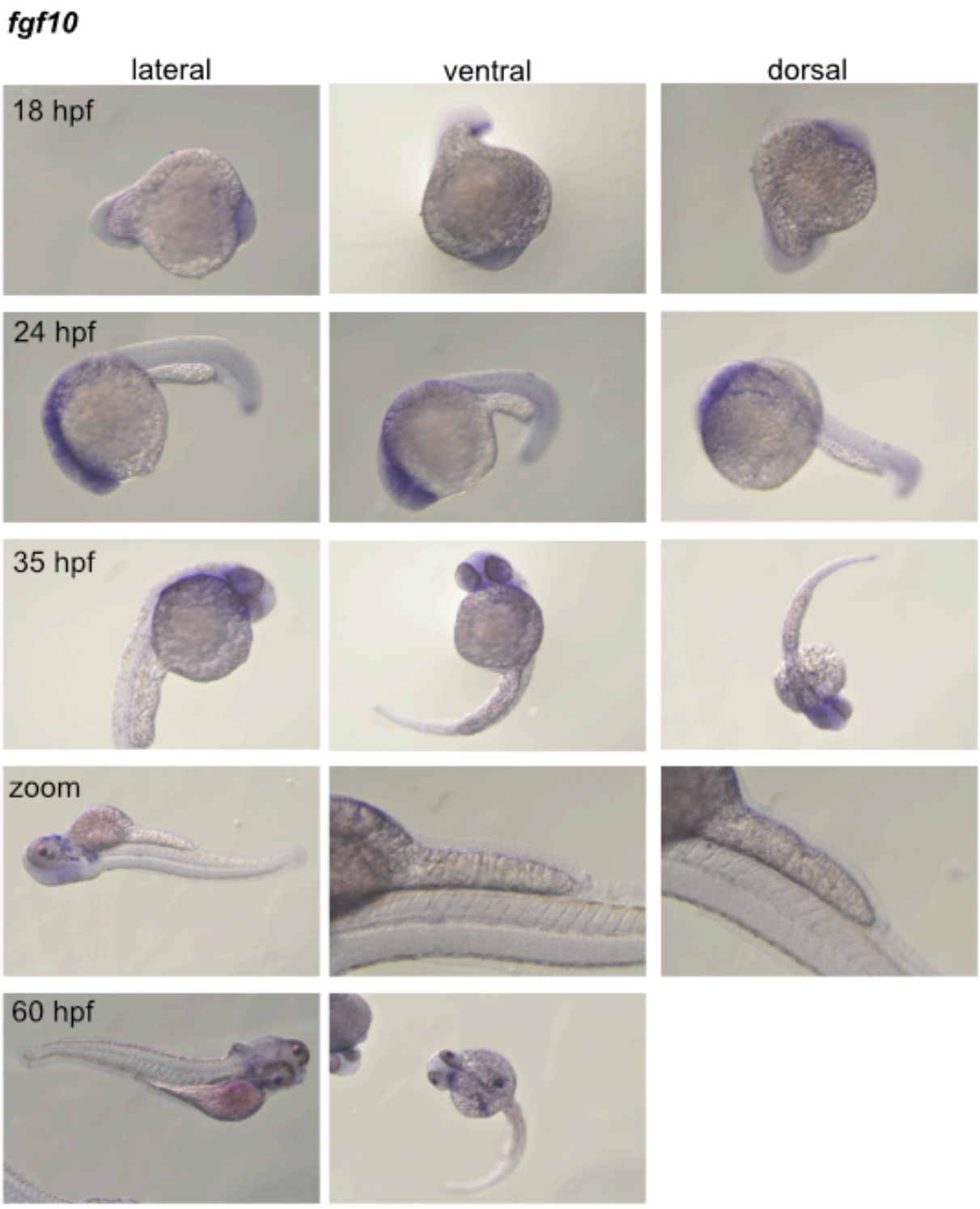

Appendix B Figure 9 - Embryo *in situ* of *fgf10a*.

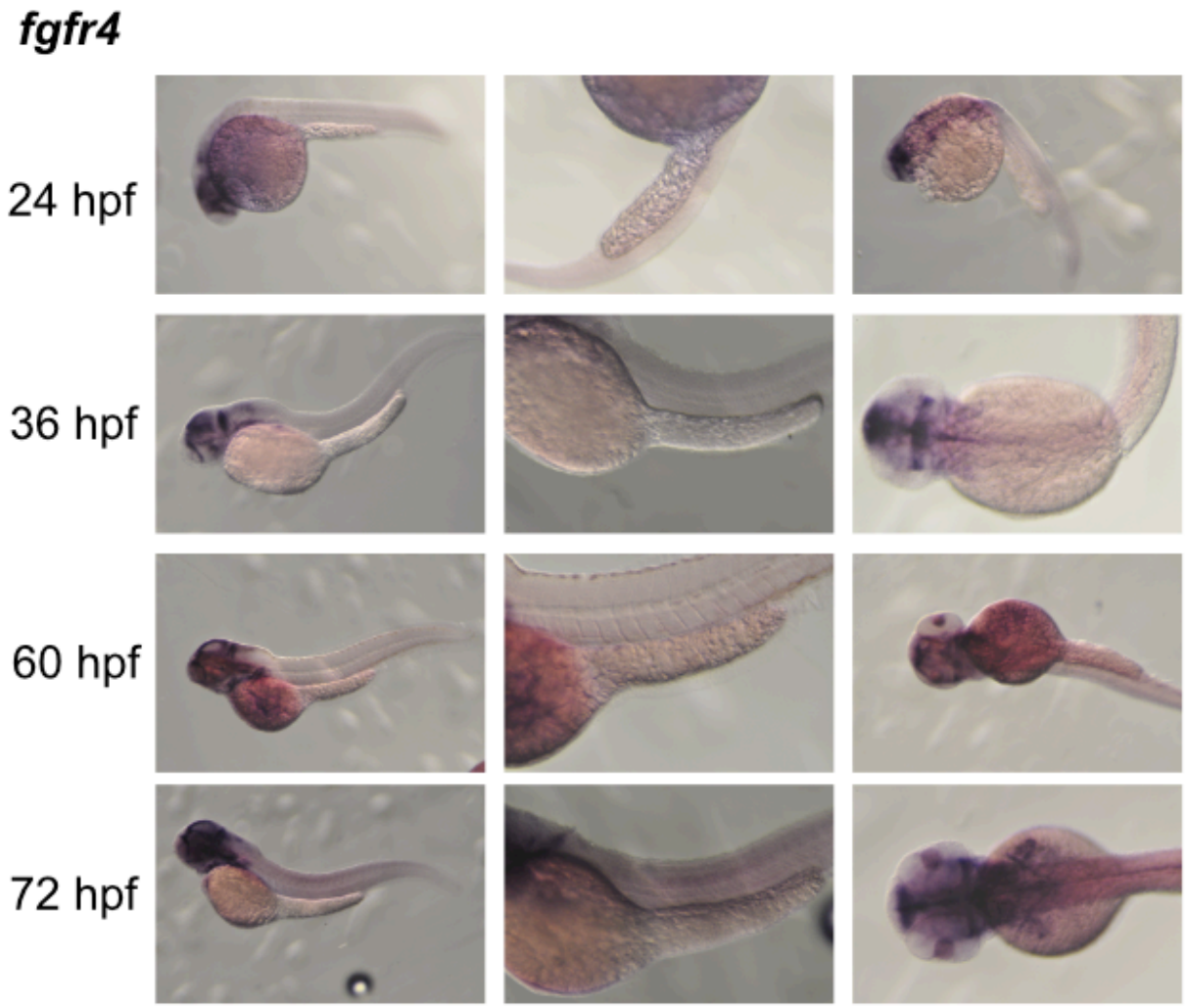

Appendix B Figure 10 – Embryo *in situs* of *fgfr4*.

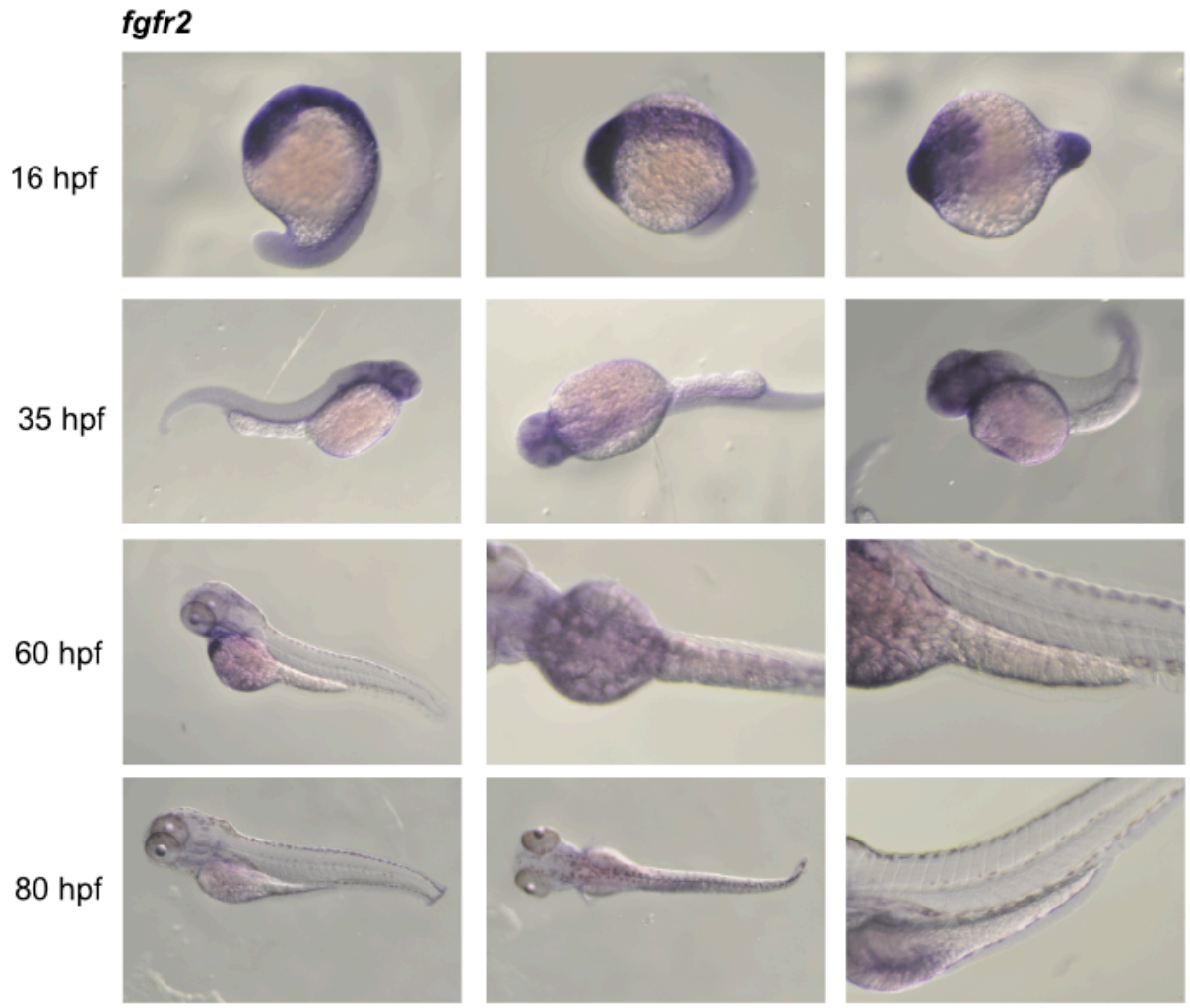

Appendix B Figure 11 – Embryo *in situs* of *fgfr2*.

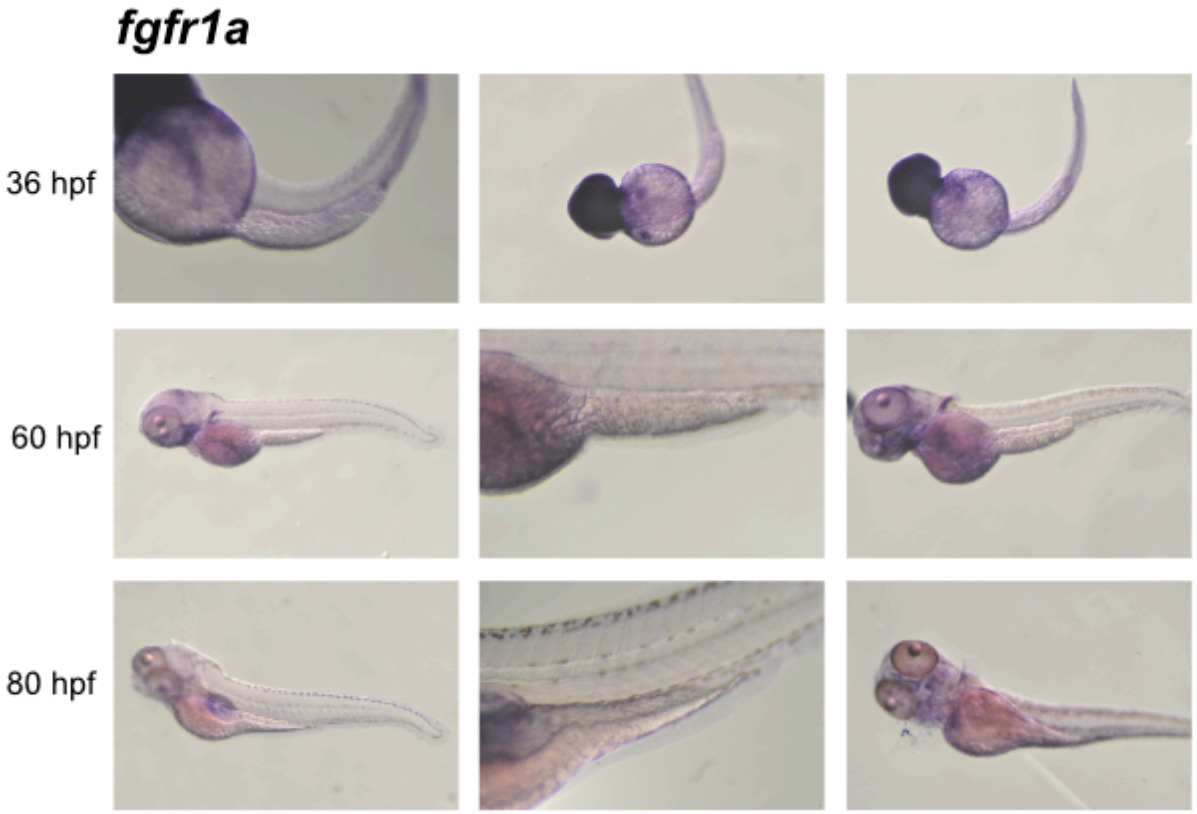

Appendix B Figure 12 – Embryo *in situs* of *fgfr1a.*

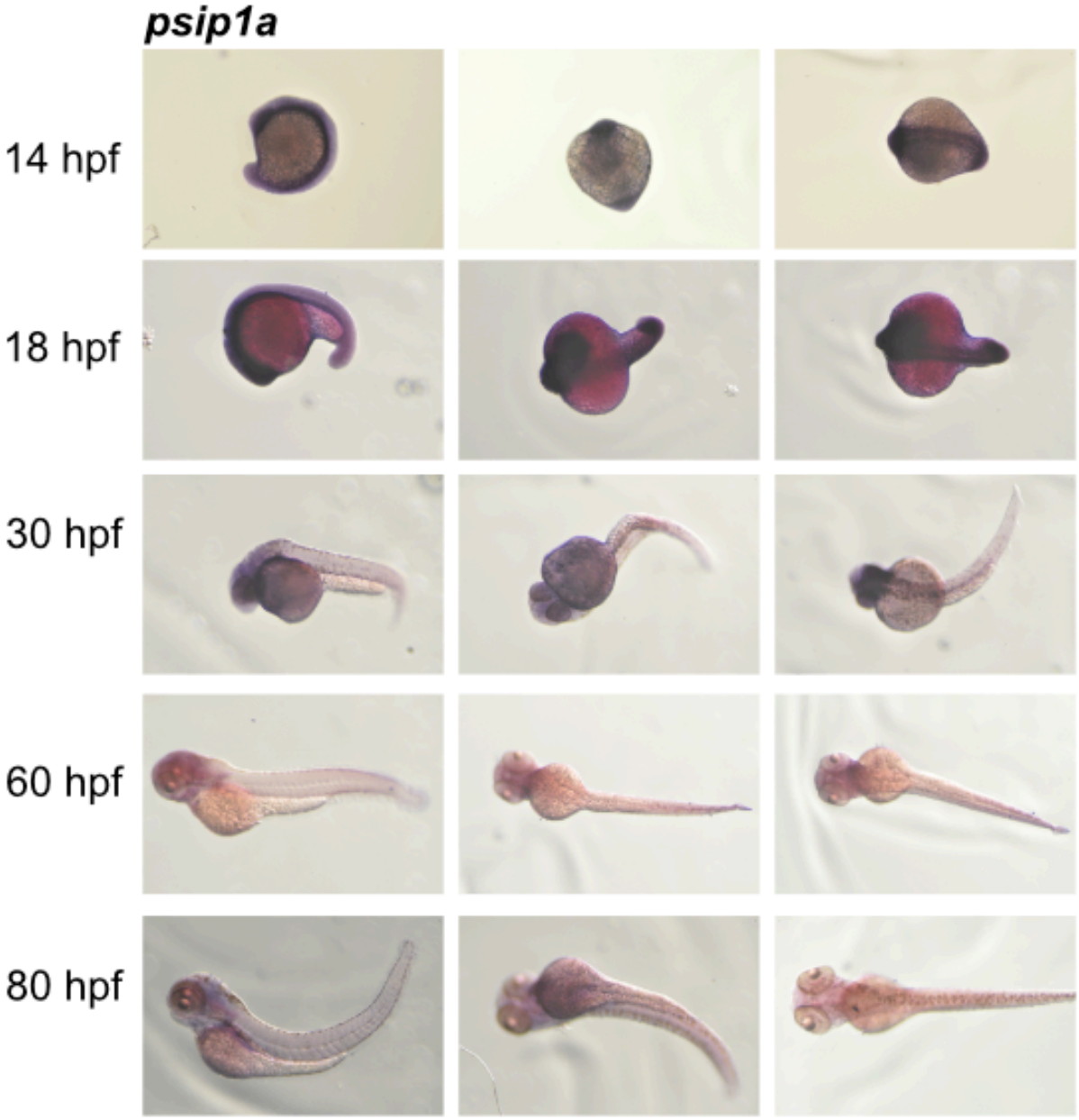

Appendix B Figure 13 – Embryo *in situs* of *psip1a.*

Appendix B Table 2 - Development of forelimbs/hindlimbs in chick/mouse/zebrafish

Misexpression/Identity Experiments

	Chick	**Mouse**
Misexpression expression of Tbx5 in hindlimb	Confer forelimb type morphology to the limb and induce ectopic expression of forelimb markers (Rodriguez-Esteban et al. 1999, Takeuchi et al. 2003)	
Misexpression expression of **Tbx4** in the forelimb in a **WT background**	Forelimb acquires hindlimb type morphology and induces ectopic expression of hindlimb markers (Takeuchi et al. 2003)	
Ectopic expression of Tbx5 in the flank	Wing-like limb (Takeuchi et al. 2003)	
Ectopic expression of Tbx4 in the flank	Induces a hindlimb-like limb (Takeuchi et al. 2003)	
Misexpression expression of **Tbx4** in a **Tbx5-null background** in the forelimb area		Tbx4 was capable of rescuing the forelimb and it had forelimb-like identity (Minguillon et al. 2005)
Misexpression of **Pitx1** in the forelimb in a **Tbx5-null background**		Pitx1 (only) cannot rescue forelimb development (Minguillon et al. 2005)
Ectopic expression of Pitx1 in the flank		No effect (unpublished from Minguillon et al. 2005)
Misexpression of Pitx1 in the forelimb in a WT background	Wing transformed to more hindlimb-like. However expression of Tbx5 not affected in the wing. (Logan and Tabin 1999)	

Appendix B Table 2 continued

	Chick	Mouse	Zebrafish
Tbx5 expression	Stage 17 – expression in the developing wing bud mesenchyme. Transient expression in the flank extending from the posterior of the wing bud to 2/3 of the interlimb flank region. (Logan et al. 1998)	Forelimb and a little bit of interlimb area Gibson-Brown et al. (2003)	Mao et al. (2015) in pectoral fin field
Absence of Tbx5	Viral infection into the prospective wing field = Wingless phenotype (**but there is a hypoplastic bud!**). If infected at later stages (before Stage 10) then wing is truncated. (Takeuchi et al. 2003)	No forelimb (no bud, sometimes there's a tiny outgrowth) (Rallis et al. 2003)	No pectoral fin, mis-migration (Mao et al. 2015)

	Chick	Mouse	Zebrafish
Tbx4 expression	Expressed throughout the early leg bud mesenchyme. At Stage 29, a very low level of Tbx4 detected in the wing? High levels of expression in the flank mesenchyme directly underneath the leg bud. (Logan et al. 1998)	**Low levels of Tbx4 expression in the developing forelimb** (Gibson-Brown et al. 1996, Naiche et al. 2011). Forelimb expression domain of Tbx4 shown to be unnecessary for forelimb morphology in mice and the enhancer is not conserved outside Mammalia (Menke et al. 2008, Naiche et al. 2011). Tbx4 ectopic forelimb expression is sufficient to rescue hindlimb-like morphology to Pitx1 null hindlimbs (Ouimette et al. 2008). Tbx4 has a unique transcriptional repressor site that is possibly responsible for hindlimb-like morphology and that this repressor site is absent in Tbx5 and ancestral Tbx4/5 cluster (Ouimette et al. 2008)	No embryonic, but in body wall and myosepta in larvae (Chapter 4)
Absence of Tbx4	Viral infection into the prospective leg field = Legless phenotype (hypoplastic bud) (Takeuchi et al. 2003. Later stages of viral infection = truncation of leg structures with normal wing formation.	Bud forms but does not outgrow (Naiche and Papaioannou 2007)	No pelvic fin, hypoplastic bud (Don et al. 2016)

Appendix B Table 2 continued

	Chick	Mouse	Zebrafish
Hindlimb buds- first appearance	3 dpf (Saunders 1977)	10 dpf (Martin 1990)	21 dpf

	Chick	Mouse	Zebrafish
Pitx1 expression	Leg bud mesenchyme (stage 18-14) and then becomes restricted to the most proximal extent of the leg and in the **flank of the embryo** at the level of the leg bud (Logan et al. 1998)	Expressed in a broad, caudal domain prior to expression of Tbx4 in the presumptive hindlimb forming region (Lanctat et al 1997)	Nothing in posterior body in embryo; body wall and myosepta in larvae (Chapter 4) But expressed in pelvic region for sticklebacks (Cole et al. 2003, Shapiro et al. 2004)
Pitx1 KO		Pitx1-null mice develop (smaller) hindlimbs where the skeleton has most hindlimb characteristics except the ilium (Lanctot et al. 1999, Szeto et al. 1999, Marcil et al. 2003) Pitx1 KO mice display reduced Tbx4 expression (Lamonerie et al. 1996, Lanctot et al. 1999). Thought to regulate Tbx4 via upstream enhancer region in tetrapods (Menke et al. 2008) – 5' HLEA and 3' HLEB, but only 3' HLEB is in fish.)	Absence of Pitx1 activity in the prospective pelvic regions of certain populations of threespine stickleblacks = failure of pelvic spine formation at an early stage (Cole et al 2003, Shapiro et al 2004)
Binding sites		Enriched near Tbx4 HLEA and HLEB, HoxC10, HoxC11, Tbx2 hindlimb enhancer. (Infante et al. 2013)	

Appendix B Table 2 continued

	Chick	Mouse	Zebrafish
Fgf8-soaked bead to the interlimb region	Induces an ectopic limb to form (Cohn et al. 1995, Mahmood et al. 1995, Ohuchi et al. 1995, Crossley et al. 1996, Vogel et al. 1996, Yonei-Tamura et al. 1999)		
Fgf signaling in general			Fgf8 expression not observed until after AER (Fischer et all 2003). Fgf8 mutant acerebellar develops normal pectoral fin (Reifers et al. 1998). But in pectoral fin buds, Fgf16 and Fgf24 seen before the expression of Fgf8 (Fischer et al. 2003, Nomura et al. 2006). Fgf8 expression is dependent on Fgf16 activity. Fgf24 mutant ikarus fails to develop pec fin but does develop pelvic fin.
Conditional removal of Fgf activity		Little effect on limb bud induction – removal of Fgf8 and Fgf4 (Boulet et al. 2004, Perantoni et al. 2005)	Fgf signaling not required for pectoral fin bud initiation but is required for later stages of limb/fin budding and development – SU5402 (Fgf receptor antagonist) treated fish are fine (Mercader et al. 2006)
Fgf10			Removal (dae mutant)- initiation is seen in pec fin but prevents later fin bud development (Norton et al. 2005)

Appendix B Table 2 continued

Other genes

	Chick	**Mouse**	**Zebrafish**
Hoxb9, Hoxc9, and Hoxd9 expression	Staggered in the prospective forelimb/pectoral fin region; strong expression also in the interlimb/fin and prospective hindlimb/pelvic fin region (Cohn et al. 1997, Tanaka et al. 2005). Hoxd9 expression disappears from interlimb regions and is restricted to domains adjacent to the prospective limb buds (Cohn et al. 1997)		See chick
Gdf11 mutants		Changes expression domain of Hoxc10 and changes the axial position of hindlimb (McPherron et al. 1999)	Changes expression domain of Hoxc10 and changes the axial position of pelvic fin (Murata et al. 2010)
RA		RA promotes forelimb induction but not necessary for hindlimb bud induction (Zhao et al 2009). Role of RA in limb dev to suppress Fgf8 activity along the flank?	RA and Tbx5 signaling is upstream of Fgf function (Gilbert e tal. 2006, Mercader et al. 2006, Grandel and Brand 2011)
Wnts	Wnt2b in forelimb and wint8c in hindlimb thought to be involved in induction (Kawakami et al 2001)	Neither wnt2b or wnt8c have been detected in the limb buds of early mice embryos (Agarwal et al 2003)	Wnt2b relays the RA fin bud induction signal to the pec fin and induces Tbx5 expression (Mercader et al. 2006)

APPENDIX C - TESTING FOR CORRELATION BETWEEN DELAY IN PELVIC FIN INITIATION AND PELVIC FIN POSITIONING

C.1 PREFACE

As mentioned in Chapter 5, the delay in timing seen in Neopterygi or Teleostei may have facilitated the ability for Neoteleostei fish to shift their pelvic fins forwards. To test this hypothesis in a comparative context, I attempted to quantify the delay in timing across actinopterygians and test whether there was a correlation in pelvic fin timing and position. Data collection was performed by a wonderful team of undergraduates: Eric Yuan, Maryam Bolouri, and Dominique Jaramillo. Initial data cleanup was performed by E. Yuan. This work was funded by the Micro-Metcalf Program at the University of Chicago.

C.2 MATERIALS AND METHODS

Larval data was primarily collected from *Early Stages of Atlantic Fish* (Richards, 2005). The following data types were collected: Egg diameter (low-high), yolk type, hatch size (low-high), incubation information, length at flexion (low-high), length at transformation (low-high), number of pelvic fin rays, and pelvic fin first length. Averages were calculated for all data that had low-high ranges. Except for the last metric, these characteristics were compiled by Richards (2005). For the pelvic fin first length, we used the staging images to find the first stage at which a pelvic fin bud is visible and recorded that length. Lengths were only recorded if the pelvic fin bud was small, and not if the pelvic fin was already fully formed. In total, 1668 species of fish

(526 families) were examined.

To quantify the delay in timing, I used two methods:

$$Method\ 1\ delay = \frac{length\ of\ fish\ at\ pelvic\ fin\ initiation - length\ at\ transformation}{length\ at\ transformation}$$

$$Method\ 2\ delay = \frac{length\ of\ fish\ at\ pelvic\ fin\ initiation - length\ at\ hatching}{length\ at\ transformation}$$

The first method relied on the length of the fish at pelvic fin initiation as the main indicator of the delay. It assumed that most fish develop pectoral fins within the first few days of development, and that the total length of the fish when the pectoral fin develops is more or less constant across actinopterygians (i.e. probably very small). The second method did not assume that all fish are similar in size when the pectoral fin develops, and instead used the "total length of the fish at hatching" as a proxy. This method assumed that fish hatch soon after the pectoral fins develop (or that the pectoral fins develop soon after hatching). For both methods, the lengths were standardized by the length at transformation, which was a proxy for metamorphosis. This is defined in Richards (2005) as "the process (synonymous with metamorphosis) at the end of the larval stage, characterized by a marked change in form of structure and involving acquisition of juvenile or adult characters and loss of larval characters" (p.29).

Only families that had both data for pelvic fin first length and length at transformation could be used for Method 1, and only families that had those two metrics in addition to length at

hatching could be used for Method 2. After filtering for these requirements, the number of families used in Method 1 and Method 2 were 59 and 36 ("trimmed dataset"), respectively.

The analyses performed follow the methods written in Chapter 2. For each method of quantifying pelvic fin delay, I visualized the trait distribution with contMap. Then, I tested whether the delay in pelvic fin initiation was correlated with pelvic fin position with a phylogenetic framework (phylogenetic generalized least squares). I fitted each model with either a Brownian motion or OU model (where lambda was initially set to 1 and allowed to vary). Finally, I checked for shifts in adaptive optima with phyloEM. The family-level tree was derived from (Rabosky et al., 2018).

C.3 RESULTS

The delay in pelvic fin initiation was first visualized with contMap across our family-level dataset. Three visualizations were generated: Figure C.1 with Method #1 and its 59 species, Figure C.2 with Method #1 and 36 species ("trimmed dataset"), and Figure C.3 with Method #2 and 36 species ("trimmed dataset"). Using Method #1, there appeared to be a slight tendency for pelvic fin initiation to be less delayed, or earlier in development compared to metamorphosis, in more nested lineages. Using Method #2, there did not seem to be a change in pelvic fin delay throughout these families.

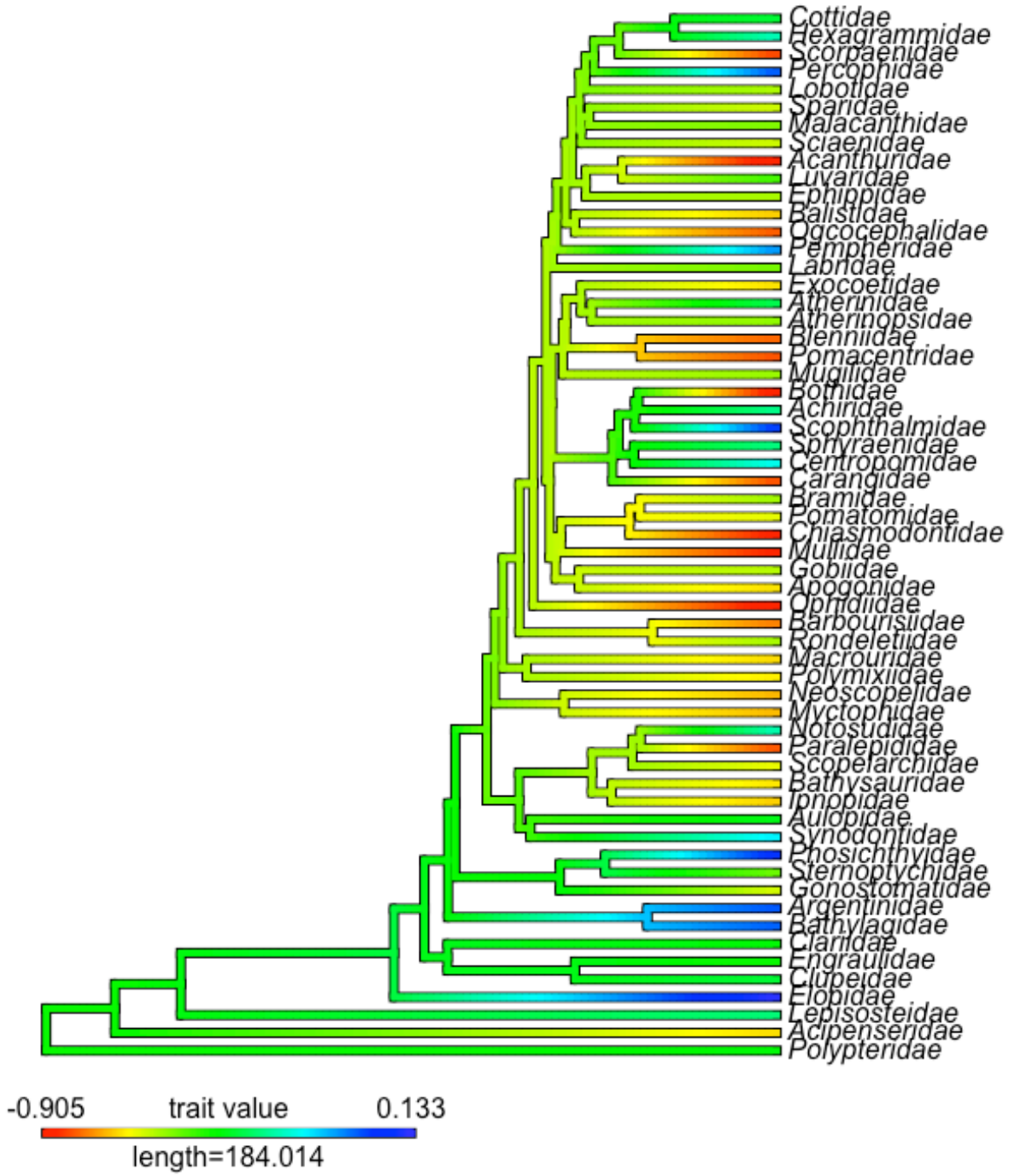

Appendix C Figure 1 - contMap of pelvic fin delay quantified by Method 1. More negative values (warmer) indicate a smaller delay in pelvic fin initiation.

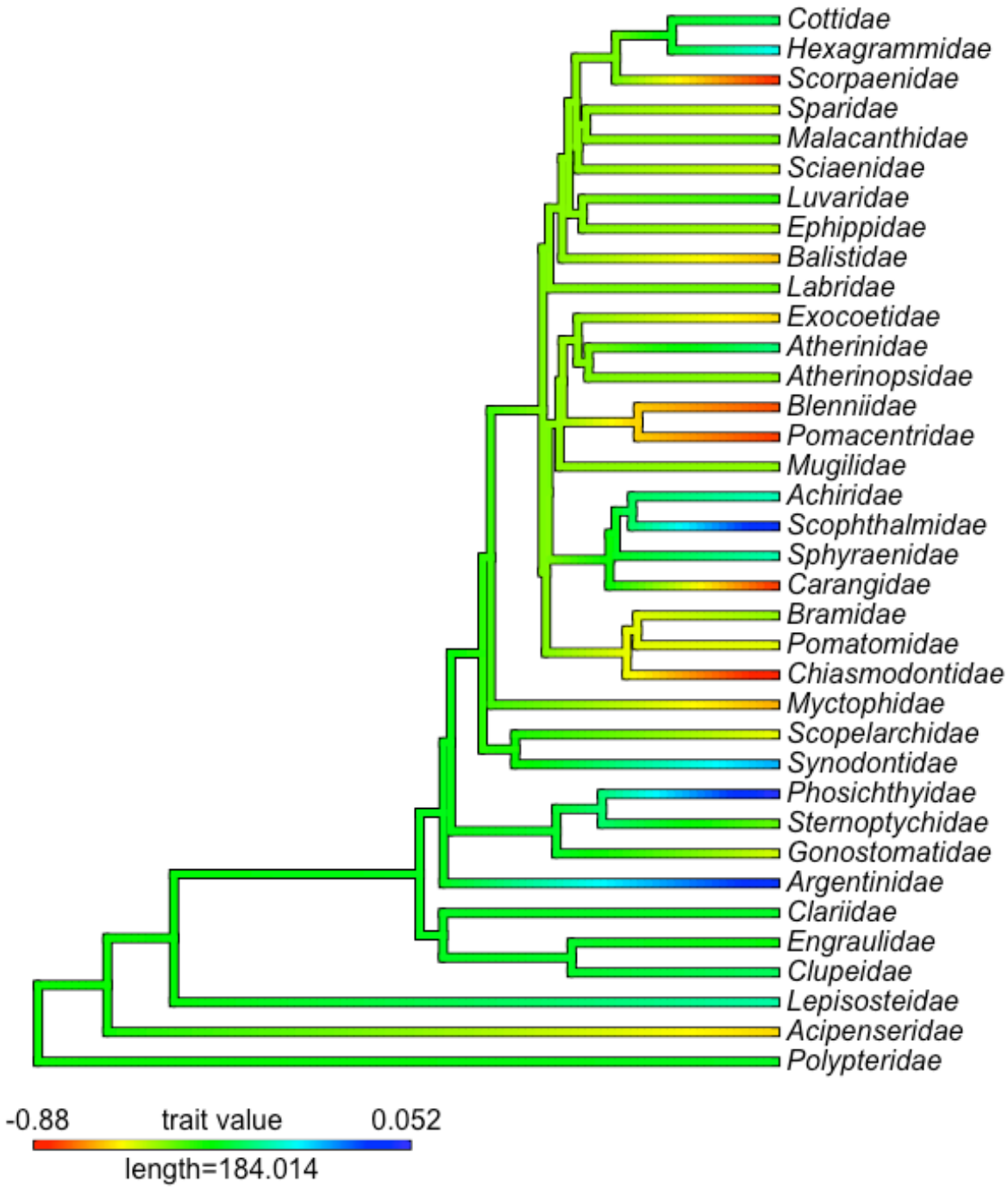

Appendix C Figure 2 - contMap of pelvic fin delay quantified by Method 1, but with the "trimmed" dataset. More negative values (warmer) indicate a smaller delay in pelvic fin initiation.

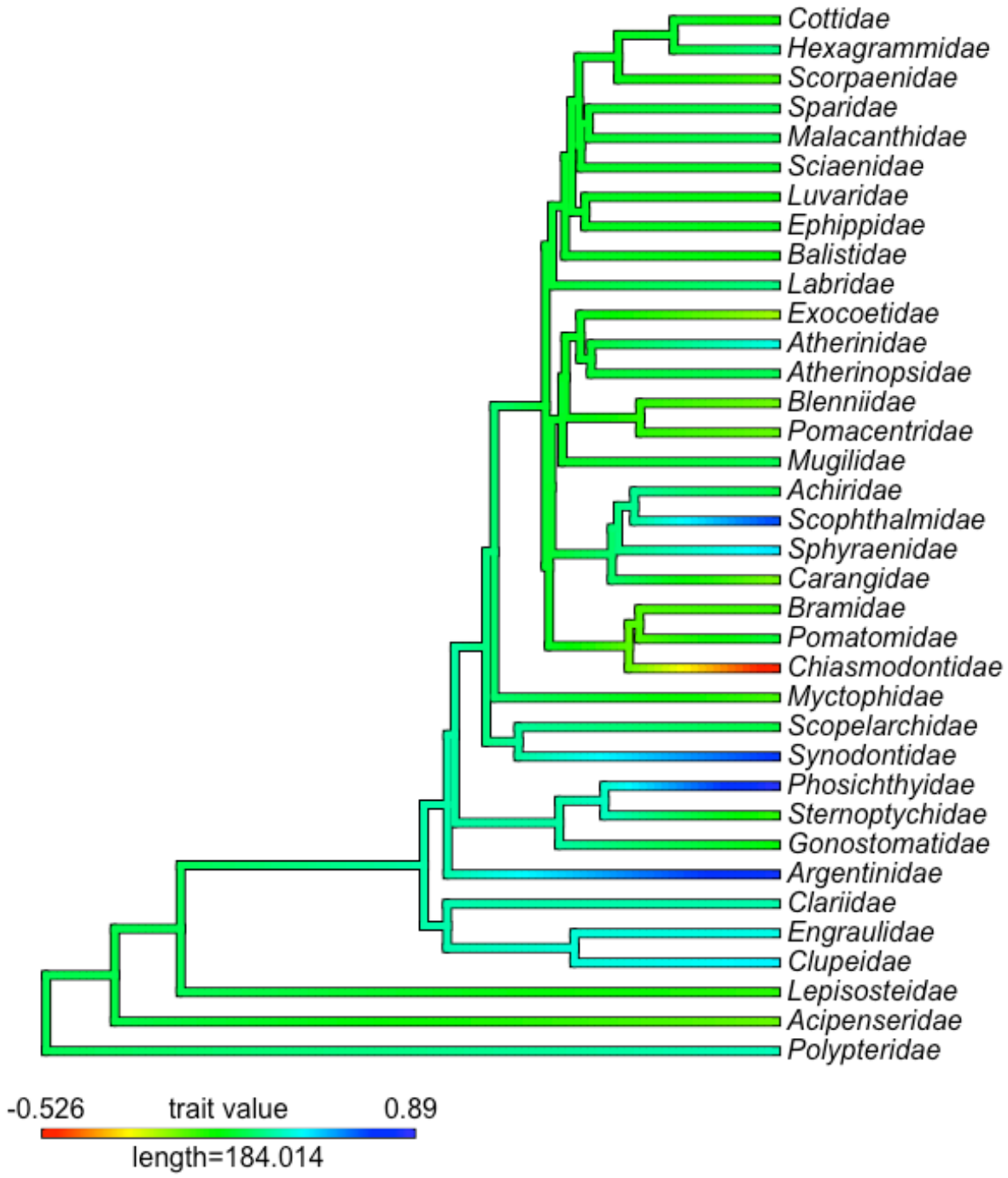

Appendix C Figure 3 – contMap of pelvic fin delay quantified by Method 2. Larger numbers (cooler) indicate a longer delay in pelvic fin initiation.

To investigate the drivers of our calculated pelvic fin delay, I also generated plots for length of fish at pelvic fin initiation, length of fish at transformation, and length of fish at hatching for the trimmed dataset (Figure C.4). Visually, it appeared that length of fish at pelvic fin initiation decreased dramatically at the base of Acanthomorpha (Figure C.4A), that there was a slight decrease of length of fish at transformation at the base of Acanthomorpha (Figure C.4B), and that most teleost fish at hatching are around the same size (Figure C.4C). Therefore, it is likely that the dramatic decrease of fish length at pelvic fin initiation stage is driving the signal that the pelvic fin is appearing earlier in more nested (e.g. acanthomorph) lineages.

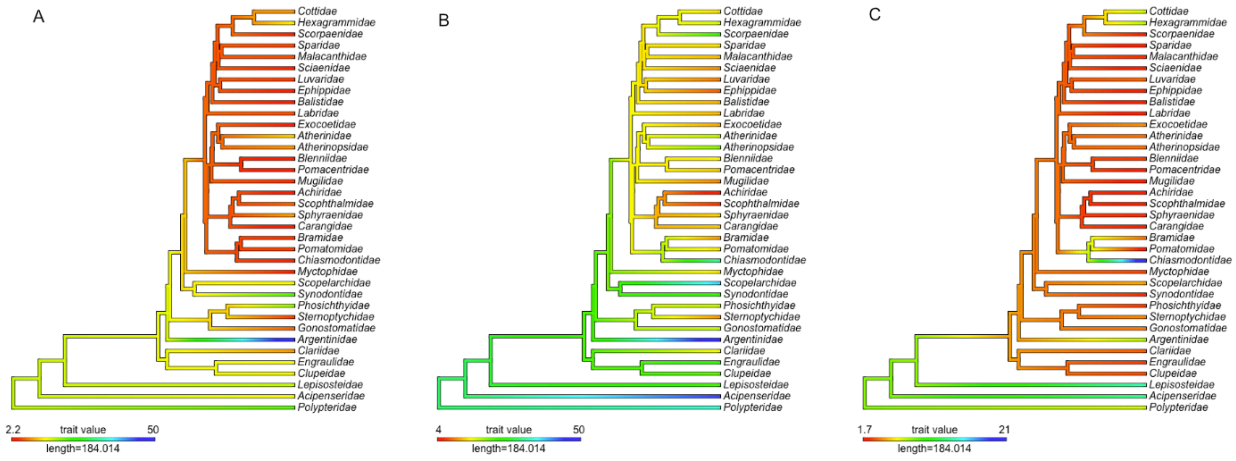

Appendix C Figure 4- contMaps of the trimmed dataset with (A) length of fish at pelvic fin initiation (B) length of fish at transformation (C) length of fish at hatching.

I next tested whether pelvic fin delay was correlated with pelvic fin position (position ~ delay) using phylogenetic generalized least squares. Three types of datasets/methods were investigated – the 59-family dataset with Method #1, and then the "trimmed" 36-species dataset

with Methods #1 and #2. None of these methods produced a significant correlation between pelvic fin delay and pelvic fin position (Table C.1).

	p-value	coefficients	lambda	AIC	df	standard error
Method 1 – Brownian	0.76	0.22	n/a	-79.88	59; 57 residual	0.18
Method 1 – OU model	0.85	0.19	1.09	-78.80	59; 57 residual	0.21
Method 1 – trimmed dataset; Brownian	0.45	0.33	n/a	-45.50	36; 34 residual	0.17
Method 1 – trimmed dataset; OU model	0.19	0.24	1.15	-44.10	36; 34 residual	0.22
Method 2 – trimmed dataset; Brownian	0.91	-0.08	n/a	-42.19	36; 34 residual	0.18
Method 2 – trimmed dataset; OU model	0.84	-0.07	1.08	-40.44	36; 34 residual	0.20

Appendix C Table 1– Testing for correlation between pelvic fin delay and position.

Finally, I checked for shifts in adaptive optima when considering both pelvic fin delay and pelvic fin position. These traits appeared to shift together at the base of Neoteleostei

according to Method #1 (full and trimmed dataset), with an additional shift detected at Pleuronectiformes in the trimmed dataset. For these, the shift is characterized by a more rostral pelvic fin, as seen in Chapter 2, and surprisingly, an earlier initiation of the pelvic fin (less of a delay). The Pleuronectiformes shift was characterized by a very rostral pelvic fin and a later initiation of the pelvic fin. Using Method #2, no shifts were detected.

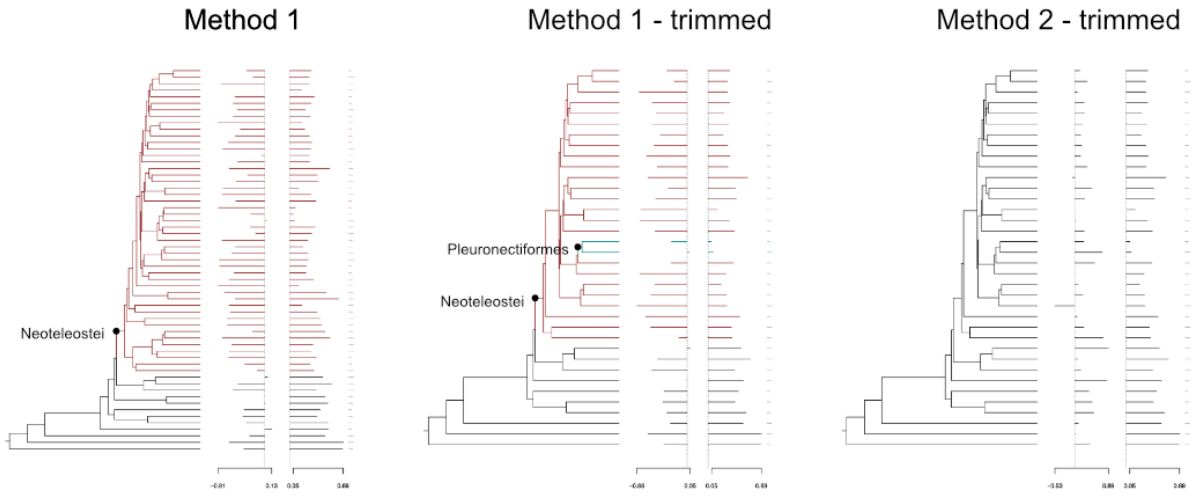

Appendix C Figure 5 - PhyloEM shifts in adaptive optima of pelvic fin delay (first column) and pelvic fin position (second column).

For Method #1, more negative values of pelvic fin delay indicate earlier initiation. A shift is seen towards earlier initiation at the base of Neoteleostei for both full and trimmed datasets in Method #1. For Method #2, larger, more positive numbers indicate a longer delay. No shift was detected using this method.

C.4 DISCUSSION AND FUTURE DIRECTIONS

I showed that there is no correlation between pelvic fin timing and pelvic fin initiation, however, Method #1 uncovered a shift in adaptive optima in these two traits at the base of

Neotelostei. In Chapter 2, I also found no correlation between pectoral and pelvic fin position but a shift at the base of Neotelostei. It is possible that here again, this shift indicates that there are two distinct sets of pelvic fin initiation times/pelvic fin position without any correlation between the total dataset.

The results from this preliminary study are extremely dependent on the quality and standardization of data collected. For the length of the fish at pelvic fin initiation, it is likely that I was unable to capture the earliest length, since the stages illustrated in Richards (2005) are generally not finely divided. The length at hatching is probably more accurate, as hatching is a defined and obvious event. However, the length of transformation can be subjective, since "transformation" is a nebulous term that refers to an author's personal definition of what a change from larval to adult characters means. Since Richards (2005) compiled the data for most of these species as a single author, it is my hope that he was able to apply a similar definition of transformation to every species.

A large surprise emerging from this data is that the delay in pelvic fin initiation appears to actually decrease (i.e. earlier pelvic fin) in Neotelostei, instead of increasing as I predicted in Chapter 5. This hypothesis predicted that a delay in pelvic fin initiation allowed for the rostral movement of pelvic fins by temporally separating pectoral and pelvic fin development so that regionalization signals would not be crossed in the lateral plate mesoderm. A later initiation of the pelvic fin in the rostral region would be accomplished by re-regionalization in the late larval stages. Clearly, this is not the pattern seen here, which may be due to a few factors:

(1) Irregular growth rate - My preliminary data in Chapter 5 relied on time (dpf) but this data is based on standard length. Using length as a proxy for time assumes a constant growth rate. Thus, if there is a larger gap between length of pelvic fin initiation and length at transformation than predicted by a constant growth rate, then the delay would look earlier than it is in reality. This increased gap could be due to an increased growth rate between pelvic fin stage and length at transformation.

(2) Bias in classifying length at transformation – Because the definition of transformation is subjective, it is possible that for Neoteleosts or Acanthomorphs, transformation was perceived to be later than the biologically equivalent stage for Non-Neoteleosts or Non-Acanthomorphs. This could be due to observational bias from the authors, or it could be the case that the "juvenile" characters in more nested lineages used to diagnose transformation appear at a later stages than in earlier lineages.

(3) Bias in classifying length at pelvic fin first initiation – Acanthomorphs appear to have body lengths at pelvic fin initiation that are markedly smaller than Non-Acanthomorphs (Figure C.4A). This could be due to a more refined staging system that has allowed for earlier observation of pelvic fin initiation, however, it is striking that the all Acanthomorphs sampled have uniformly small body lengths at pelvic fin initiation.

Given these uncertainties in the data, I believe the next step should be to verify that the growth rates of these fish are constant enough for length to be used as a proxy for time. If this is not the case, then another metric for the delay between pelvic fin and pectoral fin initiation should be developed.

If these results are accurate and there truly is a decreased delay in pelvic fin initiation in Neoteleosts that is concomitant with a rostral shift in pelvic fin position, then these Neoteleost fish need to have developmental strategies to differentiate the identities of the lateral plate mesoderm at the same axial level. This could be accomplished a few ways: (1) simultaneous regionalization and anterior migration of the pelvic fin precursors (2) novel responsiveness of *tbx4* to rostral Hox signals, perhaps through subfunctionalization if both copies of *tbx4* have been retained in Neoteleosts (3) dorsoventral separation of lateral plate mesoderm fate – perhaps cells that reach the ventral midline are specified as pelvic fin, and cells that remain dorsally are specified as pectoral fin.

In summary, this preliminary attempt at testing for a correlation between pelvic fin delay and pelvic fin position has found no correlation within actinopterygians, but has potentially uncovered a shift in adaptive optimum at the base of Neoteleostei towards earlier pelvic fin initiation. Further work will be needed to ensure that using length is an adequate proxy for time, and that standardizing by length at transformation is appropriate. In addition, the compilation of this larval/hatching dataset from digitizing information from Richards (2005) as well was other online sources will allow further investigation in linking embryonic traits to adult morphologies.

APPENDIX D - PROTOCOLS

The attached protocols are meant for bench use – I printed them out for every experiment and used them as checklists in my lab notebook. I hope that they can be useful for future graduate students – they were extremely challenging to refine for zebrafish larvae! Please refer to Chapter 6 for information on the catalogue numbers for reagents and citations for the sources of these protocols. If there are any discrepancies, Chapter 6 should take priority.

List of protocols

- D.1 - Larval *in situ* hybridization protocol
- D.2 – Embryo *in situ* hybridization protocol
- D.3 – Embedding and sectioning larvae in paraffin
- D.4 – Antibody staining on paraffin sections
- D.5 – Antibody staining on larval whole mounts
- D.6 – Hematoxylin and eosin staining on paraffin sections
- D.7 – Preparation of RNA probes for *in situ* hybridization from plasmids
- D.8 – Primer design
- D.9 – PCR workflow
- D.10 – RNA probe transcription and purification from PCR product
- D.11 – Solutions

Appendix D.1 - Larval in situ hybridization protocol

Beforehand:

**Only use fresh larvae! Typically, they are fixed in 4% PFA over the weekend and immediately used the next week. If stored in PFA or MeOH too long, the protocol is not effective.

Day 1: MeOH, Pro-K, Hyb incubation

The goal of this day is to dehydrate into 100% MeOH (good for clearing pigment and increasing permeabilization of the probe), rehydrate into PBT, and then permeabilize with either Pro-K or acetone (see next page). Then, we incubate in Hyb before adding the probe overnight to ensure that the probe can permeabilize the tissue well.

	30% MeOH (5 min)
	60% MeOH (5 min)
	100% MeOH (2x) – total time 1hr
	60% MeOH/PBT (5 min)
	30% MeOH/PBT (5 min)
	PBT – 4x (5 min)
	Pro-K treatment - 20 µg/mL ~ 3.5 mm SL = 35 min, 6-8 mm SL = 50 min For 1 mL of 20µg/mL: 2**0 µL Pro-K 100x stock + 10 µL DMSO + 970 µL PBT**
	Re-fix in 4% PFA (30 min)
	Rinse in PBT (4x)
	• Hyb (allow to sink) at RT • Hyb (2x washes) • Hyb (3 hours to overnight) @ 70 C … then move on to *in situ* steps

Overnight in _____ probe: (5 mg tRNA to 10 mL Hyb + probe) **Preheat!**

Alternative Day 1: Permeabilization with ethanol/xylene/acetone

	30% MeOH (5 min)
	60% MeOH (5 min)
	100% MeOH (2x) – total time 1hr
	100% EtOH (5 min) (2x)
	1:1 ethanol:xylene solution (1 hour)
	100% EtOH (5 min) (2x)
	60% EtOH in H2O-Tween (15 min)
	30% EtOH in H2O-Tween (15 min)
	H2O-Tween (5 min) (2x)
	Permeabilize - 80% acetone/H2O at -20C (30 min)
	PBT (5 min) (2x)
	• Hyb (allow to sink) at RT • Hyb (2x washes) • Hyb (3 hours to overnight) @ 70 C … then move on to *in situ* steps

Day 2: Hyb washes, antibody block and incubation

- Remove probe – save it!

The goal of this day is to wash out the primary probe so that we minimize background staining. The SSCT solutions are the main detergents/salts that help the probe diffuse out. Pre-warm the solutions!

	75% Hyb + 25% 2X SSCT @ 70 C (10 min)
	50% Hyb + 50% 2X SSCT @ 70 C (10 min)
	25% Hyb + 75% 2X SSCT @ 70 C (10 min)
	2X SSCT @ 70 C (10 min) @ 70 C
	0.05X SSCT @ 70 C (30 min)
	0.05X SSCT @ 70 C (30 min)
	2X SSCT @ 70C (2 hours)
	75% 2X SSCT in PBT (5 min)
	50% 2X SSCT in PBT (5 min)
	25% 2X SSCT in PBT (5 min)
	PBT (5 min)
	PI buffer, RT (2-3 hours) – blocking step
	Incubate with PI + DIG antibody overnight, 4 C on rocker (1 uL DIG into 5 mL PI, store at 4C)

Day 3: PBT washes (15 min)

	PBT wash (5 min)
	PBT wash (5 min)
	PBT wash (5 min)
	PBT2 wash (overnight – wash as long as antibody incubation) @ 4 C

Day 4: Staining with NBT/BCIP

	Replace PBT2 with AP buffer (5 min)
	AP buffer (5 min)
	AP buffer (5 min)
	NBT/BCIP staining solution – change out if it becomes yellow. May take a few days. Avoid 4C during 1st day or crystals will form.
	Stop reaction by replacing with PBS pH 5.5 (wash 10-30 min)
	Solution X rinses

ALTERNATIVELY:

Day 4: Staining with BM Purple

	PBT2 washes (10 min) (2x)
	AP buffer (20 min)
	AP buffer (20 min)
	AP buffer (20 min)
	Discard AP buffer then add 1 mL of BM purple to the tube. Avoid agitation. Incubate in the dark and check staining frequently. May take a few days.
	Stop reaction by replacing with PBS pH 5.5 (wash 10-30 min)
	Solution X rinses

** Note: I find Pro-K permeabilization more intense, and BM Purple more intense. Combining the two will lead to more background staining, so the incubation times should be monitored.

Ideal schedule: Fix larvae on Friday, leave in fixative over the weekend, start protocol on Monday. Color development should be timed for Thursday, leaving imaging for Friday. If color development takes longer than a day, consider increasing the permeabilization intensity next time, because imaging on the weekend is not the most enjoyable activity!

Appendix D.2 - Embryo *in situ* hybridization protocol

Day 1: Rehydrate + PreHyb

	60% MeOH/PBT (5 min)
	30% MeOH/PBT (5 min)
	PBT – 4x (5 min)
	Pro-K treatment – 10 ug/mL… 10 min for 24 hpf; 20 min 36 hpf; 60 min for 72 hpf For 1 mL of 10µg/mL: **10 µL Pro-K 100x stock + 990 µL PBT**
	Re-fix in 4% PFA (1 hour)
	Rinse in PBT (4x)
	If storing in Hyb: • Hyb at 70 C for 15 minutes • Hyb (2x washes) – then store at -20C, make sure to sit for 1-2 hours in 70 C hyb before probe goes in next time **If moving forwards:** • Hyb (1-3 hours) @ 70 C … then move on to *in situ* steps

Day 2: Hyb washes, antibody block and incubation

- Remove probe – save it!
- Pre-warm solutions in incubator

	75% Hyb + 25% 2X SSCT @ 70 C (10 min)
	50% Hyb + 50% 2X SSCT @ 70 C (10 min)
	25% Hyb + 75% 2X SSCT @ 70 C (10 min)
	2X SSCT @ 70 C (10 min) @ 70 C
	0.05X SSCT @ 70 C (30 min)
	0.05X SSCT @ 70 C (30 min)
	75% 0.05x SSCT in PBT (5 min)
	50% 0.05x SSCT in PBT (5 min)
	25% 0.05x SSCT in PBT (5 min)
	PBT (5 min)
	PI buffer, RT (1 hour) – blocking step
	Incubate with PI + DIG antibody overnight, 4 C on rocker (1 uL DIG into 5 mL PI, store at 4C)

Day 3: PBT washes and color development

	PBT wash (5 min) (2x)
	PBT wash (15 min) (5x) or overnight

	Replace PBT with AP buffer (5 min)
	AP buffer (5 min)
	AP buffer (5 min)
	NBT/BCIP staining solution – change out if it becomes yellow.
	Stop reaction by replacing with PBT (3x rinse)

Lazy version for clearing yolks:

	Store in 70% DMF (few hours to overnight)
	PBT rinses (5x)
	Store in 80% glycerol; TAKE PHOTOS IMMEDIATELY

Ideal version for clearing yolks:

	Store in 70% DMF (few hours to overnight)
	PBT rinses (2x)
	30% MeOH (5 min)
	60% MeOH (5 min)
	100% MeOH (5 min)
	100% MeOH (1 hour)
	60% MeOH (5 min)
	30% MeOH (5 min)
	PBT (5 min) (2x)
	4% PFA (1 hour to overnight)
	Store in 80% glycerol

Appendix D.3 – Embedding and sectioning zebrafish larvae

Adapted from K. Criswell's protocol for skates

Step 1: Grade specimens up to 100% ethanol on a rocker.

- (15 min) – 30% EtOH
- (15 min) -- 50% EtOH
- (15 min) -- 70% ethanol (can stop here for storage)
- (20 min) – 100% EtOH
- (20 min) – 100% EtOH

Beforehand: Melt paraffin wax in 65C incubator - it takes 2+ hours to melt.

Step 2: Infiltrate tissue

- (15 minutes) – 50:50 EtOH:histosol
- (15 minutes) – 25:75 EtOH:histosol
- (15 minutes) – 100% histosol
- (15 minutes) – 50:50 wax:histosol (need to heat up beforehand) @ 65C
- (20 minutes) – 100% wax @ 65C (transfer to 50 mL tubes)
- (20 minutes) – 100% wax @ 65C
- (20 minutes) – 100% wax @ 65C

Step 3: Embed tissue

- Heat wax in mold – do not pour to minimize cooling
- Transfer larvae to mold with wide-cut pipettes and position with heated forceps. Speed is of the essence!
- Cool overnight – do not attempt to speed-cool in a freezer

Appendix D.4 – Antibody staining on paraffin sections (with DAB)

Adapted from Reed Lab (UIC) protocol

Day 1: Deparafinnizing and preparing for primary antibody incubation

Deparaffinizing: 1 hour

	Xylene – 15 minutes
	100% EtOH – 5 minutes
	70% EtOH – 5 minutes
	50% EtOH – 5 minutes
	30% EtOH – 5 minutes
	1X PBS – 15 minutes

Sodium borohydride – 2 x 30 minutes - MAKE FRESH, IT WILL START TO BUBBLE

- 1X PBS – 15 mL
- NaBH4 – 0.075 grams

Citrate buffer – 10 min heated, 30 min RT

1.05 grams citric acid → 500 mL ddH2O → adjust to pH=6 using NaOH

	Preheat tap water to a boil for 6 min in the microwave
	Place on hot plate and bring to boil
	Fill PLASTIC mailer with 0.01 M citrate buffer
	Take boiling water off heat source; place PLASTIC mailer in boiling water
	Allow to cool to RT for 30 minutes

Triton wash – 3 x 5 minutes

0.5% v/v Triton-X100 in PBS. Slightly warm PBS before adding Triton. Cut pipette tip off and eject pipette tip right into the PBS.

	Wash in the mailer

MeOH wash – 3 minutes

	Fill mailer with -20C MeOH, then place slides into MeOH

Serum blocking – 1 hour

5% serum blocking solution – 1X PBS (19 mL), 1 mL animal serum

	Fill mailer with blocking solution, transfer slide right from MeOH into blocking solution

Primary antibody – overnight

Antibody used and dilution in blocking solution: _____

	Transfer slides to hydrator, wipe off excess solution around tissue
	Pipette 100 uL antibody solution onto slide
	Cover each slide with a slip of parafilm
	Cover hydrator and place into 4C overnight

Day 2: Washes and preparation for secondary antibody

Triton wash – 3 x 5 minutes

	Wash in the mailer

PBT wash – 2 x 5 minutes

	Wash in the mailer

Serum blocking – 1 hour

5% serum blocking solution – 1X PBS (19 mL), 1 mL animal serum

	Fill mailer with blocking solution, transfer slide right from MeOH into blocking solution

Secondary antibody with HRP* – overnight

Antibody used and dilution in blocking solution: _____

	Transfer slides to hydrator, wipe off excess solution around tissue
	Pipette 100 uL antibody solution onto slide
	Cover each slide with a slip of parafilm
	Cover hydrator and place into 4C overnight

*If skipping DAB, then just use a normal fluorescent secondary antibody.

Day 3: Washes and preparation for DAB staining

Triton wash – 3 x 5 minutes

	Wash in the mailer

ddH2O wash – 2 x 5 minutes

	Wash in the mailer

DAB staining – using DAB substrate kit (Vector Labs, SK-4100)

For 5 mL in ddH2O: (only need 2.5 mL for 10 slides)

- 2 drops of Buffer Stock Solution
- 4 drops of DAB Stock Solution
- 2 drops of Hydrogen Peroxide Solution

ddH2O wash – 2 x 5 minutes

	Wash in the POST DAB mailers (glass)

Dehydrate into 100% EtOH (use POST DAB mailers) – 5 minutes each

	70% EtOH
	95% EtOH
	100% EtOH
	100% EtOH

Histosol – 2 x 5 minutes; mount with permount

Appendix D.5 – Antibody staining on larval whole mounts with DAB

	Permeabilize specimens with ice-cold acetone, 10 minutes
	OR: Permeabilize specimens with Pro-K treatment Record concentration and time:
	Rinse in PBT (3X) – some protocols call for PBT with 1% DMSO
	Incubate specimens in blocking solution for 2 hours RT
	Remove blocking solution and incubate specimens in Primary Antibody 4C, several days! Primary antibody: _____ Dilution: _____ (in blocking solution) Time: _____ note that overnight is fine for embryos
	Remove and save Primary Antibody, store at -20C
	Wash 10 min with PBT (5X)
	Block for 1 hour with blocking solution
	Incubate specimens with Secondary Antibody* (conjugated with HRP!) for 2 hours at room temperature, or 4C overnight
	Incubate with DAB kit (Vector Labs, SK-4100) – move into glass tubes/vials
	Wash with H2O (10 minutes) – 3 X, careful that the fish get sticky ☹
	Fix for 30 min in 4% PFA
	Rinse with PBT (3X)
	Store embryos in 100% or 80% Glycerol. OR- dehydrate into 70% EtOH if intended for embedding later.

*If skipping DAB, then just use a normal fluorescent secondary antibody.

Appendix D.6 – Hematoxylin and Eosin Staining for Paraffin Sections

Adapted from K. Criswell

Rehydration: (total time = 30 minutes)

1. Histosol (10 min)
2. 2 x 100% EtOH (2min)
3. 70% EtOH (2min)
4. 50% EtOH (2min)
5. 30% EtOH (2min)
6. 2 x ddHOH (2min)

Staining: (total time = 10 minutes)

7. Hematoxylin - Vector (<1 min)
8. 2 x ddHOH (2 min)
9. 95% EtOH (2min)
10. 95% EtOH (2min)
11. Eosin Y (1:15 min)

Dehydration and mounting: (total time = 20 minutes before mounting)

12. 95% EtOH (2min)
13. 95% EtOH (2min)
14. 100% EtOH (2min)
15. 100% EtOH (2min)
16. Histosol (5min)
17. Histosol (5min)
18. Mount with permount

Eosin Y solution: 0.1% (w/v) solution in 95% ethanol (so 0.1g of Eosin powder in 100mL of 95% ethanol, scaled up to whatever volume you need)

Alcian blue: 7 parts 100% EtOH plus 3 parts acetic acid, scale up to desired volume. Add 2 mg/mL of Alcian blue.

Appendix D.7 – Probes for *in situ* hybridization from plasmid

Linearize Plasmids: (from mini-prepped DNA)

Probe Name			
Concentration			
2.5 uL buffer			
1 ul restriction enzyme			
2.5 uL BSA			
1-3 ug plasmid			
H2O up to 25 uL			

1. Make tube using table above (total 25 uL)
2. Digest in 37C water bath for 2-4 hours
3. Run gel (uncut, cut) – load _____ uL sample with _____ uL loading dye

Gel image here:

Ethanol Precipitation:

1. Add 0.1 volumes of 3M NaOAc and mix

If 20 uL linearized plasmid, then:

- 2 uL NaOAc
- 12 uL isopropanol

2. Add 0.6 volumes of isopropanol at room temperature and mix
3. Let mixture stand on a rack at room temperature for 20 min or overnight at 4C
4. Spin at 4ºC 14,000rpm for 15 minutes
5. Carefully remove supernatant and rinse pellet with 0.1 ml 70% EtOH
6. Spin 4ºC 14,000 rpm for 5 minutes
7. Carefully remove supernatant and air-dry pellet for 10-30 minutes
8. Suspend pellet in DNase/RNase-free water to a concentration of 0.5 – 1 µg/µl

Probe Name	**Nanodrop Concentration**

RNA Probe Transcription:

Combine:

Component	**For 1 µg of DNA**	**For 3 µg of DNA**
Plasmid DNA	2 µl	4 µl
Water	13 µl	20 µl
5x Transcription Buffer	6 µl	10 µl
DTT (10X) (100mM)	3 µl	5 µl
DIG RNA Labeling Mix	2 µl	5 µl
RNAsin	2 µl	2 µl
RNA Polymerase Enzyme	2 µl	4 µl
Total	30 µl	50 µl

1. Transcribe for 2 – 4 hours. Note: T7 and T3 at 37ºC, SP6 at 40ºC

Time in: _____ Time out: _____

2. Add 1 µl DNase into reaction and incubate for 15-30 minutes at 37ºC
3. Proceed with probe purification using lithium chloride

Probe Purification (Lithium Chloride):

1. Add 20 µl of RNase-free water to the reaction mixture.
2. Add 25 µl of LiCl precipitation solution from Ambien.
3. Mix and Chill at -20°C for 30 minutes up to overnight.
4. Spin at 4°C 14,000rpm for 15 minutes.
5. Carefully remove supernatant and rinse pellet with 0.1 ml 70% EtOH.
6. Spin 4°C 14,000 rpm for 5 minutes.
7. Carefully remove supernatant and air-dry pellet for 10-30 minutes. DO NOT OVERDRY, otherwise the pellet will not re-suspend.
8. Add 100 µl of DNase/RNase-free water to the pellet. Vortex to fully suspend.
9. Add 1 µl of RNAsin to protect RNA.
10. Run 3µl on a 1% agarose gel, 120V for 30 minutes to check RNA integrity.
11. Store at -20°C.

Gel image here:

Appendix D.8 – Primer design procedure

Ensemble.org → cDNA sequence

a) Search for gene
b) "Show Transcript Data" button
c) Sidebar > cDNA
d) Copy FASTA – just get cDNA (check)

Primer3Web

a) Paste in FASTA
b) Size – 18; opt 20; max 20
c) Tm – 55; 57; 59
d) Size range – 400 to 1000 bp
e) Pick primers

IDT OligoAnalyzer 3.1 – check for hairpins

a) Paste in primer sequence
b) Tm below 40C is okay
c) T7 seq TAATACGACTCACTATAGgg + reverse primer → check Tm
d) Use two primer pairs for safety. Overlapping is good to get more coverage.

Appendix D.9 – PCR workflow (best for probes)

	Single 50 uL reaction	Multiplier X _____	Total volumes
H2O	36 uL		
Buffer	5 uL		
Forward Primer	2 uL	**X**	**X**
Reverse Primer	2 uL	**X**	**X**
2.5 mM dNTPs	4 uL		
Taq	0.5 uL		
Template (if the same for all)	0.5 uL		

Master Mix
Don't forget negative control!
Add _____ uL of master mix into each tube + primers

PCR settings

1. 94C, 30s
2. 94C, 30s
3. _____ C, 60s (should be set to annealing temperature)
4. 68C, 60s

   Steps 2-4 run for 45x

5. 68C, 10m
6. 12C forever

Appendix D.10 – RNA probe transcription & purification from PCR product

Gene Name	Volume of DNA	Remaining H2O

Transcription master mix

	Amount	X _____
DNA	~300 ng	X
Water	15 ul - # uL of DNA	X
5X Buffer	6 uL	
DTT (10X) (100 nM)	3 uL	
RNA labeling mix (DIG or FITC)	2 uL	
RNAsin	2 uL	
RNA polymerase (T7 or SP6)	2 uL	
	Total = 30 uL	

Amount of Master Mix into each tube: _____
Chapter 1 Transcribe for 4 hours (or longer). Note: T3 and T7 at 37C, SP6 at 40C.

Start time: _____ End time: _____

Chapter 2 Add 1 uL DNase into the reaction. Incubate for 15-30 min at 37 C.

Probe purification, Day 1:

Chapter 3 Add 20 uL of RNase-free water to the reaction mixture
Chapter 4 Add 25 uL of LiCl precipitation solution from Ambien
Chapter 5 Mix and chill at -20C overnight, or -80C if desperate!

Probe purification, Day 2:
Chapter 6 Spin at 4C for 15 min @ 14,000 rpm.
Chapter 7 Remove supernatant and rinse pellet with 250 uL 70% EtOH
Chapter 8 Spin 4C for 5 min.
Chapter 9 Carefully remove supernatant and air-dry pellet for 10-30 min.
Chapter 10 Add 50 uL of DNase/RNase-free water to the pellet. Vortex to fully suspend. Drop in 37C water bath for few min if stubborn.

Check on gel, paste image below:

Nanodrop concentration: _____

Appendix D.11 - Solutions

Blocking Solution

- 1 mL 10X PBS
- 100 uL DMSO
- 10 uL BSA
- 1 mL goat serum
- 50 uL Triton-X
- Top up to 10 mL

PBT: 0.1% Tween in PBS
SSC: 20X stock solution (3M NaCl, 0.3M trisodium citrate). Add 1% Tween for SSCT.

Hybridization Mix ("Hyb"): Store at -20C. For 50 mL aliquots,

- 32.5 mL Formamide
- 12.5 mL 20X SSC
- 50 uL Heparin (50 mg/mL)
- 250 uL 20% Tween
- 920 uL 0.5M citric acid
- Top up to 50 mL with ddH2O

Pre-Incubation Buffer ("PI Buffer"): Store at -20C. For 50 mL aliquots,

- 1 mL goat serum
- 100 mg BSA powder
- Top up to 50 mL with PBT

AP Buffer – For 10 mL aliquots,

- 500 uL 2M Tris HCl, pH 9.5
- 500 uL 1M MgCl2
- 200 uL 5M NaCl
- 50 uL 20% Tween-20
- 8.750 mL ddH2O

Solution X/Clearing Solution

- 50% formamide, 2X SSC, 1% SDS

REFERENCES

Abe, G., Ide, H., & Tamura, K. (2007). Function of FGF signaling in the developmental process of the median fin fold in zebrafish. *Developmental Biology*, *304*(1), 355–366. https://doi.org/10.1016/j.ydbio.2006.12.040

Adams, D. C., & Otárola-Castillo, E. (2013). Geomorph: An r package for the collection and analysis of geometric morphometric shape data. *Methods in Ecology and Evolution*, *4*(4), 393–399. https://doi.org/10.1111/2041-210X.12035

Adrain, J. M., & Wilson, M. V. H. (1994). Early Devonian cephalaspids (Vertebrata: Osteostraci: Cornuata) from the southern MacKenzie Mountains, N.W.T., Canada. *Journal of Vertebrate Paleontology*, *14*(3), 301–319. https://doi.org/10.1080/02724634.1994.10011561

Agarwal, P., Wylie, J. N., Galceran, J., Arkhitko, O., Li, C., Deng, C., … Bruneau, B. G. (2003). Tbx5 is essential for forelimb bud initiation following patterning of the limb field in the mouse embryo. *Development (Cambridge, England)*, *130*(3), 623–633. https://doi.org/10.1242/DEV.00191

Agulnik, S. I., Garvey, N., Hancock, S., Ruvinsky, I., Chapman, D. L., Agulnik, I., … Silver, L. M. (1996). Evolution of Mouse T-box Genes by Tandem Duplication and Cluster Dispersion. *Genetics*, *144*(1).

Ahn, Dae-gwon, Kourakis, M. J., Rohde, L. A., Silver, L. M., & Ho, R. K. (2002). T-box gene tbx5 is essential for formation of the pectoral limb bud. *Nature*, *417*(6890), 754–758. https://doi.org/10.1038/nature00814

Ahn, Daegwon, & Ho, R. K. (2008). Tri-phasic expression of posterior Hox genes during development of pectoral fins in zebrafish: Implications for the evolution of vertebrate paired appendages. *Developmental Biology*, *322*(1), 220–233. https://doi.org/10.1016/j.ydbio.2008.06.032

Aiello, B. R., King, H. M., & Hale, M. E. (2014). Functional subdivision of fin protractor and retractor muscles underlies pelvic fin walking in the African lungfish Protopterus annectens. *Journal of Experimental Biology*, *217*(19), 3474–3482. https://doi.org/10.1242/jeb.105262

Alaska Seafood Marketing Institute. (2022). Coho Salmon. Retrieved June 24, 2022, from https://www.alaskaseafood.org/species/coho-salmon/

Alexander, R. (1974). Functional design of fishes.

Aman, A. J., Kim, M., Saunders, L. M., & Parichy, D. M. (2021). Thyroid hormone regulates

abrupt skin morphogenesis during zebrafish postembryonic development. *Developmental Biology*, *477*, 205–218. https://doi.org/10.1016/J.YDBIO.2021.05.019

Amores, A., Force, A., Yan, Y. L., Joly, L., Amemiya, C., Fritz, A., … Postlethwait, J. H. (1998). Zebrafish hox clusters and vertebrate genome evolution. *Science*, *282*(5394), 1711–1714. https://doi.org/10.1126/SCIENCE.282.5394.1711/SUPPL_FILE/983268.XHTML

Arratia, G. (2000). Remarkable teleostean fishes from the Late Jurassic of southern Germany and their phylogenetic relationships. *Fossil Record*, *3*(1), 137–179. https://doi.org/10.1002/MMNG.20000030108

Asleh, M. A., Zaher, M., Jadon, J., Shaulov, L., Yelin, R., & Schultheiss, T. M. (2022). A Morphogenetic Wave that Generates Mesenchymal-to-Epithelial Transition in the Lateral Plate Mesoderm. *BioRxiv*, 2022.03.01.482468. https://doi.org/10.1101/2022.03.01.482468

Balfour, F. M. (1881). On the Dedopment of the Skeleton of the Paired Fins of Elasmobranchii, considered in Relation to its Bearings on the Nature of the Limbs of the Vertebrata. *Proceedings of the Zoological Society of London*, *49*(3), 656–670. https://doi.org/10.1111/j.1096-3642.1881.tb01323.x

Ballard, W. W., & Needham, R. G. (1964). Normal embryonic stages of Polyodon spathula (Walbaum). *Journal of Morphology*, *114*(3), 465–477. https://doi.org/10.1002/jmor.1051140307

Ballard, William W. (1986). Stages and rates of normal development in the holostean fish, Amia calva. *Journal of Experimental Zoology*, *238*(3), 337–354. https://doi.org/10.1002/jez.1402380308

Bartsch, P., Gemballa, S., & Piotrowskil, T. (1997). The embryonic and larval development of Polypterus senegalus Cuvier, 1829: its staging with reference to external and skeletal features, behaviour and locomotory habits. *Acta Zoologica*, *78*(4), 309–328. https://doi.org/10.1111/j.1463-6395.1997.tb01014.x

Bemis, W. E., & Grande, L. (1992). Early development of the actinopterygian head. I. External development and staging of the paddlefish Polyodon spathula. *Journal of Morphology*, *213*(1), 47–83. https://doi.org/10.1002/JMOR.1052130106

Berger, J., & Currie, P. D. (2013). 503unc, a small and muscle-specific zebrafish promoter. *Genesis (New York, N.Y. : 2000)*, *51*(6), 443–447. https://doi.org/10.1002/DVG.22385

Betancur-R, R., Wiley, E. O., Arratia, G., Acero, A., Bailly, N., Miya, M., … Ortí, G. (2017).

Phylogenetic classification of bony fishes. *BMC Evolutionary Biology*, *17*(1), 162. https://doi.org/10.1186/s12862-017-0958-3

Bio-Atlas - Zebrafish Atlas. (2013). Retrieved June 22, 2022, from https://bio-atlas.psu.edu/about.php#citing

Blake, R. W. (2004). Fish functional design and swimming performance. *Journal of Fish Biology*, *65*(5), 1193–1222. https://doi.org/10.1111/J.0022-1112.2004.00568.X

Blom, H., & Journal, S. (2008). A New Anaspid Fish from the Middle Silurian Cowie Harbour Fish Bed of Stonehaven , Scotland, *28*(3), 594–600.

Boyle-Anderson, E. A. T., Mao, Q., & Ho, R. K. (2022). Tbx5a and Tbx5b paralogues act in combination to control separate vectors of migration in the fin field of zebrafish. *Developmental Biology*, *481*(October 2021), 201–214. https://doi.org/10.1016/j.ydbio.2021.10.008

Boyle Anderson, E. A. T., & Ho, R. K. (2018). A transcriptomics analysis of the Tbx5 paralogues in zebrafish. *PLOS ONE*, *13*(12), e0208766. https://doi.org/10.1371/JOURNAL.PONE.0208766

Brazeau, M. D., & Friedman, M. (2015). The origin and early phylogenetic history of jawed vertebrates, (Box 1). https://doi.org/10.1038/nature14438

Brittanica. (n.d.). batfish | fish. Retrieved June 24, 2022, from https://www.britannica.com/animal/batfish

Brown, D. D. (1997). The role of thyroid hormone in zebrafish and axolotl development. *Developmental Biology*, *94*, 13011–13016. Retrieved from http://www.pnas.org/content/pnas/94/24/13011.full.pdf

Budi, E. H., Patterson, L. B., & Parichy, D. M. (2011). Post-Embryonic Nerve-Associated Precursors to Adult Pigment Cells: Genetic Requirements and Dynamics of Morphogenesis and Differentiation. *PLOS Genetics*, *7*(5), e1002044. https://doi.org/10.1371/JOURNAL.PGEN.1002044

Burke, A. C., Nelson, C. E., Morgan, B. A., & Tabin, C. (1995). Hox genes and the evolution of vertebrate axial morphology. *Development*, *121*(2), 333–346. https://doi.org/10.1242/dev.121.2.333

Burke, A. C., & Nowicki, J. L. (2003). A new view of patterning domains in the vertebrate mesoderm. *Developmental Cell*, *4*(2), 159–165. https://doi.org/10.1016/S1534-

5807(03)00033-9

Carroll, S. B. (2001). Chance and necessity: the evolution of morphological complexity and diversity. *Nature 2001 409:6823*, *409*(6823), 1102–1109. https://doi.org/10.1038/35059227

Chan, Y. F., Marks, M. E., Jones, F. C., Villarreal, G., Shapiro, M. D., Brady, S. D., … Kingsley, D. M. (2010). Adaptive evolution of pelvic reduction in sticklebacks by recurrent deletion of a Pitx1 enhancer. *Science (New York, N.Y.)*, *327*(5963), 302–305. https://doi.org/10.1126/science.1182213

Chang, J., Wang, M., Gui, W., Zhao, Y., Yu, L., & Zhu, G. (2012). Changes in Thyroid Hormone Levels during Zebrafish Development. *Zoological Society of Japan ZOOLOGICAL SCIENCE*, *29*, 181–184. https://doi.org/10.2108/zsj.29.181

Chen, J., Liu, X., Yao, X., Gao, F., & Bao, B. (2017). Dorsal fin development in flounder, Paralichthys olivaceus: Bud formation and its cellular origin. *Gene Expression Patterns*, *25–26*, 22–28. https://doi.org/10.1016/j.gep.2017.04.003

Chimal-Monroy, J., Rodriguez-Leon, J., Montero, J. A., Gañan, Y., Macias, D., Merino, R., & Hurle, J. M. (2003). Analysis of the molecular cascade responsible for mesodermal limb chondrogenesis: sox genes and BMP signaling. *Developmental Biology*, *257*(2), 292–301. https://doi.org/10.1016/S0012-1606(03)00066-6

Clack, J. A. (2009). The fin to limb transition: New data, interpretations, and hypotheses from paleontology and developmental biology. *Annual Review of Earth and Planetary Sciences*, *37*, 163–179. https://doi.org/10.1146/annurev.earth.36.031207.124146

Coates, M. I. (1994). The origin of vertebrate limbs. *Development*, *1994*(Supplement), 169–180.

Coates, M. I. (2003). The evolution of paired fins. *Theory in Biosciences*, *122*(2–3), 266–287. https://doi.org/10.1078/1431-7613-00087

Coates, M. I., & Cohn, M. J. (1998). Fins, limbs, and tails: outgrowths and axial patterning in vertebrate evolution. *BioEssays*, *20*, 371–381.

Cohn, M. J., Izpisúa-Belmonte, J. C., Abud, H., Heath, J. K., & Tickle, C. (1995). Fibroblast growth factors induce additional limb development from the flank of chick embryos. *Cell*, *80*(5), 739–746. https://doi.org/10.1016/0092-8674(95)90352-6

Cole, N. J., Hall, T. E., Don, E. K., Berger, S., Boisvert, C. A., Neyt, C., … Currie, P. D. (2011). Development and evolution of the muscles of the pelvic fin. *PLoS Biology*, *9*(10), 16–18. https://doi.org/10.1371/journal.pbio.1001168

Cole, N. J., Tanaka, M., Prescott, A., & Tickle, C. (2003). Expression of limb initiation genes and clues to the morphological diversification of threespine stickleback. *Current Biology*, *13*(24), 951–952. https://doi.org/10.1016/j.cub.2003.11.039

Cooper, M. S., & Virta, V. C. (2007). Evolution of gastrulation in the ray-finned (actinopterygian) fishes. *Journal of Experimental Zoology Part B: Molecular and Developmental Evolution*, *308*(5), 591–608. https://doi.org/10.1002/JEZ.B.21142

Cunningham, T. J., Zhao, X., Sandell, L. L., Evans, S. M., Trainor, P. A., & Duester, G. (2013). Antagonism between Retinoic Acid and Fibroblast Growth Factor Signaling during Limb Development. *Cell Reports*, *3*(5), 1503–1511. https://doi.org/10.1016/J.CELREP.2013.03.036

Davis, M. C., Shubin, N. H., & Force, A. (2004). Pectoral fin and girdle development in the basal actinopterygians polyodon spathula and Acipenser transmontanus. *Journal of Morphology*, *262*(2), 608–628. https://doi.org/10.1002/jmor.10264

De Pinna, M. C. (1996). Teleostean Monophyly. In *Interrelationships of Fishes* (pp. 147–162).

Dickson, B., & Pierce, S. (2018). How (and why) fins turn into limbs: insights from anglerfish. *Earth and Environmental Science Transactions of the Royal Society of Edinburgh*, *109*(1–2), 87–103.

Draper, B. W., Stock, D. W., & Kimmel, C. B. (2003). Zebrafish fgf24 functions with fgf8 to promote posterior mesodermal development. *Development*, *130*(19), 4639–4654. https://doi.org/10.1242/DEV.00671

Drucker, E. G., & Lauder, G. V. (2002). Wake Dynamics and Locomotor Function in Fishes: Interpreting Evolutionary Patterns in Pectoral Fin Design. *Integrative and Comparative Biology*, *42*(5), 997–1008. https://doi.org/10.1093/icb/42.5.997

Drucker, Eliot G., & Lauder, G. V. (2001). Locomotor function of the dorsal fin in teleost fishes: Experimental analysis of wake forces in sunfish. *Journal of Experimental Biology*, *204*(17), 2943–2958. https://doi.org/10.1242/jeb.204.17.2943

Du, T. Y., Tissandier, S. C., & Larsson, H. C. E. (2019). Integration and modularity of teleostean pectoral fin shape and its role in the diversification of acanthomorph fishes. *Evolution*, *73*(2), 401–411. https://doi.org/10.1111/evo.13669

Esteves de Lima, J., Blavet, C., Bonnin, M. A., Hirsinger, E., Comai, G., Yvernogeau, L., … Duprez, D. (2021). Unexpected contribution of fibroblasts to muscle lineage as a

mechanism for limb muscle patterning. *Nature Communications*, *12*(1). https://doi.org/10.1038/s41467-021-24157-x

Feilich, K. L. (2016). Correlated evolution of body and fin morphology in the cichlid fishes. *Evolution*, *70*(10), 2247–2267. https://doi.org/10.1111/EVO.13021

Felsenstein, J. (1985). Phylogenies and the comparative method. *The American Naturalist*, *125*(1), 1–15.

Fishbio. (2014). The yellowfin goby: unusual, but only a little. Retrieved June 24, 2022, from https://fishbio.com/unusual-but-only-a-little/

Fox, C. H., Gibb, A. C., Summers, A. P., & Bemis, W. E. (2018). Benthic walking, bounding, and maneuvering in flatfishes (Pleuronectiformes: Pleuronectidae): New vertebrate gaits. *Zoology*, *130*, 19–29. https://doi.org/10.1016/J.ZOOL.2018.07.002

Freitas, R., Zhang, G. J., & Cohn, M. J. (2006). Evidence that mechanisms of fin development evolved in the midline of early vertebrates. *Nature*, *442*(7106), 1033–1037. https://doi.org/10.1038/nature04984

Friedman, S. T., Price, S. A., Corn, K. A., Larouche, O., Martinez, C. M., & Wainwright, P. C. (2020). Body shape diversification along the benthic – pelagic axis in marine fishes.

Friedman, S. T., Price, S. A., & Wainwright, P. C. (2021). The Effect of Locomotion Mode on Body Shape Evolution in Teleost Fishes. *Integrative Organismal Biology*, *3*(1). https://doi.org/10.1093/iob/obab016

Fujimura, K., & Okada, N. (2007). Development of the embryo, larva and early juvenile of Nile tilapia Oreochromis niloticus (Pisces: Cichlidae). Developmental staging system. *Development Growth and Differentiation*, *49*(4), 301–324. https://doi.org/10.1111/j.1440-169X.2007.00926.x

Funayama, N., Sato, Y., Matsumoto, K., Ogura, T., & Takahashi, Y. (1999). Coelom formation: Binary decision of the lateral plate mesoderm is controlled by the ectoderm. *Development*, *126*(18), 4129–4138. https://doi.org/10.1242/dev.126.18.4129

Garrity, D. M., Childs, S., & Fishman, M. C. (2002). Zebrafish heartstrings mutant is tbx5. *Development*, *129*, 4635–4645. Retrieved from http://dev.biologists.org/content/develop/129/19/4635.full.pdf

Gays, D., Hess, C., Camporeale, A., Ala, U., Provero, P., Mosimann, C., & Santoro, M. M. (2017). An exclusive cellular and molecular network governs intestinal smooth muscle cell

differentiation in vertebrates, 464–478. https://doi.org/10.1242/dev.133926

Gegenbauer, C. (1878). No Title. In *Elements of Comparative Anatomy*. London: Macmilan and Co.

Gegenbaur, C. (1876). Zur Morphologie der Gliedmaassen der Wirbelthiere.

George, A. B., & Westneat, M. W. (2021). Fin Shape, Asymmetry, and Evolutionary Ecomorphology in Triggerfishes and Filefishes (Superfamily: Balistoidea). *BioRxiv*, 2021.06.29.450391. https://doi.org/10.1101/2021.06.29.450391

Ghezelayagh, A., Harrington, R. C., Burress, E. D., Campbell, M. A., Buckner, J. C., Chakrabarty, P., … Near, T. J. (2021). Prolonged morphological expansion of spiny-rayed fishes following the end-Cretaceous. *BioRxiv*, 2021.07.12.452083. https://doi.org/10.1101/2021.07.12.452083

Gilbert, S. (2000). *Developmental Biology* (6th editio). Sunderland, MA: Sinauer Associates.

Gill, E. L. (1925). XXXI.—The Permian Fish Dorypterus. *Earth and Environmental Science Transactions of The Royal Society of Edinburgh*, *53*(3), 643–661. https://doi.org/10.1017/S0080456800027526

Gillis, J. A., Dahn, R. D., & Shubin, N. H. (2009). Shared developmental mechanisms pattern the vertebrate gill arch and paired fin skeletons. *Proceedings of the National Academy of Sciences*, *106*(14), 5720–5724. https://doi.org/10.1073/pnas.0810959106

Glasauer, S. M. K., & Neuhauss, S. C. F. (2014). Whole-genome duplication in teleost fishes and its evolutionary consequences. *Molecular Genetics and Genomics*, *289*(6), 1045–1060. https://doi.org/10.1007/s00438-014-0889-2

Goswami, A., & Polly, P. D. (2010). The Influence of Modularity on Cranial Morphological Disparity in Carnivora and Primates (Mammalia). *PLOS ONE*, *5*(3), e9517. https://doi.org/10.1371/JOURNAL.PONE.0009517

Gould, S. J., & Eldredge, N. (1972). Puncutated equilibria: an alternative to phyletic gradualism. *Models in Paleobiology*, *1972*, 82–115.

Grandel, H., & Brand, M. (2011). Zebrafish limb development is triggered by a retinoic acid signal during gastrulation. *Developmental Dynamics*, *240*(5), 1116–1126. https://doi.org/10.1002/DVDY.22461

Grandel, H., & Schulte-Merker, S. (1998). The development of the paired fins in the zebrafish (Danio rerio). *Mechanisms of Development*, *79*(1–2), 99–120.

https://doi.org/10.1016/S0925-4773(98)00176-2

Gros, J., & Tabin, C. J. (2014). Vertebrate limb bud formation is initiated by localized epithelial-to-mesenchymal transition. *Science*, *343*(6176), 1253–1256. https://doi.org/10.1126/science.1248228

Haber, A. (2016). Phenotypic covariation and morphological diversification in the ruminant skull. *American Naturalist*, *187*(5), 576–591. https://doi.org/10.1086/685811/ASSET/IMAGES/LARGE/FG12.JPEG

Hancock, A., & Howse, R. (1870). On Dorypterus Hoffmanni, Germar, from the Marl-slate fo Midderidge, Durham. *Quarterly Journal of the Geological Society*, *26*(1–2), 623–641. https://doi.org/10.1144/GSL.JGS.1870.026.01-02.58

Hans, S., Zöller, D., Hammer, J., Stucke, J., Spieß, S., Kesavan, G., … Brand, M. (2021). Cre-Controlled CRISPR mutagenesis provides fast and easy conditional gene inactivation in zebrafish. *Nature Communications 2021 12:1*, *12*(1), 1–12. https://doi.org/10.1038/s41467-021-21427-6

Harris, J. E. (1938). The role of the fins in the equilibrium of the swimming fish II. The role of the pelvic fins. *The Journal of Experimental Biology*, *15*(1866), 32–47.

Höch, R., Schneider, R. F., Kickuth, A., Meyer, A., & Woltering, J. M. (2021). Spiny and soft-rayed fin domains in acanthomorph fish are established through a BMP-gremlin-shh signaling network. *Proceedings of the National Academy of Sciences of the United States of America*, *118*(29), 1–8. https://doi.org/10.1073/pnas.2101783118

Hurley, I., Hale, M. E., & Prince, V. E. (2005). Duplication events and the evolution of segmental identity. *Evolution & Development*, *7*(6), 556–567. https://doi.org/10.1111/J.1525-142X.2005.05059.X

Hutchings Museum Institute. (2022). Atlantic Mudskipper Facts and Info. Retrieved June 24, 2022, from https://johnhutchingsmuseum.org/atlantic-mudskipper/

Infante, C. R., Park, S., Mihala, A. G., Kingsley, D. M., & Menke, D. B. (2013). Pitx1 broadly associates with limb enhancers and is enriched on hindlimb cis-regulatory elements. *Developmental Biology*, *374*(1), 234–244. https://doi.org/10.1016/J.YDBIO.2012.11.017

Jain, D., Nemec, S., Luxey, M., Gauthier, Y., Bemmo, A., Balsalobre, A., & Drouin, J. (2018). Regulatory integration of Hox factor activity with Tbox factors in limb development. *Development*, (February), dev.159830. https://doi.org/10.1242/dev.159830

Johnson, G. D. (1992). Monophyly of the Euteleostean Clades : Neoteleostei , Eurypterygii , and Ctenosquamata Author (s): G . David Johnson Published by : American Society of Ichthyologists and Herpetologists (ASIH) Stable URL : https://www.jstor.org/stable/1446531 Monophyl, *1992*(1), 8–25.

Kaneko, H., Nakatani, Y., Fujimura, K., & Tanaka, M. (2014). Development of the lateral plate mesoderm in medaka Oryzias latipes and Nile tilapia Oreochromis niloticus: Insight into the diversification of pelvic fin position. *Journal of Anatomy*, *225*(6), 659–674. https://doi.org/10.1111/joa.12244

Kanki, J. P., & Ho, R. K. (1997). The development of the posterior body in zebrafish. *Development*, *124*(4), 881–893. https://doi.org/10.1242/dev.124.4.881

Kawano, S. M., & Blob, R. W. (2013). Propulsive Forces of Mudskipper Fins and Salamander Limbs during Terrestrial Locomotion: Implications for the Invasion of Land. *Integrative and Comparative Biology*, *53*(2), 283–294. https://doi.org/10.1093/ICB/ICT051

Kikuchi, K., Holdway, J. E., Major, R. J., Blum, N., Dahn, R. D., Begemann, G., & Poss, K. D. (2011). Retinoic acid production by endocardium and epicardium is an injury response essential for zebrafish heart regeneration. *Developmental Cell*, *20*(3), 397–404. https://doi.org/10.1016/J.DEVCEL.2011.01.010

Klug, C., Kröger, B., Kiessling, W., Mullins, G. L., Servais, T., Frýda, J., … Turner, S. (2010). The Devonian nekton revolution. *Lethaia*, *43*(4), 465–477. https://doi.org/10.1111/J.1502-3931.2009.00206.X

Kucenas, S., Takada, N., Park, H. C., Woodruff, E., Broadie, K., & Appel, B. (2008). CNS-derived glia ensheath peripheral nerves and mediate motor root development. *Nature Neuroscience 2007 11:2*, *11*(2), 143–151. https://doi.org/10.1038/nn2025

Kwan, K. M., Fujimoto, E., Grabher, C., Mangum, B. D., Hardy, M. E., Campbell, D. S., … Chien, C.-B. (2007). The Tol2kit: A Multisite Gateway-Based Construction Kit for Tol2 Transposon Transgenesis Constructs. https://doi.org/10.1002/dvdy.21343

Lanctôt, C., Lamolet, B., & Drouin, J. (1997). The bicoid-related homeoprotein Ptx1 defines the most anterior domain of the embryo and differentiates posterior from anterior lateral mesoderm. *Development (Cambridge, England)*, *124*(14), 2807–2817. Retrieved from http://www.ncbi.nlm.nih.gov/pubmed/9226452

Larouche, O., Benton, B., Corn, K. A., Friedman, S. T., Gross, D., Iwan, M., … Price, S. A.

(2020). Reef-associated fishes have more maneuverable body shapes at a macroevolutionary scale. *Coral Reefs*, *39*(5), 1427–1439. https://doi.org/10.1007/S00338-020-01976-W/TABLES/5

Larouche, O., Zelditch, M. L., & Cloutier, R. (2017). Fin modules: An evolutionary perspective on appendage disparity in basal vertebrates. *BMC Biology*, *15*(1), 1–26. https://doi.org/10.1186/s12915-017-0370-x

Larouche, O., Zelditch, M. L., & Cloutier, R. (2018). Modularity promotes morphological divergence in ray-finned fishes. *Scientific Reports*, *8*(1), 7278. https://doi.org/10.1038/s41598-018-25715-y

Lauder, G. V. (1982). Patterns of Evolution in the Feeding Mechanism of Actinopterygian Fishes. *Integrative and Comparative Biology*, *22*(2), 275–285. https://doi.org/10.1093/ICB/22.2.275

Lauder, G. V. (1989). Caudal Fin Locomotion in Ray-finned Fishes: Historical and Functional Analyses. *Integrative and Comparative Biology*, *29*(1), 85–102. https://doi.org/10.1093/ICB/29.1.85

Lee, R. T. H., Knapik, E. W., Thiery, J. P., & Carney, T. J. (2013). An exclusively mesodermal origin of fin mesenchyme demonstrates that zebrafish trunk neural crest does not generate ectomesenchyme, *2932*, 2923–2932. https://doi.org/10.1242/dev.093534

Lee, R. T. H., Thiery, J. P., & Carney, T. J. (2013). Dermal fin rays and scales derive from mesoderm, not neural crest. *Current Biology*, *23*(9), R336–R337. https://doi.org/10.1016/j.cub.2013.02.055

Liu, Y.-W., Chan, W.-K., Liu, Y.-W., Chan, ¡ W-K, & Chan, W.-K. (2002). Thyroid hormones are important for embryonic to larval transitory phase in zebrafish. *Differentiation*, *70*, 36–45. Retrieved from http://citeseerx.ist.psu.edu/viewdoc/download?doi=10.1.1.658.6859&rep=rep1&type=pdf

Logan, M., Simon, H. G., & Tabin, C. (1998). Differential regulation of T-box and homeobox transcription factors suggests roles in controlling chick limb-type identity. *Development (Cambridge, England)*, *125*(15), 2825–2835. Retrieved from http://eutils.ncbi.nlm.nih.gov/entrez/eutils/elink.fcgi?dbfrom=pubmed&id=9655805&retmode=ref&cmd=prlinks%5Cnpapers3://publication/uuid/FF7D8BB8-A64D-4CF3-8FFD-22558FDCDD03

Loh, C. Y., Chai, J. Y., Tang, T. F., Wong, W. F., Sethi, G., Shanmugam, M. K., … Looi, C. Y. (2019). The E-Cadherin and N-Cadherin Switch in Epithelial-to-Mesenchymal Transition: Signaling, Therapeutic Implications, and Challenges. *Cells 2019, Vol. 8, Page 1118*, *8*(10), 1118. https://doi.org/10.3390/CELLS8101118

Long, W. L., & Ballard, W. W. (2001). Normal embryonic stages of the longnose gar, Lepisosteus osseus. *BMC Developmental Biology*, *1*, 1–8. https://doi.org/10.1186/1471-213X-1-6

Mabee, P. M., Crotwell, P. L., Bird, N. C., & Burke, A. C. (2002). Evolution of median fin modules in the axial skeleton of fishes. *Journal of Experimental Zoology*, *294*(2), 77–90. https://doi.org/10.1002/jez.10076

Mao, L. M. F., Boyle Anderson, E. A. T., & Ho, R. K. (2021). Anterior lateral plate mesoderm gives rise to multiple tissues and requires tbx5a function in left-right asymmetry, migration dynamics, and cell specification of late-addition cardiac cells. *Developmental Biology*, *472*(July 2020), 52–66. https://doi.org/10.1016/j.ydbio.2021.01.007

Mao, Q., Stinnett, H. K., & Ho, R. K. (2015). Asymmetric cell convergence-driven zebrafish fin bud initiation and pre-pattern requires Tbx5a control of a mesenchymal Fgf signal. *Development*, *142*(24), 4329–4339. https://doi.org/10.1242/dev.124750

Mao, Qiyan. (2013). *Spatial dynamics and regulation of the zebrafish limb morphogenetic field*. University of Chicago.

Marelli, F., Carra, S., Agostini, M., Cotelli, F., Peeters, R., Chatterjee, K., & Persani, L. (2016). Patterns of thyroid hormone receptor expression in zebrafish and generation of a novel model of resistance to thyroid hormone action. *Molecular and Cellular Endocrinology*, *424*, 102–117. https://doi.org/10.1016/J.MCE.2016.01.020

Meier, S. (1980). Development of the chick embryo mesoblast: Pronephros, lateral plate, and early vasculature. *Journal of Embryology and Experimental Morphology*, *Vol. 55*, 291–306. https://doi.org/10.1242/dev.55.1.291

Mercader, N. (2007). Early steps of paired fin development in zebrafish compared with tetrapod limb development. *Development Growth and Differentiation*, *49*(6), 421–437. https://doi.org/10.1111/j.1440-169X.2007.00942.x

Mercader, N., Fischer, S., & Neumann, C. J. (2006). Prdm1 acts downstream of a sequential RA, Wnt and Fgf signaling cascade during zebrafish forelimb induction. *Development*, *133*(15),

2805–2815. https://doi.org/10.1242/DEV.02455

Miller, M. J. (2009). Ecology of Anguilliform Leptocephali: Remarkable Transparent Fish Larvae of the Ocean Surface Layer. https://doi.org/10.5047/absm.2009.00204.0001

Minguillon, C., Nishimoto, S., Wood, S., Vendrell, E., Gibson-Brown, J. J., & Logan, M. P. O. (2012). Hox genes regulate the onset of Tbx5 expression in the forelimb. *Development*, *139*(17), 3180–3188. https://doi.org/10.1242/dev.084814

Minguillon, Carolina, Del Buono, J., & Logan, M. P. (2005). Tbx5 and Tbx4 are not sufficient to determine limb-specific morphologies but have common roles in initiating limb outgrowth. *Developmental Cell*, *8*(1), 75–84. https://doi.org/10.1016/j.devcel.2004.11.013

Minguillon, Carolina, Nishimoto, S., Wood, S., Vendrell, E., Gibson-Brown, J. J., & Logan, M. P. O. (2012). Hox genes regulate the onset of Tbx5 expression in the forelimb. *Development (Cambridge)*, *139*(17), 3180–3188. https://doi.org/10.1242/dev.084814

Mivart, S. G. (1879). XII. Notes on the Fins of‘ Elasmobranchs, with Considerations on the Nature and Homologues of Vertebrate Limbs. *The Transactions of the Zoological Society of London*, *10*(10), 439–484. https://doi.org/10.1111/j.1096-3642.1879.tb00460.x

Miyamoto, K., & Abe, G. (2022). Developmental Independence of Median Fins From the larval Fin Fold Revises Their Evolutionary Origin. *Scientific Reports*, 1–21. https://doi.org/10.1038/s41598-022-11180-1

Miyashita, T., Coates, M. I., Farrar, R., Larson, P., Manning, P. L., & Wogelius, R. A. (2018). Hagfish from the Cretaceous Tethys Sea and a reconciliation of the morphological – molecular conflict in early vertebrate phylogeny, (8). https://doi.org/10.1073/pnas.1814794116

Mosimann, C., Kaufman, C. K., Li, P., Pugach, E. K., Tamplin, O. J., & Zon, L. I. (2011). Ubiquitous transgene expression and Cre-based recombination driven by the ubiquitin promoter in zebrafish. *Development (Cambridge, England)*, *138*(1), 169–177. https://doi.org/10.1242/dev.059345

Murata, Y., Tamura, M., Aita, Y., Fujimura, K., Murakami, Y., Okabe, M., … Tanaka, M. (2010). Allometric growth of the trunk leads to the rostral shift of the pelvic fin in teleost fishes. *Developmental Biology*, *347*(1), 236–245. https://doi.org/10.1016/j.ydbio.2010.07.034

Naiche, L. A., & Papaioannou, V. E. (2007). Tbx4 is not required for hindlimb identity or post-

bud hindlimb outgrowth. *Development*, *134*(1), 93–103. https://doi.org/10.1242/dev.02712

Nakamura, T., Gehrke, A. R., Lemberg, J., Szymaszek, J., & Shubin, N. H. (2016). Digits and fin rays share common developmental histories. *Nature*, *537*(7619), 225–228. https://doi.org/10.1038/nature19322

NC DEQ. (n.d.). Flounder. Retrieved June 24, 2022, from https://deq.nc.gov/about/divisions/marine-fisheries/public-information-and-education/species-profiles/flounder

Near, T. J., Eytan, R. I., Dornburg, A., Kuhn, K. L., Moore, J. A., Davis, M. P., … Smith, W. L. (2012). Resolution of ray-finned fish phylogeny and timing of diversification. *PNAS*, *109*(34), 13698–13703. https://doi.org/10.1073/pnas.1206625109

Nelsen, O. E. (1953). *Comparative embryology of the vertebrates*. New York: The Blakiston Company.

Nelson, J. S., Grande, T. C., & Wilson, M. V. (2006). *Fishes of the World* (Fourth). Hoboken, New Jersey: John Wiley & Sons, Inc. Retrieved from https://books.google.com/books?hl=en&lr=&id=E-MLDAAAQBAJ&oi=fnd&pg=PT43&dq=fishes+of+the+world&ots=uVk1HKuZmT&sig=H9fSq_q3itq0BANjs4B98d9DM5A#v=onepage&q=fishes of the world&f=false

Nelson, J. S., Schultze, H., & Wilson, M. V. H. (2010). *Origin and Phylogenetic Interrelationships of Teleosts*. *Origin and Phylogenetic Interrelationships of Teleosts* (Vol. 1st). Retrieved from http://people.ku.edu/~mpdavis/GAV-19-Davis.pdf

Nemec, S., Jain, D., Sung, H., Pastinen, T., & Drouin, J. (2017). Pitx1 directly modulates the core limb development program to implement hindlimb identity, 3325–3335. https://doi.org/10.1242/dev.154864

Newton, A. H., Williams, S. M., Major, A. T., & Smith, C. A. (2022). Cell lineage specification during development of the anterior lateral plate mesoderm and forelimb field. *BioRxiv*, 2022.01.13.475748. https://doi.org/10.1101/2022.01.13.475748

Nishimoto, S., & Logan, M. P. O. (2016a). Subdivision of the lateral plate mesoderm and specification of the forelimb and hindlimb forming domains. *Seminars in Cell and Developmental Biology*, *49*, 102–108. https://doi.org/10.1016/j.semcdb.2015.11.011

Nishimoto, S., & Logan, M. P. O. (2016b). Subdivision of the lateral plate mesoderm and specification of the forelimb and hindlimb forming domains. *Seminars in Cell and*

Developmental Biology, *49*, 102–108. https://doi.org/10.1016/j.semcdb.2015.11.011

Nowicki, J. L., & Burke, A. C. (2000). Hox genes and morphological identity: axial versus lateral patterning in the vertebrate mesoderm. *Development*, *127*(19), 4265–4275. https://doi.org/10.1242/DEV.127.19.4265

Nowicki, Julie L, Takimoto, R., & Burke, A. C. (2003). The lateral somitic frontier: dorso-ventral aspects of anterio-posterior regionalization in avian embryos. *Mechanisms of Development*, *120*(2), 227–240. https://doi.org/10.1016/S0925-4773(02)00415-X

Ocaña, O. H., Córcoles, R., Fabra, Á., Moreno-Bueno, G., Acloque, H., Vega, S., … Nieto, M. A. (2012). Metastatic Colonization Requires the Repression of the Epithelial-Mesenchymal Transition Inducer Prrx1. *Cancer Cell*, *22*(6), 709–724. https://doi.org/10.1016/j.ccr.2012.10.012

Owen, R. (1849). *On the nature of limbs: a discourse delivered on Friday, February 9, at an Evening Meeting of the Royal Institution of Great Britain*.

Parichy, D. M., & Spiewak, J. E. (2015). Origins of adult pigmentation: diversity in pigment stem cell lineages and implications for pattern evolution. *Pigment Cell & Melanoma Research*, *28*(1), 31–50. https://doi.org/10.1111/PCMR.12332

Peter, I. S., & Davidson, E. H. (2011). Evolution of Gene Regulatory Networks Controlling Body Plan Development. *Cell*, *144*(6), 970–985. https://doi.org/10.1016/J.CELL.2011.02.017

Petit, F., Sears, K. E., & Ahituv, N. (2017). Limb development: A paradigm of gene regulation. *Nature Reviews Genetics*, *18*(4), 245–258. https://doi.org/10.1038/nrg.2016.167

Pietsch, T. W., & Grobecker, D. B. (1987). *Frogfishes of the world : systematics, zoogeography, and behavioral ecology*. Stanford University Press. Retrieved from http://agris.fao.org/agris-search/search.do?recordID=US8919240

Power, D. ., Llewellyn, L., Faustino, M., Nowell, M. ., Björnsson, B. T., Einarsdottir, I. ., … Sweeney, G. . (2001). Thyroid hormones in growth and development of fish. *Comparative Biochemistry and Physiology Part C: Toxicology & Pharmacology*, *130*(4), 447–459. https://doi.org/10.1016/S1532-0456(01)00271-X

Price, S. A., Friedman, S. T., & Wainwright, P. C. (2015). How predation shaped fish: The impact of fin spines on body form evolution across teleosts. *Proceedings of the Royal Society B: Biological Sciences*, *282*(1819). https://doi.org/10.1098/rspb.2015.1428

Prince, V., Joly, L., Ekker, M., Development, R. H.-, & 1998, undefined. (1998). Zebrafish hox genes: genomic organization and modified colinear expression patterns in the trunk. *Journals.Biologists.Com*. Retrieved from https://journals.biologists.com/dev/article-abstract/125/3/407/40090

Prummel, K. D., Crowell, H. L., Nieuwenhuize, S., Brombacher, E. C., Soneson, C., Kresoja-rakic, J., … Mosimann, C. (2022). Hand2 delineates mesothelium progenitors and is reactivated in mesothelioma. *Nature*.

Prummel, K. D., Nieuwenhuize, S., & Mosimann, C. (2020). The lateral plate mesoderm. *Development (Cambridge)*, *147*(12). https://doi.org/10.1242/dev.175059

Quintanilla, C. A., & Ho, R. K. (2020). The Cdx transcription factors and retinoic acid play parallel roles in antero-posterior position of the pectoral fin field during gastrulation. *Mechanisms of Development*, *164*, 103644. https://doi.org/10.1016/J.MOD.2020.103644

Rabosky, D. L., Chang, J., Title, P. O., Cowman, P. F., Sallan, L., Friedman, M., … Alfaro, M. E. (2018). An inverse latitudinal gradient in speciation rate for marine fishes. *Nature*, *559*(7714), 392–395. https://doi.org/10.1038/s41586-018-0273-1

Rallis, C. (2003). Tbx5 is required for forelimb bud formation and continued outgrowth. *Development*, *130*(12), 2741–2751. https://doi.org/10.1242/dev.00473

Rescan, P. Y. (2019). Development of myofibres and associated connective tissues in fish axial muscle: Recent insights and future perspectives. *Differentiation*, *106*(March), 35–41. https://doi.org/10.1016/j.diff.2019.02.007

Revell, L. (2012). phytools: An R package for phylogenetic comparative biology (and other things). *Methods in Ecology and Evolution*, *3*, 217–223.

Rocha, M., Singh, N., Ahsan, K., Beiriger, A., & Prince, V. E. (2020). Neural crest development: insights from the zebrafish. *Developmental Dynamics*, *249*(1), 88–111. https://doi.org/10.1002/DVDY.122

Rosen, D. (1973). Interrelationships of higher euteleostean fishes. In P. Greenwood, R. Miles, & C. Patterson (Eds.), *Interrelationships of Fishes*.

Rosen, D. E. (1982). Teleostean interrelationships, morphological function and evolutionary inference. *Integrative and Comparative Biology*, *22*(2), 261–273. https://doi.org/10.1093/icb/22.2.261

Ruvinsky, I., Oates, A. C., Silver, L. M., & Ho, R. K. (2000). The evolution of paired

appendages in vertebrates: T-box genes in the zebrafish. *Development Genes and Evolution*, *210*(2), 82–91. https://doi.org/10.1007/s004270050014

Ruvinsky, I, & Gibson-Brown, J. J. (2000). Genetic and developmental bases of serial homology in vertebrate limb evolution. *Development (Cambridge, England)*, *127*(24), 5233–5244. https://doi.org/11076746

Ruvinsky, Ilya, Silver, L. M., & Gibson-Brown, J. J. (2000). Phylogenetic Analysis of T-Box Genes Demonstrates the Importance of Amphioxus for Understanding Evolution of the Vertebrate Genome. *Genetics*, *156*(3).

Sallan, L. C. (2014). Major issues in the origins of ray-finned fish (Actinopterygii) biodiversity. *Biological Reviews*, *89*(4), 950–971. https://doi.org/10.1111/brv.12086

Scarpa, E., Szabó, A., Bibonne, A., Theveneau, E., Parsons, M., & Mayor, R. (2015). Cadherin Switch during EMT in Neural Crest Cells Leads to Contact Inhibition of Locomotion via Repolarization of Forces. *Developmental Cell*, *34*(4), 421–434. https://doi.org/10.1016/J.DEVCEL.2015.06.012

Schindelin, J., Arganda-Carreras, I., Frise, E., Kaynig, V., Longair, M., Pietzsch, T., … Cardona, A. (2012). Fiji: An open-source platform for biological-image analysis. *Nature Methods*, *9*(7), 676–682. https://doi.org/10.1038/NMETH.2019

Scott, B. R., & Wilson, M. V. H. (2012). A New Species of Waengsjoeaspis (Cephalaspidomorpha, Osteostraci) from the Early Devonian of Northwestern Canada, with a Redescription of W. nahanniensis and Implications for Growth, Variation, Morphology, and Phylogeny. *Source Journal of Vertebrate Paleontology Journal of Vertebrate Paleontology*, *32*(326). https://doi.org/10.1080/02724634.2012.694514

Sfakiotakis, M., Lane, D. M., & Davies, J. B. C. (1999). Review of fish swimming modes for aquatic locomotion. *IEEE Journal of Oceanic Engineering*, *24*(2), 237–252. https://doi.org/10.1109/48.757275

Shapiro, M. D., Marks, M. E., Peichel, C. L., Blackman, B. K., Nereng, K. S., Jonsson, B., … Kingsley, D. M. (2004). Genetic and developmental basis\rof evolutionary pelvic reduction\rin threespine sticklebacks. *Nature*, *428*(APRIL), 717–723.

Shearman, R. M., & Burke, A. C. (2009). The lateral somitic frontier in ontogeny and phylogeny. *Journal of Experimental Zoology Part B: Molecular and Developmental Evolution*, *312*(6), 603–612. https://doi.org/10.1002/jez.b.21246

Shibukawa, K., Tran, D. D., Loi, &, & Tran, X. (2012). Phallostethus cuulong, a new species of priapiumfish (Actinopterygii: Atheriniformes: Phallostethidae) from the Vietnamese Mekong. *Zootaxa*, *3363*, 45–51. Retrieved from www.mapress.com/zootaxa/

Shimada, A., Kawanishi, T., Kaneko, T., Yoshihara, H., Yano, T., Inohaya, K., … Takeda, H. (2013). Trunk exoskeleton in teleosts is mesodermal in origin. *Nature Communications*, *4*. https://doi.org/10.1038/ncomms2643

Shkil, F. N., Kapitanova, D. V., Borisov, V. B., Abdissa, B., & Smirnov, S. V. (2012). Thyroid hormone in skeletal development of cyprinids: effects and morphological consequences. *Journal of Applied Ichthyology*, *28*(3), 398–405. https://doi.org/10.1111/j.1439-0426.2012.01992.x

Siegal, M. L., & Bergman, A. (2002). Waddington's canalization revisited: Developmental stability and evolution. *Proceedings of the National Academy of Sciences of the United States of America*, *99*(16), 10528–10532. https://doi.org/10.1073/PNAS.102303999

Sloan Kettering Institute. (2019). Postdoctoral position: Pigmentation in the zebrafish. Retrieved June 24, 2022, from https://www.mskcc.org/research/ski/labs/richard-white/postdoctoral-position-pigmentation-zebrafish-richard-white-lab-msk-cancer

Smith, M., Hickman, A., Amanze, D., Lumsden, A., & Thorogood, P. (1994). Trunk neural crest origin of caudal fin mesenchyme in the zebrafish Brachydanio rerio. *Proceedings of the Royal Society of London. Series B: Biological Sciences*, *256*(1346), 137–145. https://doi.org/10.1098/RSPB.1994.0061

Stainier, D., Lee, R., & Fishman, M. (1993). Cardiovascular development in the zebrafish. I. Myocardial fate map and heart tube formation. *Development*. Retrieved from https://journals.biologists.com/dev/article-abstract/119/1/31/37848

Standen, E. M. (2008). Pelvic fin locomotor function in fishes: three-dimensional kinematics in rainbow trout (Oncorhynchus mykiss). *Journal of Experimental Biology*, *211*(18), 2931–2942. https://doi.org/10.1242/jeb.018572

Standen, E. M. (2010). Muscle activity and hydrodynamic function of pelvic fins in trout (Oncorhynchus mykiss). *Journal of Experimental Biology*, *213*(5), 831–841. https://doi.org/10.1242/jeb.033084

Standen, E. M., & Lauder, G. V. (2005). Dorsal and anal fin function in bluegill sunfish Lepomis macrochirus: Three-dimensional kinematics during propulsion and maneuvering. *Journal of*

Experimental Biology, *208*(14), 2753–2763. https://doi.org/10.1242/jeb.01706

Standen, E. M., & Lauder, G. V. (2007). Hydrodynamic function of dorsal and anal fins in brook trout (Salvelinus fontinalis). *Journal of Experimental Biology*, *210*(2), 325–339. https://doi.org/10.1242/jeb.02661

Stewart, T. A., Bonilla, M. M., Ho, R. K., & Hale, M. E. (2019). Adipose fin development and its relation to the evolutionary origins of median fins. *Scientific Reports 2019 9:1*, *9*(1), 1–12. https://doi.org/10.1038/s41598-018-37040-5

Stewart, T. A., Smith, W. L., & Coates, M. I. (2014). The origins of adipose fins: an analysis of homoplasy and the serial homology of vertebrate appendages. *Proceedings of the Royal Society B: Biological Sciences*, *281*(1781). https://doi.org/10.1098/RSPB.2013.3120

Takeuchi, J. K. (2003). Tbx5 and Tbx4 trigger limb initiation through activation of the Wnt/Fgf signaling cascade. *Development*, *130*(12), 2729–2739. https://doi.org/10.1242/dev.00474

Tamura, K., Yonei-Tamura, S., & Belmonte, J. C. I. (1999). Differential expression of Tbx4 and Tbx5 in Zebrafish Fin buds. *Mechanisms of Development*, *87*(1–2), 181–184. https://doi.org/10.1016/S0925-4773(99)00126-4

Tanaka, M., Cohn, M. J., Ashby, P., Davey, M., Martin, P., & Tickle, C. (2000). Distribution of polarizing activity and potential for limb formation in mouse and chick embryos and possible relationships to polydactyly. *Development*, *127*(18), 4011–4021. https://doi.org/10.1242/dev.127.18.4011

Tanaka, Mikiko. (2011). Revealing the mechanisms of the rostral shift of pelvic fins among teleost fishes. *Evolution and Development*, *13*(4), 382–390. https://doi.org/10.1111/j.1525-142X.2011.00493.x

Tanaka, Mikiko. (2016). Developmental Mechanism of Limb Field Specification along the Anterior–Posterior Axis during Vertebrate Evolution. *Journal of Developmental Biology*, *4*(2), 18. https://doi.org/10.3390/jdb4020018

Tanaka, Mikiko, Yu, R., & Kurokawa, D. (2015). Anterior migration of lateral plate mesodermal cells during embryogenesis of the pufferfish takifugu niphobles: Insight into the rostral positioning of pelvic fins. *Journal of Anatomy*, *227*(1), 81–88. https://doi.org/10.1111/joa.12324

Taylor, J. S., Van de Peer, Y., Braasch, I., & Meyer, A. (2001). Comparative genomics provides evidence for an ancient genome duplication event in fish. *Philosophical Transactions of the*

Royal Society of London. Series B: Biological Sciences, *356*(1414), 1661–1679. https://doi.org/10.1098/RSTB.2001.0975

Thacher, J. (1877a). Median and paired fins: a contribution to the history of vertebrate limbs. Retrieved from https://scholar.google.com/scholar?hl=en&as_sdt=0%2C14&q=Thacher+1877+median+paired+fins&btnG=&oq=thac

Thacher, J. (1877b). Median and paired fins: a contribution to the history of vertebrate limbs. Retrieved from https://scholar.google.com/scholar?hl=en&as_sdt=0%2C14&q=Thacher+1877+median+paired+fins&btnG=

Theißen, G. (2009). Saltational evolution: hopeful monsters are here to stay. *Theory in Biosciences 2009 128:1*, *128*(1), 43–51. https://doi.org/10.1007/S12064-009-0058-Z

Tickle, C. (2015). How the embryo makes a limb: Determination, polarity and identity. *Journal of Anatomy*, *227*(4), 418–430. https://doi.org/10.1111/joa.12361

Trinajstic, K., Boisvert, C., Long, J., & Maksimenko, A. (2015). Pelvic and reproductive structures in placoderms (stem gnathostomes), *90*, 467–501. https://doi.org/10.1111/brv.12118

Tulenko, F. J., McCauley, D. W., MacKenzie, E. L., Mazan, S., Kuratani, S., Sugahara, F., … Burke, A. C. (2013). Body wall development in lamprey and a new perspective on the origin of vertebrate paired fins. *Proceedings of the National Academy of Sciences*, *110*(29), 11899–11904. https://doi.org/10.1073/pnas.1304210110

Van Valen, L. (1974). Multivariate structural statistics in natural history. *Journal of Theoretical Biology*, *45*(1), 235–247. https://doi.org/10.1016/0022-5193(74)90053-8

Vauti, F., Stegemann, L. A., Vögele, V., & Köster, R. W. (2020). All-age whole mount in situ hybridization to reveal larval and juvenile expression patterns in zebrafish. *PLOS ONE*, *15*(8), e0237167. https://doi.org/10.1371/JOURNAL.PONE.0237167

Virta, V. C., & Cooper, M. S. (2009). Ontogeny and phylogeny of the yolk extension in embryonic cypriniform fishes. *Journal of Experimental Zoology Part B: Molecular and Developmental Evolution*, *312*(3), 196–223. https://doi.org/10.1002/jez.b.21284

Waddington, C. H. (1942). CANALIZATION OF DEVELOPMENT AND THE INHERITANCE OF ACQUIRED CHARACTERS. *Nature 1942 150:3811*, *150*(3811),

563–565. https://doi.org/10.1038/150563a0

Wanner, S. J., & Prince, V. E. (2013). Axon tracts guide zebrafish facial branchiomotor neuron migration through the hindbrain. *Development*, *140*(4), 906–915. https://doi.org/10.1242/DEV.087148

Webb, P. W., & Fairchild, A. G. (2001). Performance and maneuverability of three species of teleostean fishes. *Canadian Journal of Zoology*, *79*(10), 1866–1877. https://doi.org/10.1139/cjz-79-10-1866

Westerfield, M. (2000). No Title. In *The zebrafish book: a guide for the labratory use of zebrafish*.

Westoll, T. S. (1941). The Permian Fishes Dorypterus and Lekanichthys. *Proceedings of the Zoological Society of London*, *B111*(1–2), 39–58. https://doi.org/10.1111/J.1469-7998.1941.TB00042.X

Wilga, C. D., & Lauder, G. V. (1999). Locomotion in sturgeon: Function of the pectoral fins. *Journal of Experimental Biology*, *202*(18), 2413–2432. https://doi.org/10.1242/jeb.202.18.2413

Windner, S. E., Steinbacher, P., Obermayer, A., Kasiba, B., Zweimueller-Mayer, J., & Stoiber, W. (2011). Distinct modes of vertebrate hypaxial muscle formation contribute to the teleost body wall musculature. *Development Genes and Evolution*, *221*(3), 167–178. https://doi.org/10.1007/S00427-011-0369-1/FIGURES/5

Wu, F., Sun, Y., Xu, G., Hao, W., Jiang, D., & Sun, Z. (2011). New Saurichthyid Actinopterygian Fishes from the Anisian (Middle Triassic) of Southwestern China. *Https://Doi.Org/10.4202/App.2010.0007*, *56*(3), 581–614. https://doi.org/10.4202/APP.2010.0007

Yamanoue, Y., Setiamarga, D. H. E., & Matsuura, K. (2010). Pelvic fins in teleosts: Structure, function and evolution. *Journal of Fish Biology*, *77*(6), 1173–1208. https://doi.org/10.1111/j.1095-8649.2010.02674.x

Yonei-Tamura, S., Abe, G., Tanaka, Y., Anno, H., Noro, M., Ide, H., … Tamura, K. (2008). Competent stripes for diverse positions of limbs/fins in gnathostome embryos. *Evolution and Development*, *10*(6), 737–745. https://doi.org/10.1111/j.1525-142X.2008.00288.x

Yonei-Tamura, S., Ide, H., & Tamura, K. (2005). Splanchnic (Visceral) Mesoderm Has Limb-Forming Ability According to the Position Along the Rostrocaudal Axis in Chick Embryos,

(April), 256–265. https://doi.org/10.1002/dvdy.20391

Zhang, X.-G., & Hou, X.-G. (2004). Evidence for a single median fin-fold and tail in the Lower Cambrian vertebrate, Haikouichthys ercaicunensis. *Journal of Evolutionary Biology*, *17*(5), 1162–1166. https://doi.org/10.1111/j.1420-9101.2004.00741.x

Zhao, X., & Duester, G. (2009). Effect of retinoic acid signaling on Wnt/β-catenin and FGF signaling during body axis extension. *Gene Expression Patterns*, *9*(6), 430–435. https://doi.org/10.1016/J.GEP.2009.06.003

Zhu, M., Yu, X., Choo, B., Wang, J., & Jia, L. (2012). An antiarch placoderm shows that pelvic girdles arose at the root of jawed vertebrates, (January), 453–456.